

**TACKLING ALDOSTERONE-MEDIATED DISORDERS:
LEAD OPTIMIZATION PROVIDING A SERIES OF
3-PYRIDINE-BASED ALDOSTERONE SYNTHASE INHIBITORS
WITH IMPROVED PHARMACOLOGICAL PROPERTIES**

Dissertation

zur Erlangung des Grades des Doktors der Naturwissenschaften
der Naturwissenschaftlich-Technischen Fakultät III
Chemie, Pharmazie, Bio- und Werkstoffwissenschaften
der Universität des Saarlandes

von

Dipl. Chem. Simon Lucas

Saarbrücken

2008

Tag des Kolloquiums: 17. Dezember 2008
Dekan: Prof. Dr. U. Müller
Berichterstatter: Prof. Dr. R. W. Hartmann
Prof. Dr. U. Kazmaier
Prof. Dr. B. Clement

Die vorliegende Arbeit wurde von September 2005 bis August 2008 unter Anleitung von Herrn Prof. Dr. Rolf W. Hartmann an der Naturwissenschaftlich-Technischen Fakultät III der Universität des Saarlandes angefertigt.

JE PLANMÄßIGER DIE MENSCHEN VORGEHEN,
DESTO WIRKSAMER VERMAG SIE DER ZUFALL ZU TREFFEN.

FRIEDRICH DÜRRENMATT

FÜR J. F. L.

ABSTRACT

3-Pyridine substituted naphthalenes constitute a class of potent inhibitors of aldosterone synthase (CYP11B2), an innovative target for the treatment of aldosterone-mediated disorders such as congestive heart failure and myocardial fibrosis. However, these early leads exhibit several major pharmacological drawbacks, above all undesirable hepatic CYP interactions and lacking *in vivo* activity. In order to overcome these obstacles, a drug design program toward a development candidate was launched following a combined ligand- and structure-based approach. The optimization process yielded 110 new compounds, classified into four main molecular scaffolds, most of which are highly potent CYP11B2 inhibitors with IC₅₀ values in the low nanomolar to picomolar range. Beside a striking selectivity toward the highly homologous 11 β -hydroxylase (CYP11B1), the most promising compounds of the present study show virtually no inhibition of the six most important hepatic CYP enzymes as well as CYP17 and CYP19, both crucial enzymes for the metabolism of steroid hormones. A subset of the investigated inhibitors reaches excellent plasma-levels in the range of the marketed drug fadrozole after peroral application to rats. Furthermore, a derivative of the dihydro-1*H*-quinolin-2-one series exerts potent aldosterone-lowering effects *in vivo* using ACTH stimulated rats. In conclusion, the current work might give rise to a development candidate after further optimization and biological testing.

ZUSAMMENFASSUNG

3-Pyridinsubstituierte Naphthalene sind potente Hemmstoffe der Aldosteronsynthese (CYP11B2), einem innovativen Target zur Behandlung von Herzinsuffizienz und Myokardfibrose. Die entwickelten Leitverbindungen weisen jedoch unerwünschte Wechselwirkungen mit hepatischen CYP Enzymen auf und können die Aldosteronbiosynthese *in vivo* nicht hemmen. In der vorliegenden Arbeit wurden 110 neuartige Hemmstoffe, entwickelt durch Ligand- und Struktur-basiertes Design, synthetisiert und auf biologische Aktivität getestet, um diese Hindernisse auf dem Weg zu einem Entwicklungskandidaten zu überwinden. Die meisten der hierin vorgestellten Verbindungen sind nicht nur hochpotente CYP11B2 Inhibitoren mit IC_{50} -Werten im nano- bis picomolaren Bereich, sondern auch besonders selektiv gegenüber CYP11B1 (11 β -Hydroxylase), einem Enzym mit hoher Homologie zu dem eigentlichen Target. Außerdem weisen die vielversprechenden Hemmstoffe ein deutlich verbessertes pharmakologisches Gesamtprofil gegenüber den entsprechenden Naphthalenderivaten auf: Keine oder nur geringe Hemmung der sechs wichtigsten hepatischen CYP-Enzyme sowie den steroidmetabolisierenden Enzymen CYP17 und CYP19, keine Zytotoxizität, niedrige Plasmaproteinbindung, eine exzellente Bioverfügbarkeit und eine starke Hemmung der Aldosteronbiosynthese *in vivo*. Nach erweiterten pharmakologischen Untersuchungen und gegebenenfalls erforderlichen strukturellen Optimierungen sollen aus den vorgestellten Substanzklassen Entwicklungskandidaten hervorgehen.

PAPERS INCLUDED IN THIS THESIS

This thesis divided into four publications, which are referred to in the text by their Roman numerals.

- I Overcoming Undesirable CYP1A2 Inhibition of Pyridynaphthalene Type Aldosterone Synthase Inhibitors: Influence of Heteroaryl Derivatization on Potency and Selectivity**
Ralf Heim, Simon Lucas, Cornelia M. Grombein, Christina Ries, Katarzyna E. Schewe, Matthias Negri, Ursula Müller-Vieira, Barbara Birk, and Rolf W. Hartmann
J. Med. Chem. **2008**, *51*, 5064–5074
- II Novel Aldosterone Synthase Inhibitors with Extended Carbocyclic Skeleton by a Combined Ligand-Based and Structure-Based Drug Design Approach**
Simon Lucas, Ralf Heim, Matthias Negri, Iris Antes, Christina Ries, Katarzyna E. Schewe, Alessandra Bisi, Silvia Gobbi, and Rolf W. Hartmann
J. Med. Chem. **2008**, in press
- III Nonsteroidal Aldosterone Synthase Inhibitors with Improved Selectivity: Lead Optimization Providing a Series of Pyridine Substituted 3,4-Dihydro-1*H*-quinolin-2-one Derivatives**
Simon Lucas, Ralf Heim, Christina Ries, Katarzyna E. Schewe, Barbara Birk, and Rolf W. Hartmann
J. Med. Chem. **2008**, submitted
- IV Fine-Tuning the Selectivity of Aldosterone Synthase Inhibitors: SAR Insights from Studies of Heteroaryl Substituted 1,2,5,6-Tetrahydropyrrolo[3,2,1-*ij*]quinolin-4-one Derivatives**
Simon Lucas, Ralf Heim, Christina Ries, and Rolf W. Hartmann
J. Med. Chem. **2008**, manuscript

CONTRIBUTION REPORT

The author wishes to clarify his contributions to the papers **I–IV** in the thesis.

- I** Significantly contributed to the inhibitor design concept. Planned, synthesized and characterized most of the new compounds. Compounds **2**, **2a–g**, **5**, **12**, **13**, **29** and **30** were synthesized by Cornelia M. Grombein as part of a Diploma thesis. Compounds **6**, **6a–b**, **8**, **8a** and **27** were synthesized by Dr. Ralf Heim. Significantly contributed to the interpretation of the results. Wrote the manuscript.
- II** Significantly contributed to the inhibitor design concept. Planned, synthesized and characterized all new compounds. Significantly contributed to the interpretation of the results. Wrote the manuscript.
- III** Significantly contributed to the inhibitor design concept. Planned, synthesized and characterized all new compounds except of compound **1** (synthesized by Dr. Ralf Heim). Significantly contributed to the interpretation of the results. Wrote the manuscript.
- IV** Significantly contributed to the inhibitor design concept. Planned, synthesized and characterized all new compounds. Significantly contributed to the interpretation of the results. Wrote the manuscript.

ABBREVIATIONS

11 β HSD2	11 β -Hydroxysteroid dehydrogenase type 2
18-EP	18-Ethynylprogesterone
18-VDOC	18-Vinyldeoxycorticosterone
18-VP	18-Vinylprogesterone
3 β HSD	3 β -Hydroxysteroid dehydrogenase
ACE	Angiotensin-converting enzyme
ACTH	Adrenocorticotrophic hormone
Ang I	Angiotensin I
Ang II	Angiotensin II
AUC	Area under the curve
cAMP	Cyclic adenosine monophosphate
CGS 16949A	Fadrozole (racemic)
CHF	Congestive heart failure
CNS	Central nervous system
CONSENSUS	Cooperative north scandinavian enalapril survival study
CRH	Corticotrophin-releasing hormone
CYP	Cytochrome P450
CYP11A1	Cholesterol desmolase
CYP11B1	11 β -Hydroxylase
CYP11B2	Aldosterone synthase
CYP17	17 α -Hydroxylase-17,20-lyase
CYP19	Aromatase
ENaC	Epithelial sodium channel
EPHESUS	Eplerenone post-acute myocardial infarction heart failure efficacy and survival study
ER	Endoplasmatic reticulum
Et	Ethyl
FAD 286A	<i>R</i> (+)-Enantiomer of fadrozole
HPA	Hypothalamic-pituitary-adrenal
Het	Heteroaryl
IC ₅₀	Concentration required for 50 % inhibition
<i>i</i> Pr	Isopropyl
kB	Kilobase

kDa	Kilodalton
Me	Methyl
MMP1	Matrix metalloproteinase 1
MR	Mineralocorticoid receptor
mRNA	Messenger ribonucleic acid
μg	Microgram
μM	Micromolar
NADP	Nicotinamide adenine dinucleotide phosphate
nm	Nanometer
nM	Nanomolar
Ph	Phenyl
PK	Pharmacokinetic
pM	Picomolar
QSAR	Quantitative structure activity relationship
RAAS	Renin-angiotensin-aldosterone system
RALES	Randomized aldactone evaluation study
SAR	Structure activity relationship
SEM	Standard error of the mean
Å	Ångström

CONTENTS

1 Introduction	1
1.1 Adrenal corticosteroids	1
1.1.1 Mineralocorticoid physiology: The role of aldosterone	1
1.1.2 Glucocorticoid physiology: The role of cortisol	2
1.1.3 Cytochrome P450 enzymes in the biosynthesis of mineralo- and glucocorticoids	3
1.1.4 Aldosterone synthase (CYP11B2) and 11 β -hydroxylase (CYP11B1), the key enzymes in corticosteroid biosynthesis	5
1.2 Aldosterone synthase as drug target	6
1.2.1 Congestive heart failure, myocardial fibrosis, and the role of aldosterone	6
1.2.2 Significance of aldosterone receptor antagonists in cardiovascular therapy	7
1.2.3 Inhibition of CYP11B2 as promising cardiovascular therapy concept	9
1.3 State of knowledge: Inhibitors of CYP11B2	11
1.3.1 Compounds with inhibitory effect on aldosterone biosynthesis	11
1.3.2 Further developments of the aromatase inhibitor fadrozole	12
1.3.3 Development of heteroaryl substituted methyleneindanes and -tetrahydro-naphthalenes	13
1.3.4 Development of heteroaryl substituted naphthalenes and structurally modified derivatives	14
2 Aim of the present study	16
2.1 Scientific objective	16
2.2 Working strategy: Inhibitor design concept	17
3 Results	21
3.1 Overcoming Undesirable CYP1A2 Inhibition of Pyridylnaphthalene Type Aldosterone Synthase Inhibitors: Influence of Heteroaryl Derivatization on Potency and Selectivity	21
3.2 Novel Aldosterone Synthase Inhibitors with Extended Carbocyclic Skeleton by a Combined Ligand-Based and Structure-Based Drug Design Approach	45
3.3 Nonsteroidal Aldosterone Synthase Inhibitors with Improved Selectivity: Lead Optimization Providing a Series of Pyridine Substituted 3,4-Dihydro-1H-quinolin-2-one Derivatives	72

3.4 Fine-Tuning the Selectivity of Aldosterone Synthase Inhibitors: SAR Insights from Studies of Heteroaryl Substituted 1,2,5,6-Tetrahydropyrrolo[3,2,1-<i>ij</i>]quinolin-4-one Derivatives	97
4 Summary and conclusion	119
5 References	131
6 Acknowledgements	140

1 Introduction

1.1 Adrenal corticosteroids

1.1.1 Mineralocorticoid physiology: The role of aldosterone

The most important circulating mineralocorticoid, aldosterone, is mainly secreted by the zona glomerulosa of the adrenal gland and plays a crucial role in the electrolyte and fluid homeostasis. Its biosynthesis is accomplished by the mitochondrial cytochrome P450 enzyme aldosterone synthase (CYP11B2) and proceeds via oxidation of the substrate 11-deoxycorticosterone to corticosterone and subsequently to aldosterone.¹ Since its isolation and characterization by Tait *et al.* some 50 years ago,² the traditional view of aldosterone action has been that the hormone binds to specific mineralocorticoid receptors (MR) located in the cytosol of target epithelial cells.³ The steroid receptor complex translocates to the nucleus upon ligand binding where it acts as a transcription factor modulating gene expression and translation of proteins. The prevalent final effectors of aldosterone action are the apical amiloride-sensitive epithelial sodium channel (ENaC)⁴ and the basolateral Na⁺/K⁺-ATPase.⁵ As a consequence, renal sodium reabsorption and potassium secretion are promoted in the distal tubule and the collecting duct of the nephron.⁶ Elevated blood volume and thus blood pressure result from water that follows the sodium movement via osmosis. Mineralocorticoid receptors have also been localized in nonepithelial tissues, particularly in the central nervous system (CNS)⁷ and in the cardiovascular system⁸ where they mediate diverse effects.

Various factors control the aldosterone production, whereof the principal regulator is the renin-angiotensin-aldosterone system (RAAS).⁹ This compensatory mechanism reacts in response to a decreased blood pressure or a decreased sodium level by release of renin, a proteolytic enzyme, from the juxtaglomerular cells of the kidney. Renin cleaves its glycoprotein substrate angiotensinogen between Leu10 and Val11 to form the biologically inert decapeptide angiotensin I (Ang I) which is thereupon converted to angiotensin II (Ang II) by the angiotensin-converting enzyme (ACE), present in the vascular endothelium. Angiotensin II is a highly potent vasoconstrictor agent and can elevate the blood pressure. Furthermore, it stimulates the adrenal cortex to secrete aldosterone, leading to sodium and water retention. The biosynthesis of renin is in turn under control of the RAAS in a negative feedback loop by direct action of Ang II on the juxtaglomerular apparatus. Other key regulators of aldosterone release are the plasma potassium concentration and to a minor extent the adrenocorticotrophic hormone (corticotrophin, ACTH).

Recent studies, mostly of nonepithelial cells, revealed that some aldosterone effects are not mediated by classical MR binding.¹⁰ These rapid actions that are referred to as nongenomic effects are independent of gene transcription and translation and were first identified in erythrocytes which lack nuclei.¹¹ Further insight has been gained by experiments using skin fibroblasts from MR knockout mice.¹² Therein, treatment with aldosterone excited a calcium and cAMP increase within minutes. In most cases, the induced nongenomic effects proved to be insensitive to specific MR antagonists which are contrariwise capable of blocking the genomic actions.¹³ The latter findings gave reason to the suggestion that a distinct, novel receptor is responsible for the nongenomic aldosterone effects, presumably associated with the cell membrane and showing high affinity for aldosterone. Although Eisen *et al.* have isolated a putative nongenomic aldosterone receptor, an approximately 50 kDa membrane protein with high affinity for aldosterone but not for glucocorticoids, its structure and function have not yet been fully characterized.¹⁴ Furthermore, there are suggestions that these fast aldosterone effects may also be mediated by the classical MR or a closely related protein.

Beside the classical adrenal biosynthetic pathway, extra-adrenal sites of aldosterone production have been identified.¹⁵ The aldosterone biosynthesis in the CNS is well-documented and aldosterone synthase mRNA was found in whole brain and cortex, cerebellum, brain stem, hippocampus and amygdale homogenates.¹⁶ Whether aldosterone is also synthesized locally in the cardiovascular system is controversially discussed.¹⁷ Silvestre *et al.* observed aldosterone formation in both homogenate and perfusate of isolated rat hearts which was increasable by Ang II and the measured aldosterone concentrations in the heart were found to be 17-fold higher than in plasma.¹⁸ By contrast, other studies suggest that cardiac aldosterone derives from circulation.¹⁹

1.1.2 Glucocorticoid physiology: The role of cortisol

Glucocorticoids stimulate processes, such as *de novo* synthesis and uptake of glucose, that serve to control the glucose levels.²⁰ They typically exert anti-inflammatory, immune-modulating as well as bone-catabolizing functions.²¹ The major glucocorticoid in humans, cortisol, is synthesized by the enzyme 11 β -hydroxylase (CYP11B1) which is located in the zona fasciculata of the adrenal gland.¹ The production of cortisol is under control of the hypothalamic-pituitary-adrenal (HPA) axis, an extremely sensitive signaling pathway which reacts upon physical, psychological or inflammatory stimulation by expressing the corticotrophin-releasing hormone (CRH) in the hypothalamus. This, in turn, acts on the pituitary to release the effector peptide ACTH into the circulation which stimulates the biosynthesis of glucocorticoids in the adrenal cortex. The HPA axis is self-regulated by the negative feedback exerted by cortisol on the pituitary and the hypothalamus to suppress further CRH release.

Interestingly, cortisol shows *in vitro* a similar high affinity to the mineralocorticoid receptor as aldosterone.²² On the other hand, several mechanisms trigger specificity for aldosterone *in vivo* although cortisol is present at 1000-fold higher level in the plasma. These mechanisms include a different

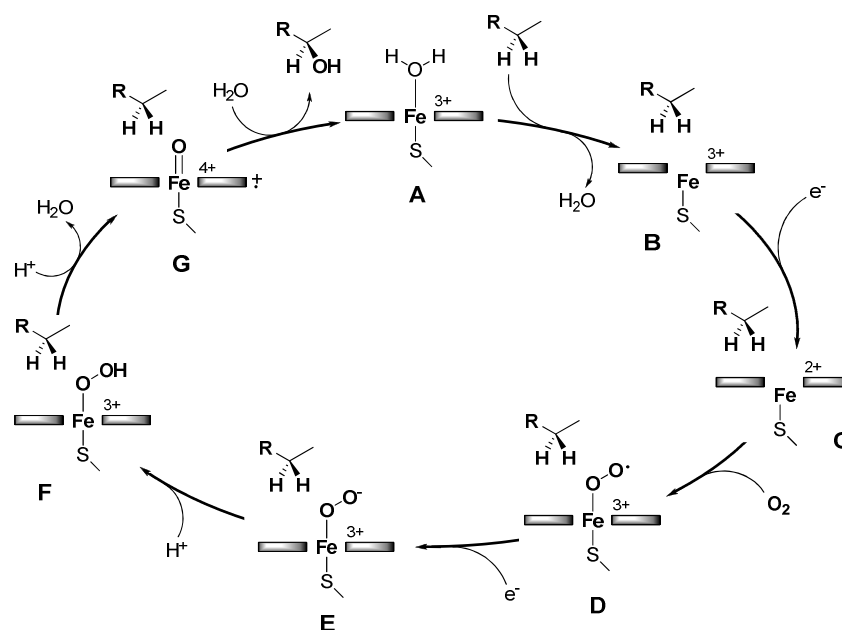
binding to plasma proteins²³ and a different dissociation rate from the MR.²⁴ Most attention has yet been attracted by the role of 11 β -hydroxysteroid dehydrogenase type 2 (11 β HSD2), an enzyme that converts cortisol to its inactive metabolite cortisone and colocalizes with MRs in aldosterone target tissues.²⁵ Analogously metabolizing aldosterone by 11 β HSD2 can not be accomplished because the hydroxy group in 11 β -position is protected by cyclization. Under normal conditions, with these specificity mechanisms operating, approximately 90 % of the epithelial MR and 99 % of the nonepithelial MRs are still occupied by cortisol. However, this occupancy can turn into an agonistic mode when 11 β HSD2 is blocked as it is in the case of tissue damage, changed redox state by reactive oxygen species, or inappropriate salt status, leading to hypertension and hypokalemia.²⁶

1.1.3 Cytochrome P450 enzymes in the biosynthesis of mineralo- and glucocorticoids

The adrenal corticosteroids are produced by multi-step syntheses with participation of cytochrome P450 (CYP) enzymes. These enzymes belong to a vast family of cysteinato-heme enzymes that are present in all forms of life (plants, bacteria, and mammals) and 'activate' molecular oxygen for the metabolism of both endogenous and exogenous substrates.²⁷ A main structural feature of all CYP enzymes is the prosthetic group, that is constituted of an iron(III)porphyrin, covalently linked to the protein by a proximal cysteine ligand. The naming 'P450' can be traced back to studies of Garfinkel²⁸ and Klingenberg²⁹ in 1958 who identified a carbon monoxide-binding 'pigment' in the microsomal fraction of rat liver cells. Omura and Sato characterized the responsible 'pigment' as a hemoprotein with a characteristic shift of the absorption peak in the carbon monoxide adduct to approximately 450 nm.³⁰

The cytochromes P450 are potent oxidation catalysts that use molecular oxygen as oxidant. Specifically, they are monooxygenases or mixed function oxidases because only one oxygen atom is inserted into the substrate while the second oxygen atom is reduced to a water molecule. The catalytic cycle starts with entropy driven substrate binding and release of an axial water molecule from the low spin resting state **A** (Figure 1).³¹ This event displaces the iron out of the porphyrin plane and changes to a pentacoordinated high spin state in the substrate bound complex **B**. The so changed redox potential makes the heme a better electron acceptor and triggers electron transfer from NADPH via a reductase protein, giving rise to the iron(II)porphyrin complex **C** which is an efficient reducing agent. Triplet dioxygen binds in η^1 -mode by accepting an electron from iron(II), forming the relatively stable intermediate **D**. The formally negatively charged iron(III)peroxo complex **E** results from the rate-determining second reduction step. Once at this stage, a network of specific amino acids affords a fast protonation to the hydroperoxo species **F** and subsequently to the iron(IV)oxo-porphyrinradical cation **G** under release of a water molecule. Insertion of oxygen into a carbon–hydrogen bond finally affords the hydroxylation product. By this or closely related mechanisms CYP enzymes can carry out a wide variety of oxidative biotransformations such as epoxidations, dehalogenations, dealkylations or cleavage of carbon–carbon bonds.

Figure 1. Catalytic cycle of cytochrome P450 mediated oxidations

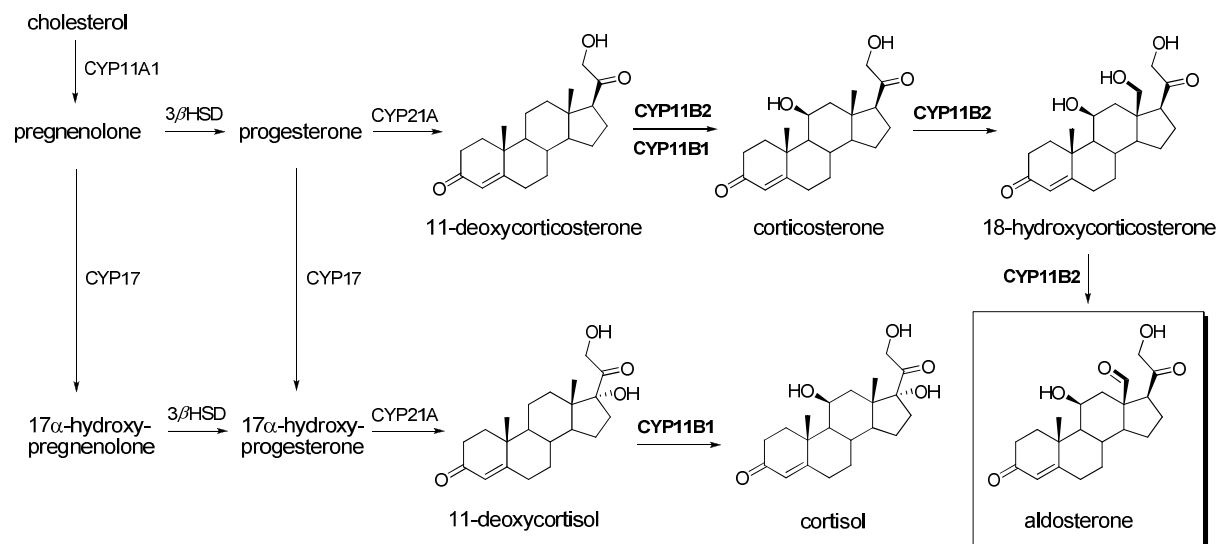


Depending on the electron providing system, CYP enzymes are classified into two main biochemical classes. Type I enzymes (including CYP11B2 and CYP11B1) which are present in the mitochondrial membrane receive their electrons from NADPH via a ferredoxin reductase and ferredoxin. Microsomal type II enzymes, found in the endoplasmic reticulum (ER), receive their electrons from NADPH through the intermediacy of a P450-oxidoreductase, sometimes under assistance of cytochrome b_5 .³²

Aldosterone and cortisol are synthesized starting from cholesterol by a cascade of several enzymes, many of which belong to the P450 superfamily (Figure 2).³³ The initial step is the conversion of cholesterol to pregnenolone, mediated by cholesterol desmolase CYP11A1 (side chain cleavage enzyme) at the inner mitochondrial membrane. The enzyme catalyzes three reactions including 20α -hydroxylation, 22 -hydroxylation, and cleavage of the carbon-carbon bond between C_{20} and C_{22} .³⁴ Pregnenolone returns to the cytosolic compartment and undergoes dehydrogenation of the 3β -hydroxy group and subsequent isomerization of the double bond at C_5 to afford progesterone. These reactions are carried out by the enzyme 3β -hydroxysteroid dehydrogenase (3β HSD), located on the membrane of the smooth endoplasmic reticulum. Alternatively, pregnenolone can be hydroxylated at position 17 by 17α -hydroxylase (CYP17) and subsequently transferred to 17α -hydroxyprogesterone by 3β HSD, initiating the cortisol synthesis. Progesterone and its 17 -hydroxylated derivative, which can also be synthesized from progesterone by CYP17, undergo 21 -hydroxylation by CYP21A on the smooth ER cytoplasmic surface, giving rise either to 11 -deoxycorticosterone or 11 -deoxycortisol. The synthesis of aldosterone takes place in the zona glomerulosa of the adrenal gland and involves three consecutive reactions. Aldosterone synthase (CYP11B2) initially hydroxylates 11 -deoxycorticosterone at 11β -position to yield corticosterone. Finally, two subsequent CYP11B2 catalyzed oxidations at C_{18} and water release yield the mineralocorticoid aldosterone. In the zona fasciculata of the adrenal gland, 11β -hydroxylase (CYP11B1) oxidizes its substrate 11 -deoxycortisol, giving rise to the glucocorticoid corti-

sol. A major difference of CYP11B1 compared to CYP11B2 is the lacking 18-hydroxylase activity. CYP11B1 can only introduce a hydroxy group in 11 β -position in both 11-deoxycortisol and 11-deoxycorticosterone whereas CYP11B2 can also carry out oxidations in 18-position.¹

Figure 2. Steroidogenic pathway to aldosterone and cortisol



1.1.4 Aldosterone synthase (CYP11B2) and 11 β -hydroxylase (CYP11B1), the key enzymes in corticosteroid biosynthesis

The corticosteroid synthesizing enzymes CYP11B2 and CYP11B1 are not coexpressed within the adrenal cortex. Aldosterone synthase is found only in the zona glomerulosa, 11 β -hydroxylase in the zona fasciculata. The genes encoding both enzymes are arranged in a tandem on human chromosome 8q, approximately 45 kB from each other, and their nucleotide sequences are 95 % identical in coding regions and about 90 % identical in introns.³⁵ The primary protein sequences differ only in 32 out of 503 amino acid positions and in the mature enzymes which are bound to the inner mitochondrial membrane, only 29 out of 479 residues are not identical.^{36,37} This high sequence identity (approximately 93 %) is reflected in the shared 11 β -hydroxylase function of both CYP11B isoforms. However, CYP11B1 is a pure 11 β -hydroxylase catalyst without 18-hydroxylase activity and can not even 11 β -hydroxylate 18-hydroxy-11-deoxycorticosterone.³⁸ By contrast, CYP11B2 catalyzes also oxidations at the steroidal 18-position, mainly in the course of converting corticosterone to 18-hydroxycorticosterone and subsequently to aldosterone, but it can also 18-hydroxylate cortisol. An interesting feature is the interspecies differences of these enzymes. In human and mouse, the corticoid synthesis involves two CYP11B isoforms, CYP11B1 and CYP11B2, as explained above. Bovine, pig and frog possess only a single enzyme CYP11B.³⁶ Four isoforms are present in the rat, whereof CYP11B1 and CYP11B2 are the most important. CYP11B3, expressed exclusively in neonatal rat, has the same activity as CYP11B2 and CYP11B4 encodes a pseudogene.³

In order to spot the amino acids responsible for the catalytic specificity, a series of site-directed mutagenesis experiments was performed attracting the putative I-helix. It was demonstrated by Böttner *et al.* that the aldosterone synthase activity decreases to approximately 10 % compared to the CYP11B2 wild type in the case of modifying the positions 301 (leucine to proline), 302 (glutamic to aspartic acid), and 320 (alanine to valine) whereas the 11 β -hydroxylase activity simultaneously increases. Vice versa swapping the aldosterone synthase specific amino acid at position 320 of CYP11B1 from valine to alanine induced aldosterone synthase activity without significant impact on the 11 β -hydroxylase efficacy.³⁹

A 3D structure of either CYP11B2 or CYP11B1 is presently not at hand which is referable to the common difficulties with crystallizing membrane bound proteins. However, recently established homology models provide elementary insight into the protein structures and inhibitor binding modes.^{37,40} It has been shown by our group that docking into the homology models of CYP11B2 and CYP11B1 built on the X-ray structure of human CYP2C9 is a useful tool to explain differences in activity and selectivity of nonsteroidal aldosterone synthase inhibitors.^{41,42} The binding affinity to either enzyme was found to be highly dependent to the geometry of the coordinative interaction between the heme iron and the heterocyclic nitrogen. An angle of the Fe–N straight line with the porphyrin plane close to 90° (i.e., when the heterocyclic nitrogen lone pair arranges in perpendicular position to the heme group) provides an optimal orbital overlap and corresponds with a high inhibitory potency. Any distortion of this geometry weakens the coordinative bond and hence the inhibitory potency.

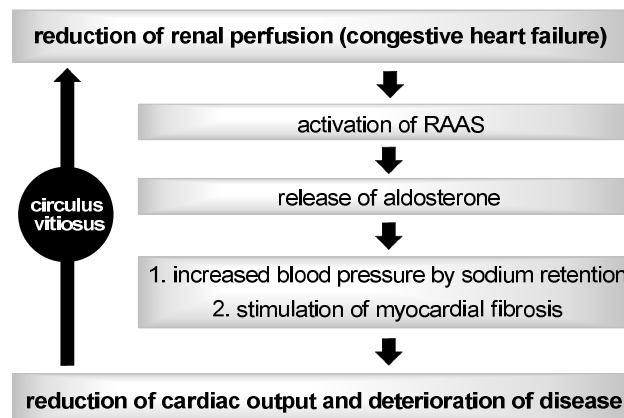
1.2 Aldosterone synthase as drug target

1.2.1 Congestive heart failure, myocardial fibrosis, and the role of aldosterone

Congestive heart failure (CHF) is a condition of insufficient cardiac output and reduced systemic blood flow, most frequently provoked by arterial hypertension and coronary artery disease, and goes along with dispnoea, fatigue and edema. The prognosis is poor: 30 % of the patients die within one year and the mortality rises to 60–70 % after five years.⁴³ The progressive nature of the disease is a consequence of a neurohormonal imbalance and involves a chronic activation of the renin-angiotensin-aldosterone system (RAAS) in response to the reduced cardiac output and the reduced renal perfusion. Aldosterone and Ang II are released excessively, leading to increased blood volume and blood pressure as a consequence of epithelial sodium retention as well as Ang II mediated vasoconstriction and finally to a further reduction of cardiac output. The RAAS is pathophysiologically stimulated in a vicious circle of neurohormonal activation that counteracts the normal negative feedback loop regulation (Figure 3). As a consequence, the aldosterone plasma levels may reach 300 ng/dL in CHF patients compared to 5–15 ng/ in normal subjects whose sodium intake is normal.⁴⁴ A decreased metabolic clearance due to reduced hepatic perfusion contributes to further aldosterone accumulation.⁴⁵

In addition to these indirect effects on the heart function, aldosterone exerts direct effects on the heart by binding to and activating nonepithelial MRs in cardiomyocytes, fibroblasts, and endothelial cells.⁴⁶ In response, aldosterone increases the expression of endothelin 1 in cardiac fibroblasts which is a growth factor stimulating collagen synthesis. As a consequence, collagen type I and type III are produced in the fibroblasts as procollagen, containing an amino-terminal and a carboxy-terminal propeptide.⁴⁷ Upon release in the extracellular space, the propeptides are cleaved by specific proteinases and the rigid collagen triple helix integrates into growing fibrils. Aldosterone may also act by increasing the endothelin receptor numbers which in turn increases the collagen synthesis.⁴⁸ In addition, Ang II, the other main effector hormone of the RAAS cascade, decreases the activity of matrix metalloproteinase 1 (MMP 1) which is the key enzyme for interstitial collagen degradation.⁴⁹ The progressive synthesis and deposition of fibrillar collagens in the fibroblasts results in myocardial fibrosis. Relatively inelastic collagen fibers stiffen the heart muscle which deteriorates the myocardial function and as a consequence enforces the neurohormonal imbalance by stimulating the RAAS. In addition to the effects of circulating aldosterone deriving from adrenal secretion, Satoh *et al.* reported that aldosterone produced locally in the heart can trigger myocardial fibrosis, too.⁵⁰ In endomyocardial tissue from CHF patients, the CYP11B2 mRNA expression was significantly increased compared to the control group, particularly in the case of advanced cardiac dysfunction. The mRNA levels correlated positively with the measured collagen volume fraction, suggesting that cardiac CYP11B2 activity has pathophysiological importance in the progression of myocardial fibrosis.

Figure 3. Pathophysiology of the renin-angiotensin-aldosterone system

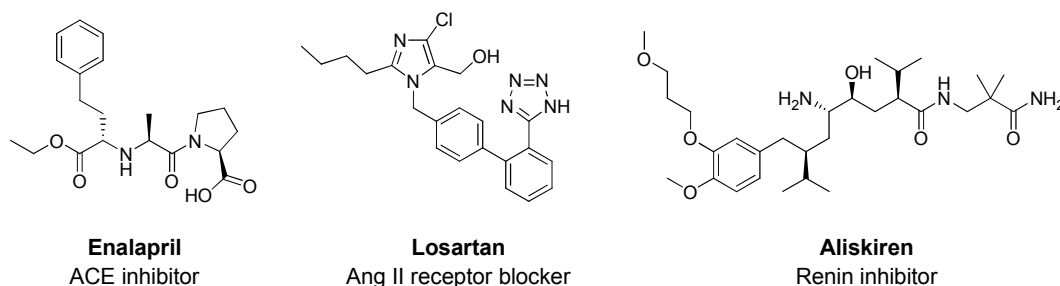


1.2.2 Significance of aldosterone receptor antagonists in cardiovascular therapy

Until today, various drug classes targeting the RAAS have been developed, acting either by inhibition of the key regulator enzymes or by blocking the actions of the effector hormones by functional antagonism, affording a successful treatment of heart failure and hypertension. The beneficial effect of inhibiting the biosynthesis of Ang II by the angiotensin converting enzyme inhibitor enalapril (Figure 4) has been shown in the CONSENSUS trial in the 1980s. The risk of mortality turned out to be reduced by 50 % within 6 months and by 46 % within 12 months upon enalapril treatment.⁵¹ However,

undesirable effects such as dry cough are observed due to potentiation of endogenous kinins. In addition, ACE independent pathways to Ang II are not blocked. Moreover, ACE inhibitors can indeed trigger an initial downregulation of circulating aldosterone, but increased levels of aldosterone may be seen after several months of therapy, presumably due to potassium stimulated secretion.⁵² This phenomenon termed ‘aldosterone escape’ is a limiting factor of ACE inhibitors and shows that novel therapeutic concepts combating the effects of elevated aldosterone levels are needed. Angiotensin II type 1 receptor blockers such as losartan (Figure 1), that were developed in the 1990s, antagonize the Ang II effects independent of their source and clearly proved to reduce mortality in heart failure but under long-term treatment, the Ang II levels are chronically elevated.⁵³ Very recently, aliskiren, the first marketed orally active renin inhibitor, co-developed by *NOVARTIS* and *SPEEDEL*, received regulatory approval by the U. S. Food and Drug Administration for the treatment of hypertension.⁵⁴ Aliskiren binds tightly and selectively to the active site of renin ($IC_{50} = 0.6$ nM) with a half-life of 20–45 h in the plasma and its efficacy and safety have been evaluated in several clinical trials.⁵⁵ Other drugs for the treatment of heart failure are beta-blockers, diuretics and digoxin. However, these drugs can not reverse cardiac fibrosis.

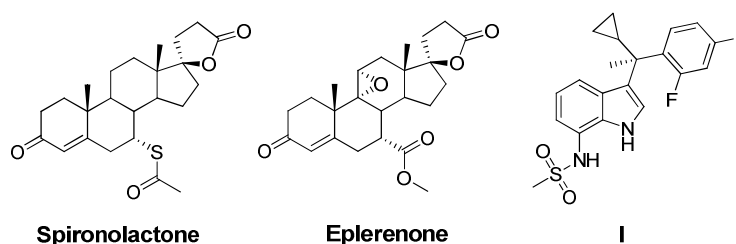
Figure 4. The RAAS targeting drugs enalapril, losartan and aliskiren



The persistence of aldosterone secretion despite treatment with ACE inhibitors and the evidence of the deleterious effects of aldosterone on cardiovascular function led to the hypothesis that blocking the mineralocorticoid receptor might provide additional benefit. In the Randomized Aldactone Evaluation Study (RALES), published in 1999, patients with moderately severe or severe congestive heart failure were treated with a 25 mg daily dose of the MR antagonist spironolactone (Figure 5) in addition to the standard therapy (ACE inhibitor, loop diuretic, digoxin) and compared to patients who received a placebo.⁵⁶ The trial was discontinued early, when the interim analysis demonstrated a reduction of mortality by 30 % and a reduction of hospitalization by 35 % compared to the placebo group. In addition, follow-up studies suggested that spironolactone treatment can not only prevent but also reverse cardiac fibrosis,⁵⁷ as reflected by reduced levels of serum procollagen type III peptides.⁵⁸ However, severe progestational and antiandrogenic side effects such as gynecomastia or menstrual disturbances were observed. *In vitro* studies revealed, that spironolactone possesses only sixfold selectivity against the androgen receptor and also activates the progesterone receptor.²⁰ Moreover, the publication of RALES was accompanied with increases in the rate of prescriptions for spironolactone and in hyperkalemia-associated morbidity and mortality.⁵⁹

In 2003, the cardioprotective effect of eplerenone (Figure 5), a more selective MR antagonist, was shown in the Eplerenone Post-acute Myocardial Infarction Heart Failure Efficacy and Survival Study (EPHESUS).⁶⁰ In the group of patients who received eplerenone (43 mg average dose daily) in addition to the standard therapy within two weeks after acute myocardial infarction, the overall mortality decreased by 15 % compared to the placebo group. Recent findings in animal models suggest that eplerenone can induce a reversal of cardiac fibrosis,⁶¹ as it has been described for spironolactone. Since eplerenone has greater selectivity for the mineralocorticoid receptor, the rate of observed endocrine side effects during the EPHESUS trial was low, although there was an increased incidence of hyperkalemia. Very recently, Bell *et al.* from *ELI LILLY* described the development of a series of indole analogues as MR antagonists.⁶² Their research culminated in the discovery of the methanesulfonamide derivative **I** (Figure 5) that shows picomolar binding affinity and *in vivo* blood pressure lowering superior to eplerenone at pharmaceutically relevant doses. Moreover, the selectivity profile of **I** against the androgen and progesterone receptor exceeds that of spironolactone and eplerenone.

Figure 5. The mineralocorticoid receptor antagonists spironolactone, eplerenone and compound **I**



1.2.3 Inhibition of CYP11B2 as promising cardiovascular therapy concept

The clinical studies with MR antagonists gave evidence for the pivotal role of aldosterone in the progression of cardiovascular diseases. Blocking the aldosterone action by functional antagonism of its receptor reduced the mortality and significantly reduced the symptoms of heart failure. Furthermore, cardiac fibrosis could not only be prevented but also reversed by use of spironolactone. However, several issues remain unsolved by this therapeutic strategy. Spironolactone binds rather unselectively to the aldosterone receptor and also has some affinity to other steroid receptors. This often results in adverse side effects during MR antagonistic therapy. Although eplerenone is more selective, clinically relevant hyperkalemia remains a principal therapy risk. Another crucial point is the high concentration of circulating aldosterone which is not lowered by MR antagonists and raises several issues. First, the elevated aldosterone plasma levels do not induce a homologous downregulation but an upregulation of the aldosterone receptor.⁶³ This fact complicates a long-term therapy as antagonists are likely to become ineffective. Furthermore, the high concentrations promote nongenomic actions of aldosterone which are in general not blocked by receptor antagonists. Pathological aldosterone concentrations have been identified to induce a negative inotropic effect in human trabeculae and to potentiate the vasocon-

strictor effect of Ang II in coronary arteries in rapid, nongenomic manner.⁶⁴ Thus, aldosterone is intrinsically capable to further deteriorate the heart function by acting nongenomically.

A novel therapy option, targeting cardiovascular diseases by interruption of the RAAS, is the blockade of aldosterone production, preferably by inhibiting CYP11B2, the key enzyme of its biosynthesis. Aldosterone synthase was proposed as a potential pharmacological target by our group as early as 1994,⁶⁵ followed soon thereafter by the hypothesis, that inhibitors of CYP11B2 could serve as drugs for the treatment of hyperaldosteronism, congestive heart failure, and myocardial fibrosis.^{66,67} This therapeutic strategy has two main advantages compared to receptor antagonism. Foremost, there is no nonsteroidal inhibitor of a steroidogenic CYP enzyme known to have affinity for a steroid receptor which is why fewer side effects on the endocrine system can be expected. Furthermore, CYP11B2 inhibition can reduce the pathologically elevated aldosterone levels, whereas interfering one step later at the receptor level leaves them unaffected. In the development process toward aldosterone synthase inhibitors, investigating the selectivity profile toward other cytochrome P450 enzymes at an early stage is a crucial point. It is known that the concept of heme-iron complexation (e.g., by nitrogen-containing heterocycles) is an appropriate strategy to discover highly potent and selective inhibitors.⁶⁸ Due to this binding mechanism, however, a putative CYP11B2 inhibitor is potentially capable of interacting with other CYP enzymes by similarly binding to the heme co-factor with its metal binding moiety. Taking into consideration that the key enzyme of glucocorticoid biosynthesis, 11 β -hydroxylase (CYP11B1), and CYP11B2 have a sequence homology of approximately 93 %, the selectivity issue is especially critical for the design of CYP11B2 inhibitors.⁶⁹

Recent experimental data presented by Fiebeler *et al.* point at the potential therapeutic utility of aldosterone synthase inhibition.¹⁹ Their studies revealed, that the *R*(+)-enantiomer of fadrozole, FAD 286A, ameliorates angiotensin II induced organ damage in transgenic rats. Fadrozole, an aromatase (CYP19) inhibitor which is used for the therapy of breast cancer, is the first described compound with ability to reduce corticoid formation.^{70,71} In their studies, Fiebeler *et al.* demonstrated, that untreated transgenic rats overexpressing both the human renin and angiotensinogen genes had a 40 % mortality rate (5/13) after 7 weeks and developed hypertension and cardiac and renal damage. FAD 286A reduced the mortality to 10 % (1/10) and also ameliorated cardiac hypertrophy. In week seven, a slight decrease of blood pressure was observed. In addition, it was shown very recently, that fadrozole reverses cardiac fibrosis in spontaneously hypertensive heart failure rats.⁷² Whether MR blockade should be preferred rather than lowering the aldosterone synthesis is a moot question and controversially debated in the literature.⁷³ The preliminary studies toward aldosterone-lowering effects in disease-oriented models, however, underline the potential therapeutic utility of aldosterone synthase inhibition. Thus, the approach to reduce aldosterone action by CYP11B2 blockade and thus tackling mineralocorticoid mediated pathologies is a promising pharmacological concept, although its clinical value still has to be proven.

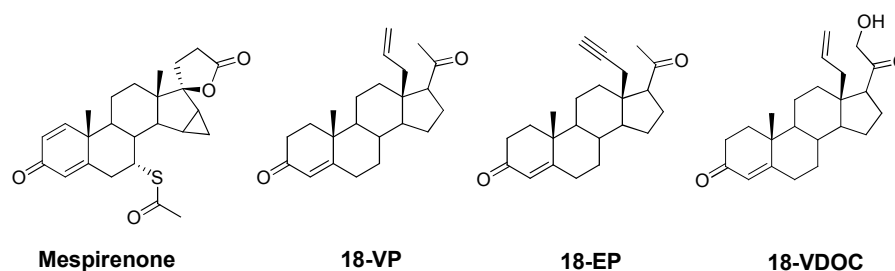
In addition to the potential therapeutic utility in cardiovascular diseases, radiolabeled ligands of CYP11B enzymes might be a useful tool for molecular imaging of CYP11B expression in adrenocortical tissue and thus for the diagnosis of adrenal tumors.⁷⁴ Due to selectively binding to CYP11B2, these compounds are also interesting for the imaging of Conn adenomas which are characterized by high expression of CYP11B2.⁷⁵

1.3 State of knowledge: Inhibitors of CYP11B2

1.3.1 Compounds with inhibitory effect on aldosterone biosynthesis

Several compounds are known to suppress the aldosterone formation. In the course of an evaluation of MR antagonists, the spironolactone derivative mespirenone (Figure 6) was found to exert an inhibitory effect on the adrenal corticosteroid synthesis. The aldosterone formation was inhibited by 40 % at a concentration of 100 μM in rat adrenal glands.⁷⁶ Among the class of steroidal compounds, progesterone and deoxycorticosterone derivatives with unsaturated C_{18} -substituents such as 18-vinylprogesterone (18-VP), 18-ethynylprogesterone (18-EP)⁷⁷ and 18-vinyldeoxycorticosterone (18-VDOC)⁷⁸ bind covalently to the bovine CYP11B enzyme. For 18-VP it was shown by difference spectroscopy that the inactivation proceeds via binding to the prosthetic heme. Catalytic oxidative activation generates a reactive intermediate which *N*-alkylates the porphyrin and as a result induces a destruction of the P450 chromophore. By this 'suicide mechanism' they block the 18-hydroxylation of corticosterone to aldosterone with K_i values in the low micromolar range.

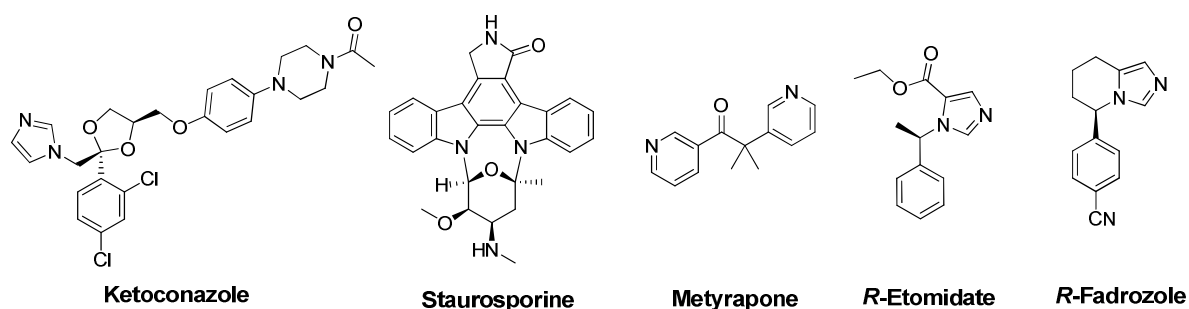
Figure 6. Steroidal compounds with inhibitory effect on aldosterone formation



Few nonsteroidal compounds have been identified as CYP11B2 inhibitors. Moderately potent inhibitors were discovered by screening azole type fungicides.⁷⁹ The most active compound of this screening turned out to be ketoconazole (Figure 7), an unspecific inhibitor of many CYP enzymes ($\text{IC}_{50} = 81 \text{ nM}$).⁴² Staurosporine, a very potent broad-range kinase inhibitor, significantly reduces the aldosterone synthase activity in V79MZh cells expressing human CYP11B2 ($\text{IC}_{50} = 11 \text{ nM}$).⁸⁰ Other compounds with well-known inhibitory action on CYP11B2 are metyrapone ($\text{IC}_{50} = 208 \text{ nM}$), a CYP11B1 inhibitor which is used in the diagnosis of Cushing's syndrome,⁸¹ *R*-etomidate ($\text{IC}_{50} = 1.7 \text{ nM}$), a clinically used anesthetic,⁸² and fadrozole which is used for the therapy of breast cancer.

Amongst the latter compounds, fadrozole is certainly the best investigated relating to aldosterone synthase inhibition. Its racemic form, CGS 16949 A, was originally designed to selectively inhibit aromatase (CYP19), the key enzyme for the conversion of adrenal androgen substrates to estrogens, for the treatment of hormone dependent breast cancer.⁸³ CYP19 is closely related to CYP11B2 as it oxidizes steroids at C₁₉ and fadrozole was accordingly found to inhibit aldosterone synthase with considerable potency *in vitro* as well.⁷⁰ Furthermore, treatment with a 16 mg daily dose led to a significant suppression of both basal and ACTH-stimulated aldosterone production in postmenopausal patients with metastatic breast cancer.⁷¹ The *R*(+)-enantiomer (Figure 7), FAD 286A, proved to be a potent and relatively specific aldosterone synthase inhibitor (CYP11B2, IC₅₀ = 6 nM; CYP11B1, IC₅₀ = 119 nM)⁴⁰ and often serves as a prototype to investigate effects of aldosterone synthase inhibition *in vivo*.^{19,72,84}

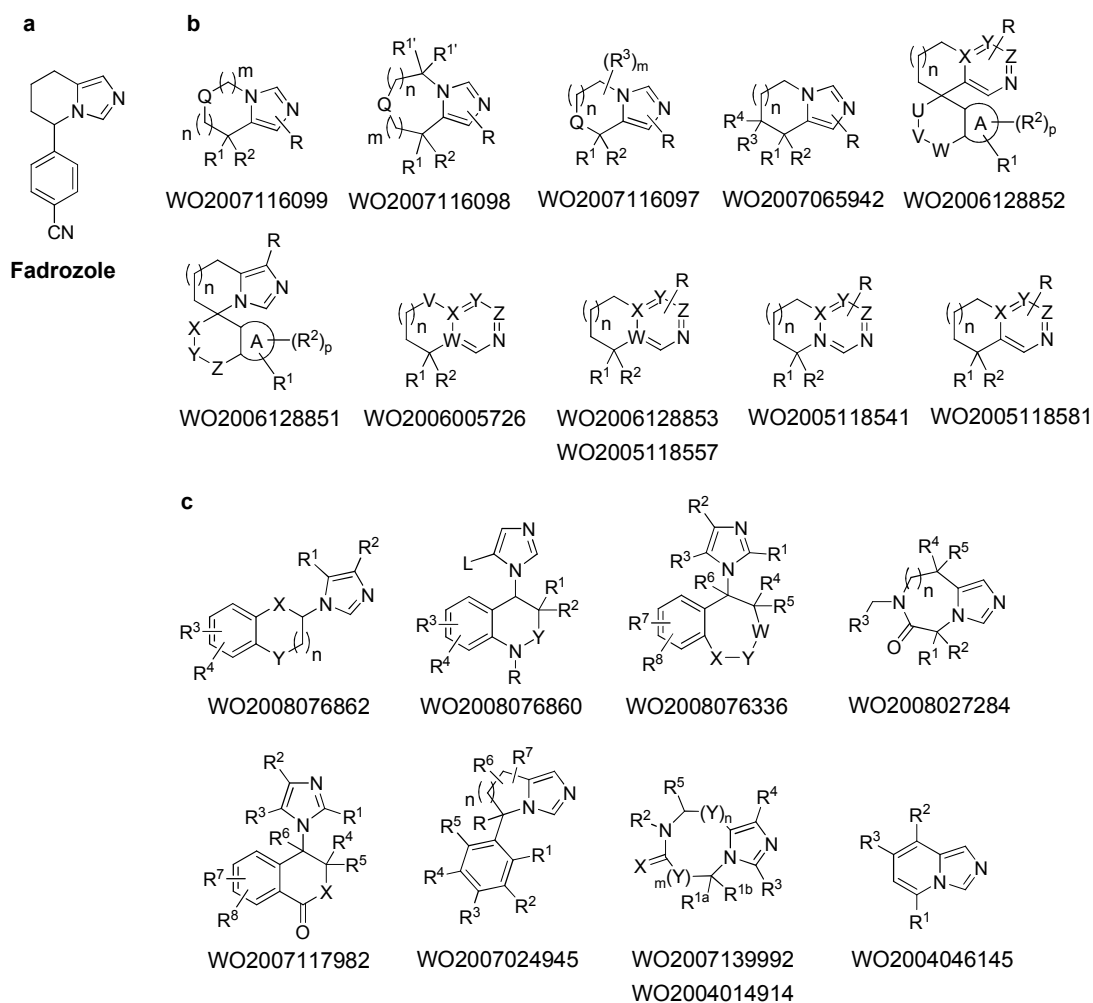
Figure 7. Nonsteroidal aldosterone synthase inhibitors



1.3.2 Further developments of the aromatase inhibitor fadrozole

Several fused heterocycles, primarily fused imidazole compounds, have been described as aldosterone synthase inhibitors in recently filed patents by *SPEEDEL*⁸⁵ and *NOVARTIS*.⁸⁶ From Figure 8 it becomes apparent, that most of these compounds are further developments of the aromatase inhibitor fadrozole (Figure 8a), consisting of a heterocycle, in most cases imidazole, condensed to a derivatized carbocycle. The carbocyclic moiety of the presented compounds has been extensively modified, for example by introduction of heteroatoms or variation of ring-size. The *para*-cyanophenyl motive of fadrozole can also be found in most of the derivatives shown in Figure 8 and is generally represented by the substituents R¹ and/or R² or by a spirocyclic connection to the bicyclic core (WO2006128852 and WO2006128851). However, some structures do not obviously derive from fadrozole. This particularly applies to recent patents of *NOVARTIS* (WO2008076862, WO2008076860, WO2008076336, and WO2007117982), that focus on dihydroisochromen-1-one and dihydroisoquinoline-1-one type inhibitors.

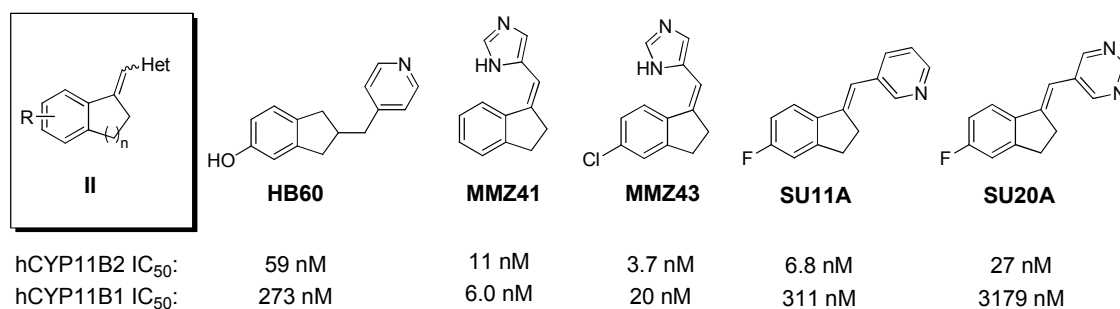
Figure 8. General structures with international publication number of nonsteroidal CYP11B2 inhibitors derived from fadrozole (a): Patents of *SPEDEL* (b) and *NOVARTIS* (c)



1.3.3 Development of heteroaryl substituted methyleneindanes and -tetrahydronaphthalenes

In our effort to identify a lead structure, that can be optimized as selective aldosterone synthase inhibitor, we performed a screening of our in-house compound library consisting of cytochrome P450 inhibitors. This search resulted in several hits. Amongst them, the hydroxylated indane derivative **HB60** (Figure 9) turned out to be of particular interest due to its strong inhibition of CYP11B2 ($IC_{50} = 59$ nM) together with slight selectivity versus CYP11B1 ($IC_{50} = 273$ nM) and no inhibition of CYP5, CYP11A1, CYP17, and CYP19.⁶⁷ Structural optimization led to imidazolyl substituted methyleneindanes and -tetrahydronaphthalenes as potent but rather unselective aldosterone synthase inhibitors such as **MMZ41** and **MMZ43** (Figure 9).⁴¹ The latter compounds have also been shown to reduce the aldosterone plasma levels *in vivo* by approximately 35–50 % in adult male rats. However, the poor selectivity makes them unsuitable drug candidates. The best compound within this series **MMZ43** displays only 5-fold selectivity versus CYP11B1 and also strongly inhibits aromatase ($IC_{50} = 39$ nM). Consecutive studies revealed that exchange of imidazole by pyridine or pyrimidine as heme complexing heterocycle clearly increases the inhibitory potency and especially the selectivity.⁴²

Figure 9. Heteroaryl (Het) substituted methyleneindanes and -tetrahydronaphthalenes (general structure **II**)

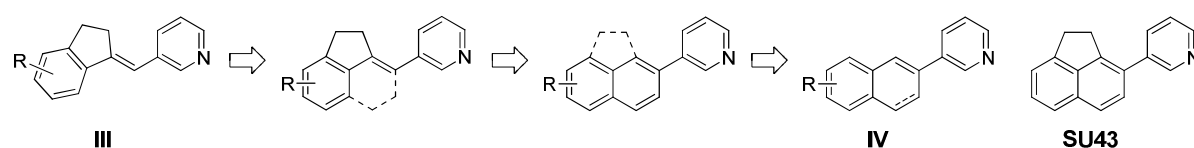


The 5-fluoro substituted *E*-methyleneindanes **SU11A** and **SU20A** (Figure 9) inhibit CYP11B2 46- and 118-fold stronger than CYP11B1. However, although the compounds are more selective toward CYP11B1 and also CYP19, several issues remain unsolved. First, compounds of the pyridyl-methyleneindane type turned out to be inhibitors of several hepatic drug-metabolizing CYP enzymes, above all CYP1A2, but also CYP2B6 and CYP2C19. Hepatic CYP enzymes are the most important catalysts for the oxidative metabolism of exogenous substrates such as drugs.⁸⁷ Inhibition of these enzymes by concomitant administration of other drugs can lead to adverse drug-drug interactions and therefore has to be avoided in either case. Furthermore, no significant lowering of aldosterone plasma levels *in vivo* could be observed in the previously used rat model. Slight variation of the lead structure which has subsequently been performed to further increase the selectivity resulted in the discovery of heteroaryl substituted naphthalenes and dihydronaphthalenes as potent and selective aldosterone synthase inhibitors.

1.3.4 Development of heteroaryl substituted naphthalenes and structurally modified derivatives

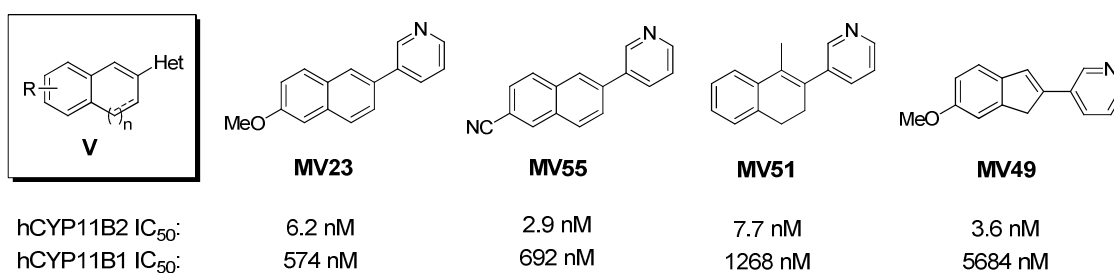
By keeping two pharmacophore points of the pyridylmethyleneindanes **III** (i.e., the aromatic ring centroid and the heterocyclic nitrogen) pyridylnaphthalenes and -dihydronaphthalenes **IV** were designed (Figure 10). The exocyclic double bond present in **III** was incorporated into a carbocycle or heterocycle (not shown) condensed to the conserved aromatic ring and the partly saturated 5-membered ring was removed to afford a naphthalene or dihydronaphthalene skeleton.^{88,89} In the corresponding acenaphthene derivatives such as **SU43**, three ring centroids are present by conserving the 5-membered ring.⁹⁰

Figure 10. Development of pyridylnaphthalenes and -dihydronaphthalenes **IV** by variation of pyridyl-methyleneindanes **III**



Structural optimization of this new lead (general structure **V** in Figure 11) revealed clear SAR. A 3-pyridine moiety as heme complexing heterocycle proved to be of high importance for a strong inhibitory potency and high selectivity toward CYP11B1. Substituents in 6-position of the naphthalene core, preferably cyano and small alkoxy residues, as accomplished in compounds **MV23** and **MV55** (Figure 11) were shown to further improve the selectivity. Some other substituents were also tolerated in terms of both activity and selectivity, e.g., 1-methyl in compound **MV51**. The indene derivative **MV49** turned out to be the most selective CYP11B2 inhibitor with a striking selectivity factor of 1500. However, these compounds exhibited no inhibitory effect on the aldosterone production *in vivo*. Another major drawback of the naphthalene and dihydronaphthalene type CYP11B2 inhibitors is a strong inhibition of the hepatic CYP1A2 enzyme that makes up approximately 10 % of the overall cytochrome P450 content in the liver and contributes to the metabolism of aromatic and heterocyclic amines as well as polycyclic aromatic hydrocarbons.⁹¹ At a concentration of 2 μM , CYP1A2 was inhibited by more than 95 %, with only a few exceptions displaying approximately 80 % inhibition which is not tolerable for a drug candidate.

Figure 11. Heteroaryl (Het) substituted naphthalenes, dihydronaphthalenes and indenes (general structure **V**)



2 Aim of the present study

2.1 Scientific objective

Pyridine substituted naphthalenes (e.g., **MV23**) and structurally related compounds constitute a class of potent inhibitors of aldosterone synthase (CYP11B2) that affect the highly homologous 11 β -hydroxylase CYP11B1 only to a minor degree (selectivity factors up to 1500). In addition, examination of availability in plasma following peroral administration of these compounds to rats showed good half-lives and reasonable to excellent plasma levels. However, these nonsteroidal inhibitors revealed two major pharmacological drawbacks: A strong inhibition of the hepatic drug metabolizing enzyme CYP1A2 and no inhibitory effect on the aldosterone production *in vivo* by using a rat model.

Hepatic CYP enzymes are the most important catalysts for the oxidative metabolism of xenobiotics, and approximately 80 % of all Phase I reactions are carried out by the CYP families 1–3. Amongst the latter, CYP1A2 makes up approximately 10 % of the overall cytochrome P450 content in the liver and mainly metabolizes amines and aromatic hydrocarbons. Inhibition of these enzymes by concomitant administration of other drugs can lead to adverse drug-drug interactions and therefore has to be avoided in either case. Hence, one major goal of the present thesis was the optimization of the selectivity profile mainly by overcoming the unwanted inhibition of hepatic CYP enzymes and CYP1A2 in particular. To achieve this goal, novel aldosterone synthase inhibitors have been designed using several rational drug design approaches.

Some highly potent and selective CYP11B2 inhibitors of the naphthalene type were investigated for their ability to reduce aldosterone levels *in vivo* using the animal model of Häusler *et al.*⁹² However, none of the investigated compounds displayed a statistically significant lowering of the aldosterone plasma levels, although being highly available in the plasma (e.g., **MV23** displays an AUC of 1753 ng·h/mL following a 5 mg/kg peroral dose). In the sequel, it has been shown in our laboratories that the lacking *in vivo* efficacy is due to species differences of the CYP11B2 enzymes (Ries *et al.*, unpublished results). The investigated molecules proved to exhibit no blockade of the aldosterone biosynthesis in V79 MZh cells expressing *rat* CYP11B2. Therefore, the present study aimed to bring forth a proof of concept by showing that a nonsteroidal *in vitro* potent CYP11B2 inhibitor has also aldosterone-lowering effects *in vivo*. To achieve this goal, the new inhibitors were routinely investigated for their ability to inhibit aldosterone formation catalyzed by the rat CYP11B2 enzyme in a

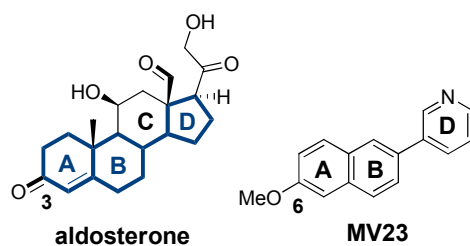
recently established assay using V79 MZh cells expressing rat CYP11B2 (unpublished) prior to *in vivo* experiments in the modified rat model of Häusler *et al.* In parallel, initial studies toward *in vivo* trials in other species were performed (e.g., *ex vivo* and pharmacokinetic investigations, unpublished).

Apart from this rather ‘pragmatic’ approach of optimizing an early lead into an *in vivo* active drug candidate, the present thesis aims to elucidate several other issues that are of major relevance for the understanding of structure activity relationships (SAR) as well as for the future design of CYP11B inhibitors. First, an extended pharmacophore model was generated following the discovery of structurally diverse molecules with inhibitory action on CYP11B2 by a compound library screening. The present work was intended to point out the scope of and thus validate the model following a pharmacophore-based synthesis project. Furthermore, docking studies in our CYP11B2 protein model were performed in order to check for consistency with the pharmacophore hypothesis. In addition, the influence of certain structural modifications on the 11 β -hydroxylase (CYP11B1) activity is of particular interest. On the one hand, CYP11B1 inhibition is an important selectivity criterion for aldosterone synthase inhibitors. On the other hand, selective CYP11B1 inhibitors could be used for the treatment of Cushing’s syndrome and metabolic syndrome. Although several potent CYP11B1 inhibitors have been described previously, in-depth SAR studies are essentially absent. In the present work, these issues were scrutinized in detail.

2.2 Working strategy: Inhibitor design concept

The preliminary studies of Voets *et al.* aiming at the design of nonsteroidal aldosterone synthase inhibitors have demonstrated, that 3-pyridine substituted naphthalenes provide an ideal molecular scaffold for a strong inhibition of the target enzyme CYP11B2 as well as high selectivity versus several other CYP enzymes (e.g., CYP11B1, CYP17, CYP19).⁸⁸ These molecules can be considered to be ABD-ring mimetics of aldosterone, imitating the AB-moiety by a naphthalene molecular scaffold and the D-ring by a 3-pyridine that binds to the heme-cofactor (Figure 12).

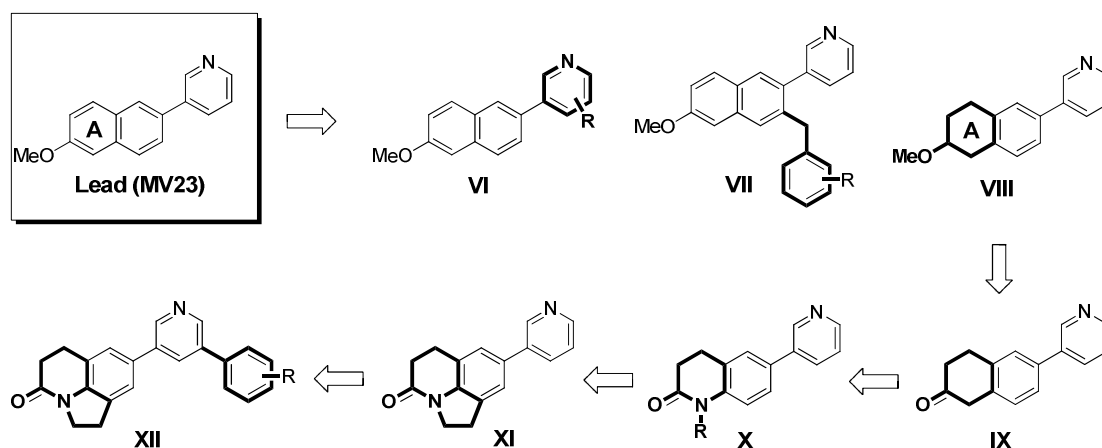
Figure 12. Chemical structures of aldosterone and the ABD-ring mimetic MV26



The previous structural optimization was focused on the carbocyclic skeleton (AB-moiety) and revealed that residues in 6-position, which obviously imitate the keto-group in the steroidal 3-position, significantly increase both activity and selectivity of the compounds. Rationalizing the obtained SAR

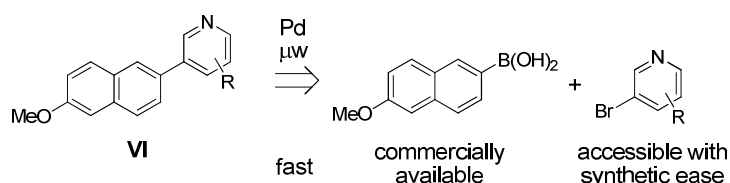
from the preliminary work, a potent aldosterone synthase inhibitor should at least exploit the following pharmacophoric features: A bicyclic core structure with a substituent in 6-position mimicking the steroidal AB-moiety and a derivative of 3-pyridine in the naphthalene 2-position imitating the D-ring to provide the appropriate molecular geometry for binding to the heme-cofactor. In the present work, pyridynaphthalene **MV23** serves as a lead structure for further structural optimization. The particular variations of the **MV23** core are outlined in Figure 13: Variation of the heterocyclic (D-ring) substitution pattern (**VI**), extension of the carbocycle by introduction of benzylic substituents into the B-ring (**VII**) and A-ring modifications giving rise to compounds with the general structures **VIII–XII**.

Figure 13. Inhibitor design concept



In the preliminary work, the substitution pattern of the AB-moiety of **MV23** has been extensively modified. The influence of substituents in the heterocyclic moiety on potency and selectivity, however, was not investigated in detail. In one subproject of the present thesis, a series of molecules (**VI**, Figure 13) bearing various substituents in the pyridine D-ring and with retained **MV23**-backbone (i.e., 6-methoxy-2-naphthyl) has been prepared following a synthesis-based strategy (Paper I). The subproject was rooted in and clearly benefited from the facile and quick synthesis, affording a considerable number of compounds over a relatively short period.⁹³ The key synthetic transformation was a microwave enhanced Suzuki coupling, starting from either commercially available or easily accessible building blocks (Figure 14). The results of these investigations are presented in Chapter 3.1.

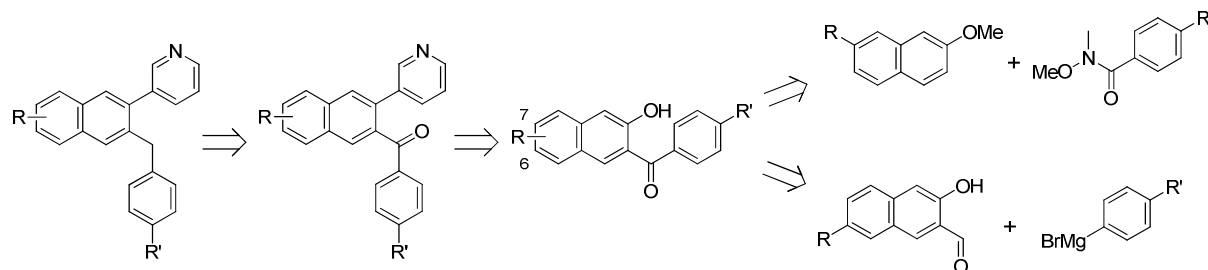
Figure 14. Synthesis of compounds with the general structure **VI**



In another subproject, novel aldosterone synthase inhibitors with extended carbocyclic skeleton (**VII**, Figure 13) were designed by a combined ligand- and structure-based approach (Paper II).⁹⁴ In our search for new lead compounds as CYP11B2 inhibitors imidazolylmethylene-substituted flavones were found to be aldosterone synthase inhibitors with moderate to high inhibitory potency by

compound library screening (for structures see Chapter 3.2). These molecules that originally have been described as aromatase inhibitors⁹⁵ display a considerable CYP11B2 inhibition, albeit without being selective toward the highly homologous CYP11B1. The chemical structures of the most potent inhibitors of this series were used for the generation of an extended pharmacophore model. The pharmacophore hypothesis led to the design of sample molecules that exploit the newly discovered pharmacophoric features (i.e., a voluminous hydrophobic area next to the heterocycle, along with two acceptor atom features) by modifying the **MV23** lead structure. Subsequently, docking studies in our CYP11B2 protein model⁴¹ were performed in order to check for spatial consistency with the pharmacophore hypothesis. It was found that 3-benzyl substituted derivatives of **MV23** such as **VII** (Figure 13) adequately fit into the binding site by exploiting a previously unexplored sub-pocket (for details of the pharmacophore modeling and docking see Chapter 3.2). Upon hit identification, a series of compounds was synthesized with the benzyl moiety being the site of major chemical modification and evaluated in several assays for biological activity. The typical synthetic procedure toward the title compounds is outlined in Figure 15 as retrosynthetic sketch. The heterocycle was introduced to the naphthalene skeleton via Pd-catalyzed cross coupling starting from a 3-benzoyl-2-naphthol derivative. This key intermediate was obtained either by *ortho*-lithiation of a 2-methoxynaphthalene derivative and subsequent addition to a Weinreb amide or by Grignard-addition of a functionalized phenyl-magnesium reagent to a 2-naphthalene-carbaldehyde derivative.

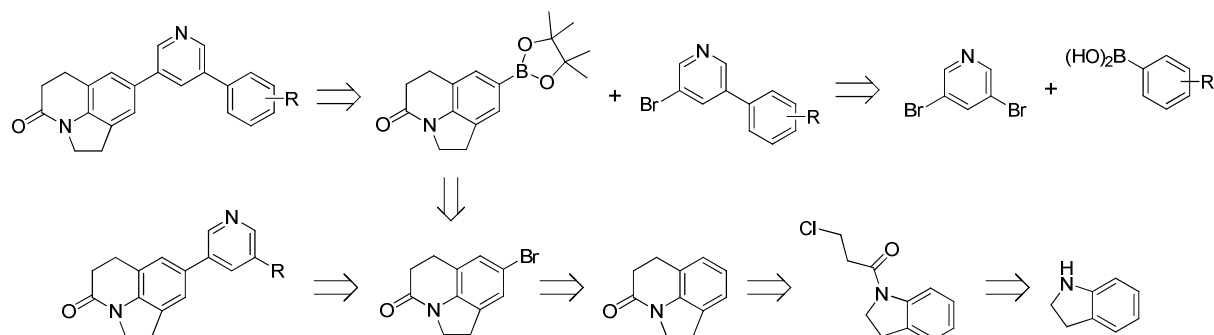
Figure 15. Synthesis of compounds with the general structure **VII**



As mentioned above, naphthalene and to a minor degree also methyleneindane type CYP11B2 inhibitors proved to be highly potent inhibitors of the hepatic drug-metabolizing enzyme CYP1A2 in an extended selectivity screening. A survey of the chemical structures revealed that these molecules largely consist of aromatic carbon atoms, thus being present in rather planar conformations. Interestingly, aromaticity has been identified to correlate positively with CYP1A2 inhibition in recent QSAR studies.⁹⁶ Furthermore, both CYP1A2 substrates and inhibitors are usually small-volume molecules with a planar shape (e.g., caffeine⁹⁷ and furafylline⁹⁸). Rationalizing these findings, our design strategy aimed at reducing the aromaticity and disturbing the planarity of the molecules while keeping the pharmacophoric points of the naphthalene molecular scaffold of **MV23** in order to reduce the CYP1A2 potency. The above considerations led to the development of pyridine substituted tetrahydronaphthalene (e.g., **VIII**, Figure 13) and tetralone (**IX**) derivatives with (partly) saturated A-ring moiety (Paper III). Bioisosteric exchange due to cytotoxic side effects of tetralone **IX** afforded a series of

highly potent and selective 3,4-dihydro-1*H*-quinolin-2-one derivatives (**X**, Paper III).⁹⁹ Rigidification of these molecules by incorporation of the lactam residue into a 5- or 6-membered ring afforded compounds with a pyrroloquinolinone or pyridoquinolinone (not shown) molecular scaffold (**XI**, Figure 13, Paper IV).¹⁰⁰ Introduction of an additional benzene moiety into the heterocycle (**XII**) was accomplished with the aid of the SAR of the preceding studies (Paper I and Paper II). Figure 16 outlines the typical synthetic procedure toward derivatives with the general structures **XI** and **XII** comprising Suzuki coupling reactions to form the biaryl bonds and Friedel Crafts cyclization reactions to synthesize the tricyclic molecular backbone as key transformations.

Figure 16. Synthesis of compounds with the general structures **XI** and **XII**



3 Results

3.1 Overcoming Undesirable CYP1A2 Inhibition of Pyridyl-naphthalene Type Aldosterone Synthase Inhibitors: Influence of Heteroaryl Derivatization on Potency and Selectivity

Ralf Heim, Simon Lucas, Cornelia M. Grombein, Christina Ries, Katarzyna E. Schewe, Matthias Negri, Ursula Müller-Vieira, Barbara Birk, and Rolf W. Hartmann

This manuscript has been published as an article in the

Journal of Medicinal Chemistry **2008**, *51*, 5064–5074.

Paper I

Abstract: Recently, we reported on the development of potent and selective inhibitors of aldosterone synthase (CYP11B2) for the treatment of congestive heart failure and myocardial fibrosis. A major drawback of these non-steroidal compounds was a strong inhibition of the hepatic drug-metabolizing enzyme CYP1A2. In the present study, we examined the influence of substituents in the heterocycle of lead structures with a naphthalene molecular scaffold to overcome this unwanted side effect. With respect to CYP11B2 inhibition, some substituents induced a dramatic increase in inhibitory potency. The methoxyalkyl derivatives **22** and **26** are the most potent CYP11B2 inhibitors up to now ($IC_{50} = 0.2$ nM). Most compounds also clearly discriminated between CYP11B2 and CYP11B1 and the CYP1A2 potency significantly decreased in some cases (e.g., isoquinoline derivative **30** displayed only 6 % CYP1A2 inhibition at 2 μ M concentration). Furthermore, isoquinoline derivative **28** proved to be capable of passing the gastrointestinal tract and reached the general circulation after peroral administration to male Wistar rats.

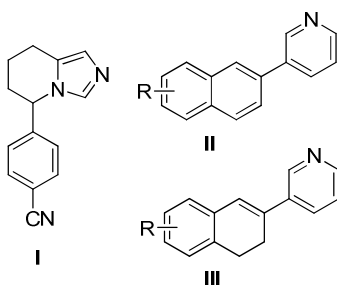
Introduction

The most important circulating mineralocorticoid aldosterone is secreted by the zona glomerulosa of the adrenal gland and is to a minor extent also synthesized in the cardiovascular system.¹ The hormone plays a key role in the electrolyte and fluid homeostasis and thus for the regulation of blood pressure. Its biosynthesis is accomplished by the mitochondrial cytochrome P450 enzyme aldosterone synthase (CYP11B2) and proceeds via catalytic oxidation of the substrate 11-deoxycorticosterone to corticosterone and subsequently to aldosterone.² The adrenal aldosterone synthesis is regulated by several physiological parameters such as the renin-angiotensin-aldosterone system (RAAS) and the plasma potassium concentration. Chronically elevated plasma aldosterone levels increase the blood pressure and are closely associated with certain forms of myocardial fibrosis and congestive heart failure.³ An insufficient renal flow chronically activates the RAAS and aldosterone is excessively released. The therapeutic benefit of reducing aldosterone effects by use of the mineralocorticoid receptor (MR) antagonists spironolactone and eplerenone has been reported in two recent clinical studies (RALES and EPHEBUS).^{4,5} The studies showed that treatment with these antagonists reduces mortality in patients with chronic congestive heart failure and in patients after myocardial infarction, respectively. Spironolactone, however, showed severe side effects presumably due to its steroidal structure.^{4,6} Although the development of non-steroidal aldosterone receptor antagonists has been reported recently,⁷ several issues associated with the unaffected and pathophysiologically elevated plasma aldosterone levels remain unsolved by this therapeutic strategy such as the up-regulation of the mineralocorticoid receptor expression⁸ and non-genomic aldosterone effects.⁹ A novel approach for the treatment of diseases affected by elevated aldosterone levels is the blockade of aldosterone biosynthesis by inhibition of CYP11B2.^{10,11} Aldosterone synthase has previously been proposed as a potential pharmacological target,¹² and preliminary work focused on the development of steroidal inhibitors, i.e., progesterone¹³ and deoxycorticosterone¹⁴ derivatives with unsaturated C₁₈-substituents. These compounds were found to be mechanism-based inhibitors binding covalently to the active site of bovine CYP11B, however, data on inhibitory action towards human enzyme are essentially absent in these studies. The strategy of inhibiting the aldosterone formation has two main advantages compared to MR antagonism. First, there is no non-steroidal inhibitor of a steroidogenic CYP enzyme known to have affinity to a steroid receptor. For this reason, fewer side effects on the endocrine system should be expected. Furthermore, CYP11B2 inhibition can reduce the pathologically elevated aldosterone levels whereas the latter remain unaffected by interfering one step later at the receptor level. By this approach, however, it is a challenge to reach selectivity versus other CYP enzymes. Taking into consideration that the key enzyme of glucocorticoid biosynthesis, 11 β -hydroxylase (CYP11B1), and CYP11B2 have a sequence homology of more than 93 %, ¹⁵ the selectivity issue becomes especially critical for the design of CYP11B2 inhibitors.

The aromatase (CYP19) inhibitor fadrozole (**I**, Chart 1) which is used in the therapy of breast cancer was found to significantly reduce the corticoid formation.¹⁶ This compound is a potent inhibitor of

CYP11B2 displaying an IC_{50} value of 1 nM (Table 1). The R(+)-enantiomer of fadrozole (FAD 286) was recently shown to reduce mortality and to ameliorate angiotensin II-induced organ damage in transgenic rats overexpressing both the human renin and angiotensinogen genes.¹⁷ These findings underline the potential therapeutic utility of aldosterone synthase inhibition, and up to now, several structurally modified fadrozole derivatives are investigated as CYP11B2 inhibitors.^{18,19} Recently, the development of imidazolyl- and pyridylmethylenetetrahydronaphthalenes and -indanes as highly active and in some cases selective CYP11B2 inhibitors has been described by our group.^{20,21} By keeping the pharmacophore and rigidization of the core structure, pyridine substituted naphthalenes²² **II** and dihydronaphthalenes²³ **III** were shown to be potent and selective CYP11B2 inhibitors (Chart 1). Combining the structural features of these substance classes to a hybrid core structure led to pyridine substituted acenaphthenes as potent CYP11B2 inhibitors with remarkable selectivity.²⁴ Furthermore, most of the naphthalene and dihydronaphthalene type compounds exhibited a favorable selectivity profile versus selected hepatic CYP enzymes. However, they turned out to be potent inhibitors of the hepatic CYP1A2 enzyme (see examples **1**, **3**, and **4** in Table 1). CYP1A2 makes up about 10 % of the overall cytochrome P450 content in the liver and metabolizes aromatic and heterocyclic amines as well as polycyclic aromatic hydrocarbons.²⁵ This experimental result turned these naphthalene type aldosterone synthase inhibitors into unsuitable drug candidates since adverse drug-drug interactions are mainly caused by inhibition of hepatic cytochrome P450 enzymes and have to be avoided in either case. In our preceding studies, the attention was focused on the optimization of the naphthalene skeleton, the substitution pattern of the heme complexing 3-pyridine moiety, however, was not investigated in detail. Herein, we describe the synthesis of a series of naphthalenes and dihydronaphthalenes with various substituents in the pyridine heterocycle to examine their influence on potency and selectivity (Table 1). The biological activity of the synthesized compounds was determined *in vitro* on human CYP11B2 for potency and human CYP11B1 and CYP1A2 for selectivity. In addition, selected compounds were tested for inhibitory activity at human CYP17 (17 α -hydroxylase-C17,20-lyase), CYP19, and selected hepatic CYP enzymes (CYP2B6, CYP2C9, CYP2C19, CYP2D6, CYP3A4). The *in vivo* pharmacokinetic profile of two promising compounds was determined in a cassette dosing experiment using male Wistar rats.

Chart 1. Non-steroidal inhibitors of CYP11B2

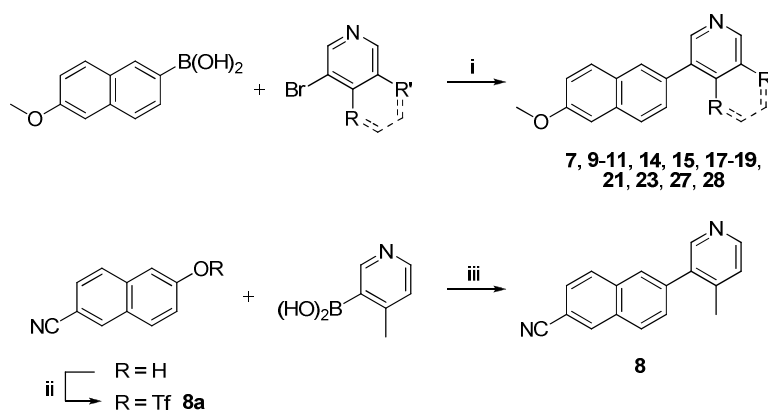


Results

Chemistry

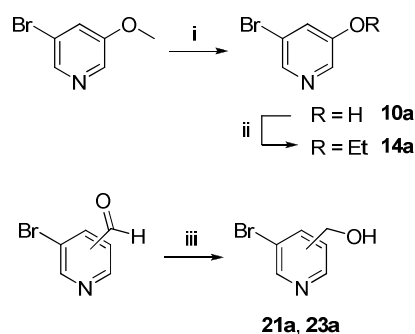
The key step for the synthesis of pyridine substituted naphthalenes was a Suzuki cross coupling (Scheme 1).²⁶ A microwave enhanced method developed by van der Eycken et al. was chosen for this purpose.²⁷ By applying this method, various substituted bromopyridines were coupled with 6-methoxy-2-naphthaleneboronic acid to afford compounds **7**, **9–11**, **14**, **15**, **17–19**, **21**, **23**, **27**, and **28**. Compound **8** was obtained by coupling of 4-methyl-3-pyridineboronic acid with triflate **8a** which was accessible by treating 6-cyano-2-naphthol with $\text{ Tf}_2\text{NPh}$ and $\text{ K}_2\text{CO}_3$ in THF under microwave irradiation.²⁸ The bromopyridines could be derivatized prior to Suzuki coupling according to Scheme 2 to provide heterocycles bearing a hydroxy, ethoxy or hydroxymethyl substituent (**10a**, **14a**, **21a**, and **23a**).²⁹

Scheme 1^a



^a Reagents and conditions: i) $\text{ Pd}(\text{PPh}_3)_4$, DMF, aq. NaHCO_3 , μw , $150\text{ }^\circ\text{C}$; ii) $\text{ Tf}_2\text{NPh}$, $\text{ K}_2\text{CO}_3$, THF, μw , $120\text{ }^\circ\text{C}$; iii) $\text{ Pd}(\text{dppf})\text{Cl}_2$, toluene/acetone, aq. $\text{ Na}_2\text{CO}_3$, μw , $150\text{ }^\circ\text{C}$.

Scheme 2^a

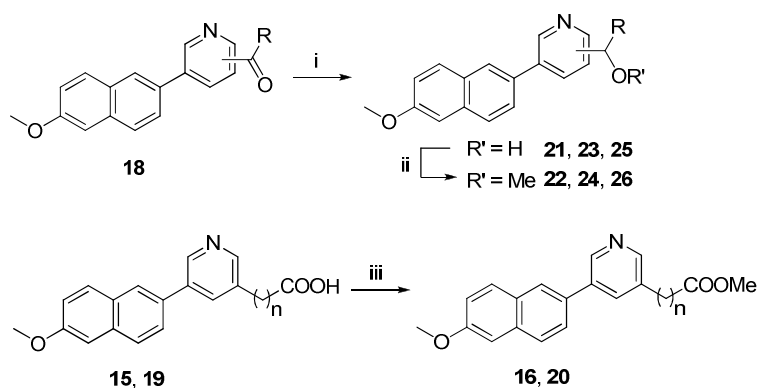


^a Reagents and conditions: i) conc. HBr , reflux; ii) EtBr , $\text{ K}_2\text{CO}_3$, DMF, rt; iii) NaBH_4 , methanol, $0\text{ }^\circ\text{C}$.

For compounds **21–26**, the substitution pattern was modified after the cross-coupling reaction as shown in Scheme 3 by sodium borohydride reduction and optional methylation. Esterification of the carboxylic acids **15** and **19** by refluxing in methanol under acid catalysis afforded the corresponding

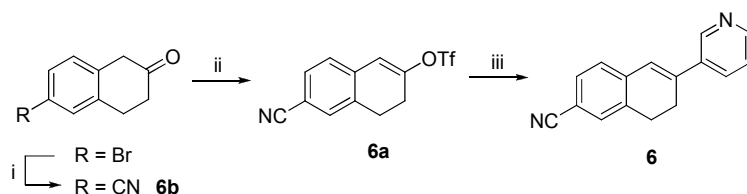
methyl esters **16** and **20**. The synthesis of 6-cyanodihydronaphthalene **6** was accomplished by the sequence shown in Scheme 4. Using 6-bromo-2-tetralone, Pd-catalyzed cyanation³⁰ led to intermediate **6b** which was transformed into the alkenyltriflate **6a** by deprotonation with KHMDS and subsequent treatment with Tf₂NPh.³¹ Compound **6a** underwent Suzuki coupling with 3-pyridineboronic acid to afford **6**.

Scheme 3^a



^a Reagents and conditions: i) NaBH₄, methanol, 0 °C; ii) MeI, NaH, THF, rt; iii) methanol, H₂SO₄, reflux.

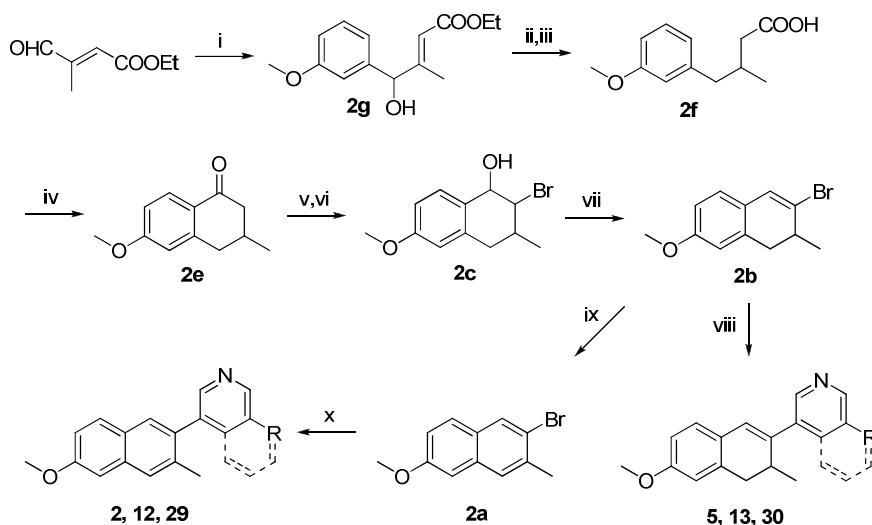
Scheme 4^a



^a Reagents and conditions: i) Zn(CN)₂, Pd(PPh₃)₄, DMF, 100 °C; ii) Tf₂NPh, KHMDS, THF/toluene, -78 °C; iii) 3-pyridineboronic acid, Pd(PPh₃)₄, DMF, aq. NaHCO₃, μw, 150 °C.

The naphthalenes **2**, **12**, **29** and the dihydronaphthalenes **5**, **13**, **30** were obtained as shown in Scheme 5. The sequence for the synthesis of intermediate **2e** was described previously and was only slightly modified by us (see supplementary material).³² Regioselective α -bromination was accomplished by treating **2e** with CuBr₂ in refluxing ethyl acetate/CHCl₃.³³ After a subsequent reduction/elimination step,²³ the intermediate alkenylbromide **2b** underwent Suzuki coupling³⁴ with the appropriate boronic acid to afford the dihydronaphthalenes **5**, **13**, and **30**. The corresponding naphthalenes **2**, **12**, and **29** were obtained by aromatization of **2b** with DDQ in refluxing toluene³⁵ followed by Suzuki coupling.²⁷ The synthesis of compounds **1**, **3**, and **4** has been reported previously by our group.^{22,23}

Scheme 5^a



^a Reagents and conditions: i) 3-methoxyphenylmagnesium bromide, THF, $-5\text{ }^{\circ}\text{C}$; ii) KOH, NaOH/water, reflux; iii) H_2 , Pd/C, AcOH, $60\text{ }^{\circ}\text{C}$; iv) $(\text{COCl})_2$, CH_2Cl_2 , rt, then AlCl_3 , CH_2Cl_2 , $-10\text{ }^{\circ}\text{C}$; v) CuBr_2 , ethyl acetate/ CHCl_3 , reflux; vi) NaBH_4 , methanol, $0\text{ }^{\circ}\text{C}$; vii) *p*-toluenesulfonic acid, toluene, reflux; viii) boronic acid, $\text{Pd}(\text{OAc})_2$, TBAB, acetone, aq. Na_2CO_3 , μw , $150\text{ }^{\circ}\text{C}$; ix) DDQ, toluene, reflux; x) boronic acid, $\text{Pd}(\text{PPh}_3)_4$, DMF, aq. NaHCO_3 , μw , $150\text{ }^{\circ}\text{C}$.

Biological Results

Inhibition of Human Adrenal Corticoid Producing CYP11B2 and CYP11B1 *In Vitro* (Table 1).

The inhibitory activities of the compounds were determined in V79 MZh cells expressing either human CYP11B2 or CYP11B1.^{10,36} The V79 MZh cells were incubated with [^{14}C]-deoxycorticosterone as substrate and the inhibitor at different concentrations. The product formation was monitored by HPTLC using a phosphoimager. Fadrozole, an aromatase (CYP19) inhibitor with proven ability to reduce corticoid formation *in vitro* and *in vivo* was used as a reference compound (CYP11B2, $\text{IC}_{50} = 1\text{ nM}$; CYP11B1, $\text{IC}_{50} = 10\text{ nM}$).¹⁶

Most of the substituted pyridyl naphthalenes showed a high inhibitory activity at the target enzyme CYP11B2 with IC_{50} values in the low nanomolar range (Table 1). Some of the compounds displayed subnanomolar potency ($\text{IC}_{50} < 1\text{ nM}$) and turned out to be even stronger aldosterone synthase inhibitors than the reference substance fadrozole. The methoxyalkyl substituted compounds **22** and **26** exhibited IC_{50} values of 0.2 nM each. Hence, they are 5-fold more active than fadrozole ($\text{IC}_{50} = 1\text{ nM}$) and 30-fold more active than the unsubstituted parent compound **1** ($\text{IC}_{50} = 6.2\text{ nM}$). However, derivatization by polar and acidic residues in 5'-position resulted in a decrease in potency. This particularly applies to the carboxylic acids **15** and **19** showing no or only low inhibitory activity and to a minor extent also to the phenolic compound **10** and the carboxamide **17** with IC_{50} values of 94 nM each.

Table 1. Inhibition of human adrenal CYP11B2, CYP11B1 and human CYP1A2 *in vitro*

compd	R ₁	R ₂	IC ₅₀ value ^a (nM)		selectivity factor ^d	% inhibition ^e CYP1A2 ^f
			V79 11B2 ^b	V79 11B1 ^c		
			hCYP11B2	hCYP11B1		
1^g	6-OMe	H	6.2	1577	254	98
2	6-OMe-3-Me	H	7.0	1047	150	93
3^g	6-CN	H	2.9	691	239	97
4^g	6-OMe	H	2.1	578	275	98
5	6-OMe-3-Me	H	3.3	248	79	73
6	6-CN	H	4.5	461	103	91
7	6-OMe	4'-Me	0.8	114	143	98
8	6-CN	4'-Me	0.6	52	87	86
9	6-OMe	4'-NH ₂	13	1521	117	58
10	6-OMe	5'-OH	94	8925	95	93
11	6-OMe	5'-OMe	4.2	238	57	91
12	6-OMe-3-Me	5'-OMe	3.8	875	230	91
13	6-OMe-3-Me	5'-OMe	1.2	100	83	18
14	6-OMe	5'-OEt	5.1	373	73	85
15	6-OMe	5'-COOH	n.a. ^h	n.d.	n.d.	n.d.
16	6-OMe	5'-COOMe	0.8	15	19	n.d.
17	6-OMe	5'-CONH ₂	94	41557	442	n.d.
18	6-OMe	5'-COMe	2.1	255	121	80
19	6-OMe	5'-CH ₂ COOH	1216	37796	31	n.d.
20	6-OMe	5'-CH ₂ COOMe	6.9	199	29	n.d.
21	6-OMe	5'-CH ₂ OH	9.1	614	68	93
22	6-OMe	5'-CH ₂ OMe	0.2	31	155	83
23	6-OMe	4'-CH ₂ OH	22	1760	80	92
24	6-OMe	4'-CH ₂ OMe	2.2	435	198	97
25	6-OMe	5'-CH(OH)Me	0.5	99	198	78
26	6-OMe	5'-CH(OMe)Me	0.2	10	50	n.d.
27	6-OMe	5'-Ph	4.8	151	32	n.d.
28	6-OMe	-	0.6	67	112	57
29	6-OMe-3-Me	-	3.1	843	272	45
30	-	-	0.5	64	128	6
fadrozole	-	-	1.0	10	10	8

^a Mean value of four experiments, standard deviation usually less than 25 %, n.d. = not determined. ^b Hamster fibroblasts expressing human CYP11B2; substrate deoxycorticosterone, 100 nM. ^c Hamster fibroblasts expressing human CYP11B1; substrate deoxycorticosterone, 100 nM. ^d IC₅₀ CYP11B1/IC₅₀ CYP11B2. ^e Mean value of two experiments, standard deviation less than 5 %; n.d. = not determined. ^f Recombinantly expressed enzyme from baculovirus-infected insect microsomes (Supersomes); inhibitor concentration, 2.0 μM; furafylline, 55 % inhibition. ^g These compounds were described previously.^{22,23} ^h n.a. = no activity (7 % inhibition at an inhibitor concentration of 500 nM).

Beside introduction of small residues in 4'- and 5'-position, an extension of the heterocyclic moiety by a condensed phenyl ring afforded the extraordinary potent isoquinoline compounds **28–30** with IC_{50} values in the range of 0.5–3.1 nM. Even the sterically demanding 5'-phenyl residue of compound **27** was still tolerated (IC_{50} = 4.8 nM). In general, changing the carbocyclic core (naphthalene, 3-methyl- or dihydro-derivative) while simultaneously keeping the substitution pattern of the heterocycle had only little effect on the CYP11B2 inhibition as shown by the series **11–13** (IC_{50} = 1.2–4.2 nM) and **28–30** (IC_{50} = 0.5–3.1 nM). With regard to the inhibitory activity at the highly homologous CYP11B1, most of the tested compounds were less active than at CYP11B2. However, a noticeable inhibition with IC_{50} values in the range of 10–100 nM was observed in some cases. In particular, the 5'-methoxyalkylpyridine derivatives **22** (IC_{50} = 31 nM) and **26** (IC_{50} = 10 nM) as well as the methyl ester **16** (IC_{50} = 15 nM) turned out to be potent CYP11B1 inhibitors. Although introduction of substituents in the heterocyclic moiety mostly resulted in a moderate decrease in selectivity compared to the unsubstituted derivatives, the selectivity factors were still high for most of the tested compounds (factor 100–200). In case of 6-methoxy-3-methylnaphthalene **2**, the introduction of substituents in the heterocyclic moiety led to an enhanced selectivity. A methoxy substituent in 5'-position as accomplished in compound **12** increased the selectivity factor from 150 to 230 and the isoquinoline derivative **29** proved to be one of the most selective CYP11B2 inhibitors of the series with a selectivity factor of 272, thus being 27-fold more selective than fadrozole (selectivity factor = 10).

Inhibition of Hepatic and Steroidogenic CYP Enzymes (Tables 1 and 2). In order to further examine the influence of heteroaryl substitution on selectivity, the compounds were tested for inhibition of the hepatic CYP1A2 enzyme. CYP1A2 was strongly inhibited by all previous CYP11B2 inhibitors of the naphthalene and dihydronaphthalene type with unsubstituted heme-coordinating heterocycle, e.g., **1–4** exhibited more than 90 % inhibition at an inhibitor concentration of 2 μ M (Table 1). With regard to the potent CYP1A2 inhibitor **1**, derivatization of the heterocycle gave rise to compounds with a slightly reduced inhibitory potency, e.g., compounds **14**, **18**, **22**, and **25** displaying approximately 80 % inhibition. A pronounced decrease of CYP1A2 inhibition was observed in case of compounds **9**, **13**, and **29–30** (6–57 %). However, the dihydronaphthalenes **6**, **13**, and **30** turned out to be chemically unstable and decomposition in DMSO solution was observed after storage at 2 °C (~80 % purity after three days) yielding considerable amounts of the aromatized analogues and traces of unidentified degradation products. Therefore, they were not taken into account for further biological evaluations despite their outstanding CYP1A2 selectivity. The CYP1A2 inhibition of some compounds was not determined at all due to either a low CYP11B2 potency (**15**, **17**, and **19**) or low CYP11B1 selectivity (**16**, **20**, **26**, and **27**).

For a set of four structurally diverse compounds (**9**, **11**, **18**, and **28**), an extended selectivity profile including inhibition of the steroidogenic enzymes CYP17 and CYP19 as well as inhibition of some crucial hepatic CYP enzymes (CYP2B6, CYP2C9, CYP2C19, CYP2D6, CYP3A4) was determined (Table 2). The inhibition of CYP17 was determined with the 50,000 g sediment of the *E. coli* homo-

genate recombinantly expressing human CYP17, progesterone (25 μM) as substrate, and the inhibitors at a concentration of 2 μM .³⁷ The tested compounds turned out to be moderately potent inhibitors of CYP17. The inhibition values ranked around 40 % corresponding with IC_{50} values of approximately 2000 nM or higher. The inhibition of CYP19 at an inhibitor concentration of 500 nM was determined *in vitro* by use of human placental microsomes and [1β - ^3H]androstenedione as substrate as described by Thompson and Siiteri³⁸ using our modification.³⁹ In this assay, no inhibition of CYP19 was observed for compounds **11**, **18**, and **28**. Only the amino substituted compound **9** displayed a moderate inhibition of 47 %. The IC_{50} values of the compounds for the inhibition of the hepatic CYP enzymes CYP1A2, CYP2B6, CYP2C9, CYP2C19, CYP2D6, and CYP3A4 were determined using recombinantly expressed enzymes from baculovirus-infected insect microsomes (Supersomes). The values of the CYP1A2 inhibition matched well the previously determined percental inhibition (Table 1). Methoxy compound **11** with 91 % inhibition at 500 nM turned out to be a potent CYP1A2 inhibitor (IC_{50} = 83 nM) whereas the inhibitory potency decreased to 488 nM in case of the ketone derivative **18**. A pronounced selectivity regarding the CYP1A2 inhibition was observed in case of compounds **9** and **28** with IC_{50} values of approximately 1.5 μM . In most cases, the other investigated CYP enzymes were unaffected, e.g., IC_{50} values of **9** were greater than 10 μM versus CYP2B6, CYP2C9, CYP2C19, CYP2D6, and CYP3A4.

Table 2. Inhibition of selected steroidogenic and hepatic CYP enzymes *in vitro*

compd	% inhibition ^a		IC_{50} value ^b (nM)					
	CYP17 ^c	CYP19 ^d	CYP1A2 ^{e,f}	CYP2B6 ^{e,g}	CYP2C9 ^{e,h}	CYP2C19 ^{e,i}	CYP2D6 ^{e,j}	CYP3A4 ^{e,k}
9	42	47	1420	> 50000	48970	45800	11100	21070
11	41	14	83	> 25000	1888	> 25000	> 25000	1913
18	36	< 5	488	> 50000	> 200000	> 200000	> 200000	9070
28	39	7	1619	16540	1270	3540	33110	3540

^a Mean value of four experiments, standard deviation less than 10 %. ^b Mean value of two experiments, standard deviation less than 5 %. ^c *E. coli* expressing human CYP17; substrate progesterone, 25 μM ; inhibitor concentration 2.0 μM ; ketoconazole, IC_{50} = 2780 nM. ^d Human placental CYP19; substrate androstenedione, 500 nM, inhibitor concentration 500 nM; fadrozole, IC_{50} = 30 nM. ^e Recombinantly expressed enzymes from baculovirus-infected insect microsomes (Supersomes). ^f Furafylline, IC_{50} = 2419 nM. ^g Tranylcypromine, IC_{50} = 6240 nM. ^h Sulfaphenazole, IC_{50} = 318 nM. ⁱ Tranylcypromine, IC_{50} = 5950 nM. ^j Quinidine, IC_{50} = 14 nM. ^k Ketoconazole, IC_{50} = 57 nM.

Pharmacokinetic Profile of Compounds 1, 9, and 28 (Table 3). The pharmacokinetic profile of compounds **9** and **28** was determined after peroral application to male Wistar rats and compared to the unsubstituted parent compound **1**. After administration of a 5 mg/kg dose in a cassette (N = 5), plasma samples were collected over 24 h and plasma concentrations were determined by HPLC-MS/MS. Fadrozole which was used as a reference compound displayed the highest plasma levels ($\text{AUC}_{0-\infty}$ = 3575 ng·h/mL), followed by **1** (1544 ng·h/mL) and **28** (762 ng·h/mL). At all sampling points, the amounts of **9** detected were found below the limit of quantification (1.5 ng per mL plasma). This experimental result may be either due to a fast metabolism of the aromatic amine or due to a lacking ability of this compound to permeate the cell membrane under physiological conditions. The half-lives were between 2.2–5.4 h in which the elimination of fadrozole occurs faster than the elimination of the

naphthalenes **1** and **28**. Compound **28** is slowly absorbed as indicated by the t_{\max} of 6 h whereas **1** is absorbed as fast as fadrozole ($t_{\max} = 1$ h). Furthermore, no obvious sign of toxicity was noted in any animal over the duration of the experiment (24 h).

Table 3. Pharmacokinetic profile of compounds **1**, **9**, and **28**

compd ^a	$t_{1/2z}$ (h) ^b	t_{\max} (h) ^c	C_{\max} (ng/mL) ^d	$AUC_{0-\infty}$ (ng·h/mL) ^e
1	5.4	1.0	222	1544
9	n.d. ^f	n.d. ^f	< 1.5 ^g	n.d. ^f
28	3.2	6.0	81	762
fadrozole	2.2	1.0	454	3575

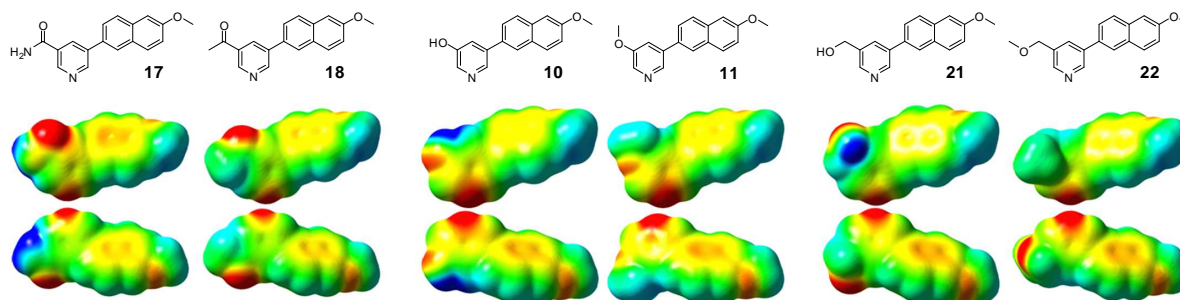
^a All compounds were applied perorally at a dose of 5 mg per kg body weight in four different cassette dosing experiments using male Wistar rats. ^b Terminal half-life. ^c Time of maximal concentration. ^d Maximal concentration. ^e Area under the curve. ^f n.d. = not detectable. ^g Below the limit of quantification.

Discussion and Conclusion

The results obtained in the present study revealed that a variety of substituents in 4'- and 5'-position is tolerated with regard to the CYP11B2 potency. Most of the tested compounds were more potent than the unsubstituted parent compounds and IC_{50} values less than 1 nM were observed in 7 cases (e.g., **22** and **26**, $IC_{50} = 0.2$ nM). Some of the compounds were also potent CYP11B1 inhibitors (e.g., **26**, $IC_{50} = 10$ nM). Interestingly, a precise relationship between the inhibition of CYP11B2 and CYP11B1 was observed: An increased or decreased inhibitory activity at the one enzyme was accompanied by an increased or decreased inhibitory activity at the other enzyme. For instance, based on the unsubstituted parent compound **1**, introduction of the methoxyalkyl substituent in compound **26** resulted in an enhanced inhibition of both CYP11B2 ($IC_{50} = 0.2$ nM) and CYP11B1 ($IC_{50} = 10$ nM), whereas introduction of the hydroxy group in compound **10** resulted in a decreased inhibitory potency at both CYP11B isoforms in a comparable order of magnitude (CYP11B2, $IC_{50} = 94$ nM; CYP11B1, $IC_{50} = 8925$ nM). This trend becomes particularly evident when plotting the CYP11B2 versus the CYP11B1 pIC_{50} values of the compounds presented in Table 1 revealing a reasonable linear correlation ($r^2 = 0.86$, $n = 29$). The finding that it is to some extent possible to change the inhibitory potency by the heteroaryl derivatization without significantly changing the selectivity versus either CYP11B2 or CYP11B1 is an indication that the inhibitor binding proceeds via similar protein-inhibitor interactions of the heterocyclic moiety with both CYP11B isoforms. Contrariwise, it has been shown earlier by us that variation of the carbocyclic skeleton instead of the heterocycle can significantly influence the selectivity. Therefore, no correlation is observed for a plot of the CYP11B2 and CYP11B1 pIC_{50} values of the naphthalenes²² and dihydronaphthalenes²³ described previously by us that are functionalized with an unsubstituted 3-pyridine as heme complexing heterocycle ($r^2 = 0.30$, $n = 20$). Consistent with these findings, it can be assumed that both enzymes, CYP11B2 and CYP11B1, are structurally more diverse in the naphthalene binding site than in the heterocyclic binding site. Interesting structure-activity relationships could also be observed with respect to electronic properties. Compounds bearing protic substituents in 5'-position rather poorly inhibited

CYP11B2 whereas bioisosteric exchange by aprotic residues gave rise to highly potent aldosterone synthase inhibitors, e.g., the inhibitory potency increased by a factor of 40 from carboxamide **17** ($IC_{50} = 94$ nM) to the ethanone **18** ($IC_{50} = 2.1$ nM). A comparable increase of potency was observed when the protic hydroxy group was replaced by the aprotic methoxy group, e.g., the IC_{50} value decreased by a factor of 20 in case of compound **11** compared to the phenol **10** or by a factor of 40 in case of compound **22** compared to the primary alcohol **21**. Similarly, the methyl esters **16** and **20** were more active than the corresponding carboxylic acids **15** and **19**. However, a lack of membrane permeability must be taken into consideration as an alternative explanation. Figure 1 shows the molecular electrostatic potentials (MEP) mapped on the electron density surface of compounds **17**, **10**, and **21** and their bioisosteric analogues **18**, **11**, and **22**. Both the shape and the geometry of the compounds as well as the electrostatic potential distribution in the naphthalene moiety are very similar. In addition, all compounds contain a region in which the nitrogen of the pyridine ring presents a negative potential. However, areas with a distinct positive potential in the pyridine moiety are present in compounds **17**, **10**, and **21** showing low inhibitory potency. In case of the highly potent bioisosters, these areas display less positive potential values with a more uniformly distributed electron charge. Hence, the difference in the electrostatic potential distribution is a reasonable explanation for the varying binding behavior within this set of compounds.

Figure 1^a



^a MEP of compounds **17**, **18**, **10**, **11**, **21**, and **22** (front and back view). The electrostatic potential surfaces were plotted with GaussView 3.0 in a range of -18.83 kcal/mol (red) to $+21.96$ kcal/mol (blue).

The heteroaryl derivatization had also a noticeable influence on the CYP1A2 potency of the compounds. Most of the substituted derivatives were still inhibiting CYP1A2 for more than 90 % at a concentration of 2 μ M. With respect to the compounds with a 6-methoxynaphthalene core, a slight decrease to approximately 80 % inhibition was observed in some cases. This effect was due to the introduction of substituents in 5'-position of the heterocycle. While no decrease of CYP1A2 inhibition was observed in case of the rather small substituents in compounds **10**, **11**, and **21** (hydroxy, methoxy, and hydroxymethyl), a slight increase of the sterical bulk in compounds **14**, **18**, **22**, and **25** (ethoxy, acetyl, methoxymethyl, and hydroxyethyl) resulted in a decrease in CYP1A2 inhibition to 78–85 %. On the other hand, some derivatives proved to be significantly less active with approximately 50 % inhibition of CYP1A2, including the 4'-amino-substituted compound **9** and the isoquinoline **28** with

IC₅₀ values of 1420 nM and 1619 nM, respectively. The effect of changing 3-pyridine by 4-isoquinoline as heme-complexing heterocycle is particularly noteworthy. The three isoquinoline derivatives **28**, **29**, and **30** are considerably less active at CYP1A2 (6–57 % inhibition) than their unsubstituted analogues **1**, **2**, and **5** (73–98 % inhibition). An explanation might be found in the geometry of these molecules. The isoquinoline constrains the rotation around the carbon–carbon bond between the heterocycle and the naphthalene, especially in presence of the additional *ortho*-methyl groups in **29** and **30**. Thus, a coplanar conformation becomes energetically disfavored compared to the pyridine analogues and the sterically demanding heterocycle rotates out of the naphthalene plane. This loss of planarity is a reasonable explanation for the reduced inhibitory potency since both CYP1A2 substrates and inhibitors are usually small-volume molecules with a planar shape (e.g., caffeine⁴⁰ and furafylline⁴¹). An even more drastic effect on the CYP1A2 potency was observed in case of the dihydronaphthalene type compounds. While the unsubstituted parent compound **5** exhibited 74 % inhibition, introduction of the methoxy substituent in compound **13** led to a reduction to 18 % and the isoquinoline derivative **30** displayed only 6 % inhibition. The partly saturated core structure becomes flexible and disturbs the planarity. Factors other than steric might play an additional role for the decreased CYP1A2 inhibition, e.g., disturbed π - π -stacking contacts with aromatic amino acids in the CYP1A2 binding pocket due to the reduced number of aromatic carbons. Aromaticity has been identified to correlate positively with CYP1A2 inhibition in recent QSAR studies.⁴² As dihydronaphthalenes **13** and **30** were found to be unstable in DMSO solution, the low potencies might be due to substance degradation. However, the decomposition (~20 % after three days) afforded mainly the aromatized naphthalene analogues, i.e., **12** and **29** both displaying higher CYP1A2 inhibition than **13** and **30**.

In conclusion, we have shown that modifying the lead compounds **I** and **II** by introduction of substituents in the heterocyclic moiety has a clear effect on the activity and selectivity profile. Some substituents induced a significant increase in inhibitory potency versus CYP11B2. Compounds **22** and **26** with subnanomolar IC₅₀ values are the most potent aldosterone synthase inhibitors so far. The undesirable high CYP1A2 inhibition that is present in the previously investigated derivatives could be overcome by certain residues, giving rise to compounds with an advantageous overall selectivity profile. It was also demonstrated that the naphthalene type aldosterone synthase inhibitors **1** and **28** were able to cross the gastrointestinal tract and reached the general circulation. Presently, the elucidated concepts are used to systematically modify other lead structures whereof some are under investigation for their ability to reduce aldosterone levels *in vivo*.

Experimental Section

Chemical and Analytical Methods. Melting points were measured on a Mettler FP1 melting point apparatus and are uncorrected. ¹H NMR and ¹³C spectra were recorded on a Bruker DRX-500 instrument. Chemical shifts are given in parts per million (ppm), and tetramethylsilane (TMS) was used as internal standard for spectra obtained in DMSO-*d*₆ and CDCl₃. All coupling constants (*J*) are

given in hertz. Mass spectra (LC/MS) were measured on a TSQ Quantum (Thermo Electron Corporation) instrument with a RP18 100-3 column (Macherey Nagel) and with water/acetonitrile mixtures as eluents. Elemental analyses were carried out at the Department of Chemistry, University of Saarbrücken. Reagents were used as obtained from commercial suppliers without further purification. Solvents were distilled before use. Dry solvents were obtained by distillation from appropriate drying reagents and stored over molecular sieves. Flash chromatography was performed on silica gel 40 (35/40–63/70 μM) with hexane/ethyl acetate mixtures as eluents, and the reaction progress was determined by thin-layer chromatography analyses on Alugram SIL G/UV254 (Macherey Nagel). Visualization was accomplished with UV light and KMnO_4 solution. All microwave irradiation experiments were carried out in a CEM-Discover monomode microwave apparatus.

The following compounds were prepared according to previously described procedures: 6-Methoxy-3-methyl-3,4-dihydronaphthalen-1(2*H*)-one (**2e**),³² (*E*)-4-hydroxy-4-(3-methoxyphenyl)-3-methyl-2-butenic acid (**2g**),³² 5-bromopyridin-3-ol (**10a**).²⁹

Synthesis of the Target Compounds

Procedure A.²⁷ Pyridine boronic acid (0.75 mmol, 1 equivalent), aryl bromide or -triflate (0.9–1.3 equivalents), and tetrakis(triphenylphosphane)palladium(0) (43 mg, 37.5 μmol , 5 mol %) were suspended in 1.5 mL DMF in a 10 mL septum-capped tube containing a stirring magnet. To this was added a solution of NaHCO_3 (189 mg, 2.25 mmol, 3 equivalents) in 1.5 mL water and the vial was sealed with a Teflon cap. The mixture was irradiated with microwaves for 15 min at a temperature of 150 °C with an initial irradiation power of 100 W. After the reaction, the vial was cooled to 40 °C, the crude mixture was partitioned between ethyl acetate and water and the aqueous layer was extracted three times with ethyl acetate. The combined organic layers were dried over MgSO_4 and the solvents were removed in vacuo. The coupling products were obtained after flash chromatography on silica gel (petroleum ether/ethyl acetate mixtures) and/or crystallization. If an oil was obtained, it was transferred into the hydrochloride salt by 1N HCl solution in diethyl ether.

Procedure B.³⁴ In a microwave tube alkenyl bromide **7** (1 equivalent), pyridine boronic acid (1.3 equivalent), tetrabutylammonium bromide (1 equivalent), sodium carbonate (3.5 equivalents) and palladium acetate (1.5 mol %) were suspended in water/acetone 3.5/3 to give a 0.15 M solution of bromide **7** under an atmosphere of nitrogen. The septum sealed vessel was irradiated under stirring and simultaneous cooling for 15 min at 150 °C with an initial irradiation power of 150 W. The reaction mixture was cooled to room temperature, diluted with a saturated ammonium chloride solution and extracted several times with diethyl ether. The combined extracts were washed with brine, dried over MgSO_4 , concentrated and purified by flash chromatography on silica gel. The resulting oil was transferred into the hydrochloride salt by a 5-6 N HCl solution in 2-propanol and crystallized from ethanol.

Procedure C. To a suspension of NaH (1.15 equivalents, 60 % dispersion in oil) in 5 mL dry THF at was added dropwise a solution of alcohol (1 equivalent) in 5 mL THF at room temperature under an atmosphere of nitrogen. After hydrogen evolution ceased, a solution of methyl iodide (3.3 equivalents) in 5 mL THF was added dropwise, and the resulting mixture was stirred for 5 h at room temperature. The mixture was then treated with saturated aqueous NH₄Cl solution and extracted three times with ethyl acetate. The combined organic layers were washed with water and brine, dried over MgSO₄ and the solvent was evaporated in vacuo. The crude product was flash chromatographed on silica gel (petroleum ether/ethyl acetate mixtures) to afford the pure methylether. If an oil was obtained, it was transferred into the hydrochloride salt by 1N HCl solution in diethyl ether.

Procedure D. To a 0.05 M solution of carbonyl compound in dry methanol was added sodium borohydride (2 equivalents). The reaction mixture was stirred for 1 h, diluted with diethylether and treated with saturated aqueous NaHCO₃ solution. The mixture was then extracted three times with ethyl acetate, washed twice with saturated aqueous NaHCO₃ solution and once with brine and dried over MgSO₄. The filtrate was concentrated in vacuo, and the residue was filtered through a short pad of silica gel or flash chromatographed on silica gel (petroleum ether/ethyl acetate mixtures) to afford the corresponding alcohols.

3-(6-Methoxy-3-methylnaphthalen-2-yl)pyridine (2) was obtained according to procedure A starting from **2a** (377 mg, 1.50 mmol) and 3-pyridineboronic acid (240 mg, 1.95 mmol) after flash chromatography on silica gel (petroleum ether/ethyl acetate, 4/1, $R_f = 0.16$) as a white solid (304 mg, 1.22 mmol, 81 %), mp 106–107 °C. MS m/z 250.06 (MH⁺). Anal. (C₁₇H₁₅NO) C, H, N.

3-(6-Methoxy-3-methyl-3,4-dihydronaphthalen-2-yl)pyridine (5) was obtained according to procedure B starting from **2b** (127 mg, 0.50 mmol) and 3-pyridineboronic acid (80 mg, 0.65 mmol) after flash chromatography on silica gel (petroleum ether/ethyl acetate, 4/1, $R_f = 0.20$), precipitation as HCl salt and crystallization from ethanol as a white solid (50 mg, 0.17 mmol, 35 %), mp (HCl salt) 186–187 °C. MS m/z 252.02 (MH⁺). Anal. (C₁₇H₁₇NO·HCl·0.2H₂O) C, H, N.

6-(Pyridin-3-yl)-7,8-dihydronaphthalene-2-carbonitrile (6) was prepared according to procedure A starting from 3-pyridineboronic acid (107 mg, 0.87 mmol) and **6a** (189 mg, 0.62 mmol). After flash chromatography on silica gel (petroleum ether/ethyl acetate, 2/1, $R_f = 0.10$) pure **6** was obtained as a white, crystalline solid (100 mg, 0.43 mmol, 69 %). Treatment with hydrochloric acid (0.1 N in Et₂O) yielded the hydrochloride salt of **6** (110 mg, 0.41 mmol, 66 %) as a white solid, mp (HCl salt) 264–268 °C. MS m/z 223.23 (MH⁺). Anal. (C₁₆H₁₂N₂·HCl·0.4H₂O) C, H, N.

3-(6-Methoxynaphthalen-2-yl)-4-methylpyridine (7) was prepared according to procedure A starting from 6-methoxy-2-naphthaleneboronic acid (131 mg, 0.65 mmol) and 3-bromo-4-methylpyridine (86 mg, 0.50 mmol). After flash chromatography on silica gel (petroleum ether/ethyl acetate, 7/3, $R_f = 0.10$) pure **7** was obtained as a white solid (65 mg, 0.26 mmol, 52 %), mp (HCl salt) 172–174 °C. MS m/z 250.30 (MH⁺). Anal. (C₁₇H₁₅NO·HCl·0.1H₂O) C, H, N.

6-(4-Methylpyridin-3-yl)-2-naphthonitrile (8). Triflate **8a** (151 mg, 0.50 mmol), 4-methyl-3-pyridineboronic acid (89 mg, 0.65 mmol), K_2CO_3 (138 mg, 1.0 mmol) and $Pd(dppf)Cl_2$ (37 mg, 0.05 mmol) were suspended in 4.0 mL of a 4:4:1 mixture of toluene/acetone/water. This mixture was heated to 125 °C by microwave irradiation for 15 minutes (initial irradiation power 150 W). After cooling to room temperature, 15 mL of distilled water were added and the reaction mixture was extracted four times with 10 mL of Et_2O . After washing the combined organic fractions with water (twice) and brine, drying over $MgSO_4$ and evaporation of the solvent crude product **8** was obtained as a yellow solid (127 mg). Further purification by flash chromatography on silica gel (petroleum ether/ethyl acetate, 2/5, $R_f = 0.20$) and subsequent crystallization of the free base as hydrochloride salt gave 52 mg (0.19 mmol, 37 %) of pure **8** (HCl salt) as a yellowish solid, mp (HCl salt) decomposition above 210 °C. MS m/z 245.30 (MH^+). Anal. ($C_{17}H_{12}N_2 \cdot HCl \cdot 0.5H_2O$) C, H, N.

3-(6-Methoxynaphthalen-2-yl)pyridin-4-amine (9) was prepared according to procedure A starting from 6-methoxy-2-naphthaleneboronic acid (131 mg, 0.65 mmol) and 3-bromopyridin-4-amine (86 mg, 0.50 mmol). After crystallization from acetone pure **9** was obtained as a white solid (39 mg, 0.16 mmol, 31 %), mp 155–156 °C. MS m/z 251.28 (MH^+). Anal. ($C_{16}H_{14}N_2O$) C, H, N.

5-(6-Methoxynaphthalen-2-yl)pyridin-3-ol (10) was prepared according to procedure A starting from 6-methoxy-2-naphthaleneboronic acid (131 mg, 0.65 mmol) and **10a** (87 mg, 0.50 mmol). After crystallization from acetone/diethyl ether pure **10** was obtained as an off-white solid (86 mg, 0.34 mmol, 68 %), mp 172–175 °C. MS m/z 252.02 (MH^+). Anal. ($C_{16}H_{13}NO_2 \cdot 0.7H_2O$) C, H, N: calcd, 5.31, found, 5.79.

3-Methoxy-5-(6-methoxynaphthalen-2-yl)pyridine (11) was prepared according to procedure A starting from 6-methoxy-2-naphthaleneboronic acid (131 mg, 0.65 mmol) and 3-bromo-5-methoxypyridine (94 mg, 0.50 mmol). After flash chromatography on silica gel (petroleum ether/ethyl acetate, 7/3, $R_f = 0.10$) pure **11** was obtained as a white solid (80 mg, 0.30 mmol, 60 %), mp (HCl salt) 211–214 °C. 1H -NMR (500 MHz, CD_3OD): $\delta = 3.96$ (s, 3H), 4.15 (s, 3H), 7.23 (dd, $^3J = 9.1$ Hz, $^4J = 2.5$ Hz, 1H), 7.32 (d, $^4J = 2.2$ Hz, 1H), 7.85 (dd, $^3J = 8.5$ Hz, $^4J = 1.9$ Hz, 1H), 7.92 (d, $^3J = 8.8$ Hz, 1H), 7.97 (d, $^3J = 8.5$ Hz, 1H), 8.29 (d, $^4J = 1.5$ Hz, 1H), 8.52 (s, 1H), 8.54 (s, 1H), 8.86 (s, 1H). ^{13}C -NMR (125 MHz, CD_3OD): $\delta = 57.9, 58.3, 108.5, 120.9, 121.9, 128.1, 128.5, 130.2, 131.4, 132.5, 134.5, 136.7, 138.9, 139.1, 142.6, 158.4, 160.4$. MS m/z 266.26 (MH^+). Anal. ($C_{17}H_{15}NO_2 \cdot HCl \cdot 0.3H_2O$) C, H, N.

3-Methoxy-5-(6-methoxy-3-methylnaphthalen-2-yl)pyridine (12) was obtained according to procedure A starting from **2a** (377 mg, 1.50 mmol) and 5-methoxy-3-pyridineboronic acid (298 mg, 1.95 mmol) after flash chromatography on silica gel (petroleum ether/ethyl acetate, 3/1, $R_f = 0.16$) as a white solid (328 mg, 1.17 mmol, 78 %), mp 106–107 °C. 1H -NMR (500 MHz, $CDCl_3$): $\delta = 2.40$ (s, 3H), 3.91 (s, 3H), 3.94 (s, 3H), 7.12 (m, 2H), 7.23 (dd, $^4J = 2.8$ Hz, $^4J = 1.9$ Hz, 1H), 7.62 (s, 1H), 7.64 (s, 1H), 7.71 (d, $^3J = 8.8$ Hz, 1H), 8.28 (d, $^4J = 1.9$ Hz, 1H), 8.33 (d, $^4J = 2.8$ Hz, 1H). ^{13}C -NMR (125

MHz, CDCl₃): δ = 21.0, 55.3, 55.6, 104.9, 118.6, 121.5, 127.4, 127.5, 128.6, 129.2, 134.1, 134.4, 134.5, 135.8, 138.0, 142.6, 155.2, 158.1. MS m/z 280.08 (MH⁺). Anal. (C₁₈H₁₇NO₂) C, H, N.

3-Methoxy-5-(6-methoxy-3-methyl-3,4-dihydronaphthalen-2-yl)pyridine (13) was obtained according to procedure B starting from **2b** (253 mg, 1.00 mmol) and 5-methoxy-3-pyridineboronic acid (199 mg, 1.30 mmol) after flash chromatography on silica gel (petroleum ether/ethyl acetate, 4/1, R_f = 0.14), precipitation as HCl salt and crystallization from ethanol as a yellow solid (84 mg, 0.26 mmol, 26 %), mp (HCl salt) 181–182 °C. ¹H-NMR (500 MHz, CD₃OD): δ = 0.94 (d, ³ J = 7.0 Hz, 3H), 2.71 (dd, ² J = 15.3 Hz, ³ J = 1.2 Hz, 1H), 3.02 (m, 1H), 3.13 (dd, ² J = 15.5 Hz, ³ J = 6.4 Hz, 1H), 3.74 (s, 3H), 4.01 (s, 3H), 6.72 (m, 2H), 7.15 (d, ³ J = 8.2 Hz, 1H), 7.19 (s, 1H), 8.22 (m, 1H), 8.34 (d, ⁴ J = 2.4 Hz, 1H), 8.59 (d, ⁴ J = 1.5 Hz, 1H). ¹³C-NMR (125 MHz, CD₃OD): δ = 17.8, 30.6, 36.7, 55.8, 57.9, 112.9, 115.6, 116.6, 127.0, 127.2, 127.8, 129.8, 130.3, 132.3, 137.1, 137.2, 150.9, 160.1. MS m/z 281.96 (MH⁺). Anal. (C₁₈H₁₉NO₂·HCl·0.2H₂O) C, H, N.

3-Ethoxy-5-(6-methoxynaphthalen-2-yl)pyridine (14) was prepared according to procedure A starting from 6-methoxy-2-naphthaleneboronic acid (131 mg, 0.65 mmol) and **14a** (101 mg, 0.50 mmol). After crystallization from ethyl acetate/petroleum ether pure **14** was obtained as a white solid (33 mg, 0.17 mmol, 23 %), mp decomposition above 130 °C. MS m/z 280.05 (MH⁺). Anal. (C₁₈H₁₇NO₂·0.2H₂O) C, H, N.

5-(6-Methoxynaphthalen-2-yl)pyridine-3-carboxylic acid (15) was prepared according to procedure A starting from 6-methoxy-2-naphthaleneboronic acid (131 mg, 0.65 mmol) and 5-bromonicotinic acid (101 mg, 0.50 mmol). After crystallization from methanol/water pure **15** was obtained as an off-white solid (74 mg, 0.26 mmol, 53 %), mp decomposition above 300 °C. MS m/z 279.98 (MH⁺). Anal. (C₁₇H₁₃NO₃·HCl·0.3H₂O) C, H, N.

Methyl 5-(6-methoxynaphthalen-2-yl)pyridine-3-carboxylate (16). Carboxylic acid **15** (45 mg, 0.16 mmol) was dissolved in 20 mL dry methanol and 0.05 mL concentrated H₂SO₄ (98%) was added. The whole mixture was refluxed for 10 h and thereafter the excess methanol was distilled off. The residue was taken up in 50 mL ethyl acetate and the organic layer was washed several times with 5 % aqueous Na₂CO₃ solution, water and brine. After drying over MgSO₄, the solvent was evaporated in vacuo. After flash chromatography on silica gel (petroleum ether/ethyl acetate, 7/3, R_f = 0.34) pure **16** was obtained as an off-white solid (28 mg, 0.10 mmol, 60 %), mp 150–151 °C. MS m/z 293.97 (MH⁺). Anal. (C₁₈H₁₄NO₃) C, H, N.

5-(6-Methoxynaphthalen-2-yl)pyridine-3-carboxamide (17) was prepared according to procedure A starting from 6-methoxy-2-naphthaleneboronic acid (131 mg, 0.65 mmol) and 5-bromonicotinamide (92 mg, 0.50 mmol). After crystallization from acetone/diethyl ether pure **17** was obtained as a white solid (55 mg, 0.20 mmol, 40 %), mp 245–247 °C. MS m/z 279.07 (MH⁺). Anal. (C₁₇H₁₄N₂O₂) C, H, N.

1-[5-(6-Methoxynaphthalen-2-yl)pyridin-3-yl]ethanone (18) was prepared according to procedure A starting from 6-methoxy-2-naphthaleneboronic acid (131 mg, 0.65 mmol) and 3-acetyl-5-bromopyridine (100 mg, 0.50 mmol). After crystallization from acetone/diethyl ether pure **18** was

obtained as a white solid (75 mg, 0.27 mmol, 54 %), mp 159–160 °C. MS m/z 278.09 (MH⁺). Anal. (C₁₈H₁₅NO₂·0.1H₂O) C, H, N.

[5-(6-Methoxynaphthalen-2-yl)pyridin-3-yl]acetic acid (19) was prepared according to procedure A starting from 6-methoxy-2-naphthaleneboronic acid (131 mg, 0.65 mmol) and 5-bromo-3-pyridine-acetic acid (108 mg, 0.50 mmol). After crystallization from methanol/water pure **19** was obtained as a white solid (70 mg, 0.24 mmol, 48 %), mp decomposition above 210 °C. MS m/z 293.97 (MH⁺). Anal. (C₁₈H₁₅NO₃·0.5H₂O) C, H, N.

Methyl [5-(6-methoxynaphthalen-2-yl)pyridin-3-yl]acetate (20) was prepared as described for **16** starting from **19** (145 mg, 0.49 mmol). After flash chromatography on silica gel (petroleum ether/ethyl acetate, 1/1, R_f = 0.18) pure **20** was obtained as a white solid (81 mg, 0.26 mmol, 53 %), mp 145–146 °C. MS m/z 308.04 (MH⁺). Anal. (C₁₉H₁₇NO₃) C: calcd, 74.25, found, 74.72, H, N.

[5-(6-Methoxynaphthalen-2-yl)pyridin-3-yl]methanol (21) was prepared according to procedure A starting from 6-methoxy-2-naphthaleneboronic acid (131 mg, 0.65 mmol) and **21a** (94 mg, 0.50 mmol). After crystallization from acetone/diethyl ether pure **21** was obtained as a white solid (86 mg, 0.32 mmol, 65 %), mp 193–194 °C. MS m/z 266.05 (MH⁺). Anal. (C₁₇H₁₅NO₂·0.1H₂O) C, H, N.

3-(Methoxymethyl)-5-(6-methoxynaphthalen-2-yl)pyridine (22) was prepared according to procedure C starting from **21** (150 mg, 0.57 mmol) using methyl iodide (82 μ L, 1.32 mmol). After flash chromatography on silica gel (petroleum ether/ethyl acetate, 1/1, R_f = 0.22) pure **22** was obtained as an off-white solid (80 mg, 0.29 mmol, 50 %), mp 121–122 °C. MS m/z 279.91 (MH⁺). Anal. (C₁₈H₁₇NO₂) C, H, N.

[4-(6-Methoxynaphthalen-2-yl)pyridin-3-yl]methanol (23) was prepared according to procedure A starting from 6-methoxy-2-naphthaleneboronic acid (131 mg, 0.65 mmol) and **23a** (94 mg, 0.50 mmol). After crystallization from acetone/diethyl ether pure **23** was obtained as a white solid (90 mg, 0.34 mmol, 68 %), mp decomposition above 240 °C. MS m/z 266.05 (MH⁺). Anal. (C₁₇H₁₅NO₂·0.2H₂O) C, H, N.

4-(Methoxymethyl)-3-(6-methoxynaphthalen-2-yl)pyridine (24) was prepared according to procedure C starting from **23** (150 mg, 0.57 mmol) using methyl iodide (82 μ L, 1.32 mmol). After flash chromatography on silica gel (petroleum ether/ethyl acetate, 1/1, R_f = 0.23) pure **24** was obtained as an off-white solid (74 mg, 0.26 mmol, 46 %), mp (HCl salt) 174–177 °C. MS m/z 279.91 (MH⁺). Anal. (C₁₈H₁₇NO₂·0.2H₂O) C, H, N.

1-[5-(6-Methoxynaphthalen-2-yl)-pyridin-3-yl]ethanol (25) was prepared according to procedure D starting from **18** (50 mg, 0.18 mmol) using NaBH₄ (8.0 mg, 0.21 mmol). After flash chromatography on silica gel (petroleum ether/ethyl acetate, 1/1, R_f = 0.24) pure **25** was obtained as a white solid (28 mg, 0.10 mmol, 56 %), mp 154–155 °C. MS m/z 280.05 (MH⁺). Anal. (C₁₈H₁₇NO₂) C, H, N.

3-(1-Methoxyethyl)-5-(6-methoxynaphthalen-2-yl)pyridine (26) was prepared according to procedure C starting from **25** (70 mg, 0.25 mmol) using methyl iodide (41 μ L, 0.66 mmol). After flash

chromatography on silica gel (petroleum ether/ethyl acetate, 1/1, $R_f = 0.23$) pure **26** was obtained as a yellowish solid (26 mg, 0.08 mmol, 35 %), mp 124–125 °C. MS m/z 294.11 (MH^+). Anal. ($C_{19}H_{19}NO_2$) C, H, N.

3-(6-Methoxynaphthalen-2-yl)-5-phenylpyridine (27) was prepared according to procedure A starting from 6-methoxy-2-naphthaleneboronic acid (394 mg, 1.95 mmol) and 3-bromo-5-phenylpyridine (351 mg, 1.50 mmol). After flash chromatography on silica gel (petroleum ether/ethyl acetate, 2/1, $R_f = 0.23$) pure **27** was obtained as a white, crystalline solid (455 mg, 1.46 mmol, 97 %), mp 216–217 °C. MS m/z 312.09 (MH^+). Anal. ($C_{22}H_{17}NO \cdot 0.4H_2O$) C, H, N.

4-(6-Methoxynaphthalen-2-yl)isoquinoline (28) was prepared according to procedure A starting from 6-methoxy-2-naphthaleneboronic acid (131 mg, 0.65 mmol) and 4-bromoisquinoline (104 mg, 0.50 mmol). After flash chromatography on silica gel (petroleum ether/ethyl acetate, 7/3, $R_f = 0.21$) pure **28** was obtained as a white solid (44 mg, 0.16 mmol, 31 %), mp 185–186 °C. MS m/z 286.07 (MH^+). Anal. ($C_{20}H_{15}NO \cdot 0.1H_2O$) C, H, N.

4-(6-Methoxy-3-methylnaphthalen-2-yl)isoquinoline (29) was obtained according to procedure A starting from **2a** (377 mg, 1.50 mmol) and 4-isoquinolineboronic acid (337 mg, 1.95 mmol) after flash chromatography on silica gel (dichloromethane/methanol 99/1, $R_f = 0.26$) as yellow oil which solidified with diethyl ether as a pale yellow solid (178 mg, 0.59 mmol, 40 %), mp 156–157 °C. MS m/z 300.10 (MH^+). Anal. ($C_{21}H_{11}NO$) C, H, N.

4-(6-Methoxy-3-methyl-3,4-dihydronaphthalen-2-yl)isoquinoline (30) was obtained according to procedure B starting from **2b** (253 mg, 1.00 mmol) and 4-isoquinolineboronic acid (225 mg, 1.30 mmol) after two flash chromatographical separations on silica gel (petroleum ether/ethyl acetate, 5/1, $R_f = 0.20$ and dichloromethane/methanol 99/1, $R_f = 0.27$) and precipitation as HCl salt as a yellow solid (112 mg, 0.33 mmol, 17 %), mp 149–150 °C. MS m/z 302.18 (MH^+). Anal. ($C_{21}H_{19}NO \cdot HCl \cdot 0.2H_2O$) C, H, N.

Biological Methods. 1. Enzyme Preparations. CYP17 and CYP19 preparations were obtained by described methods: the 50,000 g sediment of *E. coli* expressing human CYP17³⁷ and microsomes from human placenta for CYP19.³⁹ **2. Enzyme Assays.** The following enzyme assays were performed as previously described: CYP17³⁷ and CYP19.³⁹ **3. Activity and Selectivity Assay Using V79 Cells.** V79 MZh 11B1 and V79 MZh 11B2 cells³⁶ were incubated with [4-¹⁴C]-11-deoxycorticosterone as substrate and inhibitor in at least three different concentrations. The enzyme reactions were stopped by addition of ethyl acetate. After vigorous shaking and a centrifugation step (10,000 g, 2 min), the steroids were extracted into the organic phase, which was then separated. The conversion of the substrate was analyzed by HPTLC and a phosphoimaging system as described.^{10,22} **4. Inhibition of Human Hepatic CYP Enzymes.** The recombinantly expressed enzymes from baculovirus-infected insect microsomes (Supersomes) were used and the manufacturer's instructions (www.gentest.com) were followed. **5. In Vivo Pharmacokinetics.** Animal trials were conducted in accordance with institutional and international ethical guidelines for the use of laboratory animals. Male Wistar rats

weighing 317–322 g (Janvier, France) were housed in a temperature-controlled room (20–22 °C) and maintained in a 12 h light/12 h dark cycle. Food and water were available *ad libitum*. The animals were anaesthetised with a ketamine (135mg/kg)/xylazine (10mg/kg) mixture, and cannulated with silicone tubing via the right jugular vein. Prior to the first blood sampling, animals were connected to a counterbalanced system and tubing, to perform blood sampling in the freely moving rat. Separate stock solutions (5 mg/mL) were prepared for the tested compounds in Labrasol/Water (1:1; v/v), leading to a clear solution. Immediately before application, the cassette dosing mixture was prepared by adding equal volumes of the 5 stock solutions to end up with a final concentration of 1 mg/mL for each compound. The mixture was applied perorally to 3 rats with an injection volume of 5 mL/kg (Time 0). 400 μ L of blood were taken via jugularis catheter 1 hour before application and then 1 and 2 hours after application. Immediately, equal volume (400 μ L) of 0.9 % NaCl (37 °C) was re-injected intravenously to keep the blood volume stable. 4, 6, 8, 10 and 24 hours after application 250 μ L of blood were sampled without balancing the blood volume. Blood samples were centrifuged at 3000 g for 10 minutes at 4 °C. Plasma was harvested and kept at –20 °C until analysis. The mean of absolute plasma concentrations (\pm SEM) was calculated for the 3 rats and the regression was performed on group mean values. The pharmacokinetic analysis was performed using a noncompartment model (PK Solutions 2.0, Summit Research Services). HPLC-MS/MS analysis and quantification of the samples was carried out on a Surveyor-HPLC-system coupled with a TSQ Quantum (ThermoFinnigan) triple quadrupole mass spectrometer equipped with an electrospray interface (ESI).

Computational Methods. MEP. For each docked compound geometry optimization was performed at the B3LYP/6-31G* density functional levels by means of the Gaussian03 software and the molecular electrostatic potential (MEP) maps were plotted using GaussView3, the 3-D molecular graphics package of Gaussian.⁴³ These electrostatic potential surfaces were generated by mapping 6-31G* electrostatic potentials onto surfaces of molecular electron density (isovalue = 0.002 electron/ \AA).⁴⁴

Acknowledgement. We thank Ms. Gertrud Schmitt and Ms. Jeannine Jung for their help in performing the *in vitro* tests. S. L. is grateful to Saarland University for a scholarship (Landesgraduierten-Förderung). Thanks are due to Prof. J. J. Rob Hermans, University of Maastricht, The Netherlands, for supplying the V79 CYP11B1 cells, and Prof. Rita Bernhardt, Saarland University, for supplying the V79 CYP11B2 cells.

Supporting Information Available: Individual plasma levels of each compound and animal, graphs and equations of the linear regression of pIC₅₀ values, NMR-spectroscopic data of compounds **2**, **5–10**, **14–30**, full experimental details and spectroscopic characterization of the reaction intermediates **2a–2d**, **2f**, **6a**, **6b**, **8a**, **14a**, **21a**, **23a**, elemental analysis results of compounds **2**, **5–30**. This information is available free of charge via the Internet at <http://pubs.acs.org>.

References

- (1) (a) Takeda Y. Vascular synthesis of aldosterone: role in hypertension. *Mol. Cell. Endocrinol.* **2004**, *217*, 75–79. (b) Davies, E.; MacKenzie, S. M. Extra-adrenal production of corticosteroids. *Clin. Exp. Pharmacol. Physiol.* **2003**, *30*, 437–445.
- (2) Kawamoto, T.; Mitsuuchi, Y.; Toda, K.; Yokoyama, Y.; Miyahara, K.; Miura, S.; Ohnishi, T.; Ichikawa, Y.; Nakao, K.; Imura, H.; Ulick, S.; Shizuta, Y. Role of steroid 11 β -hydroxylase and steroid 18-hydroxylase in the biosynthesis of glucocorticoids and mineralocorticoids in humans. *Proc. Natl. Acad. Sci. U.S.A.* **1992**, *89*, 1458–1462.
- (3) (a) Brilla, C. G. Renin-angiotensin-aldosterone system and myocardial fibrosis. *Cardiovasc. Res.* **2000**, *47*, 1–3. (b) Lijnen, P.; Petrov, V. Induction of cardiac fibrosis by aldosterone. *J. Mol. Cell. Cardiol.* **2000**, *32*, 865–879.
- (4) Pitt, B.; Zannad, F.; Remme, W. J.; Cody, R.; Castaigne, A.; Perez, A.; Palensky, J.; Wittes, J. The effect of spironolactone on morbidity and mortality in patients with severe heart failure. *N. Engl. J. Med.* **1999**, *341*, 709–717.
- (5) Pitt, B.; Remme, W.; Zannad, F.; Neaton, J.; Martinez, F.; Roniker, B.; Bittman, R.; Hurley, S.; Kleiman, J.; Gatlin, M. Eplerenone, a selective aldosterone blocker, in patients with left ventricular dysfunction after myocardial infarction. *N. Eng. J. Med.* **2003**, *348*, 1309–1321.
- (6) Khan, N. U. A.; Movahed, A. The role of aldosterone and aldosterone-receptor antagonists in heart failure. *Rev. Cardiovasc. Med.* **2004**, *5*, 71–81.
- (7) Bell, M. G.; Gernert, D. L.; Grese, T. A.; Belvo, M. D.; Borromeo, P. S.; Kelley, S. A.; Kennedy, J. H.; Kolis, S. P.; Lander, P. A.; Richey, R.; Sharp, V. S.; Stephenson, G. A.; Williams, J. D.; Yu, H.; Zimmerman, K. M.; Steinberg, M. I.; Jadhav, P. K. (S)-N-{3-[1-Cyclopropyl-1-(2,4-difluoro-phenyl)-ethyl]-1H-indol-7-yl}-methanesulfonamide: A potent, nonsteroidal, functional antagonist of the mineralocorticoid receptor. *J. Med. Chem.* **2007**, *50*, 6443–6445.
- (8) (a) Delcayre, C.; Swynghedauw, B. Molecular mechanisms of myocardial remodeling. The role of aldosterone. *J. Mol. Cell. Cardiol.* **2002**, *34*, 1577–1584. (b) de Resende, M. M.; Kauser, K.; Mill, J. G. Regulation of cardiac and renal mineralocorticoid receptor expression by captopril following myocardial infarction in rats. *Life Sci.* **2006**, *78*, 3066–3073.
- (9) (a) Wehling, M. Specific, nongenomic actions of steroid hormones. *Annu. Rev. Physiol.* **1997**, *59*, 365–393. (b) Lösel, R.; Wehling, M. Nongenomic actions of steroid hormones. *Nature Rev. Mol. Cell. Biol.* **2003**, *4*, 46–55. (c) Chai, W.; Garrelds, I. M.; Arulmani, U.; Schoemaker, R. G.; Lamers, J. M. J.; Danser, A. H. J.; Genomic and nongenomic effects of aldosterone in the rat heart: Why is spironolactone cardioprotective? *Br. J. Pharmacol.* **2005**, *145*, 664–671. (d) Chai, W.; Garrelds, I. M.; de Vries, R.; Batenburg, W. W.; van Kats, J. P.; Danser, A. H. J. Nongenomic effects of aldosterone in the human heart: Interaction with angiotensin II. *Hypertension* **2005**, *46*, 701–706.

- (10) Ehmer, P. B.; Bureik, M.; Bernhardt, R.; Müller, U.; Hartmann, R. W. Development of a test system for inhibitors of human aldosterone synthase (CYP11B2): Screening in fission yeast and evaluation of selectivity in V79 cells. *J. Steroid Biochem. Mol. Biol.* **2002**, *81*, 173–179.
- (11) Hartmann, R. W.; Müller, U.; Ehmer, P. B. Discovery of selective CYP11B2 (aldosterone synthase) inhibitors for the therapy of congestive heart failure and myocardial fibrosis. *Eur. J. Med. Chem.* **2003**, *38*, 363–366.
- (12) (a) Yamakita, N.; Chiou, S.; Gomez-Sanchez, C. E. Inhibition of aldosterone biosynthesis by 18-ethynyl-deoxycorticosterone. *Endocrinology* **1991**, *129*, 2361–2366. (b) Hartmann, R. W. Selective inhibition of steroidogenic P450 enzymes: Current status and future perspectives. *Eur. J. Pharm. Sci.* **1994**, *2*, 15–16.
- (13) (a) Viger, A.; Coustal, S.; Perard, S.; Piffeteau, A.; Marquet, A. 18-Substituted progesterone derivatives as inhibitors of aldosterone biosynthesis. *J. Steroid Biochem.* **1989**, *33*, 119–124. (b) Delorme, C.; Piffeteau, A.; Viger, A.; Marquet, A. Inhibition of bovine cytochrome P-450_{11 β} by 18-unsaturated progesterone derivatives. *Eur. J. Biochem.* **1995**, *232*, 247–256. (c) Delome, C.; Piffeteau, A.; Sobrio, F.; Marquet, A. Mechanism-based inactivation of bovine cytochrome P-450_{11 β} by 18-unsaturated progesterone derivatives. *Eur. J. Biochem.* **1997**, *248*, 252–260.
- (14) Davioud, E.; Piffeteau, A.; Delorme, C.; Coustal, S.; Marquet, A. 18-Vinyldeoxycorticosterone: a potent inhibitor of the bovine cytochrome P-450_{11 β} . *Bioorg. Med. Chem.* **1998**, *6*, 1781–1788.
- (15) Taymans, S. E.; Pack, S.; Pak, E.; Torpy, D. J.; Zhuang, Z.; Stratakis, C. A. Human CYP11B2 (aldosterone synthase) maps to chromosome 8q24.3. *J. Clin. Endocrinol. Metab.* **1998**, *83*, 1033–1036.
- (16) (a) Häusler, A.; Monnet, G.; Borer, C.; Bhatnagar, A. S. Evidence that corticosterone is not an obligatory intermediate in aldosterone biosynthesis in the rat adrenal. *J. Steroid Biochem.* **1989**, *34*, 567–570. (b) Demers, L. M.; Melby, J. C.; Wilson, T. E.; Lipton, A.; Harvey, H. A.; Santen, R. J. The effects of CGS 16949A, an aromatase inhibitor on adrenal mineralocorticoid biosynthesis. *J. Clin. Endocrinol. Metab.* **1990**, *70*, 1162–1166.
- (17) Fiebeler, A.; Nussberger, J.; Shagdarsuren, E.; Rong, S.; Hilfenhaus, G.; Al-Saadi, N.; Dechend, R.; Wellner, M.; Meiners, S.; Maser-Gluth, C.; Jeng, A. Y.; Webb, R. L.; Luft, F. C.; Muller, D. N. Aldosterone synthase inhibitor ameliorates angiotensin II-induced organ damage. *Circulation* **2005**, *111*, 3087–3094.
- (18) (a) Ksander, G.; Hu, Q.-Y. Fused imidazole derivatives for the treatment of disorders mediated by aldosterone synthase and/or 11-beta-hydroxylase and/or aromatase. PCT Int. Appl. WO2008027284, 2008. (b) Papillon J.; Ksander, G. M.; Hu, Q.-Y. Preparation of tetrahydroimidazo[1,5-a]pyrazine derivatives as aldosterone synthase and/or 11 β -hydroxylase inhibitors. PCT Int. Appl. WO2007139992, 2007. (c) Adams, C.; Papillon, J.; Ksander, G. M. Preparation of imidazole derivatives as aldosterone synthase inhibitors. PCT Int. Appl. WO2007117982, 2007. (d) Ksander, G. M.; Meredith, E.; Monovich, L. G.; Papillon, J.; Firooznia, F.; Hu, Q.-Y. Preparation of condensed imidazole derivatives for the inhibition of aldosterone synthase and aromatase. PCT Int. Appl. WO2007024945, 2007. (e) Firooznia, F. Preparation of imidazo[1,5a]pyridine derivatives for treatment of aldosterone mediated diseases. PCT Int. Appl.

- WO2004046145, 2004. (f) McKenna, J. Preparation of imidazopyrazines and imidazodiazepines as agents for the treatment of aldosterone mediated conditions. PCT Int. Appl. WO2004014914, 2004.
- (19) (a) Herold, P.; Mah, R.; Tschinke, V.; Stojanovic, A.; Marti, C.; Jelakovic, S.; Stutz, S. Preparation of imidazo compounds as aldosterone synthase inhibitors. PCT Int. Appl. WO2007116099, 2007. (b) Herold, P.; Mah, R.; Tschinke, V.; Stojanovic, A.; Marti, C.; Jelakovic, S.; Bennacer, B.; Stutz, S. Preparation of spiro-imidazo derivatives as aldosterone synthase inhibitors. PCT Int. Appl. WO2007116098, 2007. (c) Herold, P.; Mah, R.; Tschinke, V.; Stojanovic, A.; Marti, C.; Stutz, S. Preparation of imidazo compounds as aldosterone synthase inhibitors. PCT Int. Appl. WO2007116097, 2007. (d) Herold, P.; Mah, R.; Tschinke, V.; Quirnbach, M.; Marti, C.; Stojanovic, A.; Stutz, S. Preparation of fused imidazoles as aldosterone synthase inhibitors. PCT Int. Appl. WO2007065942, 2007. (e) Herold, P.; Mah, R.; Tschinke, V.; Stojanovic, A.; Marti, C.; Jotterand, N.; Schumacher, C.; Quirnbach, M. Preparation of heterocyclic spiro-compounds as aldosterone synthase inhibitors. PCT Int. Appl. WO2006128853, 2006. (f) Herold, P.; Mah, R.; Tschinke, V.; Stojanovic, A.; Marti, C.; Jotterand, N.; Schumacher, C.; Quirnbach, M. Preparation of heterocyclic spiro-compounds as aldosterone synthase inhibitors. PCT Int. Appl. WO2006128852, 2006. (g) Herold, P.; Mah, R.; Tschinke, V.; Stojanovic, A.; Marti, C.; Jotterand, N.; Schumacher, C.; Quirnbach, M. Preparation of fused imidazoles as aldosterone synthase inhibitors. PCT Int. Appl. WO2006128851, 2006. (h) Herold, P.; Mah, R.; Tschinke, V.; Schumacher, C.; Marti, C.; Quirnbach, M. Preparation of fused heterocycles as aldosterone synthase inhibitors. PCT Int. Appl. WO2006005726, 2006. (i) Herold, P.; Mah, R.; Tschinke, V.; Schumacher, C.; Quirnbach, M. Preparation of imidazopyridines and related analogs as aldosterone synthase inhibitors. PCT Int. Appl. WO2005118557, 2005. (j) Herold, P.; Mah, R.; Tschinke, V.; Schumacher, C.; Quirnbach, M. Preparation of tetrahydro-imidazo[1,5-a]pyridin derivatives as aldosterone synthase inhibitors. PCT Int. Appl. WO2005118581, 2005. (k) Herold, P.; Mah, R.; Tschinke, V.; Schumacher, C.; Behnke, D.; Quirnbach, M. Preparation of nitrogen-containing heterobicyclic compounds as aldosterone synthase inhibitors. PCT Int. Appl. WO2005118541, 2005.
- (20) Ulmschneider, S.; Müller-Vieira, U.; Mitrenga, M.; Hartmann, R. W.; Oberwinkler-Marchais, S.; Klein, C. D.; Bureik, M.; Bernhardt, R.; Antes, I.; Lengauer, T. Synthesis and evaluation of imidazolylmethylenetetrahydronaphthalenes and imidazolylmethyleneindanes: Potent inhibitors of aldosterone synthase. *J. Med. Chem.* **2005**, *48*, 1796–1805.
- (21) Ulmschneider, S.; Müller-Vieira, U.; Klein, C. D.; Antes, I.; Lengauer, T.; Hartmann, R. W. Synthesis and evaluation of (pyridylmethylene)tetrahydronaphthalenes/-indanes and structurally modified derivatives: Potent and selective inhibitors of aldosterone synthase. *J. Med. Chem.* **2005**, *48*, 1563–1575.
- (22) Voets, M.; Antes, I.; Scherer, C.; Müller-Vieira, U.; Biemel, K.; Barassin, C.; Oberwinkler-Marchais, S.; Hartmann, R. W. Heteroaryl substituted naphthalenes and structurally modified derivatives: Selective inhibitors of CYP11B2 for the treatment of congestive heart failure and myocardial fibrosis. *J. Med. Chem.* **2005**, *48*, 6632–6642.
- (23) Voets, M.; Antes, I.; Scherer, C.; Müller-Vieira, U.; Biemel, K.; Oberwinkler-Marchais, S.; Hartmann, R. W. Synthesis and evaluation of heteroaryl-substituted dihydronaphthalenes and indenes: Potent and selective inhibitors of aldosterone synthase (CYP11B2) for the treatment of congestive heart failure and myocardial fibrosis. *J. Med. Chem.* **2006**, *49*, 2222–2231.

- (24) Ulmschneider, S.; Negri, M.; Voets, M.; Hartmann, R. W. Development and evaluation of a pharmacophore model for inhibitors of aldosterone synthase (CYP11B2). *Bioorg. Med. Chem. Lett.* **2006**, *16*, 25–30.
- (25) (a) Eaton, D. L.; Gallagher, E. P.; Bammler, T. K.; Kunze, K. L. Role of cytochrome P4501A2 in chemical carcinogenesis: Implications for human variability in expression and enzyme activity. *Pharmacogenetics* **1995**, *5*, 259–274. (b) Guengerich, F.; Parikh, A.; Turesky, R. J.; Josephy, P. D. Interindividual differences in the metabolism of environmental toxicants: Cytochrome P450 1A2 as a prototype. *Mutat. Res.* **1999**, *428*, 115–124.
- (26) Miyaura, N.; Suzuki, A. Palladium-catalyzed cross-coupling reactions of organoboron compounds. *Chem. Rev.* **1995**, *95*, 2457–2483.
- (27) Appukkuttan, P.; Orts, A. B.; Chandran, R. P.; Goeman, J. L.; van der Eycken, J.; Dehaen, W.; van der Eycken, E. Generation of a small library of highly electron-rich 2-(hetero)aryl-substituted phenethylamines by the Suzuki-Miyaura reaction: A short synthesis of an apogalanthamine analogue. *Eur. J. Org. Chem.* **2004**, 3277–3285.
- (28) Bengtson, A.; Hallberg, A.; Larhed, M. Fast synthesis of aryl triflates with controlled microwave heating. *Org. Lett.* **2002**, *4*, 1231–1233.
- (29) Kertesz, D. J.; Martin, M.; Palmer, W. S. Process for preparing pyridazinone compounds. PCT Int. Appl. WO2005100323, 2005.
- (30) Lézé, M.-P.; Le Borgne, M.; Pinson, P.; Paluszczak, A.; Duflos, M.; Le Baut, G.; Hartmann, R. W. Synthesis and biological evaluation of 5-[(aryl)(1H-imidazol-1-yl)methyl]-1H-indoles: Potent and selective aromatase inhibitors. *Bioorg. Med. Chem. Lett.* **2006**, *16*, 1134–1137.
- (31) Carreño, M. C.; García-Cerrada, S.; Urbano, A. From central to helical chirality: Synthesis of P and M enantiomers of [5]helicenequinones and bisquinones from (SS)-2-(p-tolylsulfinyl)-1,4-benzoquinone. *Chem. Eur. J.* **2003**, *9*, 4118–4131.
- (32) Heyer, D.; Fang, J.; Navas III, F.; Katamreddy, S. R.; Peckham, J. P.; Turnbull, P. S.; Miller, A. B.; Akwabi-Ameyaw, A. Chemical compounds. PCT Int. Appl. WO2006002185, 2006.
- (33) Fitzgerald, D. H.; Muirhead, K. M.; Botting, N. P. A comparative study on the inhibition of human and bacterial kynureninase by novel bicyclic kynurenine analogues. *Bioorg. Med. Chem.* **2001**, *9*, 983–989.
- (34) (a) Leadbeater, N. E.; Marco, M. Ligand-free palladium catalysis of the suzuki reaction in water using microwave heating. *Org. Lett.* **2002**, *4*, 2973–2976. (b) Liu, L.; Zhang, Y.; Xin, B. Synthesis of biaryls and polyaryls by ligand-free suzuki reaction in aqueous phase. *J. Org. Chem.* **2006**, *71*, 3994–3997.
- (35) Li, D.; Zhao, B.; Sim, S.; Li, T.; Liu, A.; Liu, L. F.; LaVoie, E. J. 8,9-Methylenedioxybenzo[*i*]-phenanthridines: Topoisomerase I-targeting activity and cytotoxicity. *Bioorg. Med. Chem.* **2003**, *11*, 3795–3805.
- (36) (a) Denner, K.; Bernhardt, R. Inhibition studies of steroid conversions mediated by human CYP11B1 and CYP11B2 expressed in cell cultures. In *Oxygen Homeostasis and Its Dynamics*, 1st ed.; Ishimura, Y., Shimada, H., Suematsu, M., Eds.; Springer-Verlag: Tokyo, Berlin, Heidelberg, New York, 1998; pp 231–

236. (b) Denner, K.; Doehmer, J.; Bernhardt, R. Cloning of CYP11B1 and CYP11B2 from normal human adrenal and their functional expression in COS-7 and V79 chinese hamster cells. *Endocr. Res.* **1995**, *21*, 443–448. (c) Böttner, B.; Denner, K.; Bernhardt, R. Conferring aldosterone synthesis to human CYP11B1 by replacing key amino acid residues with CYP11B2-specific ones. *Eur. J. Biochem.* **1998**, *252*, 458–466.
- (37) (a) Ehmer, P. B.; Jose, J.; Hartmann, R. W. Development of a simple and rapid assay for the evaluation of inhibitors of human 17 α -hydroxylase-C_{17,20}-lyase (P450c17) by coexpression of P450c17 with NADPH-cytochrome-P450-reductase in *Escherichia coli*. *J. Steroid Biochem. Mol. Biol.* **2000**, *75*, 57–63; (b) Hutschenreuter, T. U.; Ehmer, P. B.; Hartmann, R. W. Synthesis of hydroxy derivatives of highly potent nonsteroidal CYP17 inhibitors as potential metabolites and evaluation of their activity by a non cellular assay using recombinant enzyme. *J. Enzyme Inhib. Med. Chem.* **2004**, *19*, 17–32.
- (38) Thompson, E. A.; Siiteri, P. K. Utilization of oxygen and reduced nicotinamide adenine dinucleotide phosphate by human placental microsomes during aromatization of androstenedione. *J. Biol. Chem.* **1974**, *249*, 5364–5372.
- (39) Hartmann, R. W.; Batzl, C. Aromatase inhibitors. Synthesis and evaluation of mammary tumor inhibiting activity of 3-alkylated 3-(4-aminophenyl)piperidine-2,6-diones. *J. Med. Chem.* **1986**, *29*, 1362–1369.
- (40) Butler, M. A.; Iwasaki, M.; Guengerich, F. P.; Kadlubar, F. F. Human cytochrome P-450_{PA} (P-450IA2), the phenacetin O-deethylase, is primarily responsible for the hepatic 3-demethylation of caffeine and N-oxidation of carcinogenic arylamines. *Proc. Natl. Acad. Sci. U.S.A.* **1989**, *86*, 7696–7700.
- (41) Sesardic, D.; Boobis, A. R.; Murray, B. P.; Murray, S.; Segura, J.; de la Torre, R.; Davies, D. S. Furfurylline is a potent and selective inhibitor of cytochrome P450IA2 in man. *Br. J. Clin. Pharmacol.* **1990**, *29*, 651–663.
- (42) (a) Chohan, K. K.; Paine, S. W.; Mistry, J.; Barton, P.; Davis, A. M. A rapid computational filter for cytochrome P450 1A2 inhibition potential of compound libraries. *J. Med. Chem.* **2005**, *48*, 5154–5161. (b) Korhonen, L. E.; Rahnasto, M.; Mähönen, N. J.; Wittekindt, C.; Poso, A.; Juvonen, R. O.; Raunio, H. Predictive three-dimensional quantitative structure-activity relationship of cytochrome P450 1A2 inhibitors. *J. Med. Chem.* **2005**, *48*, 3808–3815.
- (43) GaussView, Version 3.0, Dennington I.; Roy; Keith, T.; Millam, J.; Eppinnett, K.; Hovell, W. L.; Gilliland, R.; Semichem, Inc., Shawnee Mission, KS, **2003**.
- (44) Petti, M. A.; Shepodd, T. J.; Barrans, R. E.; Dougherty, D. A. "Hydrophobic" binding of water-soluble guests by high-symmetry, chiral hosts. An electron-rich receptor site with a general affinity for quaternary ammonium compounds and electron-deficient π systems. *J. Am. Chem. Soc.* **1988**, *110*, 6825–6840.

3.2 Novel Aldosterone Synthase Inhibitors with Extended Carbocyclic Skeleton by a Combined Ligand-Based and Structure-Based Drug Design Approach

Simon Lucas, Ralf Heim, Matthias Negri, Iris Antes, Christina Ries, Katarzyna E. Schewe, Alessandra Bisi, Silvia Gobbi, and Rolf W. Hartmann

This manuscript has been accepted for publication as an article by the

Journal of Medicinal Chemistry **2008**, in press

Paper II

Abstract: Pharmacophore modeling of a series of aldosterone synthase (CYP11B2) inhibitors triggered the design of compounds **11** and **12** by extending a previously established naphthalene molecular scaffold (e.g., present in molecules **1** and **2**) via introduction of a phenyl or benzyl residue in 3-position. These additional aromatic moieties have been hypothesized to fit into the newly identified hydrophobic pharmacophore feature HY3. Subsequent docking studies in our refined CYP11B2 protein model have been performed prior to synthesis to estimate the inhibitory properties of the proposed molecules. While phenyl-substituted compound **11** ($IC_{50} > 500$ nM) did not dock under the given pharmacophore constraint (i.e., the Fe(heme)-N(ligand) interaction), benzyl-substituted compound **12** ($IC_{50} = 154$ nM) was found to exploit a previously unexplored sub-pocket of the inhibitor binding site. By structural optimization based on the pharmacophore hypothesis, 25 novel compounds were synthesized, amongst them highly potent CYP11B2 inhibitors (e.g., **17**, $IC_{50} = 2.7$ nM) with pronounced selectivity toward the most important steroidogenic and hepatic CYP enzymes.

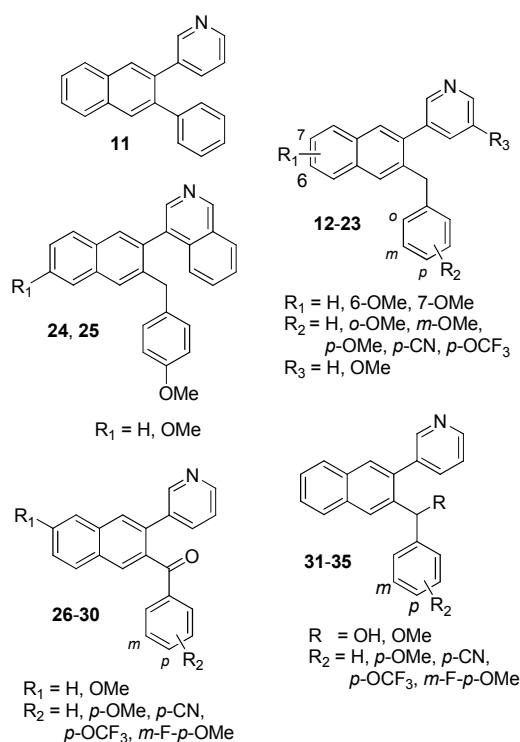
Introduction

Aldosterone synthase (CYP11B2), a mitochondrial cytochrome P450 enzyme that is localized mainly in the adrenal cortex, is the key enzyme of mineralocorticoid biosynthesis. It catalyzes the terminal three oxidation steps in the biogenesis of aldosterone in humans.¹ This hormone is the most important circulating mineralocorticoid and plays a crucial role in the electrolyte and fluid homeostasis mainly by binding to epithelial mineralocorticoid receptors (MR) promoting sodium reabsorption and potassium secretion. Since the sodium movement is followed by water via osmosis, aldosterone is a key regulator of blood volume and blood pressure. Abnormally increased plasma levels of aldosterone have been diagnosed in different cardiovascular diseases such as elevated blood pressure, congestive heart failure, and myocardial fibrosis.² Inhibitors of the angiotensin-converting enzyme (ACE) which are in use for the treatment of hypertension and congestive heart failure can initially induce a down-regulation of circulating aldosterone. However, increased levels of aldosterone are frequently observed after several months of therapy.³ This phenomenon termed ‘aldosterone escape’ is a limiting factor of ACE inhibitors and shows that novel therapeutic concepts combating the effects of elevated aldosterone levels are needed. Two recent clinical studies (RALES and EPHEBUS) demonstrated that treatment with mineralocorticoid receptor antagonists in addition to the standard therapy resulted in a decrease of mortality in patients with chronic congestive heart failure and in patients after myocardial infarction, respectively.^{4,5} The use of spironolactone, however, is accompanied by severe progestational and antiandrogenic side effects due to its affinity to other steroid receptors. Moreover, the elevated plasma aldosterone concentrations are left unaffected on a pathological level which raises several issues. First, the elevated aldosterone plasma levels do not induce a homologous down-regulation but an up-regulation of the aldosterone receptor.⁶ This fact complicates a long-term therapy as MR antagonists are likely to become ineffective. Furthermore, the high concentrations promote nongenomic actions of aldosterone which are in general not blocked by receptor antagonists.⁷ Pathological aldosterone concentrations have been identified to induce a negative inotropic effect in human trabeculae and to potentiate the vasoconstrictor effect of angiotensin II in coronary arteries in rapid, nongenomic manner.⁸ Thus, aldosterone is intrinsically capable to further deteriorate heart function by acting nongenomically.

A novel therapeutic strategy with potential to overcome the drawbacks of MR antagonists is the blockade of aldosterone formation, preferably by inhibiting CYP11B2, the key enzyme of its biosynthesis. Aldosterone synthase has been proposed as a potential pharmacological target by our group as early as 1994,⁹ followed soon thereafter by the hypothesis that inhibitors of CYP11B2 could serve as drugs for the treatment of hyperaldosteronism, congestive heart failure and myocardial fibrosis.^{10,11} Consequent structural optimization of a hit discovered by a compound library screening led to a series of nonsteroidal aldosterone synthase inhibitors with high selectivity toward other cytochrome P450 enzymes.^{12–15}

In the present study, we describe the design and synthesis of a series of 3-benzyl-substituted pyridylnaphthalenes and structurally related compounds (Chart 1) by a combined ligand-based and structure-based drug design approach as well as the determination of their biological activity regarding human CYP11B2 for potency. Selectivity is a prerequisite for a CYP11B2 inhibitor, especially with regard to other cytochrome P450 enzymes as they are likely to interact with other CYP enzymes in a similar way (e.g., by complexation of the heme iron). Taking into consideration that the key enzyme of glucocorticoid biosynthesis, 11 β -hydroxylase (CYP11B1), and CYP11B2 have a sequence homology of approximately 93 %, ¹⁶ the selectivity issue becomes especially critical for the design of CYP11B2 inhibitors. On that account, all compounds were tested for their inhibitory potency versus CYP11B1 to determine their selectivity. A set of compounds was additionally tested for inhibitory activity versus the steroidogenic enzymes CYP17 (17 α -hydroxylase-C17,20-lyase) and CYP19 (aromatase) as well as selected hepatic drug-metabolizing CYP enzymes (CYP1A2, CYP2B6, CYP2C9, CYP2C19, CYP2D6, and CYP3A4).

Chart 1. Title Compounds



Results

Inhibitor Design Concept

In our search for new lead compounds as CYP11B2 inhibitors structurally differing from the previously discovered pyridylnaphthalenes such as **1** and **2**,¹⁴ we identified imidazolylmethylene-substituted flavones (e.g., **3–10**) to be aldosterone synthase inhibitors with moderate to high inhibitory potency by compound library screening (Table 1). These compounds that originally have been described as aromatase inhibitors¹⁷ display CYP11B2 inhibition in a range of 73–94 % at a con-

centration of 500 nM with methoxy-functionalized **6** being most active ($IC_{50} = 11$ nM), albeit without showing selectivity versus the highly homologous CYP11B1 (see supplementary material for selectivity data).

Table 1. Inhibition of Human Adrenal CYP11B2 In Vitro (Compounds **1–10**)

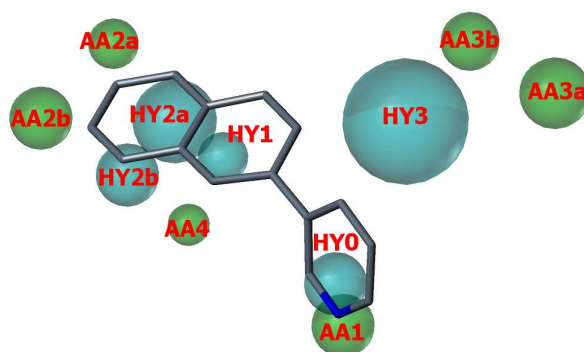
compd	R	% inhibition ^a CYP11B2 ^b	
		[IC ₅₀ (nM)] ^c	
1	H	92	[28]
2	OMe	91	[6.2]
3	H	88	[28]
4	NO ₂	81	[95]
5	Br	90	[25]
6	OMe	94	[11]
7	H	86	[124]
8	Br	80	[n.d.]
9	NO ₂	73	[n.d.]
10		77	[187]

^a Mean value of at least two experiments, standard deviation usually less than 10 %; inhibitor concentration, 500 nM. ^b Hamster fibroblasts expressing human CYP11B2; substrate deoxycorticosterone, 100 nM. ^c Mean value of at least four experiments, standard deviation usually less than 25 %, n.d. = not determined; fadrozole, $IC_{50} = 1$ nM.

Recently, a pharmacophore model for aldosterone synthase inhibitors was built by superimposition of a series of heteroaryl-substituted methyleneindanes^{12,13} and naphthalenes^{14,15} synthesized in our laboratory and subsequently validated by pyridine-substituted acenaphthenes as hybrid structures that fit into the four identified pharmacophoric points (i.e., a heterocyclic nitrogen and three ring centroids).¹⁸ The most potent compounds of the latter substance classes together with the most potent flavone type inhibitors were used as training set for the generation of an extended pharmacophore model by applying the GALAHAD¹⁹ pharmacophore generation module of SYBYL molecular modeling software. In the top ranked pharmacophore model, best in three of the most indicative ranking criteria of this software (Pareto ranking,²⁰ Specificity, and Mol-query), the earlier pharma-

cophoric points¹⁸ were confirmed, namely the hydrophobic features HY0, HY1, HY2a, HY2b as well as the acceptor atom features AA1, AA2a, and AA2b (Figure 1).

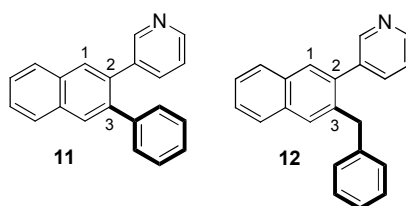
Figure 1^a



^a Compound **1** mapped to the pharmacophore model. The newly identified hydrophobic feature HY3 as well as the acceptor atom features AA3a and AA3b are not exploited by inhibitors with a naphthalene molecular scaffold. Pharmacophoric features are color-coded: Cyan for hydrophobic regions (HY0–HY3) and green for acceptor atom features (AA1–4).

A novel and voluminous hydrophobic area HY3 was identified next to HY1, along with the acceptor atom features AA3a and AA3b (see supplementary material for exact pharmacophore geometric properties) as well as an additional acceptor atom feature AA4. Rationalizing the given information, the two sample compounds **11** and **12** (Chart 2) were designed by modifying our previously reported naphthalene derivatives **1** and **2** to exploit the newly discovered pharmacophoric feature HY3. As suggested by the model and visualized in Figure 1, introduction of a hydrophobic substituent in 3-position of the naphthalene skeleton should be favorable to exploit the voluminous hydrophobic feature HY3 of the pharmacophore. The phenyl residue directly bound to the naphthalene core in compound **11** creates a conformationally constrained structure in which both rotational degrees of freedom of the two aryl–aryl bonds are limited since they are located *ortho* to each other. The benzyl motive in compound **12** leads to an increased flexibility of the spatial property distribution by rotation around the two benzylic carbon–carbon bonds. Furthermore, the aromatic ring moves apart from the naphthalene core by one methylene unit.

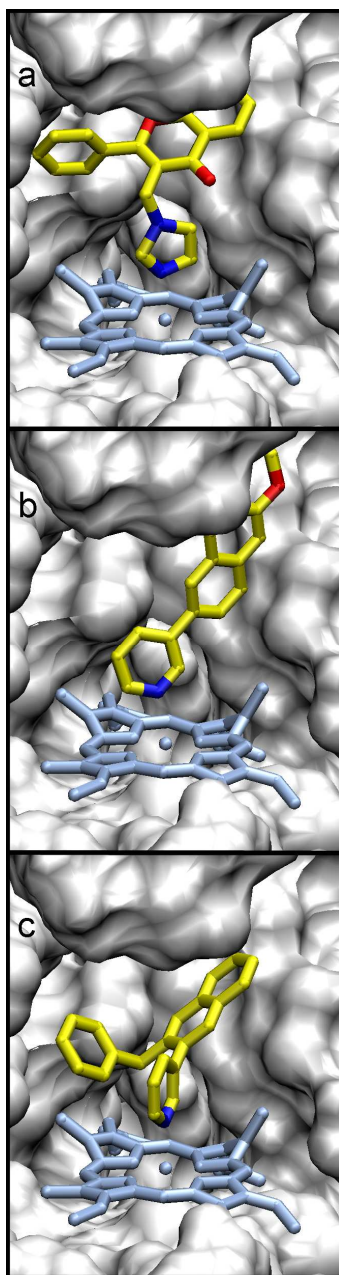
Chart 2. Proposed Lead Structures **11** and **12**



In order to elucidate the role of conformational flexibility and the exact position of the aryl moiety for optimal inhibitor binding, docking studies were performed (Figure 2). For this purpose, we used

the CYP11B2 protein model that has been built¹² and subsequently validated¹³⁻¹⁵ by our group as well as the same docking calculations that have been performed in these studies.

Figure 2^a



^a Structure of the CYP11B2–inhibitor complexes of **3** (a), **2** (b) and **12** (c). Surface of the binding pocket (grey) surrounding the inhibitor and the heme co-factor (light blue). The inhibitors are presented in yellow; nitrogen atoms are colored in blue and oxygen atoms are in red. Unlike **2**, the inhibitors **3** and **12** exploit an additional sub-pocket of the inhibitor binding site.

Previous investigations have identified the binding affinity to the target enzyme to be highly dependent on the geometry of the coordinative bond between the heme iron and the heterocyclic nitrogen. An angle of the Fe–N straight line with the porphyrin plane close to 90° (i.e., the hetero-

cyclic nitrogen lone pair arranges perpendicular to the heme group) provides an optimal orbital overlap corresponding to a high inhibitory potency.^{14,15} The analysis of the docking mode of compound **3** led to the identification of a new sub-pocket which interacts with the aryl moiety (Figure 2a). This sub-pocket was not considered as potential binding site during our previous design efforts due to the fact that the formerly investigated compounds such as **2** did not occupy this binding site (Figure 2b). The above considerations led to the design of compounds **11** and **12**. Both compounds combine the pyridylnaphthalene skeleton of compound **1** with an additional aryl motive which should be able to interact with the newly identified sub-pocket. However, compound **11** proved to be too rigid to fit into the binding site and could thus not be docked successfully into the binding pocket under the given pharmacophore constraint, that is the Fe(heme)-N(ligand) interaction. A directed heme-Fe-N interaction was defined perpendicular to the heme-plane. This pharmacophore constraint was applied to ensure the right binding mode of the inhibitors with the heme-cofactor. The constraint requires the existence of an inhibitor-nitrogen-atom on the surface of an interaction cone with a 20 degree radius, which has its origin at the Fe-atom and points perpendicular to the heme-plane (with a length of 2.2 Å). Obviously, the conformationally restricted phenyl moiety of compound **11** undergoes repulsive interaction with amino acids of the binding pocket or with the heme-cofactor under the above mentioned constraint (i.e., when the pyridine moiety forms a coordinative bond to the heme iron), thus preventing that the molecule successfully docks into the CYP11B2 protein model. Contrariwise, the 3-benzyl substituted analog **12** is more flexible due to an additional methylene spacer between the two ring systems and thus fitted adequately into the binding site (Figure 2c). From these docking results we concluded that the methylene group of the potential inhibitor should provide the flexibility necessary to adapt to the binding site geometry.

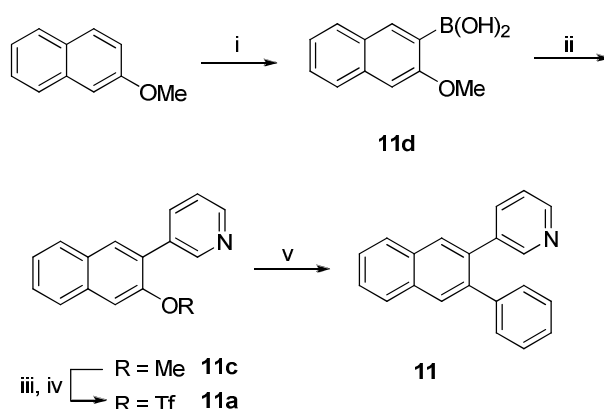
Chemistry

The phenyl-substituted pyridylnaphthalene **11** was obtained as shown in Scheme 1 by two subsequent Suzuki coupling²¹ steps, whereof the first proceeded between 3-bromopyridine and 3-methoxy-2-naphthaleneboronic acid **11d**. The boronic acid **11d** was accessible by *ortho*-lithiation of 2-methoxynaphthalene and in situ addition of trimethylborate as described previously.²² After demethylation of **11c** by refluxing in concentrated hydrobromic acid, the intermediate naphthol was transferred into the triflate **11a** by a microwave-enhanced method described by Bengtson et al.²³ A second Suzuki coupling using controlled microwave heating afforded compound **11**.²⁴

The benzyl-substituted derivatives **12–16**, **19**, and **21–25** were synthesized by the route shown in Scheme 2. Starting from a 3-hydroxy-2-naphthoic acid, few functional group inversions led to the carbaldehydes **12e–14e**. These transformations were performed by a 4-step sequence starting with an esterification²⁵ and subsequent introduction of a protection group to the naphthalene hydroxy group of **12h** and **13h** (i.e., methyl in **12g** or benzyl in **13g** and **14g**).²⁶ Lithium borohydride reduction²⁷ followed by TEMPO oxidation²⁸ (of primary alcohol **12f**) or Parik-Doehring oxidation²⁹ (of **13f** and

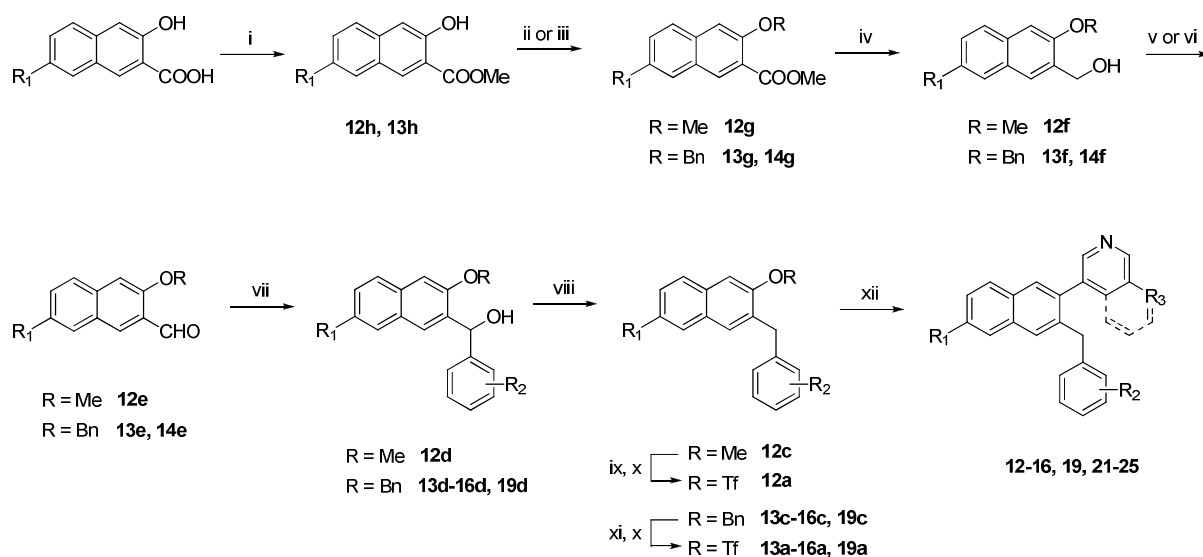
14f) afforded the corresponding carbaldehydes **12e–14e**. Grignard reaction with various substituted phenylmagnesium halogenides afforded the phenyl-naphthylalcohols **12d–16d**, and **19d**. Hydrogenolytic removal of the hydroxy group was accomplished by treatment with NaBH₄ and AlCl₃ in refluxing THF.³⁰ After deprotection using BBr₃ (for de-methylation of **12c**) or ammonium formate under Pd-catalysis³¹ (for de-benzylation of **13c–16c**, and **19c**) and subsequent triflate formation,²³ the heterocycle was introduced by microwave-enhanced Suzuki coupling²⁴ giving rise to the benzyl-substituted pyridynaphthalenes **12–16**, **19**, and **21–25**.

Scheme 1^a



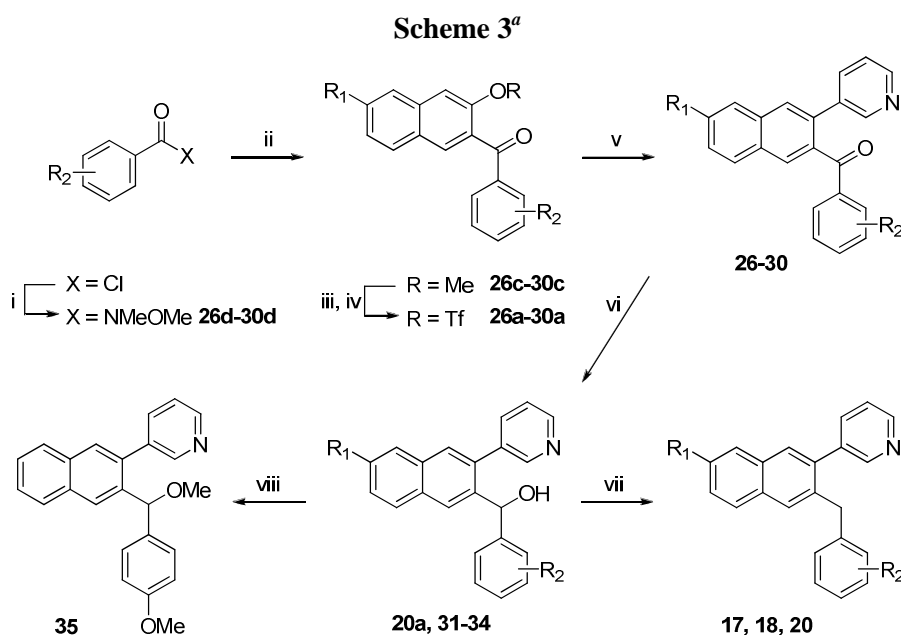
^a Reagents and conditions: i) *n*BuLi, B(OMe)₃, THF, -78 °C, then HCl/water; ii) 3-bromopyridine, Pd(PPh₃)₄, toluene/ethanol, aq. Na₂CO₃, reflux; iii) conc. HBr, reflux; iv) Tf₂NPh, K₂CO₂, THF, μw, 120 °C; v) phenylboronic acid, Pd(PPh₃)₄, aq. NaHCO₃, DMF, μw, 150 °C.

Scheme 2^a



^a Reagents and conditions: i) methanol, H₂SO₄, reflux; ii) MeI, K₂CO₃, 18-crown-6, acetone, reflux (for R = Me); iii) BnBr, K₂CO₃, 18-crown-6, acetone, reflux (for R = Bn); iv) LiBH₄, THF/toluene, reflux; v) NCS, TEMPO, *n*Bu₄NCl, aq. Na₂CO₃/NaHCO₃, CH₂Cl₂; rt (for R = Me); vi) SO₃py, NEt₃, DMSO, rt (for R = Bn); vii) ArMgX, THF, 0 °C, then aq. NH₄Cl; viii) NaBH₄, AlCl₃, THF, reflux; ix) BBr₃, CH₂Cl₂, -20 °C; x) Tf₂NPh, K₂CO₂, THF, μw, 120 °C; xi) ammonium formate, Pd/C, THF/methanol, reflux; xii) heteroarylboronic acid, Pd(PPh₃)₄, aq. NaHCO₃, DMF, μw, 150 °C.

Alternatively, the benzyl-substituted pyridylnaphthalenes **17**, **18**, and **20** were obtained by the route shown in Scheme 3. Applying the presented transformations afforded the benzoyl-substituted derivatives **26–30** and the corresponding hydroxymethylene analogues **31–34** as reaction intermediates. The sequence toward the 3-benzoyl-substituted 2-naphthols **26b–30b** was reported previously by Li et al. and starts with an *ortho*-lithiation of 2-methoxy- or 2,7-dimethoxynaphthalene, followed by in situ addition of a Weinreb amide. Regioselective demethylation of the obtained methanones **26c–30c** at the naphthalene-position *ortho* to the benzoyl residue was accomplished by treatment with $\text{BCl}_3/n\text{Bu}_4\text{NI}$ at $-78\text{ }^\circ\text{C}$.³² After triflate formation, a 3-pyridyl residue was introduced by Suzuki coupling to afford compounds **26–30**. The corresponding alcohols **20a** and **31–34** were obtained by sodium borohydride reduction. The methyl ether **35** was synthesized by treating **31** with methyl iodide and NaH in THF. The benzyl-substituted pyridylnaphthalenes **17**, **18**, and **20** were obtained by in situ iodotrimethylsilane mediated reduction.^{33,34} However, reduction by this method did not succeed in the case of **32**, neither by other commonly used hydrogenolysis protocols.^{30,35}



^a Reagents and conditions: i) *N,O*-dimethylhydroxylamine hydrochloride, NEt_3 , CH_2Cl_2 , rt; ii) *n*BuLi, 2-methoxynaphthalene (for $\text{R}_1 = \text{H}$) or 2,7-dimethoxynaphthalene (for $\text{R}_1 = \text{OMe}$), TMEDA, THF, $-78\text{ }^\circ\text{C}$, then HCl/water; iii) BCl_3 , *n*Bu₄NI, CH_2Cl_2 , $-78\text{ }^\circ\text{C}$ to rt; iv) TiF_2O , pyridine, CH_2Cl_2 , $0\text{ }^\circ\text{C}$; v) pyridineboronic acid, $\text{Pd}(\text{PPh}_3)_4$, aq. Na_2CO_3 , toluene/ethanol, reflux; vi) NaBH_4 , methanol, $0\text{ }^\circ\text{C}$; vii) Me_3SiCl , NaI, CH_3CN , $55\text{ }^\circ\text{C}$; viii) MeI, NaH, THF, rt.

Biological Results

Inhibition of Human Adrenal Corticoid Producing CYP11B2 and CYP11B1 In Vitro (Table 2). The inhibitory activities of the compounds were determined in V79 MZh cells expressing either human CYP11B2 or CYP11B1.^{10,36} The V79 MZh cells were incubated with [¹⁴C]-deoxycorticosterone as substrate and the inhibitor in different concentrations. The product formation was monitored by HPTLC using a phosphoimager. Fadrozole, an aromatase (CYP19) inhibitor with proven ability to

reduce corticoid formation in vitro³⁷ and in vivo³⁸ was used as a reference (CYP11B2, IC₅₀ = 1 nM; CYP11B1, IC₅₀ = 10 nM).

Table 2. Inhibition of Human Adrenal CYP11B2 and CYP11B1 In Vitro (Compounds **11–35**)

						% inhibition ^a		IC ₅₀ value ^b (nM)			
						V79 11B2 ^c		V79 11B2 ^c		V79 11B1 ^d	
compd	R ₁	R ₂	R ₃	R	hCYP11B2	hCYP11B2	hCYP11B2	hCYP11B1	selectivity	factor ^e	
11					8	n.d.	n.d.	n.d.	n.d.		
12	H	H	H	H	76	154	953	6			
13	6-OMe	H	H	H	85	53	640	12			
14	H	<i>o</i> -OMe	H	H	24	n.d.	n.d.	n.d.			
15	H	<i>m</i> -OMe	H	H	62	n.d.	n.d.	n.d.			
16	H	<i>p</i> -OMe	H	H	89	7.8	2804	359			
17	H	<i>p</i> -CN	H	H	93	2.7	1956	724			
18	H	<i>p</i> -OCF ₃	H	H	95	3.9	3559	913			
19	6-OMe	<i>p</i> -OMe	H	H	95	11	4329	394			
20	7-OMe	<i>p</i> -OMe	H	H	35	n.d.	n.d.	n.d.			
21	H	<i>p</i> -OMe	OMe	H	93	7.7	1811	235			
22	6-OMe	<i>p</i> -OMe	OMe	H	96	7.6	2452	322			
23	6-OMe	H	OMe	H	90	24	2936	122			
24	H				98	3.0	785	262			
25	OMe				94	5.0	735	147			
26	H	<i>p</i> -OMe	H		79	119	24003	202			
27	H	<i>m</i> -F- <i>p</i> -OMe	H		78	65	19816	305			
28	H	<i>p</i> -CN	H		88	30	9639	321			
29	H	<i>p</i> -OCF ₃	H		91	28	11307	404			
30	OMe	<i>p</i> -OMe	H		25	n.d.	n.d.	n.d.			
31	H	<i>p</i> -OMe	H	OH	57	n.d.	n.d.	n.d.			
32	H	<i>m</i> -F- <i>p</i> -OMe	H	OH	51	n.d.	n.d.	n.d.			
33	H	<i>p</i> -CN	H	OH	59	n.d.	n.d.	n.d.			
34	H	<i>p</i> -OCF ₃	H	OH	63	n.d.	n.d.	n.d.			
35	H	<i>p</i> -OMe	H	OMe	23	n.d.	n.d.	n.d.			
fadrozole					-	1	10	10			

^a Mean value of at least two experiments, standard deviation usually less than 10 %; inhibitor concentration, 500 nM. ^b Mean value of at least four experiments, standard deviation usually less than 25 %, n.d. = not determined. ^c Hamster fibroblasts expressing human CYP11B2; substrate deoxycorticosterone, 100 nM. ^d Hamster fibroblasts expressing human CYP11B1; substrate deoxycorticosterone, 100 nM. ^e IC₅₀ CYP11B1/IC₅₀ CYP11B2, n.d. = not determined.

Compound **11** with a phenyl residue directly bound to the naphthalene core shows no significant activity at the target enzyme with only 8 % inhibition at an inhibitor concentration of 500 nM (Table

2). Insertion of a methylene linker into the biaryl bond results in an increased inhibitory potency at CYP11B2 in compound **12** ($IC_{50} = 154$ nM). Introduction of a methoxy residue in *ortho*- or *meta*-position of the benzylic moiety as accomplished in compounds **14** and **15** results in a significantly decreased inhibitory potency whereas the same substituent in *para*-position gives rise to the highly potent CYP11B2 inhibitor **16** ($IC_{50} = 7.8$ nM) with pronounced selectivity versus CYP11B1 ($IC_{50} = 2804$). The cyano and trifluoromethoxy-substituted analogues **17** and **18** are highly potent as well and about 700-fold and 900-fold more selective for CYP11B2. Derivatization of the naphthalene core by a methoxy group is readily tolerated in 6-position as accomplished in compounds **13**, **19**, **22**, **23**, and **25**. The inhibitory profile of the 6-methoxy derivatives regarding the two CYP11B isoforms is thereby comparable to the corresponding hydrogen analogues with a slightly increased selectivity factor in most cases. On the other hand, introduction of methoxy in 7-position results in a decrease of the inhibition to less than 40 % at an inhibitor concentration of 500 nM (**20** and **30**). Modification of the pyridine moiety which has recently been shown to increase the activity and selectivity of naphthalene type CYP11B2 inhibitors³⁹ affords compounds **21–25** with IC_{50} values in the range of 3–24 nM. Replacing the methylene linker by a carbonyl group as accomplished in compounds **26–29** results in a slightly reduced inhibitory potency ($IC_{50} = 16–118$ nM), albeit the high CYP11B1 selectivity is retained (factor 200–500). Introducing hydroxymethylene (**31–34**) or methoxymethylene (**35**) as linker between the aryls leads to a significant loss of inhibitory activity to approximately 60 % at an inhibitor concentration of 500 nM in the case of compounds **31–34** and to an almost complete loss in the case of compound **35**.

Inhibition of Steroidogenic and Hepatic CYP Enzymes (Tables 3 and 4). A set of 12 compounds was investigated for inhibition of the steroidogenic enzymes CYP17 and CYP19 (Table 3). The inhibition of CYP17 was investigated using the 50,000 g sediment of the *E. coli* homogenate recombinantly expressing human CYP17 and progesterone (25 μ M) as substrate.⁴⁰ The inhibition values were measured at an inhibitor concentration of 2 μ M. In general, the compounds show no or only little inhibition of less than 25 %. As an exception, compound **22** exhibits 51 % inhibition which is in the range of the reference ketoconazole ($IC_{50} = 2780$ nM). The inhibition of CYP19 at an inhibitor concentration of 500 nM was determined in vitro with human placental microsomes and [1β -³H]androstenedione as substrate as described by Thompson and Siiteri⁴¹ using our modification.⁴² Most of the compounds display only a moderate aromatase inhibition of less than 40 % whereof four compounds do not inhibit CYP19 at all (**21**, **24**, **25**, and **28**). The *para*-cyano-substituted derivative **17** shows a pronounced activity (60 %) and introduction of methoxy in 6-position of the naphthalene core as accomplished in compounds **19**, **22**, and **23** results likewise in a remarkably increased inhibition. Most notably, compound **19** is a highly potent CYP19 inhibitor exhibiting an IC_{50} value of 38 nM, thus being almost as active as the reference fadrozole ($IC_{50} = 30$ nM).

Table 3. Inhibition of Human CYP17 and CYP19 In Vitro

compd	% inhibition ^a		compd	% inhibition ^a	
	CYP17 ^b	CYP19 ^c		CYP17 ^b	CYP19 ^c
16	< 5	39	23	26	73
17	25	60	24	< 5	< 5
18	10	45	25	21	6
19	< 5	92 ^d	26	5	19
21	28	6	28	7	< 5
22	51	49	29	8	17

^a Mean value of three experiments, standard deviation usually less than 10 %. ^b *E. coli* expressing human CYP17; substrate progesterone, 25 μ M; inhibitor concentration, 2.0 μ M; ketoconazole, IC₅₀ = 2.78 μ M. ^c Human placental CYP19; substrate androstenedione, 500 nM; inhibitor concentration, 500 nM; fadrozole, IC₅₀ = 30 nM. ^d IC₅₀ = 38 nM.

A selectivity profile relating to inhibition of crucial hepatic CYP enzymes (CYP1A2, CYP2B6, CYP2C9, CYP2C19, CYP2D6, and CYP3A4) was determined for compounds **16**, **17**, **19**, and **28** by use of recombinantly expressed enzymes from baculovirus-infected insect microsomes. Table 4 shows the inhibition at a concentration of 10 μ M and 1 μ M. It becomes apparent that some enzymes are affected only to a minor degree by all compounds including CYP2B6 and CYP2D6. On the other hand, CYP2C9 is strongly inhibited in most cases. The benzoyl derivative **28** with less than 40 % inhibition at 1 μ M concentration at all CYP enzymes is the most selective compound within this series. The worst selectivity profile is observed in the case of **19** inhibiting CYP2C9, CYP2C19, and CYP3A4 with pronounced potency.

Table 4. Inhibition of Selected Hepatic CYP Enzymes In Vitro

compd	% inhibition ^a											
	CYP1A2 ^{b,c}		CYP2B6 ^{b,d}		CYP2C9 ^{b,e}		CYP2C19 ^{b,f}		CYP2D6 ^{b,g}		CYP3A4 ^{b,h}	
	10 μ M	1 μ M	10 μ M	1 μ M	10 μ M	1 μ M	10 μ M	1 μ M	10 μ M	1 μ M	10 μ M	1 μ M
16	77	23	48	< 5	92	51	32	< 5	6	< 5	79	30
17	83	41	69	24	96	78	87	62	62	23	17	9
19	59	13	61	8	98 ⁱ	96 ⁱ	96	74	7	< 5	89	60
28	47	22	43	14	74	35	43	< 5	51	23	62	23

^a Mean value of two experiments, standard deviation usually less than 10 %. ^b Recombinantly expressed enzymes from baculovirus-infected insect microsomes (Supersomes). ^c Furafylline, IC₅₀ = 2.42 μ M. ^d Tranylcypromine, IC₅₀ = 6.24 μ M. ^e Sulfaphenazole, IC₅₀ = 318 nM. ^f Tranylcypromine, IC₅₀ = 5.95 μ M. ^g Quinidine, IC₅₀ = 14 nM. ^h Ketoconazole, IC₅₀ = 57 nM. ⁱ IC₅₀ = 64 nM.

Discussion and Conclusion

The inhibitor design concept of the present study triggered the synthesis of compounds **11** and **12** as potential new lead structures by extending a previously established naphthalene molecular scaffold via introduction of a phenyl or benzyl residue in 3-position. Subsequently, docking studies in our CYP11B2 protein model were performed in order to check for spatial consistency with the pharmacophore hypothesis. It was found that while phenyl-substituted **11** did not dock under the given pharmacophore constraint (Fe(heme)-N(ligand) interaction), benzyl-substituted **12** adequately fits into

the binding site by exploiting a previously unexplored sub-pocket. These findings were confirmed by experimental results showing that 3-phenyl-substituted pyridylnaphthalene **11** exhibits no significant CYP11B2 inhibition in vitro. In accordance with the docking results, benzyl analog **12** is a moderately potent aldosterone synthase inhibitor ($IC_{50} = 154$ nM). The selectivity versus CYP11B1, however, is rather poor with an only 6-fold increased IC_{50} value compared to CYP11B2. The following lead optimization was accomplished by considering the SAR results obtained previously from the structures of the known inhibitors which have been used for the generation of the pharmacophore model (e.g., **1–10**). Methoxy substitution in compound **6** afforded the most active compound of the flavone series ($IC_{50} = 11$ nM) and was therefore chosen as a model substituent to figure out the optimal substituent position in the benzyl moiety of **12**. In case of the pyridylnaphthalenes, methoxy in 6-position as accomplished in **2** proved to be favorable in terms of both inhibitory potency and selectivity.¹⁴

Within the present set of compounds, interesting structure-activity and structure-selectivity relationships can be observed, particularly with regard to the benzyl and the naphthalene moieties. The benzylic part of the investigated molecules represents a pivotal region for structural optimization and is to a great extent dependent on the position of substituents in terms of both inhibitory activity and selectivity toward the highly homologous CYP11B1. Placing methoxy in *ortho*- or *meta*-position of the benzyl residue significantly reduces the inhibitory potency. Most notably, the inhibition decreases to 24 % at an inhibitor concentration of 500 nM in case of *ortho*-methoxy-derivatized compound **14**. Contrariwise, methoxy in *para*-position as accomplished in compound **16** increases the CYP11B2 activity by a factor of 20 compared to the hydrogen analog **12** and the selectivity toward CYP11B1 clearly improves (selectivity factor = 359). The experimental observations can be explained by the docking results of compounds **16** and **19**, both bearing a *para*-methoxy group (Figure 3). The introduction of this substituent into the benzyl moiety as accomplished in **16** leads to interactions of the compound with the residues of Pro452, Val339, and Thr279, thus stabilizing the complex formed by coordination of the heme iron by the heterocyclic nitrogen considerably (Figure 3a). In compound **19**, a second methoxy group was introduced at the 6-position of the naphthalene scaffold (Figure 3b). This leads to no additional stabilization of the complex, but to a slightly increased selectivity versus CYP11B1. The same trend was observed previously for the binding properties of a series of substituted pyridylnaphthalenes.^{14,15} The *para*-cyano and *para*-trifluoromethoxy derivatives **17** and **18** are likewise highly potent and display IC_{50} values of 2.7 nM and 3.9 nM, respectively, which corroborates the importance of *para*-substitution for activity. Keeping in mind the high homology of the two CYP11B isoforms, the selectivity factors relating to CYP11B1 inhibition of the latter compounds are particularly noteworthy. Compound **17** displays an approximately 700-fold and compound **18** a 900-fold stronger inhibition of CYP11B2 versus CYP11B1.

Figure 3.

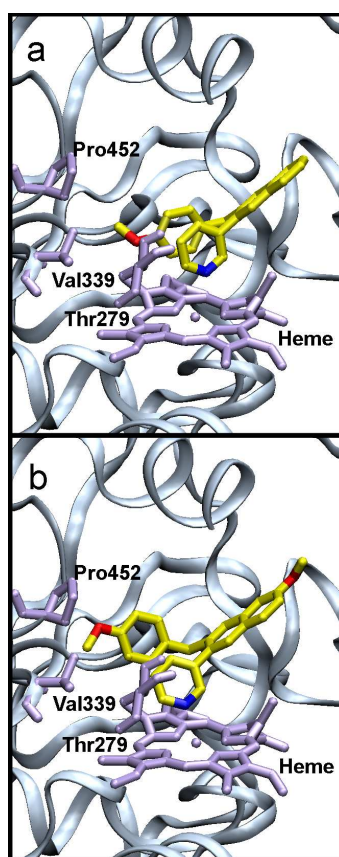
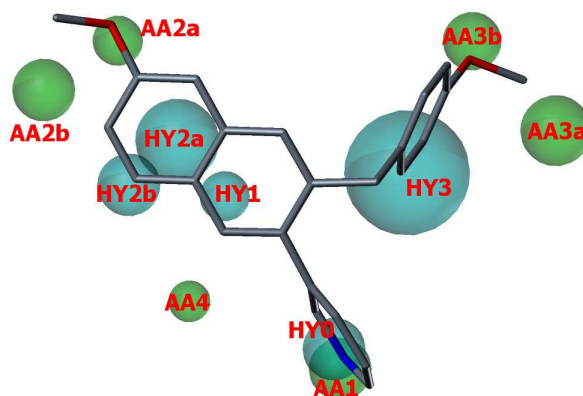


Figure 3. Structure of the CYP11B2 binding pocket with the docked inhibitors **16** (a) and **19** (b). Details of the active site, showing inhibitor, heme co-factor and the interacting residues of Pro452, Val339, and Thr279.

In the naphthalene molecular scaffold, introduction of a methoxy substituent in 7-position results in a decreased inhibitory potency (**20**, **30**) whereas the same substituent is readily tolerated in 6-position and even slightly increases the CYP11B1 selectivity in most cases. Figure 4 shows the 6-methoxy substituted derivative **19** mapped to the pharmacophore model. It is obvious that this compound nearly perfectly exploits both the well known (HY0, HY1, HY2a, AA1, AA2a) and the newly identified (HY3, AA3b) interaction areas which is reflected by the high inhibitory potency of this compound and underlines the predictive power of our pharmacophore hypothesis.

The *para*-methoxy group in the benzyl moiety of **19** which has been found to be responsible for both high inhibitory activity at CYP11B2 and selectivity versus CYP11B1 fits to the acceptor atom feature AA3b. Hence, targeting this interaction area is a promising strategy in the future design of potent and selective aldosterone synthase inhibitors. With respect to the selectivity profile relating to inhibition of several other CYP enzymes, it becomes apparent that 6-methoxylation endows the benzylnaphthalenes with an increased inhibitory potency at CYP19 as in the case of compounds **19**, **22**, and **23**, for example 6-methoxy derivative **19** is a highly potent CYP19 inhibitor displaying an activity similar to fadrozole. In addition, the latter compound strongly inhibits several hepatic CYP enzymes (i.e., CYP2C9, CYP2C19, and CYP3A4).

Figure 4.



Compound **19** shows an enhanced fit to the pharmacophore hypothesis compared to **1** by additionally exploiting the features HY3 and AA3b. Pharmacophoric features are color-coded: Cyan for hydrophobic regions (HY0–HY3) and green for acceptor atom features (AA1–4).

Varying the substitution pattern of the pyridine site induces no distinct changes of the CYP11B2 potency in case of **21** and **22**. Again, 6-methoxylation in compound **22** increases the selectivity versus CYP11B1 compared to **21**. A slightly decreased selectivity versus CYP11B1 is observable in case of the isoquinoline derivatives **24** and **25** due to a moderate increase in CYP11B1 potency ($IC_{50} < 1000$ nM) which corresponds to previously observed results within the pyridynaphthalene series.³⁹ Contrary to the finding that 6-methoxylation effects a slightly improved selectivity (as shown in previous studies^{14,15} and observed in case of compounds **13**, **19**, and **22** compared to **12**, **16**, and **21**), the 6-methoxynaphthalene compound **25** is less selective than the hydrogen analog **24**. Derivatization of the methylene linker in compounds **26–35** leads to a decrease in inhibitory potency. The carbonyl analogues **26**, **28**, and **29** are slightly less active than their methylene analogues. On the other hand, CYP11B1 inhibition is reduced to the same degree and the high selectivity is maintained. Again, *para*-trifluoromethoxy has the strongest effect on the inhibitory discrimination between the two CYP11B isoforms and derivative **29** is approximately 400-fold less active at CYP11B1 compared to CYP11B2. In case of the *para*-cyanobenzoyl compound **28**, a decreased inhibition of the sex-hormone producing CYP17, CYP19 as well as the hepatic CYP1A2, CYP2B6, CYP2C9, CYP2C19, and CYP2D6 enzymes is found compared to the benzyl analog **17**, thus providing an advantageous overall CYP selectivity profile for this compound. Other variations of the methylene moiety as accomplished in the hydroxy- and methoxymethylene derivatives **30–35** lead to a pronounced decrease of inhibitory activity compared to the unsubstituted analogues. These compounds display 51–63 % inhibition at an inhibitor concentration of 500 nM in case of hydroxy substitution (**30–34**) and only 23 % in case of methoxy substitution (**35**). Obviously, the decrease in potency with increasing substituent size (hydrogen < carbonyl < hydroxy < methoxy) reflects the increase of steric repulsion between the aryl–aryl spacer and the enzyme parts (i.e., Leu343 and heme co-factor) separating the naphthalene binding site from the sub-pocket interacting with the benzyl residue.

In summary, it has been shown that our CYP11B2 pharmacophore model has predictive power to identify prospective lead structures. Based on the results of the pharmacophore model, a new class of pyridylnaphthalene derivatives with extended carbocyclic skeleton was synthesized. Derivatives with *para*-functionalized benzyl moiety in 3-position of the naphthalene molecular scaffold thoroughly satisfied the spatial constraints imposed by the pharmacophore model and turned out to be highly potent aldosterone synthase inhibitors. The most active compound, *para*-cyanobenzyl derivative **17**, displayed nanomolar potency at the target enzyme ($IC_{50} = 2.7$ nM). In addition, docking studies using our CYP11B2 protein model proved to be a useful tool to estimate the inhibitory properties of proposed new molecules and to explain structure-activity relationships. The binding behavior of compounds **11** and **12** was adequately predicted by the docking results. Furthermore, it was shown that the high inhibitory potency of the *para*-substituted derivative **16** is the outcome of stabilizing interactions with the residues of Pro452, Val339, and Thr279. The selectivity versus CYP11B1 (up to a factor of 900) which is especially remarkable with respect to the high homology of the two CYP11B isoforms was found to be a consequence of *para*-substitution and hence of exploiting the AA3b pharmacophoric feature as well. Currently, further studies are underway to evaluate selected compounds for their *in vivo* properties.

Experimental Section

Chemical and Analytical Methods. Melting points were measured on a Mettler FP1 melting point apparatus and are uncorrected. 1H NMR and ^{13}C spectra were recorded on a Bruker DRX-500 instrument. Chemical shifts are given in parts per million (ppm), and tetramethylsilane (TMS) was used as internal standard for spectra obtained in $DMSO-d_6$ and $CDCl_3$. All coupling constants (J) are given in Hertz. Mass spectra (LC/MS) were measured on a TSQ Quantum (Thermo Electron Corporation) instrument with a RP18 100-3 column (Macherey Nagel) and with water/acetonitrile mixtures as eluents. Elemental analyses were carried out at the Department of Chemistry, University of Saarbrücken. Reagents were used as obtained from commercial suppliers without further purification. Solvents were distilled before use. Dry solvents were obtained by distillation from appropriate drying reagents and stored over molecular sieves. Flash chromatography was performed on silica gel 40 (35/40–63/70 μ M) with petroleum ether/ethyl acetate mixtures as eluents, and the reaction progress was determined by thin-layer chromatography analyses on Alugram SIL G/UV254 (Macherey Nagel). Visualization was accomplished with UV light and $KMnO_4$ solution. All microwave irradiation experiments were carried out in a CEM-Discover monomode microwave apparatus.

The following compounds were prepared according to previously described procedures: 3-(3-methoxynaphthalen-2-yl)pyridine (**11c**),¹⁴ (3-methoxynaphthalen-2-yl)boronic acid (**11d**),²² methyl 3-methoxynaphthalene-2-carboxylate (**12g**),²⁶ methyl 3-hydroxynaphthalene-2-carboxylate (**12h**),²⁵ (3-hydroxynaphthalen-2-yl)(4-methoxyphenyl)methanone (**26b**),³² (3-methoxynaphthalen-2-yl)(4-

methoxyphenyl)methanone (**26c**),³² *N*,4-Dimethoxy-*N*-methylbenzamide (**26d**),³² 4-[(3-hydroxynaphthalen-2-yl)carbonyl]benzotrile (**28b**),³² 4-[(3-mehoxynaphthalen-2-yl)carbonyl]benzotrile (**28c**),³² 4-Cyano-*N*-methoxy-*N*-methylbenzamide (**28d**).³²

Synthesis of the Target Compounds

Procedure A.²⁴ Boronic acid (0.75 mmol, 1 equivalent), aryl bromide or -triflate (0.9–1.3 equivalents), and tetrakis(triphenylphosphane)palladium(0) (43 mg, 37.5 μ mol, 5 mol %) were suspended in 1.5 mL DMF in a 10 mL septum-capped tube containing a stirring magnet. To this was added a solution of NaHCO₃ (189 mg, 2.25 mmol, 3 equivalents) in 1.5 mL water and the vial was sealed with a Teflon cap. The mixture was irradiated with microwaves for 15 min at a temperature of 150 °C with an initial irradiation power of 100 W. After the reaction, the vial was cooled to 40 °C, the crude mixture was partitioned between ethyl acetate and water and the aqueous layer was extracted three times with ethyl acetate. The combined organic layers were dried over MgSO₄ and the solvents were removed in vacuo. The coupling products were obtained after flash chromatography on silica gel (petroleum ether/ethyl acetate mixtures) and/or crystallization. If an oil was obtained, it was dissolved in diethyl ether/methanol and tranferred into the hydrochloride salt by 1N HCl solution in isopropanol/diethyl ether, followed by filtration and optional crystallization from acetone. Analytical data refer to the free base unless otherwise noted.

Procedure B. Boronic acid (1 equivalent), aryl bromide or -triflate (1.3–1.5 equivalents), and tetrakis(triphenylphosphane)palladium(0) (5 mol %) were suspended in toluene/ethanol 4/1 to give a 0.07–0.1 M solution of boronic acid under an atosphere of nitrogen. To this was added a 1 N aqueous solution of Na₂CO₃ (6 equivalents). The mixture was then refluxed for 12–18 h, cooled to room temperature, diluted with water and extracted several times with ethyl acetate. The combined extracts were dried over MgSO₄, concentrated and purified by flash chromatography on silica gel (petroleum ether/ethyl acetate mixtures) and/or crystallization. If an oil was obtained, it was dissolved in diethyl ether/methanol and tranferred into the hydrochloride salt by 1N HCl solution in isopropanol/diethyl ether, followed by filtration and optional crystallization from acetone. Analytical data refer to the free base unless otherwise noted.

Procedure C.^{33,34} To a 0.6 M solution of NaI (6 equivalents) in acetonitrile was added chlorotrimethylsilane (6 equivalents) at room temperature, and the mixture was stirred for 30 min before cooling to 0 °C with an ice-water bath. Then, a 1 M solution of the phenylnaphthylalcohol (1 equivalent) in acetonitrile was added dropwise. After complete addition the mixture was heated at 55 °C for 3 h. After recooling to room temperature, the reaction was quenched by addition of saturated aqueous NaHCO₃ solution. The layers were separated, and the aqueous layer extracted twice with ethyl acetate The combined organic layers were washed with a solution of Na₂S₂O₃, water and brine. The extracts were dried over MgSO₄, concentrated and purified by flash chromatography on silica gel (petroleum ether/ethyl acetate mixtures). If an oil was obtained, it was dissolved in diethyl ether/methanol and tranferred into the hydrochloride salt by 1N HCl solution in isopropanol/diethyl

ether, followed by filtration and optional crystallization from acetone. Analytical data refer to the free base unless otherwise noted.

Procedure D. To a 0.05 M solution of benzoynaphthalene in dry methanol was added sodium borohydride (2 equivalents) at such a rate as to maintain the internal reaction temperature below 5 °C. The reaction mixture was stirred for 1 h, diluted with diethylether and treated with saturated aqueous NaHCO₃ solution. The mixture was then extracted three times with ethyl acetate, washed twice with saturated aqueous NaHCO₃ solution and once with brine and dried over MgSO₄. The filtrate was concentrated in vacuo, and the residue was flash chromatographed on silica gel (petroleum ether/ethyl acetate mixtures) to afford the corresponding alcohols.

3-(3-Phenyl-naphthalen-2-yl)pyridine (11) was obtained according to procedure A from **11a** (657 mg, 1.86 mmol) and phenylboronic acid (854 mg, 4.00 mmol) after flash chromatography on silica gel (petroleum ether/ethyl acetate, 7/3, *R_f* = 0.22) as a colorless oil (195 mg, 0.69 mmol, 37 %), precipitation of the hydrochloride salt afforded a highly hygroscopic solid, mp (HCl salt) 106–109 °C. MS *m/z* 282.70 (MH⁺). Anal. (C₂₁H₁₅N·HCl·1.5H₂O) C, H, N.

3-(3-Benzyl-naphthalen-2-yl)pyridine (12) was obtained according to procedure A from **12a** (433 mg, 1.18 mmol) and 3-pyridineboronic acid (105 mg, 0.85 mmol) after flash chromatography on silica gel (petroleum ether/ethyl acetate, 4/1, *R_f* = 0.19) as a colorless oil (186 mg, 0.63 mmol, 74 %), mp (HCl salt) 197–198 °C. MS *m/z* 296.14 (MH⁺). Anal. (C₂₂H₁₇N·HCl·0.6H₂O) C, H, N.

3-(3-Benzyl-6-methoxynaphthalen-2-yl)pyridine (13) was obtained according to procedure A from **13a** (462 mg, 1.17 mmol) and 3-pyridineboronic acid (100 mg, 0.81 mmol) after flash chromatography on silica gel (petroleum ether/ethyl acetate, 4/1, *R_f* = 0.18) as a colorless oil (196 mg, 0.60 mmol, 74 %), mp (HCl salt) 170–172 °C. MS *m/z* 326.09 (MH⁺). Anal. (C₂₃H₁₉NO·HCl·0.6H₂O) C, H, N.

3-[3-(2-Methoxybenzyl)naphthalen-2-yl]pyridine (14) was obtained according to procedure A from **14a** (462 mg, 1.17 mmol) and 3-pyridineboronic acid (100 mg, 0.81 mmol) after flash chromatography on silica gel (petroleum ether/ethyl acetate, 7/3, *R_f* = 0.26) as colorless oil (161 mg, 0.50 mmol, 61 %), mp (HCl salt) 214–216 °C. MS *m/z* 326.02 (MH⁺). Anal. (C₂₃H₁₉NO·HCl·0.6H₂O) C, H, N.

3-[3-(3-Methoxybenzyl)naphthalen-2-yl]pyridine (15) was obtained according to procedure A from **15a** (433 mg, 1.09 mmol) and 3-pyridineboronic acid (92 mg, 0.75 mmol) after flash chromatography on silica gel (petroleum ether/ethyl acetate, 4/1, *R_f* = 0.13) as a colorless oil (162 mg, 0.50 mmol, 66 %), mp (HCl salt) 161–162 °C. MS *m/z* 326.02 (MH⁺). Anal. (C₂₃H₁₉NO·HCl·0.6H₂O) C, H, N.

3-[3-(4-Methoxybenzyl)naphthalen-2-yl]pyridine (16) was obtained according to procedure A from **16a** (476 mg, 1.20 mmol) and 3-pyridineboronic acid (92 mg, 0.75 mmol) after flash chromatography on silica gel (petroleum ether/ethyl acetate, 4/1, *R_f* = 0.14) as a colorless oil (199 mg, 0.56 mmol, 75 %), mp (HCl salt) 180–182 °C. ¹H-NMR (500 MHz, CDCl₃): δ = 3.75 (s, 3H), 4.00 (s,

2H), 6.72 (d, $^3J = 8.8$ Hz, 2H), 6.82 (d, $^3J = 8.8$ Hz, 2H), 7.26 (ddd, $^3J = 7.9$ Hz, $^3J = 4.7$ Hz, $^5J = 0.9$ Hz, 1H), 7.45–7.52 (m, 3H), 7.68 (s, 1H), 7.70 (s, 1H), 7.79–7.83 (m, 2H), 8.55 (dd, $^4J = 2.2$ Hz, $^5J = 0.9$ Hz, 1H), 8.59 (dd, $^3J = 4.7$ Hz, $^4J = 1.9$ Hz, 1H). $^{13}\text{C-NMR}$ (125 MHz, CDCl_3): $\delta = 39.0, 55.2, 113.7, 122.7, 126.0, 126.4, 127.3, 127.6, 128.9, 129.4, 129.7, 132.0, 132.4, 133.1, 136.6, 137.06, 137.13, 148.2, 149.9, 157.9$. MS m/z 326.16 (MH^+). Anal. ($\text{C}_{23}\text{H}_{19}\text{NO}\cdot\text{HCl}\cdot 0.6\text{H}_2\text{O}$) C, H, N.

4-(3-Pyridin-3-yl-naphthalen-2-ylmethyl)benzotrile (17) was obtained according to procedure C from **33** (841 mg, 2.50 mmol), sodium iodide (2.25 g, 15.0 mmol) and chlorotrimethylsilane (1.63 g, 15.0 mmol) after flash chromatography on silica gel (petroleum ether/ethyl acetate, 7/3, $R_f = 0.15$) as a colorless oil (486 mg, 1.52 mmol, 61 %), mp (HCl salt) 130–131 °C. MS m/z 321.33 (MH^+). Anal. ($\text{C}_{23}\text{H}_{16}\text{N}_2\cdot\text{HCl}\cdot 0.8\text{H}_2\text{O}$) C, H, N.

3-[3-(4-Trifluoromethoxybenzyl)naphthalen-2-yl]pyridine (18) was obtained according to procedure C from **34** (395 mg, 1.00 mmol), sodium iodide (899 mg, 6.0 mmol) and chlorotrimethylsilane (652 mg, 6.0 mmol) after flash chromatography on silica gel (petroleum ether/ethyl acetate, 4/1, $R_f = 0.28$) as a colorless oil (292 mg, 0.77 mmol, 77 %), precipitation of the hydrochloride salt afforded a highly hygroscopic solid, mp (HCl salt) 139–142 °C. MS m/z 379.90 (MH^+). Anal. ($\text{C}_{24}\text{H}_{17}\text{F}_3\text{NO}\cdot\text{HCl}\cdot 0.2\text{H}_2\text{O}$) C, H, N.

3-[6-Methoxy-3-(4-methoxybenzyl)naphthalen-2-yl]pyridine (19) was obtained according to procedure A from **19a** (512 mg, 1.20 mmol) and 3-pyridineboronic acid (113 mg, 0.92 mmol) after flash chromatography on silica gel (petroleum ether/ethyl acetate, 7/3, $R_f = 0.18$) as a colorless oil (189 mg, 0.55 mmol, 60 %), mp (HCl salt) 114–115 °C. $^1\text{H-NMR}$ (500 MHz, CDCl_3): $\delta = 3.75$ (s, 3H), 3.91 (s, 3H), 3.98 (s, 2H), 6.73 (d, $^3J = 8.5$ Hz, 2H), 6.84 (d, $^3J = 8.5$ Hz, 2H), 7.09 (d, $^4J = 2.5$ Hz, 1H), 7.13 (dd, $^3J = 9.0$ Hz, $^4J = 2.5$ Hz, 1H), 7.25 (dd, $^3J = 8.0$ Hz, $^3J = 4.8$ Hz, 1H), 7.51 (m, 1H), 7.57 (s, 1H), 7.60 (s, 1H), 7.71 (d, $^3J = 8.9$ Hz, 1H), 8.54 (d, $^4J = 1.9$ Hz, 1H), 8.56 (dd, $^3J = 4.8$ Hz, $^4J = 1.5$ Hz, 1H). $^{13}\text{C-NMR}$ (125 MHz, CDCl_3): $\delta = 38.9, 55.2, 55.3, 105.2, 113.7, 119.0, 122.8, 127.5, 127.8, 129.1, 129.2, 129.8, 132.6, 134.4, 134.8, 136.8, 137.3, 137.6, 148.1, 150.1, 157.9, 158.1$. MS m/z 356.25 (MH^+). Anal. ($\text{C}_{24}\text{H}_{21}\text{NO}_2\cdot\text{HCl}\cdot 0.8\text{H}_2\text{O}$) C, H, N.

3-[7-Methoxy-3-(4-methoxybenzyl)naphthalen-2-yl]pyridine (20) was obtained according to procedure C from **20a** (400 mg, 1.08 mmol), sodium iodide (1.65 g, 11.0 mmol) and chlorotrimethylsilane (1.20 g, 11.0 mmol) after flash chromatography on silica gel (petroleum ether/ethyl acetate, 7/3, $R_f = 0.11$) as a colorless oil (148 mg, 0.42 mmol, 39 %), mp (HCl salt) 101–103 °C. MS m/z 356.04 (MH^+). Anal. ($\text{C}_{24}\text{H}_{21}\text{NO}_2\cdot\text{HCl}\cdot 0.1\text{H}_2\text{O}$) C, H, N.

3-Methoxy-5-[3-(4-methoxybenzyl)naphthalen-2-yl]pyridine (21) was obtained according to procedure A from **16a** (396 mg, 1.00 mmol) and 5-methoxy-3-pyridineboronic acid acid (130 mg, 0.85 mmol) after flash chromatography on silica gel (petroleum ether/ethyl acetate, 7/3, $R_f = 0.21$) as a colorless oil (149 mg, 0.42 mmol, 49 %), mp (HCl salt) 106–108 °C. MS m/z 356.09 (MH^+). Anal. ($\text{C}_{24}\text{H}_{21}\text{NO}_2\cdot\text{HCl}\cdot 0.5\text{H}_2\text{O}$) C, H, N.

3-Methoxy-5-[6-methoxy-3-(4-methoxybenzyl)naphthalen-2-yl]pyridine (22) was obtained according to procedure A from **19a** (426 mg, 1.00 mmol) and 5-methoxy-3-pyridineboronic acid acid (130 mg, 0.85 mmol) after flash chromatography on silica gel (petroleum ether/ethyl acetate, 7/3, $R_f = 0.18$) as colorless plates (244 mg, 0.63 mmol, 75 %), mp 129–130 °C. MS m/z 385.91 (MH^+). Anal. ($C_{25}H_{23}NO_3$) C, H, N.

3-(3-Benzyl-6-methoxynaphthalen-2-yl)5-methoxypyridine (23) was obtained according to procedure A from **13a** (396 mg, 1.00 mmol) and 5-methoxy-3-pyridineboronic acid acid (130 mg, 0.85 mmol) after flash chromatography on silica gel (petroleum ether/ethyl acetate, 7/3, $R_f = 0.21$) as a colorless oil (221 mg, 0.62 mmol, 73 %), mp (HCl salt) 119–121 °C. MS m/z 356.09 (MH^+). Anal. ($C_{24}H_{21}NO_2 \cdot HCl \cdot 0.2H_2O$) C, H, N.

4-[3-(4-Methoxybenzyl)naphthalen-2-yl]isoquinoline (24) was obtained according to procedure A from **16a** (396 mg, 1.00 mmol) and 4-isoquinolineboronic acid (130 mg, 0.75 mmol) after flash chromatography on silica gel (petroleum ether/ethyl acetate, 7/3, $R_f = 0.20$) as a colorless oil (178 mg, 0.47 mmol, 63 %), mp (HCl salt) 202–203 °C. MS m/z 376.12 (MH^+). Anal. ($C_{27}H_{21}NO \cdot HCl \cdot 0.5H_2O$) C, H, N.

4-[6-Methoxy-3-(4-methoxybenzyl)naphthalen-2-yl]isoquinoline (25) was obtained according to procedure A from **19a** (456 mg, 1.07 mmol) and 4-isoquinolineboronic acid (130 mg, 0.75 mmol) after flash chromatography on silica gel (petroleum ether/ethyl acetate, 7/3, $R_f = 0.18$) and crystallization from acetone/diethyl ether as colorless plates (178 mg, 0.44 mmol, 59 %), mp 158–159 °C. MS m/z 406.00 (MH^+). Anal. ($C_{28}H_{23}NO_2$) C, H, N.

(4-Methoxyphenyl)(3-pyridin-3-yl-naphthalen-2-yl)methanone (26) was obtained according to procedure B from **26a** (4.02 g, 9.80 mmol) and 3-pyridineboronic acid (1.02 g, 8.33 mmol) after flash chromatography on silica gel (petroleum ether/ethyl acetate, 1/1, $R_f = 0.22$) as an off-white solid (2.66 g, 7.84 mmol, 94 %), mp 69–72 °C. MS m/z 340.07 (MH^+). Anal. ($C_{23}H_{17}NO_2 \cdot 0.2H_2O$) C, H, N.

(3-Fluoro-4-methoxyphenyl)(3-pyridin-3-yl-naphthalen-2-yl)methanone (27) was obtained according to procedure B from **27a** (4.19 g, 9.78 mmol) and 3-pyridineboronic acid (1.02 g, 8.33 mmol) after flash chromatography on silica gel (petroleum ether/ethyl acetate, 1/1, $R_f = 0.16$) as an off-white solid (2.52 g, 7.05 mmol, 85 %), mp 96–97 °C. MS m/z 358.00 (MH^+). Anal. ($C_{23}H_{16}FNO_2 \cdot 0.1H_2O$) C, H, N.

4-(3-Pyridin-3-yl-naphthalene-2-carbonyl)benzotrile (28) was obtained according to procedure B from **28a** (3.0 g, 7.40 mmol) and 3-pyridineboronic acid (1.0 g, 8.20 mmol) after flash chromatography on silica gel (petroleum ether/ethyl acetate, 7/3, $R_f = 0.15$) as yellowish needles (1.67 g, 5.0 mmol, 68 %), mp 135–136 °C. MS m/z 335.05 (MH^+). Anal. ($C_{23}H_{14}N_2O \cdot 0.1H_2O$) C, H, N.

(3-Pyridin-3-yl-naphthalen-2-yl)(4-trifluoromethoxyphenyl)methanone (29) was obtained according to procedure B from **29a** (4.57 g, 9.84 mmol) and 3-pyridineboronic acid (1.02 g, 8.33 mmol) after flash chromatography on silica gel (petroleum ether/ethyl acetate, 7/3, $R_f = 0.20$) as a colorless oil (3.20 g, 8.14 mmol, 98 %), precipitation of the hydrochloride salt afforded a highly

hygroscopic solid, mp (HCl salt) 116–118 °C. MS m/z 393.89 (MH⁺). Anal. (C₂₃H₁₄F₃NO₂·HCl) C, H, N.

(4-Methoxyphenyl)(6-methoxy-3-pyridin-3-yl-naphthalen-2-yl)methanone (30) was obtained according to procedure B from **30a** (1.54 g, 3.50 mmol) and 3-pyridineboronic acid (374 mg, 3.0 mmol) after flash chromatography on silica gel (petroleum ether/ethyl acetate, 1/1, R_f = 0.08) and crystallization from methanol as a white solid (723 mg, 1.96 mmol, 65 %), mp 140–141 °C. MS m/z 370.10 (MH⁺). Anal. (C₂₄H₁₉NO₃·0.2H₂O) C, H, N.

(4-Methoxyphenyl)(3-pyridin-3-yl-naphthalen-2-yl)methanol (31) was obtained according to procedure D from **26** (1.02 g, 3.0 mmol) and sodium borohydride (226 mg, 6.0 mmol) after flash chromatography on silica gel (petroleum ether/ethyl acetate, 1/1, R_f = 0.18) as a colorless solid (597 mg, 1.75 mmol, 58 %), mp 77–78 °C. MS m/z 342.10 (MH⁺). Anal. (C₂₃H₁₉NO₂·0.3H₂O) C, H, N.

(3-Fluoro-4-methoxyphenyl)(3-pyridin-3-yl-naphthalen-2-yl)methanol (32) was obtained according to procedure D from **27** (2.11 g, 5.91 mmol) and sodium borohydride (246 mg, 6.50 mmol) after flash chromatography on silica gel (petroleum ether/ethyl acetate, 1/1, R_f = 0.19) as a yellowish solid (543 mg, 1.51 mmol, 26 %), mp 75–76 °C. MS m/z 359.96 (MH⁺). Anal. (C₂₃H₁₈FNO₂·0.5H₂O) C, H, N.

4-[Hydroxy-(3-pyridin-3-yl-naphthalen-2-yl)methyl]benzotrile (33) was obtained according to procedure D from **28** (1.46 g, 4.37 mmol) and sodium borohydride (182 mg, 4.80 mmol) after flash chromatography on silica gel (petroleum ether/ethyl acetate, 1/1, R_f = 0.16) as a colorless solid (1.22 g, 3.63 mmol, 83 %), mp 101–103 °C. MS m/z 336.93 (MH⁺). Anal. (C₂₃H₁₆N₂O·0.5H₂O) C, H, N.

(3-Pyridin-3-yl-naphthalen-2-yl)(4-trifluoromethoxyphenyl)methanol (34) was obtained according to Procedure D from **29** (2.80 g, 7.12 mmol) and sodium borohydride (295 mg, 7.80 mmol) after flash chromatography on silica gel (petroleum ether/ethyl acetate, 1/1, R_f = 0.32) as a colorless solid (1.86 g, 4.70 mmol, 66 %), mp 65–66 °C. MS m/z 396.20 (MH⁺). Anal. (C₂₃H₁₆F₃NO₂·0.2H₂O) C, H, N.

3-{3-[Methoxy-(4-methoxyphenyl)methyl]naphthalen-2-yl}pyridine (35). To a suspension of NaH (40 mg, 1.0 mmol, 60% dispersion in oil) in 5 mL dry THF at was added dropwise a solution of **31** (300 mg, 0.88 mmol) in 5 mL THF at room temperature under an atmosphere of nitrogen. After hydrogen evolution ceased, a solution of methyl iodide (59 μ L, 0.95 mmol) in 5 mL THF was added dropwise, and the resulting mixture was stirred for 5 h at room temperature. After 2 h an additional 59 μ L methyl iodide was added. The mixture was then treated with saturated aqueous NH₄Cl solution and extracted three times with ethyl acetate. The combined organic layers were washed with water and brine, dried over MgSO₄ and the solvent was evaporated in vacuo. **35** was obtained after flash chromatography on silica gel (petroleum ether/ethyl acetate, 1/1, R_f = 0.39) as colorless oil (226 mg, 0.64 mmol, 72 %), mp (HCl salt) 113–114 °C. MS m/z 356.11 (MH⁺). Anal. (C₂₄H₂₁NO₂·HCl·0.7H₂O) C, H, N.

Biological Methods. 1. Enzyme Preparations. CYP17 and CYP19 preparations were obtained by described methods: the 50,000 g sediment of *E. coli* expressing human CYP17⁴⁰ and microsomes from human placenta for CYP19.⁴² **2. Enzyme Assays.** The following enzyme assays were performed as previously described: CYP17⁴⁰ and CYP19.⁴² **3. Activity and Selectivity Assay Using V79 Cells.** V79 MZh 11B1 and V79 MZh 11B2 cells³⁶ were incubated with [4-¹⁴C]-11-deoxycorticosterone as substrate and inhibitor in at least three different concentrations. The enzyme reactions were stopped by addition of ethyl acetate. After vigorous shaking and a centrifugation step (10,000 g, 2 min), the steroids were extracted into the organic phase, which was then separated. The conversion of the substrate was analyzed by HPTLC and a phosphoimaging system as described.^{10,36} **4. Inhibition of Human Hepatic CYP Enzymes.** The recombinantly expressed enzymes from baculovirus-infected insect microsomes (Supersomes) were used and the manufacturer's instructions (www.gentest.com) were followed.

Computational Methods. 1. Pharmacophore Modeling. The most potent compounds of the heteroaryl substituted methyleneindane and naphthalene derivatives and the most potent flavones were selected as training set (see supplementary material for composition of the training set) for the generation of an extended pharmacophore model. GALAHAD,¹⁹ the pharmacophore generation module of SYBYL 7.3.2 (Sybyl, Tripos Inc., St. Louis, Missouri, USA), was used to generate pharmacophore hypotheses of the series of inhibitors from hypermolecules incorporating the structural information of the dataset and alignments from sets of ligand molecules. In the genetic algorithm, default values were used. In the present case, 100 models were generated and the best 20 pharmacophore-hypotheses were saved. GALAHAD takes into account energetics, steric similarity, and pharmacophoric overlap, while accommodating conformational flexibility, ambiguous stereochemistry, alternative ring configurations, multiple partial match constraints, and alternative feature mappings among molecules. All the other molecules of the library were then aligned using each of the 20 pharmacophores as a template, and the best pharmacophore was selected. The top ranked model was the best in three of the most indicative ranking criteria of the used software (Pareto ranking,²⁰ Specificity, and Mol-query). An additional donor site feature not shown in the figures) was manually added to simulate the complexation of the heme iron by the sp²-hybridized nitrogen (AA1) in order to fix the orientation of the lone pair of the sp²-hybridized nitrogen. This refined pharmacophore model was selected as molecular query for the alignment of our database library. The core of the pharmacophoric scheme is formed by five hydrophobic features (HY0, HY1, HY2a, HY2b) and the acceptor atom (AA) spheres represent the H-bond acceptors. In some cases, the acceptor feature AA2a overlapped a donor feature (data not shown), indicating the presence of an OH function. The final pharmacophore model consists of 12 pharmacophoric features: 4 essential ones (HY0, AA1, HY1), necessary for basal inhibitory potency, and 8 partial matches (HY2, HY2b, AA2a, AA2b, HY3, AA3a, AA3b, and AA4). **2. Protein Modeling and Docking.** Using the resolved human cytochrome CYP2C9 structure (PDB code: 1OG5)⁴³ as template, a homology model was build and

refined for CYP11B2. This work has been described in more detail by our group in four recent papers.^{12–15} In this study selected compounds were docked into the refined homology model using FlexX-Pharm.⁴⁴ A pharmacophore constraint was applied to ensure the right binding mode of the inhibitors with the heme-cofactor. For this purpose the standard Fe–N interaction parameters of FlexX^{45,46} were modified and a directed heme-Fe–N interaction was defined perpendicular to the heme-plane. The constraint requires the existence of an inhibitor-nitrogen-atom on the surface of an interaction cone with a 20 degree radius, which has its origin at the Fe-atom and points perpendicular to the heme-plane (with a length of 2.2 Å). Only docking solutions were accepted, which fulfill this constraint. For all other ligand-protein interactions the standard FlexX interaction parameters and geometries were used. The protein-ligand interactions were analyzed using the FlexX software.

Acknowledgement. We thank Gertrud Schmitt and Jeannine Jung for their help in performing the in vitro tests. The investigation of the hepatic CYP profile by Dr. Ursula Müller-Vieira, Pharmacelus CRO, Saarbrücken, is highly appreciated. S. L. is grateful to Saarland University for a scholarship (Landesgraduierten-Förderung). Thanks are due to Prof. J. J. Rob Hermans, University of Maastricht, The Netherlands, for supplying the V79 CYP11B1 cells, and Prof. Rita Bernhardt, Saarland University, for supplying the V79 CYP11B2 cells.

Supporting Information Available: Additional inhibitory data of compounds **1–10** (CYP11B1 inhibition and selectivity factors), NMR spectroscopic data of the target compounds **11–15**, **17**, **18**, **20–35**, full experimental details and spectroscopic characterization of the reaction intermediates **11a–16a**, **19a**, **20a**, **26a–30a**, **11b–16b**, **19b**, **26b–30b**, **11c–16c**, **19c**, **11d–16d**, **19d**, **26d–30d**, **12e–14e**, **12f–14f**, **12g–14g**, **12h**, **13h**, elemental analysis results and purity data (LC/MS) of compounds **11–35**, pharmacophore modeling training set and pharmacophore geometric properties. This information is available free of charge via the Internet at <http://pubs.acs.org>.

References

- (1) Kawamoto, T.; Mitsuuchi, Y.; Toda, K.; Yokoyama, Y.; Miyahara, K.; Miura, S.; Ohnishi, T.; Ichikawa, Y.; Nakao, K.; Imura, H.; Ulick, S.; Shizuta, Y. Role of steroid 11 β -hydroxylase and steroid 18-hydroxylase in the biosynthesis of glucocorticoids and mineralocorticoids in humans. *Proc. Natl. Acad. Sci. U.S.A.* **1992**, *89*, 1458–1462.
- (2) (a) Brilla, C. G. Renin-angiotensin-aldosterone system and myocardial fibrosis. *Cardiovasc. Res.* **2000**, *47*, 1–3. (b) Lijnen, P.; Petrov, V. Induction of cardiac fibrosis by aldosterone. *J. Mol. Cell. Cardiol.* **2000**, *32*, 865–879.
- (3) (a) Struthers, A. D. Aldosterone escape during angiotensin-converting enzyme inhibitor therapy in chronic heart failure. *J. Card. Fail.* **1996**, *2*, 47–54. (b) Sato, A.; Saruta, T. Aldosterone escape during angiotensin-converting enzyme inhibitor therapy in essential hypertensive patients with left ventricular hypertrophy. *J. Int. Med. Res.* **2001**, *29*, 13–21.

- (4) Pitt, B.; Zannad, F.; Remme, W. J.; Cody, R.; Castaigne, A.; Perez, A.; Palensky, J.; Wittes, J. The effect of spironolactone on morbidity and mortality in patients with severe heart failure. *N. Engl. J. Med.* **1999**, *341*, 709–717.
- (5) Pitt, B.; Remme, W.; Zannad, F.; Neaton, J.; Martinez, F.; Roniker, B.; Bittman, R.; Hurley, S.; Kleiman, J.; Gatlin, M. Eplerenone, a selective aldosterone blocker, in patients with left ventricular dysfunction after myocardial infarction. *N. Eng. J. Med.* **2003**, *348*, 1309–1321.
- (6) Delcayre, C.; Swynghedauw, B. Molecular mechanisms of myocardial remodeling. The role of aldosterone. *J. Mol. Cell. Cardiol.* **2002**, *34*, 1577–1584.
- (7) (a) Wehling, M. Specific, nongenomic actions of steroid hormones. *Annu. Rev. Physiol.* **1997**, *59*, 365–393. (b) Lösel, R.; Wehling, M. Nongenomic actions of steroid hormones. *Nature Rev. Mol. Cell. Biol.* **2003**, *4*, 46–55.
- (8) Chai, W.; Garrelds, I. M.; de Vries, R.; Batenburg, W. W.; van Kats, J. P.; Danser, A. H. J. Nongenomic effects of aldosterone in the human heart: Interaction with angiotensin II. *Hypertension* **2005**, *46*, 701–706.
- (9) Hartmann, R. W. Selective inhibition of steroidogenic P450 enzymes: Current status and future perspectives. *Eur. J. Pharm. Sci.* **1994**, *2*, 15–16.
- (10) Ehmer, P. B.; Bureik, M.; Bernhardt, R.; Müller, U.; Hartmann, R. W. Development of a test system for inhibitors of human aldosterone synthase (CYP11B2): Screening in fission yeast and evaluation of selectivity in V79 cells. *J. Steroid Biochem. Mol. Biol.* **2002**, *81*, 173–179.
- (11) Hartmann, R. W.; Müller, U.; Ehmer, P. B. Discovery of selective CYP11B2 (aldosterone synthase) inhibitors for the therapy of congestive heart failure and myocardial fibrosis. *Eur. J. Med. Chem.* **2003**, *38*, 363–366.
- (12) Ulmschneider, S.; Müller-Vieira, U.; Mitrenga, M.; Hartmann, R. W.; Oberwinkler-Marchais, S.; Klein, C. D.; Bureik, M.; Bernhardt, R.; Antes, I.; Lengauer, T. Synthesis and evaluation of imidazolymethylenetetrahydronaphthalenes and imidazolymethyleneindanes: Potent inhibitors of aldosterone synthase. *J. Med. Chem.* **2005**, *48*, 1796–1805.
- (13) Ulmschneider, S.; Müller-Vieira, U.; Klein, C. D.; Antes, I.; Lengauer, T.; Hartmann, R. W. Synthesis and evaluation of (pyridylmethylene)tetrahydronaphthalenes/-indanes and structurally modified derivatives: Potent and selective inhibitors of aldosterone synthase. *J. Med. Chem.* **2005**, *48*, 1563–1575.
- (14) Voets, M.; Antes, I.; Scherer, C.; Müller-Vieira, U.; Biemel, K.; Barassin, C.; Oberwinkler-Marchais, S.; Hartmann, R. W. Heteroaryl substituted naphthalenes and structurally modified derivatives: Selective inhibitors of CYP11B2 for the treatment of congestive heart failure and myocardial fibrosis. *J. Med. Chem.* **2005**, *48*, 6632–6642.
- (15) Voets, M.; Antes, I.; Scherer, C.; Müller-Vieira, U.; Biemel, K.; Oberwinkler-Marchais, S.; Hartmann, R. W. Synthesis and evaluation of heteroaryl-substituted dihydronaphthalenes and indenes: Potent and selective inhibitors of aldosterone synthase (CYP11B2) for the treatment of congestive heart failure and myocardial fibrosis. *J. Med. Chem.* **2006**, *49*, 2222–2231.

- (16) Taymans, S. E.; Pack, S.; Pak, E.; Torpy, D. J.; Zhuang, Z.; Stratakis, C. A. Human CYP11B2 (aldosterone synthase) maps to chromosome 8q24.3. *J. Clin. Endocrinol. Metab.* **1998**, *83*, 1033–1036.
- (17) (a) Cavalli, A.; Bisi, A.; Bertucci, C.; Rosini, C.; Paluszczak, A.; Gobbi, S.; Giorgio, E.; Rampa, A.; Belluti, F.; Piazzini, L.; Valenti, P.; Hartmann, R. W.; Recanatini, M. Enantioselective nonsteroidal aromatase inhibitors identified through a multidisciplinary medicinal chemistry approach. *J. Med. Chem.* **2005**, *48*, 7282–7289. (b) Gobbi, S.; Cavalli, A.; Rampa, A.; Belluti, F.; Piazzini, L.; Paluszczak, A.; Hartmann, R. W.; Recanatini, M.; Bisi, A. Lead optimization providing a series of flavone derivatives as potent nonsteroidal inhibitors of the cytochrome P450 aromatase enzyme. *J. Med. Chem.* **2006**, *49*, 4777–4780.
- (18) Ulmschneider, S.; Negri, M.; Voets, M.; Hartmann, R. W. Development and evaluation of a pharmacophore model for inhibitors of aldosterone synthase (CYP11B2). *Bioorg. Med. Chem. Lett.* **2006**, *16*, 25–30.
- (19) (a) Richmond, N. J.; Abrams, C. A.; Wolohan, P. R.; Abrahamian, E.; Willett, P.; Clark, R. D. GALAHAD: 1. Pharmacophore identification by hypermolecular alignment of ligands in 3D. *J. Comput. Aided Mol. Des.* **2006**, *20*, 567–587. (b) Shepphird, J. K.; Clark, R. D. A marriage made in torsional space: Using GALAHAD models to drive pharmacophore multiplet searches. *J. Comput. Aided Mol. Des.* **2006**, *20*, 763–771. (c) <http://www.tripos.com>.
- (20) Gillet, V. J.; Willett, P.; Fleming, P. J.; Green, D. V. S. Designing focused libraries using MoSELECT. *J. Mol. Graph. Model.* **2003**, *20*, 491–498.
- (21) Miyaura, N.; Suzuki, A. Palladium-catalyzed cross-coupling reactions of organoboron compounds. *Chem. Rev.* **1995**, *95*, 2457–2483.
- (22) Chowdhury, S.; Georghiou, P. E. Synthesis and properties of a new member of the calixnaphthalene family: A C₂-symmetrical endo-calix[4]naphthalene. *J. Org. Chem.* **2002**, *67*, 6808–6811.
- (23) Bengtson, A.; Hallberg, A.; Larhed, M. Fast synthesis of aryl triflates with controlled microwave heating. *Org. Lett.* **2002**, *4*, 1231–1233.
- (24) Appukkuttan, P.; Orts, A. B.; Chandran, R., P.; Goeman, J. L.; van der Eycken, J.; Dehaen, W.; van der Eycken, E. Generation of a small library of highly electron-rich 2-(hetero)aryl-substituted phenethylamines by the Suzuki-Miyaura reaction: A short synthesis of an apogalanthamine analogue. *Eur. J. Org. Chem.* **2004**, 3277–3285.
- (25) Miller, L. E.; Hanneman, W. W.; St. John, W. L.; Smeby, R. R. The reactivity of the methyl group in 2-methyl-3-nitronaphthalene. *J. Am. Chem. Soc.* **1954**, *76*, 296–297.
- (26) Wu, K.-C.; Lin, Y.-S.; Yeh, Y.-S.; Chen, C.-Y.; Ahmed, M. O.; Chou, P.-T.; Hon, Y.-S. Design and synthesis of intramolecular hydrogen bonding systems. Their application in metal cation sensing based on excited-state proton transfer reaction. *Tetrahedron* **2004**, *60*, 11861–11868.
- (27) Brown, H. C.; Narasimhan, S.; Choi, Y. M.; Selective reductions. 30. Effect of cation and solvent on the reactivity of saline borohydrides for reduction of carboxylic esters. Improved procedures for the conversion of esters to alcohols by metal borohydrides. *J. Org. Chem.* **1982**, *47*, 4702–4708.

- (28) Einhorn, J.; Einhorn, C.; Ratajczak, F.; Pierre, J.-L. Efficient and highly selective oxidation of primary alcohols to aldehydes by N-chlorosuccinimide mediated by oxoammonium salts. *J. Org. Chem.* **1996**, *61*, 7452–7454.
- (29) Parikh, J. R.; Doering, W. v. E. Sulfur trioxide in the oxidation of alcohols by dimethyl sulfoxide. *J. Am. Chem. Soc.* **1967**, *89*, 5505–5507.
- (30) Ono, A.; Suzuki, N.; Kamimura, J. Hydrogenolysis of diaryl and aryl alkyl ketones and carbinols by sodium borohydride and anhydrous aluminum(III) chloride. *Synthesis* **1987**, 736–738.
- (31) Bieg, T.; Szeja, W. Removal of O-benzyl protective groups by catalytic transfer hydrogenation. *Synthesis* **1985**, 76–77.
- (32) Li, X.; Hewgley, J. B.; Mulrooney, C. A.; Yang, J.; Kozlowski, M. C. Enantioselective oxidative biaryl coupling reactions catalyzed by 1,5-diazadecalin metal complexes: Efficient formation of chiral functionalized BINOL derivatives. *J. Org. Chem.* **2003**, *68*, 5500–5511.
- (33) Stoner, E. J.; Cothron, D. A.; Balmer, M. K.; Roden, B. A. Benzylation via tandem Grignard reaction-iodotrimethylsilane (TMSI) mediated reduction. *Tetrahedron* **1995**, *51*, 11043–11062.
- (34) Cain, G. A.; Holler, E. R. Extended scope of in situ iodotrimethylsilane mediated selective reduction of benzylic alcohols. *Chem. Commun.* **2001**, 1168–1169.
- (35) (a) Nakamura, H.; Wu, C.; Inouye, S.; Murai, A. Design, synthesis, and evaluation of the transition-state inhibitors of coelenterazine bioluminescence: Probing the chiral environment of active site. *J. Am. Chem. Soc.* **2001**, *123*, 1523–1524. (b) Gribble, G. W.; Leese, R. M.; Evans, B. E. Reactions of sodium borohydride in acidic media; IV. Reduction of diarylmethanols and triarylmethanols in trifluoroacetic acid. *Synthesis* **1977**, 172–176.
- (36) (a) Denner, K.; Bernhardt, R. Inhibition studies of steroid conversions mediated by human CYP11B1 and CYP11B2 expressed in cell cultures. In *Oxygen Homeostasis and Its Dynamics*, 1st ed.; Ishimura, Y., Shimada, H., Suematsu, M., Eds.; Springer-Verlag: Tokyo, Berlin, Heidelberg, New York, 1998; pp 231–236. (b) Denner, K.; Doehmer, J.; Bernhardt, R. Cloning of CYP11B1 and CYP11B2 from normal human adrenal and their functional expression in COS-7 and V79 chinese hamster cells. *Endocr. Res.* **1995**, *21*, 443–448. (c) Böttner, B.; Denner, K.; Bernhardt, R. Conferring aldosterone synthesis to human CYP11B1 by replacing key amino acid residues with CYP11B2-specific ones. *Eur. J. Biochem.* **1998**, *252*, 458–466.
- (37) Lamberts, S. W.; Bruining, H. A.; Marzouk, H.; Zuiderwijk, J.; Uitterlinden, P.; Blijd, J. J.; Hackeng, W. H.; de Jong, F. H. The new aromatase inhibitor CGS-16949A suppresses aldosterone and cortisol production by human adrenal cells in vitro. *J. Clin. Endocrinol. Metab.* **1989**, *69*, 896–901.
- (38) Demers, L. M.; Melby, J. C.; Wilson, T. E.; Lipton, A.; Harvey, H. A.; Santen, R. J. The effects of CGS 16949A, an aromatase inhibitor on adrenal mineralocorticoid biosynthesis. *J. Clin. Endocrinol. Metab.* **1990**, *70*, 1162–1166.
- (39) Heim, R.; Lucas, S.; Grombein, C. M.; Ries, C.; Schewe, K. E.; Negri, M.; Müller-Vieira, U.; Birk, B.; Hartmann, R. W. Overcoming undesirable CYP1A2 inhibition of pyridyl-naphthalene type aldosterone

- synthase inhibitors: Influence of heteroaryl derivatization on potency and selectivity. *J. Med. Chem.* **2008**, *51*, 5064–5074.
- (40) (a) Ehmer, P. B.; Jose, J.; Hartmann, R. W. Development of a simple and rapid assay for the evaluation of inhibitors of human 17 α -hydroxylase-C_{17,20}-lyase (P450c17) by coexpression of P450c17 with NADPH-cytochrome-P450-reductase in *Escherichia coli*. *J. Steroid Biochem. Mol. Biol.* **2000**, *75*, 57–63; (b) Hutschenreuter, T. U.; Ehmer, P. B.; Hartmann, R. W. Synthesis of hydroxy derivatives of highly potent nonsteroidal CYP17 inhibitors as potential metabolites and evaluation of their activity by a non cellular assay using recombinant enzyme. *J. Enzyme Inhib. Med. Chem.* **2004**, *19*, 17–32.
- (41) Thompson, E. A.; Siiteri, P. K. Utilization of oxygen and reduced nicotinamide adenine dinucleotide phosphate by human placental microsomes during aromatization of androstenedione. *J. Biol. Chem.* **1974**, *249*, 5364–5372.
- (42) Hartmann, R. W.; Batzl, C. Aromatase inhibitors. Synthesis and evaluation of mammary tumor inhibiting activity of 3-alkylated 3-(4-aminophenyl)piperidine-2,6-diones. *J. Med. Chem.* **1986**, *29*, 1362–1369.
- (43) Williams, P. A.; Cosme, J.; Ward, A.; Angove, H. C.; Matak Vinkovic, D.; Jhoti, H. Crystal structure of human cytochrome P4502C9 with bound warfarin. *Nature* **2003**, *424*, 464–468.
- (44) Hindle, S. A.; Rarey, M.; Buning, C.; Lengauer, T. Flexible docking under pharmacophore type constraints. *J. Comput. Aided Mol. Des.* **2002**, *16*, 129–149.
- (45) Rarey, M.; Kramer, B.; Lengauer, T.; Klebe G. A fast flexible docking method using an incremental construction algorithm. *J. Mol. Biol.* **1996**, *261*, 470–489.
- (46) Rarey, M.; Kramer, B.; Lengauer, T. Multiple automatic base selection: Protein-ligand docking based on incremental construction without manual intervention. *J. Comput. Aided Mol. Des.* **1997**, *11*, 369–384.

3.3 Nonsteroidal Aldosterone Synthase Inhibitors with Improved Selectivity: Lead Optimization Providing a Series of Pyridine Substituted 3,4-Dihydro-1*H*-quinolin-2-one Derivatives

Simon Lucas, Ralf Heim, Christina Ries, Katarzyna E. Schewe, Barbara Birk, and Rolf W. Hartmann

This manuscript has been submitted for publication as an article to the

Journal of Medicinal Chemistry **2008**

Paper III

Abstract: Pyridine substituted naphthalenes (e.g., **I–III**) constitute a class of potent inhibitors of aldosterone synthase (CYP11B2). To overcome the unwanted inhibition of the hepatic enzyme CYP1A2, we aimed at reducing the number of aromatic carbons of these molecules since aromaticity has previously been identified to correlate positively with CYP1A2 inhibition. As hypothesized, inhibitors with a tetrahydronaphthalene type molecular scaffold (**1–11**) exhibit a decreased CYP1A2 inhibition, however, tetralone **9** turned out to be cytotoxic to the human cell line U-937 at higher concentrations. Consequent structural optimization culminated in the discovery of heteroaryl substituted 3,4-dihydro-1*H*-quinolin-2-ones (**12–26**), with **12**, a bioisoster of **9**, being not toxic up to 200 μ M. The investigated molecules are highly selective versus both CYP1A2 and a wide range of other cytochrome P450 enzymes and show a good pharmacokinetic profile *in vivo* (e.g., **12** with a peroral bioavailability of 71 %).

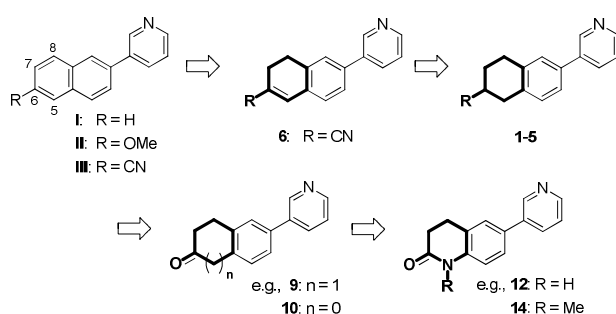
Introduction

The progressive nature of congestive heart failure (CHF) is a consequence of a neurohormonal imbalance that involves a chronic activation of the renin-angiotensin-aldosterone system (RAAS) in response to reduced cardiac output and reduced renal perfusion. Aldosterone and angiotensin II (Ang II) are excessively released, leading to increased blood volume and blood pressure as a consequence of epithelial sodium retention as well as Ang II mediated vasoconstriction and finally to a further reduction of cardiac output.¹ The RAAS is pathophysiologically stimulated in a vicious circle of neurohormonal activation that counteracts the normal negative feedback loop regulation. The most important circulating mineralocorticoid aldosterone acts by binding to specific mineralocorticoid receptors (MR) located in the cytosol of target epithelial cells. Thereby, renal sodium reabsorption and potassium secretion are promoted in the distal tubule and the collecting duct of the nephron. Elevated blood volume and thus blood pressure results from water that follows the sodium movement via osmosis. In addition to these indirect effects on heart function, aldosterone exerts direct effects on the heart by activating nonepithelial MRs in cardiomyocytes, fibroblasts and endothelial cells. Synthesis and deposition of fibrillar collagens in the fibroblasts result in myocardial fibrosis.² Relatively inelastic collagen fibers stiffen the heart muscle which deteriorates the myocardial function and consequently enhances the neurohormonal imbalance by further stimulation of the RAAS. In addition to the effects of circulating aldosterone deriving from adrenal secretion, Satoh et al. reported that aldosterone produced locally in the heart triggers myocardial fibrosis, too.³ Recent clinical studies with the MR antagonists spironolactone and eplerenone gave evidence for the pivotal role of aldosterone in the progression of cardiovascular diseases. Blocking the aldosterone action by functional antagonism of its receptor reduced the mortality and significantly reduced the symptoms of heart failure.⁴ Furthermore, follow-up studies revealed that cardiac fibrosis can not only be prevented but also reversed by use of spironolactone.⁵

However, several issues are unsolved by this therapeutic strategy. Spironolactone binds rather unselectively to the aldosterone receptor and also has some affinity to other steroid receptors, provoking adverse side effects.⁴ Although eplerenone is more selective, clinically relevant hyperkalemia remains a principal therapeutic risk.⁶ Another crucial point is the high concentration of circulating aldosterone which is not lowered by MR antagonistic therapy and raises several issues. First, the elevated aldosterone plasma levels do not induce a homologous down-regulation but an up-regulation of the aldosterone receptor which complicates a long-term therapy since MR antagonists are likely to become ineffective.⁷ Furthermore, the nongenomic actions of aldosterone are in general not blocked by receptor antagonists and can occur despite MR antagonistic treatment.⁸ A novel therapeutic strategy for the treatment of hyperaldosteronism, congestive heart failure and myocardial fibrosis with potential to overcome the drawbacks of MR antagonists was recently suggested by us:^{9,10} Blockade of aldosterone production by inhibiting the key enzyme of its biosynthesis, aldosterone synthase (CYP11B2), a mitochondrial cytochrome P450 enzyme that is localized mainly in the adrenal cortex

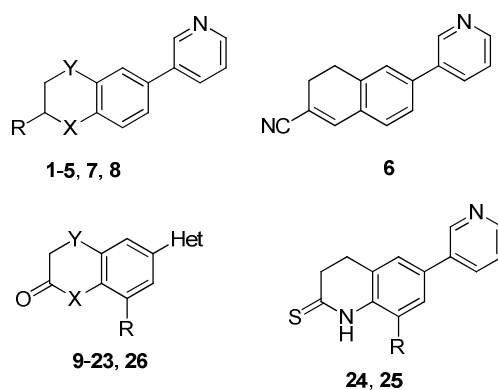
and catalyzes the terminal three oxidation steps in the biogenesis of aldosterone in humans.¹¹ Consequent structural optimization of a hit discovered by compound library screening led to a series of nonsteroidal aldosterone synthase inhibitors with high selectivity versus other cytochrome P450 enzymes.^{12,13} Pyridine-substituted naphthalenes^{14,15} such as **I–III** (Chart 1) and dihydronaphthalenes,¹⁶ the most potent and selective compounds that emerged from our drug discovery program, however, revealed two major pharmacological drawbacks: A strong inhibition of the hepatic drug metabolizing enzyme CYP1A2 and no inhibitory effect on the aldosterone production in vivo by using a rat model.

Chart 1. Pyridylnaphthalene Type CYP11B2 Inhibitors **I–III** and Design Strategy for 3,4-Dihydro-1*H*-quinolin-2-one Derivatives (e.g., **12** and **14**)



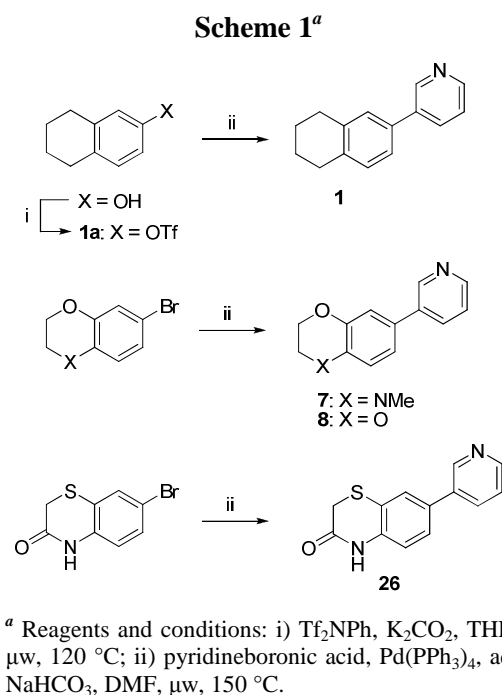
In the present study, we describe the design and the synthesis of pyridine-substituted 3,4-dihydro-1*H*-quinolin-2-ones and structurally related compounds as highly potent and selective CYP11B2 inhibitors (Chart 2). The design concept toward these molecules is based on a systematic reduction of aromaticity by saturation of the hydrocarbons C₅ to C₈ of the naphthalene moiety and subsequent chemical modification of the fully saturated ring (Chart 1). The inhibitory activity of the title compounds was determined in V79 MZh cells expressing human CYP11B2. The selectivity was investigated with respect to the highly homologous 11β-hydroxylase (CYP11B1) as well as other crucial steroid- or drug-metabolizing cytochrome P450 enzymes (CYP17, CYP19, CYP1A2, CYP2B6, CYP2C9, CYP2C19, CYP2D6, and CYP3A4). The in vivo pharmacokinetic profile of some promising compounds was determined in male Wistar rats in both cassette and single dosing experiments. Furthermore, plasma protein binding and cytotoxicity studies were performed.

Chart 2. Title Compounds

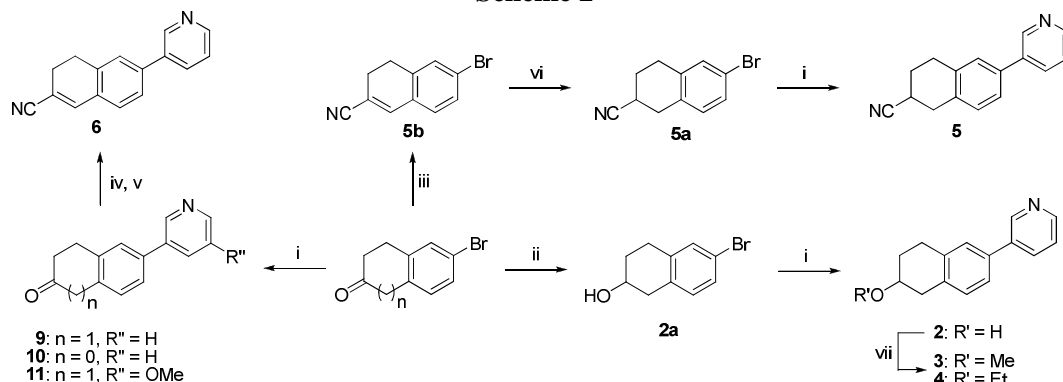


Results Chemistry

The key step for the synthesis of the title compounds was a Suzuki coupling to introduce the heterocycle, mostly 3-pyridine. In case of the unsubstituted tetrahydronaphthalene **1** the cross-coupling was accomplished by a microwave enhanced method¹⁷ using 3-pyridineboronic acid and triflate **1a** which was prepared from the corresponding tetrahydronaphthol (Scheme 1).¹⁸ Compounds **7**, **8**, and **26** were synthesized via Suzuki coupling from commercially available arylbromides and 3-pyridineboronic acid under microwave heating.

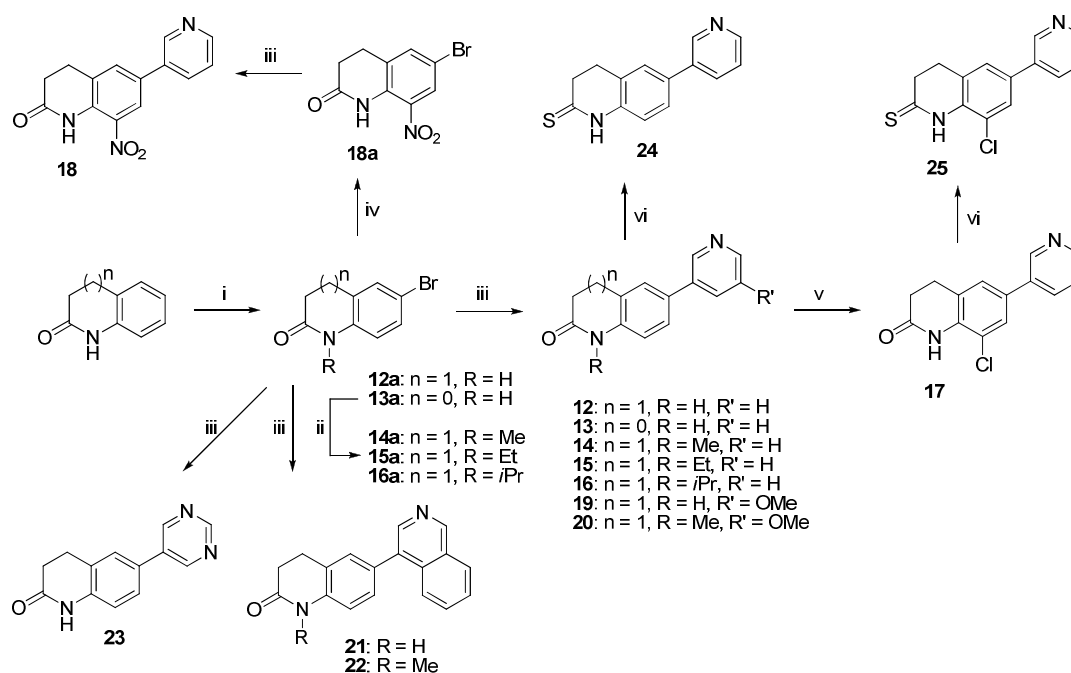


The synthesis of compounds **2–6** and **9–11** (Scheme 2) started from either 6-bromo-2-tetralone ($n = 1$) or 5-bromo-1-indanone ($n = 0$) as key building block. Suzuki coupling afforded the heterocycle-substituted analogues **9–11**. Dihydronaphthalene derivative **6** was prepared by treatment of tetralone **9** with KHMDS, *in situ* quenching the enolate with $\text{ Tf}_2\text{NPh}$ ¹⁹ and Pd-catalyzed cyanation²⁰ of the intermediate enoltriflate. The hydroxy-substituted tetrahydronaphthalene **2** was obtained by sodium borohydride reduction of the carbonyl group²¹ to afford **2a** and subsequent Suzuki coupling. *O*-Alkylation of **2** afforded the corresponding methoxy- (**3**) and ethoxy-substituted (**4**) derivatives. The 6-cyano-derivatized analog **5** was prepared in three consecutive steps starting with a one-pot cyanhydrin/elimination step.²² The intermediate α,β -unsaturated nitrile **5b** was treated with NaBH_4 in refluxing ethanol to reduce the double bond.²³ Final Suzuki coupling of **5a** with 3-pyridineboronic acid afforded the tetrahydronaphthalene **5**.

Scheme 2^a

^a Reagents and conditions: i) heteroarylboronic acid, Pd(PPh₃)₄, aq. NaHCO₃, DMF, μ w, 150 °C; ii) NaBH₄, methanol, 0 °C; iii) Me₃SiCN, ZnI₂, toluene, rt, then POCl₃, pyridine, reflux; iv) Tf₂NPh, KHMDS, THF/toluene, -78 °C; v) Zn(CN)₂, Pd(PPh₃)₄, DMF, 100 °C; vi) NaBH₄, ethanol, reflux; vii) alkyl halogenide, NaH, THF, 50 °C.

The synthetic route for the compounds with a dihydro-1*H*-quinolin-2-one or structurally related scaffold was accomplished as outlined in Scheme 3. The initial bromination procedures yielding either **12a** or **13a** have been described previously.^{24,25} Subsequent *N*-alkylation was accomplished by treating the quinolinones with alkyl halogenide and potassium *tert*-butylate in DMF to afford the intermediates **14a–16a**.²⁶ A nitro substituent was selectively introduced in 8-position of **10a** by sulphonitric acid to yield **18a**.²⁷ The obtained bromoarenes were transformed into the heterocycle-substituted analogues **12–16** and **18–23** by Suzuki coupling. Treating **12** with *N*-chlorosuccinimide in DMF at 65 °C afforded the 8-chloro derivative **17** as the only regioisomer. Conversion of the dihydroquinolinones **12** and **17** into the thio analogues **24** and **25** was carried out using Lawesson's reagent in refluxing toluene.

Scheme 3^a

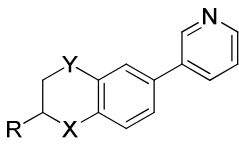
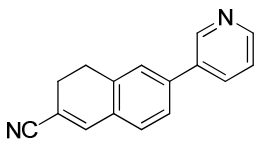
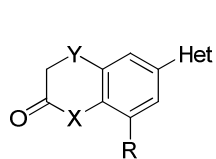
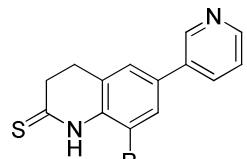
^a Reagents and conditions: i) NBS, DMF, 0 °C (n = 1) or: Br₂, KBr, water, reflux (n = 0); ii) alkyl halogenide, KO^tBu, DMF, rt; iii) heteroarylboronic acid, Pd(PPh₃)₄, aq. NaHCO₃, DMF, μ w, 150 °C or: Pd(PPh₃)₄, aq. Na₂CO₃, toluene/ethanol, reflux; iv) HNO₃/H₂SO₄, rt; v) NCS, DMF, 65 °C; vi) Lawesson's reagent, toluene, reflux.

Biological Results

Inhibition of Human Adrenal Corticoid Producing CYP11B2 and CYP11B1 In Vitro (Table 1). The inhibitory activities of the compounds were determined in V79 MZh cells expressing either human CYP11B2 or CYP11B1.^{10,28} The V79 MZh cells were incubated with [¹⁴C]-deoxycorticosterone as substrate and the inhibitor in different concentrations. The product formation was monitored by HPTLC using a phosphoimager. Fadrozole, an aromatase (CYP19) inhibitor with ability to reduce corticoid formation in vitro²⁹ and in vivo³⁰ was used as a reference (CYP11B2, IC₅₀ = 1 nM; CYP11B1, IC₅₀ = 10 nM).

Most of the compounds presented in Table 1 show a strong inhibition of the target enzyme. Within the tetrahydro- and dihydronaphthalene series (compounds **1–6**), a substituent in 6-position of the carbocyclic skeleton induces an increased inhibitory potency in case of methoxy- (compound **3**) and cyano-substituents (compounds **5, 6**) as well as a dramatic increase in selectivity toward CYP11B1, most notably in methoxy derivative **3** (selectivity factor = 347). Contrariwise, introduction of heteroatoms into the saturated ring leads to a decrease of CYP11B2 inhibition (e.g., **7** and **8**). The carbonyl derivatives **9–11** are also highly potent (IC₅₀ = 1.8–7.8 nM) and selective aldosterone synthase inhibitors. Tetralone **9** is the most selective compound of the present series displaying a CYP11B1 IC₅₀ value 496-fold higher than the CYP11B2 IC₅₀ value. The derivatives with dihydro-1*H*-quinolin-2-one molecular scaffold (**12–26**) exhibit a pronounced inhibitory potency at the target enzyme (IC₅₀ = 0.1–64 nM) and are selective with respect to CYP11B1 inhibition (selectivity factor = 44–440). A significant decrease in inhibitory potency can be observed for derivatization of the lactam nitrogen by an isopropyl residue (compound **16**) whereas methyl (compound **14**) and ethyl (compound **15**) are tolerated in this position. The activity also decreases for 3-pyridine being replaced by 5-pyrimidine (compound **23**) as heterocyclic moiety. Introduction of a nitro substituent in 8-position results in the rather moderate CYP11B2 inhibitor **18** (IC₅₀ = 64 nM) with lower CYP11B1 selectivity. Contrariwise, a chloro substituent in the same position (compound **17**) increases the inhibitory potency by a factor of 7 compared to the hydrogen analog **12**. The most potent inhibitors are obtained when the 3-pyridine moiety is modified by 5-methoxylation or replaced by 4-isoquinoline resulting in subnanomolar IC₅₀ values for compounds **20–22** (IC₅₀ = 0.1–0.2 nM). Isoquinoline derivative **22** displays an IC₅₀ value as low as 0.1 nM and is the most potent aldosterone synthase inhibitor known so far and also shows a pronounced inhibitory potency at CYP11B1 (IC₅₀ = 6.9 nM). The same trend was observed previously for the binding properties of a series of heteroaryl-substituted naphthalenes.³¹ Thionation of the lactam carbonyl results in a slightly reduced CYP11B1 selectivity as seen in compounds **24** and **25** compared to the oxygen analogues **12** and **17**. Moreover, incorporation of a sulfur atom into the lactam moiety in compound **26** induces a dramatic loss of CYP11B1 selectivity (selectivity factor = 44).

Table 1. Inhibition of Human Adrenal CYP11B2 and CYP11B1 In Vitro

				   				
				% inhibition ^a				
				IC ₅₀ value ^b (nM)				
				V79 11B2 ^c		V79 11B1 ^d		selectivity factor ^e
compd	R	X	Y	hCYP11B2	hCYP11B2	hCYP11B1		
1	H	CH ₂	CH ₂		82	29	1977	68
2	OH	CH ₂	CH ₂		86	44	4921	112
3	OMe	CH ₂	CH ₂		97	3.3	1145	347
4	OEt	CH ₂	CH ₂		92	30	4371	146
5	CN	CH ₂	CH ₂		94	5.1	745	146
6					97	1.6	290	181
7	H	NMe	O		71	101	5970	59
8	H	O	O		70	154	13378	87
9	H	CH ₂	CH ₂	3-pyridine	97	7.8	3964	496
10	H	-	CH ₂	3-pyridine	90	4.4	819	186
11	H	CH ₂	CH ₂	5-methoxy-3-pyridine	94	1.8	191	106
12	H	NH	CH ₂	3-pyridine	88	28	6746	241
13	H	NH	-	3-pyridine	85	14	5952	425
14	H	NMe	CH ₂	3-pyridine	92	2.6	742	289
15	H	NEt	CH ₂	3-pyridine	93	22	5177	235
16	H	NiPr	CH ₂	3-pyridine	39	n.d.	n.d.	n.d.
17	Cl	NH	CH ₂	3-pyridine	97	3.8	1671	440
18	NO ₂	NH	CH ₂	3-pyridine	78	64	5402	84
19	H	NH	CH ₂	5-methoxy-3-pyridine	91	2.7	339	126
20	H	NMe	CH ₂	5-methoxy-3-pyridine	94	0.2	87	435
21	H	NH	CH ₂	4-isoquinoline	94	0.2	33	165
22	H	NMe	CH ₂	4-isoquinoline	99	0.1	6.9	69
23	H	NH	CH ₂	5-pyrimidine	57	n.d.	n.d.	n.d.
24	H				97	3.1	580	187
25	Cl				97	4.2	769	183
26	H	NH	S	3-pyridine	92	12	525	44
fadrozole						1	10	10

^a Mean value of at least four experiments, standard deviation less than 10 %; inhibitor concentration, 500 nM. ^b Mean value of at least four experiments, standard deviation usually less than 25 %, n.d. = not determined. ^c Hamster fibroblasts expressing human CYP11B2; substrate deoxycorticosterone, 100 nM. ^d Hamster fibroblasts expressing human CYP11B1; substrate deoxycorticosterone, 100 nM. ^e IC₅₀ CYP11B1/IC₅₀ CYP11B2, n.d. = not determined.

Inhibition of Steroidogenic and Hepatic CYP Enzymes (Tables 2 and 3). The inhibition of CYP17 was investigated using the 50,000 *g* sediment of the *E. coli* homogenate recombinantly expressing human CYP17 and progesterone (25 μM) as substrate.³² The percental inhibition values were measured at an inhibitor concentration of 2.5 μM. Most of the investigated compounds display rather low inhibitory action on CYP17 (Table 2). However, a distinct inhibition in the range of 31–74

% at a concentration of 2.5 μM is observed in case of the tetrahydro- and dihydronaphthalenes **2–6** which is comparable to the naphthalene parent compounds **I–III** (40–73 %). All other derivatives, including the keto analogues **9–11** and the investigated dihydro-1*H*-quinolin-2-ones, are considerably less active at CYP17 (< 22 %). Exceptions from this are lactam **12** (41 % inhibition) and the thiolactam analog **24** (72 %). The inhibition of CYP19 at a concentration of 500 nM was determined in vitro with human placental microsomes and [1β - ^3H]androstenedione as substrate as described by Thompson and Siiteri³³ using our modification.³⁴ In most cases, the inhibitory action on CYP19 is low (< 30 %) at the chosen concentration (Table 2). Exceptions are observed in case of the keto derivatives **10** and **11** as well as the lactam derivatives **13–15** displaying aromatase inhibition in the range of 53–63 %.

Table 2. Inhibition of Human CYP17, CYP19, and CYP1A2 In Vitro

compd	% inhibition ^a		
	[IC ₅₀ value ^b (μM)]		
	CYP17 ^c	CYP19 ^d	CYP1A2 ^e
I	40	[5.727]	99 [n.d.]
II	72	[0.586]	98 [n.d.]
III	73	[> 36]	97 [n.d.]
2	49	23	74 [0.598]
3	44	22	80 [0.443]
4	31	10	73[0.619]
5	38	< 5	72 [0.658]
6	74	< 5	90 [0.181]
9	20	31	60 [1.55]
10	< 5	53	57 [1.55]
11	21	58	57 [1.56]
12	41	21	50 [1.95]
13	< 5	62	25 [6.58]
14	8	54	53 [1.79]
15	< 5	63	36 [3.48]
17	7	17	14 [30.6]
19	12	< 5	25 [5.24]
20	< 5	5	20 [16.5]
21	22	< 5	< 5 [> 150]
24	72	< 5	77 [0.637]

^a Mean value of three experiments, standard deviation less than 10 %. ^b Mean value of two experiments, standard deviation less than 5 %. ^c *E. coli* expressing human CYP17; substrate progesterone, 25 μM ; inhibitor concentration, 2.5 μM ; ketoconazole, IC₅₀ = 2.78 μM . ^d Human placental CYP19; substrate androstenedione, 500 nM; inhibitor concentration, 500 nM; fadrozole, IC₅₀ = 30 nM. ^e Recombinantly expressed enzymes from baculovirus-infected insect microsomes (Supersomes); inhibitor concentration, 2.0 μM ; furafylline, IC₅₀ = 2.42 μM .

A selectivity profile relating to inhibition of crucial hepatic CYP enzymes (CYP1A2, CYP2B6, CYP2C9, CYP2C19, CYP2D6, and CYP3A4) was determined by use of recombinantly expressed enzymes from baculovirus-infected insect microsomes. As previous studies have shown that aldosterone synthase inhibitors of the naphthalene type are potent inhibitors of CYP1A2 but otherwise rather selective versus important hepatic CYP enzymes,^{14,15} most of the newly prepared compounds were first and foremost tested for their inhibitory action on CYP1A2 (Table 2). The parent compounds **I–III** are highly potent inhibitors of CYP1A2 (> 95 % inhibition at concentration of 2 μ M). Based on these naphthalene type compounds, the inhibitory potency slightly decreases in case of the dihydronaphthalene derivative **6** (90 %) and the tetrahydronaphthalene derivatives **2–5** (72–80 %). The keto analogues **9–11** exhibit 57–60 % inhibition corresponding with IC₅₀ values of 1.55–1.56 μ M. A further decrease of CYP1A2 inhibition to less than 50 % is observed for the investigated lactam bioisosters **12–15**, **17**, and **19–21**. This is especially true for chloro-substituted **17** as well as compounds **20** and **21** with modified heterocycle displaying IC₅₀ values greater than 15 μ M, but also for indanone **13** and methoxypyridine derivative **19** with IC₅₀ values greater than 5 μ M. However, compound **24**, the thio analog of **12**, displays a pronounced inhibitory potency (IC₅₀ = 0.637 μ M). Some compounds were also scrutinized for inhibition of other crucial hepatic CYP enzymes (Table 3). The data presented in Table 3 reveal that the investigated CYP enzymes are rather unaffected by the compounds with tetrahydronaphthalene (**3**), tetralone (**9–11**) as well as dihydro-1*H*-quinolin-2-one (**12**, **14**, and **21**) type molecular scaffold and with few exceptions (i.e., **9**, **11** at CYP3A4 and **21** at CYP2C9), the IC₅₀ values measured are significantly greater than 10 μ M.

Table 3. Inhibition of Selected Hepatic CYP Enzymes In Vitro

compd	IC ₅₀ value ^a (μ M)				
	CYP2B6 ^{b,c}	CYP2C9 ^{b,d}	CYP2C19 ^{b,e}	CYP2D6 ^{b,f}	CYP3A4 ^{b,g}
3	47.4	16.3	> 200	> 200	12.2
9	> 50	28.3	41.5	171	6.21
10	> 50	123	147	> 200	> 200
11	> 50	12.9	45.4	> 200	3.75
12	> 50	58.9	> 200	171	127
14	> 50	125	122	> 200	> 200
21	> 100	2.86	9.15	> 50	> 50

^b Mean value of two experiments, standard deviation less than 5 %. ^c Recombinantly expressed enzymes from baculovirus-infected insect microsomes (Supersomes). ^d Tranylcypromine, IC₅₀ = 6.24 μ M. ^e Sulfaphenazole, IC₅₀ = 318 nM. ^f Tranylcypromine, IC₅₀ = 5.95 μ M. ^g Quinidine, IC₅₀ = 14 nM. ^h Ketoconazole, IC₅₀ = 57 nM.

Plasma Protein Binding (Table 4). The plasma protein binding of compounds **9**, **10**, and **12** was determined by ultrafiltration. Test solutions of an aliquot of concentrated test compound and rat or human plasma were incubated at 37 °C for 1 hour and then centrifuged at 8000 *g* for 20 min. Ultrafiltrates were analyzed for drug concentrations by LC-MS/MS. The plasma protein binding of the investigated CYP11B2 inhibitors was found to be low. The bound form of keto compounds **9** and **10**

ranks between 22–25 % in both human and rat plasma. In case of the bioisosteric dihydro-1*H*-quinolin-2-one **12**, the amount of freely available compound is lower (approximately 60 % bound).

Table 4. Plasma Protein Binding of Compounds **9**, **10**, and **12**

compd	PPB ^a (% bound)	
	rat	human
9	25	24
10	24	22
12	60	61

^a Determined by analysis of the ultrafiltrates via LC-MS/MS; the degree of binding to the plasma proteins (PPB) is calculated by the following equation: % PPB = (1-[ligand_{ultrafiltrate}]/[ligand_{total}])·100.

In Vivo Pharmacokinetics (Table 5). The pharmacokinetic profile of selected compounds was determined after peroral application to male Wistar rats. Plasma samples were collected over 24 h and plasma concentrations were determined by HPLC-MS/MS. Compounds **9–12** and **14** were investigated in cassette dosing experiments (peroral dose = 5 mg/kg) and compared to fadrozole. All five compounds show comparable absorption rates (t_{\max} = 4–6 h) and terminal half-lives ($t_{1/2z}$ = 2.3–3.9 h). The slowest elimination is observed in case of tetralone **11** ($t_{1/2z}$ = 3.9 h) and dihydro-1*H*-quinolin-2-one **12** ($t_{1/2z}$ = 3.8 h). Within this series, compound **10** shows the highest maximal concentration (C_{\max}) in plasma (300 ng/mL) followed in the same range by compound **12** (261 ng/mL). Using the area under the curve ($AUC_{0-\infty}$) as a ranking criterion, the bioavailability after peroral cassette dosing increases in the order **11** (212 ng·h/mL) < **14** (659 ng·h/mL) < **9** (727 ng·h/mL) < **12** (1753 ng·h/mL) < **10** (3178 ng·h/mL). Compounds **12** and **21** were investigated in single dosing experiments (peroral dose = 25 mg/kg). The amounts of the test compounds found in the plasma after peroral application are rather high in case of **21** ($AUC_{0-\infty}$ = 1658 ng·h/mL) and high in case of **12** ($AUC_{0-\infty}$ = 4762 ng·h/mL). Comparing the AUC of peroral with intravenous (dose = 1 mg/kg) application of dihydro-1*H*-quinolin-2-one **12** reveals an absolute bioavailability of 71 %.

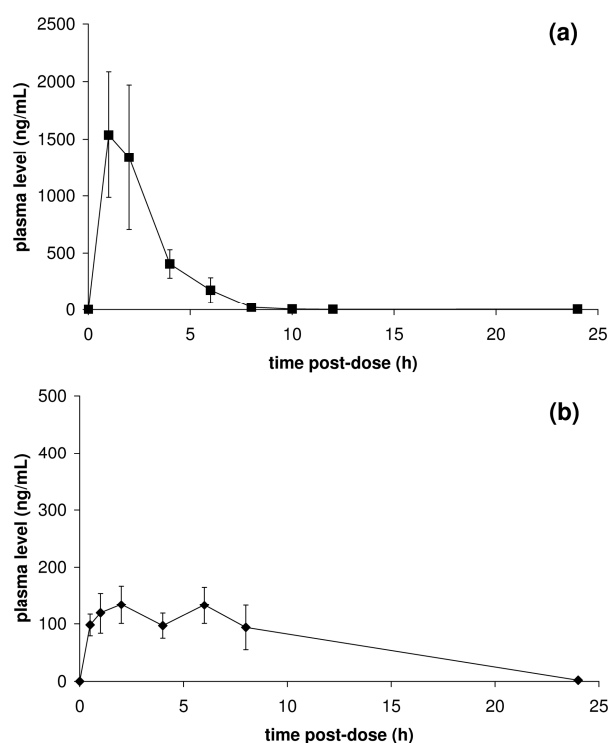
Table 5. Pharmacokinetic Profile of Compounds **9–12**, **14**, and **21**

compd	dose (mg/kg) ^a	$t_{1/2z}$ (h) ^b	t_{\max} (h) ^c	C_{\max} (ng/mL) ^d	$AUC_{0-\infty}$ (ng·h/mL) ^e
9 ^f	5	3.5	4.0	104	727
10 ^f	5	2.4	4.0	300	3178
11 ^f	5	3.9	4.0	35	212
12 ^{f,g}	5	3.8	4.0	261	1753
12	25	1.2	1.0	1537	4762
12	1 ^h	1.7	-	-	270
14 ^f	5	2.3	6.0	86	659
21	25	2.9	2.0	134	1658
fadrozole ^{f,g}	5	3.2	1.0	471	3207

^a Compounds were applied perorally to male Wistar rats. ^b Terminal half-life. ^c Time of maximal concentration. ^d Maximal concentration. ^e Area under the curve. ^f These compounds were investigated in a cassette dosing approach. ^g Mean value of two experiments. ^h Intravenous application.

Among the molecules with a cyclic ketone molecular scaffold, indanone **10** shows the highest availability in the plasma in the cassette dosing experiment with an $AUC_{0-\infty}$ in the range of the marketed drug fadrozole ($AUC_{0-\infty} = 3207 \text{ ng}\cdot\text{h/mL}$). The tetralone derivatives **9** and **11** exhibit significantly lower $AUC_{0-\infty}$ values (factor 4–15) albeit being eliminated in a decelerated rate ($t_{1/2z} = 3.5\text{--}3.9 \text{ h}$). Similarly, *N*-alkylation of **12** as accomplished in **14** decreases the $AUC_{0-\infty}$ value by a factor of approximately 3. Obviously, introduction of additional methyl or methylene units lowers the bioavailability which might be due to the metabolic vulnerability of these residues and providing potential sites for oxidative transformations. In the single dosing experiments, isoquinoline derivative **21** (with additional benzene moiety compared to **12**) displays an $AUC_{0-\infty}$ somewhat lower than that of unsubstituted **12** (factor 3) as well as a lower maximal concentration in the plasma (factor 11). Contrariwise, the terminal half-life of **21** is greater. This becomes particularly apparent from Figure 1 where the mean profile of plasma levels (ng/mL) in rat versus time after oral application (25 mg/kg) of compounds **12** (Figure 1a) and **21** (Figure 1b) are shown. The concentrations of **21** are rather constant and rank between 90–130 ng/mL in a timeframe of 0.5–8 hours after application, albeit the plasma levels are considerably lower than the plasma levels of **12**.

Figure 1^a



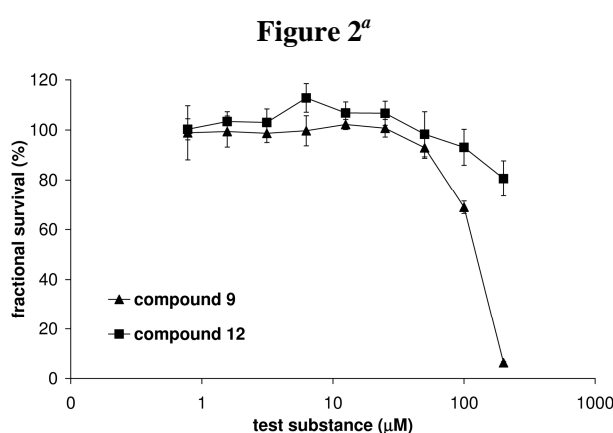
^a Mean profile (\pm) SEM of plasma levels (ng/ml) in rat versus time after oral application (25 mg/kg) of compounds **12** (a) and **21** (b) determined in single dosing experiments.

Discussion and Conclusion

Selectivity is a prerequisite of any drug candidate to avoid adverse side effects. In the development process of aldosterone synthase inhibitors, it is a crucial point to investigate the selectivity profile toward other cytochrome P450 enzymes at an early stage. It is known that the concept of heme-iron complexation (e.g., by nitrogen-containing heterocycles) is an appropriate strategy to discover highly potent and selective inhibitors. Due to this binding mechanism, however, a putative CYP11B2 inhibitor is potentially capable of interacting with other CYP enzymes by similarly binding to the heme cofactor with its metal binding moiety. Taking into consideration that the key enzyme of glucocorticoid biosynthesis, 11 β -hydroxylase (CYP11B1), and CYP11B2 have a sequence homology of approximately 93 %, ³⁵ the selectivity issue is especially critical for the design of CYP11B2 inhibitors. Recently, we have demonstrated that 3-pyridine substituted naphthalenes such as **I–III** provide an ideal molecular scaffold for high inhibitory potency at the target enzyme CYP11B2 as well as high selectivity toward several other CYP enzymes (e.g., CYP11B1, CYP17, CYP19).¹⁴ However, these compounds strongly inhibit the hepatic enzyme CYP1A2 (e.g., compounds **I–III** in Table 2) that makes up about 10 % of the overall cytochrome P450 content in the liver and metabolizes aromatic and heterocyclic amines as well as polycyclic aromatic hydrocarbons. In recent QSAR studies, CYP1A2 inhibition has been identified to correlate positively with aromaticity and lipophilicity.³⁶ Furthermore, both CYP1A2 substrates and inhibitors are usually small-volume molecules with a planar shape (e.g., caffeine³⁷ and furafylline³⁸). Rationalizing these findings, our design strategy aimed at reducing the aromaticity and disturbing the planarity of the molecules while keeping the pharmacophoric points³⁹ of the naphthalene molecular scaffold (see Chart 1).

These considerations led to the development of pyridine substituted dihydro- and tetrahydronaphthalenes **1–6**. The compounds are potent aldosterone synthase inhibitors (IC_{50} = 1.6–44 nM) with pronounced selectivity versus CYP11B1 (selectivity factor = 68–347). As hypothesized, a decrease of CYP1A2 inhibition can be observed along with decreased aromaticity (i.e., number of aromatic carbons) and planarity within this series. While the fully aromatized naphthalenes **I–III** exhibit 97–99 % inhibition at a concentration of 2 μ M, dihydronaphthalene **6** is slightly less potent (90 %) and the tetrahydro derivatives **1–5** are significantly less potent (72–80 %) inhibitors of CYP1A2. However, IC_{50} values are still below 1 μ M and thus the molecules are rather strongly inhibiting CYP1A2. Further increase in CYP1A2 selectivity is achieved by introduction of a keto group into the saturated ring as accomplished in compounds **9–11**. The inhibitory potencies toward CYP1A2 decrease to IC_{50} values in the range of 1.55–1.56 μ M. Presumably, the decrease in CYP1A2 inhibition is due to a reduced lipophilicity of the cyclic ketone scaffold compared to the tetrahydronaphthalene scaffold. Lipophilicity has been hypothesized to be one of the most important variables influencing CYP1A2 inhibition.³⁶ Furthermore, the highly potent aldosterone synthase inhibitors **9** (IC_{50} = 7.8 nM) and **10** (IC_{50} = 4.4 nM) show reasonable plasma levels after peroral application to male Wistar rats (Table 5). However, tetralone **9** turned out to be cytotoxic to the human cell line U-937 at a concentration of 100

μM (Figure 2). Subsequent bioisosteric exchange of the cyclic ketone in **9** by a lactam gave rise to the dihydro-1*H*-quinolin-2-one derivatives **12–26**. Contrary to tetralone **9**, dihydro-1*H*-quinolin-2-one **12** exhibits no distinct cytotoxic effect on U-937 cells up to the highest concentration tested (Figure 2). In addition, compound **12** is an even slightly less potent inhibitor of CYP1A2 ($\text{IC}_{50} = 1.95 \mu\text{M}$) than the analogous tetralone ($\text{IC}_{50} = 1.55 \mu\text{M}$) which is again in correspondence with the reduced lipophilicity compared to the bioisosteric **9**. Contrariwise, lipophilicity does not basically influence the CYP1A2 potency within the series of dihydro-1*H*-quinolin-2-ones (**12–21**) as does the substitution pattern of the molecules, especially in the heterocyclic binding site (**20**, **21**). It is also striking that even minor structural variations such as introduction of a chloro substituent into the dihydro-1*H*-quinolin-2-one core as accomplished in **17** can trigger an almost complete loss of CYP1A2 activity.



^a Mean profile (\pm) SEM of fractional survival (%) of human U-937 cells in presence of compound **9** or **12**.

Pharmacokinetic investigations performed with compound **12** reveal a peroral absolute bioavailability of 71%. Compounds **14** and **21** are also capable of crossing the gastrointestinal tract and reach the general circulation after peroral application. However, their total range of absorption is below that of **12**. The plasma protein binding of inhibitor **12** was found to be low in both rat and human plasma (approximately 60%), indicating that a sizeable free fraction of circulating compound is present in the plasma. Within the series of dihydro-1*H*-quinolin-2-one type inhibitors **12–26**, most compounds are highly active at the target enzyme. This particularly applies to the derivatives with a functionalized pyridine heterocycle, for example methoxy derivative **20** ($\text{IC}_{50} = 0.2 \text{ nM}$) and isoquinoline derivatives **21** ($\text{IC}_{50} = 0.2 \text{ nM}$) and **22** ($\text{IC}_{50} = 0.1 \text{ nM}$). By introduction of a chloro substituent in 8-position or methoxy in 5-position of the pyridine heterocycle, the selectivity increases to a factor of greater than 400 (**17**, **20**). Hence, these compounds are approximately 40-fold more selective than fadrozole (selectivity factor = 10). With respect to the high homology of the two CYP11B isoforms, this experimental result is particularly noteworthy.

In order to determine a suitable candidate to investigate aldosterone-lowering effects in rats, we investigated the most potent and selective inhibitors of the present series for their ability to block aldosterone biosynthesis in V79 MZh cells expressing *rat* CYP11B2 prior to in vivo experiments. The

results revealed that only compound **21** (and to a minor degree also the *N*-methyl analog **22**) shows a moderate inhibitory action on rat CYP11B2 in vitro (unpublished results). Recently, this finding was corroborated by in vivo trials showing that isoquinoline derivative **21** induces a significant aldosterone-lowering effect in ACTH stimulated rats (data to be published separately).

In summary, nonsteroidal aldosterone synthase inhibitors with a dihydro-1*H*-quinolin-2-one molecular scaffold are superior to the previously investigated pyridyl-naphthalenes such as **I–III**. Most compounds exhibit a potent inhibitory activity at the target enzyme and isoquinoline derivative **22** is the most potent CYP11B2 inhibitor described so far ($IC_{50} = 0.1$ nM). The selectivity versus other steroidogenic as well as hepatic cytochrome P450 enzymes is generally high. Most notably, the strong inhibition of the hepatic CYP1A2 enzyme (> 95 % at a concentration of 2 μ M) present in the naphthalene type inhibitors is significantly lower in case of the dihydro-1*H*-quinolin-2-ones with IC_{50} values up to > 150 μ M (**21**). The investigated molecules reach the circulation after peroral administration to rats (e.g., **12** with a peroral bioavailability of 71 %). Moreover, it has been found recently that isoquinoline derivative **21** significantly reduces the plasma aldosterone levels of ACTH stimulated rats (data to be published separately). Our current research focuses on further in vivo investigations of compound **21** and structurally related compounds in disease oriented models to determine their capability to prevent or reverse myocardial fibrosis and reduce CHF induced mortality.

Experimental Section

Chemical and Analytical Methods. Melting points were measured on a Mettler FP1 melting point apparatus and are uncorrected. 1H NMR and ^{13}C spectra were recorded on a Bruker DRX-500 instrument. Chemical shifts are given in parts per million (ppm), and tetramethylsilane (TMS) was used as internal standard for spectra obtained in DMSO- d_6 and $CDCl_3$. All coupling constants (J) are given in hertz. Mass spectra (LC/MS) were measured on a TSQ Quantum (Thermo Electron Corporation) instrument with a RP18 100-3 column (Macherey Nagel) and with water/acetonitrile mixtures as eluents. GC/MS spectra were measured on a GCD Series G1800A (Hewlett Packard) instrument with an Optima-5-MS (0.25 μ M, 30 m) column (Macherey Nagel). Elemental analyses were carried out at the Department of Chemistry, University of Saarbrücken. Reagents were used as obtained from commercial suppliers without further purification. Solvents were distilled before use. Dry solvents were obtained by distillation from appropriate drying reagents and stored over molecular sieves. Flash chromatography was performed on silica gel 40 (35/40–63/70 μ M) with petroleum ether/ethyl acetate mixtures as eluents, and the reaction progress was determined by thin-layer chromatography analyses on Alugram SIL G/UV254 (Macherey Nagel). Visualization was accomplished with UV light and $KMnO_4$ solution. All microwave irradiation experiments were carried out in a CEM-Discover monomode microwave apparatus.

The following compounds were prepared according to previously described procedures: 6-bromo-1,2,3,4-tetrahydronaphthalen-2-ol (**2a**),²¹ 6-bromo-3,4-dihydroquinolin-2(1*H*)-one (**12a**),²⁴ 5-bromo-1,3-dihydro-2*H*-indol-2-one (**13a**),²⁵ 6-bromo-8-nitro-3,4-dihydroquinolin-2(1*H*)-one (**18a**).²⁷

Synthesis of the Target Compounds

Procedure A.¹⁷ Boronic acid (0.75 mmol, 1 equivalent), aryl bromide or -triflate (0.9–1.3 equivalents), and tetrakis(triphenylphosphane)palladium(0) (43 mg, 37.5 μ mol, 5 mol %) were suspended in 1.5 mL DMF in a 10 mL septum-capped tube containing a stirring magnet. To this was added a solution of NaHCO₃ (189 mg, 2.25 mmol, 3 equivalents) in 1.5 mL water and the vial was sealed with a Teflon cap. The mixture was irradiated with microwaves for 15 min at a temperature of 150 °C with an initial irradiation power of 100 W. After the reaction, the vial was cooled to 40 °C, the crude mixture was partitioned between ethyl acetate and water and the aqueous layer was extracted three times with ethyl acetate. The combined organic layers were dried over MgSO₄ and the solvents were removed in vacuo. The coupling products were obtained after flash chromatography on silica gel (petroleum ether/ethyl acetate mixtures) and/or crystallization.

Procedure B. Boronic acid (1 equivalent), aryl bromide or (1.3–1.5 equivalents), and tetrakis(triphenylphosphane)palladium(0) (5 mol %) were suspended in toluene/ethanol 4/1 to give a 0.07–0.1 M solution of boronic acid under an atmosphere of nitrogen. To this was added a 1 N aqueous solution of Na₂CO₃ (6 equivalents). The mixture was then refluxed for 12–18 h, cooled to room temperature, diluted with water and extracted several times with ethyl acetate. The combined extracts were dried over MgSO₄, concentrated and purified by flash chromatography on silica gel (petroleum ether/ethyl acetate mixtures) and/or crystallization.

3-(5,6,7,8-tetrahydronaphthalen-2-yl)pyridine (1) was obtained according to procedure A from **1a** (280 mg, 1.0 mmol), 3-pyridineboronic acid (160 mg, 1.3 mmol) and NaHCO₃ (252 mg, 3.0 mmol) after flash chromatography on silica gel (petroleum ether/ethyl acetate, 2/1, *R_f* = 0.20) as a pale yellow oil (142 mg, 0.68 mmol, 68 %), mp (HCl salt) 200–202 °C. LC/MS *m/z* 210.27 (MH⁺). Anal. (C₁₅H₁₅N·HCl) C, H, N.

6-Pyridin-3-yl-1,2,3,4-tetrahydronaphthalen-2-ol (2) was obtained according to procedure A from **2a** (114 mg, 0.50 mmol) and 3-pyridineboronic acid (80 mg, 0.65 mmol) after flash chromatography on silica gel (ethyl acetate, *R_f* = 0.27) as a colorless solid (96 mg, 0.43 mmol, 86 %), mp 118–120 °C. LC/MS *m/z* 226.23 (MH⁺). Anal. (C₁₅H₁₅NO·0.1H₂O) C, H, N.

3-(6-Methoxy-5,6,7,8-tetrahydronaphthalen-2-yl)pyridine (3). To a suspension of NaH (73 mg, 1.84 mmol, 60 % dispersion in oil) in 10 mL dry THF was added dropwise a solution of **2** (345 mg, 1.53 mmol) in 5 mL THF at room temperature. The mixture was heated to 50 °C until evolution of hydrogen ceased and then cooled to room temperature again. Thereupon, a solution of methyl iodide (326 mg, 2.30 mmol) in 5 mL THF was added via canula and stirring was continued at 50 °C for 3 h. The mixture was treated with saturated NH₄Cl solution and extracted three times with ethyl acetate. The combined organic extracts were washed with water and brine, dried over MgSO₄ and evaporated

to dryness. The crude product was purified by flash chromatography on silica gel (petroleum ether/ethyl acetate, 7/3, $R_f = 0.09$) to afford **3** as a colorless oil (289 mg, 1.21 mmol, 79 %), mp (HCl salt) 188–190 °C. LC/MS m/z 240.29 (MH^+). Anal. ($C_{16}H_{17}NO \cdot HCl \cdot 0.6H_2O$) C, H, N.

3-(6-Ethoxy-5,6,7,8-tetrahydronaphthalen-2-yl)pyridine (4) was obtained as described for **3** starting from **2** (270 mg, 1.20 mmol), NaH (58 mg, 1.44 mmol, 60 % dispersion in oil) and ethyl bromide (196 mg, 1.80 mmol) after flash chromatography on silica gel (petroleum ether/ethyl acetate, 1/1, $R_f = 0.31$) as a colorless oil (198 mg, 0.78 mmol, 65 %), mp (HCl salt) 186–188 °C. LC/MS m/z 254.29 (MH^+). Anal. ($C_{17}H_{19}NO \cdot HCl \cdot 0.5H_2O$) C, H, N.

6-Pyridin-3-yl-1,2,3,4-tetrahydronaphthalene-2-carbonitrile (5) was obtained according to procedure A from **5a** (130 mg, 0.55 mmol) and 3-pyridineboronic acid (88 mg, 0.72 mmol) after flash chromatography on silica gel (petroleum ether/ethyl acetate, 1/1, $R_f = 0.17$) as a colorless solid (91 mg, 0.39 mmol, 71 %), mp 110–111 °C. 1H -NMR (500 MHz, $CDCl_3$): $\delta = 2.12$ (m, 1H), 2.23 (m, 1H), 2.92 (m, 1H), 3.02–3.13 (m, 3H), 3.18 (dd, $^2J = 16.4$ Hz, $^3J = 5.7$ Hz, 1H), 7.19 (d, $^3J = 7.9$ Hz, 1H), 7.31 (s, 1H), 7.33–7.37 (m, 2H), 7.83 (m, 1H), 8.57 (dd, $^3J = 5.0$ Hz, $^4J = 1.6$ Hz, 1H), 8.80 (d, $^4J = 1.6$ Hz, 1H). ^{13}C -NMR (125 MHz, $CDCl_3$): $\delta = 25.5, 26.1, 27.1, 32.1, 121.8, 123.5, 125.1, 127.8, 129.8, 132.3, 134.2, 135.5, 136.2, 136.4, 148.2, 148.5$. LC/MS m/z 235.26 (MH^+). Anal. ($C_{16}H_{14}N_2 \cdot 0.1H_2O$) C, H, N.

6-Pyridin-3-yl-3,4-dihydronaphthalene-2-carbonitrile (6). To a solution of **6a** (562 mg, 1.58 mmol) in 10 mL degassed DMF were added zinc cyanide (117 mg, 1.00 mmol) and tetrakis(triphenylphosphane)palladium(0) (173 mg, 0.15 mmol) and the mixture was heated at 100 °C for 2 h. After cooling to room temperature, the mixture was diluted with 200 mL of water and extracted three times with ethyl acetate. The combined organic extracts were washed with water and brine, dried over $MgSO_4$ and evaporated to dryness. The crude product was crystallized from petroleum ether/ethyl acetate to afford **6** as colorless needles (286 mg, 1.23 mol, 78 %), mp 142–143 °C. LC/MS m/z 233.23 (MH^+). Anal. ($C_{16}H_{12}N_2$) C, H, N.

4-Methyl-7-pyridin-3-yl-3,4-dihydro-2H-1,4-benzoxazine (7) was obtained according to procedure A from 7-bromo-4-methyl-3,4-dihydro-2H-1,4-benzoxazine (228 mg, 1.00 mmol) and 3-pyridineboronic acid (160 mg, 1.30 mmol) after flash chromatography on silica gel (petroleum ether/ethyl acetate, 1/1, $R_f = 0.26$) as an off-white solid (102 mg, 0.45 mmol, 45 %), mp 70–72 °C. LC/MS m/z 227.21 (MH^+). Anal. ($C_{14}H_{14}N_2O$) C, H, N.

3-(2,3-Dihydro-1,4-benzodioxin-6-yl)pyridine (8) was obtained according to procedure A from 6-bromo-2,3-dihydro-1,4-benzodioxine (215 mg, 1.00 mmol) and 3-pyridineboronic acid (160 mg, 1.30 mmol) after flash chromatography on silica gel (petroleum ether/ethyl acetate, 7/3, $R_f = 0.14$) as a colorless solid (184 mg, 0.86 mmol, 86 %), mp 59–61 °C. LC/MS m/z 214.19 (MH^+). Anal. ($C_{16}H_{12}N_2$) C, H, N.

6-Pyridin-3-yl-3,4-dihydronaphthalen-2(1H)-one (9) was obtained according to procedure A from 6-bromo-2-tetralone (113 mg, 0.50 mmol) and 3-pyridineboronic acid (80 mg, 0.65 mmol) after

flash chromatography on silica gel (petroleum ether/ethyl acetate, 1/1, $R_f = 0.15$) as a colorless oil (97 mg, 0.43 mmol, 86 %), mp (HCl salt) 180–182 °C. LC/MS m/z 224.20 (MH^+). Anal. ($C_{15}H_{13}NO \cdot HCl \cdot 0.4H_2O$) C, H, N.

5-Pyridin-3-yl-2,3-dihydro-1H-inden-1-one (10) was obtained according to procedure A from 5-bromo-1-indanone (211 mg, 1.00 mmol) and 3-pyridineboronic acid (160 mg, 1.30 mmol) after flash chromatography on silica gel (petroleum ether/ethyl acetate, 1/1, $R_f = 0.14$) as a colorless solid (146 mg, 0.69 mmol, 69 %), mp 122–123 °C. LC/MS m/z 210.69 (MH^+). Anal. ($C_{14}H_{11}NO \cdot 0.1H_2O$) C, H, N.

6-(5-Methoxypyridin-3-yl)-3,4-dihydronaphthalen-2(1H)-one (11) was obtained according to procedure A from 6-bromo-2-tetralone (225 mg, 1.00 mmol) and 5-methoxy-3-pyridineboronic acid (199 mg, 1.30 mmol) after flash chromatography on silica gel (petroleum ether/ethyl acetate, 1/1, $R_f = 0.15$) as an off-white solid (133 mg, 0.53 mmol, 53 %), mp 109–110 °C. LC/MS m/z 254.01 (MH^+). Anal. ($C_{16}H_{15}NO_2$) C, H, N.

6-Pyridin-3-yl-3,4-dihydroquinolin-2(1H)-one (12) was obtained according to procedure B from **12a** (2.71 g, 12.0 mmol) and 3-pyridineboronic acid (1.23 g, 10.0 mmol) after crystallization from acetone/diethyl ether as colorless needles (2.15 g, 9.59 mmol, 96 %), mp 181–183 °C. 1H -NMR (500 MHz, $DMSO-d_6$): $\delta = 2.49$ (t, $^3J = 7.3$ Hz, 2H), 2.95 (t, $^3J = 7.3$ Hz, 2H), 6.95 (d, $^3J = 8.2$ Hz, 1H), 7.43 (ddd, $^3J = 7.9$ Hz, $^3J = 4.7$ Hz, $^5J = 0.6$ Hz, 1H), 7.51 (dd, $^3J = 8.2$ Hz, $^4J = 2.2$ Hz, 1H), 7.56 (d, $^4J = 2.1$ Hz, 1H), 8.00 (ddd, $^3J = 7.9$ Hz, $^4J = 2.2$ Hz, $^4J = 1.6$ Hz, 1H), 8.50 (dd, $^3J = 4.7$ Hz, $^4J = 1.5$ Hz, 1H), 8.84 (d, $^4J = 2.2$ Hz, 1H), 10.19 (s, 1H). ^{13}C -NMR (125 MHz, $DMSO-d_6$): $\delta = 24.8, 30.3, 115.6, 123.8, 124.3, 125.6, 126.2, 130.6, 133.4, 135.2, 138.4, 147.2, 147.8, 170.2$. LC/MS m/z 225.25 (MH^+). Anal. ($C_{14}H_{12}N_2O \cdot 0.1H_2O$) C, H, N.

5-Pyridin-3-yl-1,3-dihydro-2H-indol-2-one (13) was obtained according to procedure A from **13a** (159 mg, 0.75 mmol) and 3-pyridineboronic acid (123 mg, 1.00 mmol) after crystallization from acetone/diethyl ether as colorless needles (129 mg, 0.61 mmol, 81 %), mp 218–220 °C. LC/MS m/z 211.01 (MH^+). Anal. ($C_{13}H_{10}N_2O \cdot 0.3H_2O$) C, H, N.

1-Methyl-6-pyridin-3-yl-3,4-dihydroquinolin-2(1H)-one (14) was obtained according to procedure A from **14a** (110 mg, 0.46 mmol) and 3-pyridineboronic acid (74 mg, 0.60 mmol) after flash chromatography on silica gel (petroleum ether/ethyl acetate, 2/3, $R_f = 0.07$) as colorless needles (83 mg, 0.35 mmol, 76 %), mp 100–101 °C. LC/MS m/z 239.80. Anal. ($C_{15}H_{14}N_2O \cdot 0.1H_2O$) C, H, N.

1-Ethyl-6-pyridin-3-yl-3,4-dihydroquinolin-2(1H)-one (15) was obtained according to procedure A from **15a** (229 mg, 0.90 mmol) and 3-pyridineboronic acid (92 mg, 0.75 mmol) after flash chromatography on silica gel (petroleum ether/ethyl acetate, 1/1, $R_f = 0.09$) and crystallization from acetone/diethyl ether as colorless plates (125 mg, 0.50 mmol, 55 %), mp 91–92 °C. LC/MS m/z 253.00 (MH^+). Anal. ($C_{16}H_{16}N_2O \cdot 0.1H_2O$) C, H, N.

1-(1-Methylethyl)-6-pyridin-3-yl-3,4-dihydroquinolin-2(1H)-one (16) was obtained according to procedure A from **16a** (174 mg, 0.65 mmol) and 3-pyridineboronic acid (74 mg, 0.60 mmol) after

flash chromatography on silica gel (petroleum ether/ethyl acetate, 1/1, $R_f = 0.14$) as a colorless solid (47 mg, 0.18 mmol, 29 %), mp 100–101 °C. LC/MS m/z 267.10 (MH^+). Anal. ($C_{17}H_{18}N_2O$) C, H, N.

8-Chloro-6-pyridin-3-yl-3,4-dihydroquinolin-2(1H)-one (17). To a solution of **12** (560 mg, 2.50 mmol) in 5 mL DMF was added *N*-chlorosuccinimide (368 mg, 2.75 mmol) in 5 mL DMF over a period 2 h at 65 °C. After additional 3 h at 65 °C, the mixture was poured into ice water and extracted three times with ethyl acetate. The combined organic layers were washed with water and brine, dried over $MgSO_4$ and the solvent was evaporated in vacuo. **17** was obtained after flash chromatography on silica gel (petroleum ether/ethyl acetate, 3/7, $R_f = 0.15$) and crystallization from acetone/diethyl ether as colorless needles (225 mg, 0.87 mmol, 35 %), mp 177–178 °C. GC/MS m/z 258.95 (M^+). Anal. ($C_{14}H_{11}ClN_2O \cdot 0.1H_2O$) C, H, N.

8-Nitro-6-pyridin-3-yl-3,4-dihydroquinolin-2(1H)-one (18) was obtained according to procedure B from **18a** (1.0 g, 3.70 mmol) and 3-pyridineboronic acid (546 mg, 4.44 mmol) after flash chromatography on silica gel (ethyl acetate, $R_f = 0.15$) as yellow needles (311 mg, 1.16 mmol, 31 %), mp 187–189 °C. LC/MS m/z 269.94 (MH^+). Anal. ($C_{14}H_{11}N_3O_3$) C, H, N.

6-(5-Methoxy-pyridin-3-yl)-3,4-dihydroquinolin-2(1H)-one (19) was obtained according to procedure A from **12a** (170 mg, 0.75 mmol) and 5-methoxy-3-pyridineboronic acid (150 mg, 0.98 mmol) after crystallization from acetone/diethyl ether as colorless needles (77 mg, 0.30 mmol, 40 %), mp 213–215 °C. LC/MS m/z 255.02 (MH^+). Anal. ($C_{15}H_{14}N_2O_2$) C, H, N.

6-(5-methoxy-pyridin-3-yl)-1-methyl-3,4-dihydroquinolin-2(1H)-one (20) was obtained according to procedure A from **14a** (200 mg, 0.83 mmol) and 5-methoxy-3-pyridineboronic acid (115 g, 0.75 mmol) after crystallization from acetone/diethyl ether as colorless needles (132 mg, 0.49 mmol, 66 %), mp 158–159 °C. LC/MS m/z 268.95 (MH^+). Anal. ($C_{16}H_{16}N_2O_2 \cdot 0.1H_2O$) C, H, N.

6-Isoquinolin-4-yl-3,4-dihydroquinolin-2(1H)-one (21) was obtained according to procedure B from **12a** (1.55 g, 6.85 mmol) and 4-isoquinolineboronic acid (950 mg, 5.50 mmol) after crystallization from acetone/diethyl ether as colorless needles (800 mg, 2.92 mmol, 53 %), mp 221–222 °C. LC/MS m/z 275.04 (MH^+). Anal. ($C_{18}H_{14}N_2O \cdot 0.1H_2O$) C, H, N.

6-Isoquinolin-4-yl-1-methyl-3,4-dihydroquinolin-2(1H)-one (22) was obtained according to procedure A from **14a** (264 mg, 1.10 mmol) and 4-isoquinolineboronic acid (172 mg, 1.00 mmol) after crystallization from acetone/diethyl ether as colorless needles (163 mg, 0.57 mmol, 57 %), mp 175–176 °C. LC/MS m/z 289.91 (MH^+). Anal. ($C_{19}H_{16}N_2O$) C, H, N.

6-Pyrimidin-5-yl-3,4-dihydroquinolin-2(1H)-one (23) was obtained according to procedure A from **12a** (226 mg, 1.00 mmol) and 5-pyrimidineboronic acid (103 mg, 0.83 mmol) after crystallization from ethanol as colorless needles (75 mg, 0.33 mmol, 40 %), mp 232–233 °C. LC/MS m/z 225.74 (MH^+). Anal. ($C_{13}H_{11}N_3O \cdot 0.2H_2O$) C, H, N.

6-Pyridin-3-yl-3,4-dihydroquinoline-2(1H)-thione (24). A suspension of **12** (395 mg, 1.76 mmol) and Lawesson's reagent (356 mg, 0.88 mmol) in dry toluene was refluxed for 30 min under an atmosphere of nitrogen. After cooling to room temperature, the solvent was removed in vacuo and the

residue was purified by flash chromatography on silica gel (petroleum ether/ethyl acetate, 3/7, $R_f = 0.31$) to afford **24** as yellow plates (63 mg, 0.26 mmol, 15 %), mp 265–267 °C. LC/MS m/z 241.05 (MH^+). Anal. ($C_{14}H_{12}N_2S$) C, H, N.

8-Chloro-6-pyridin-3-yl-3,4-dihydroquinoline-2(1H)-thione (25) was obtained as described for **24** starting from **17** (900 mg, 3.48 mmol) and Lawesson's reagent (985 mg, 2.44 mmol) after flash chromatography on silica gel (ethyl acetate, $R_f = 0.26$) and crystallization from acetone/diethyl ether as yellow needles (212 mg, 0.77 mmol, 22 %), mp 174–175 °C. GC/MS m/z 273.95 ($M^{35}Cl^+$), 275.95 ($M^{37}Cl^+$). Anal. ($C_{14}H_{11}ClN_2S$) C, H, N.

7-Pyridin-3-yl-2H-1,4-benzothiazin-3(4H)-one (26) was obtained according to general procedure B from 7-bromo-2H-1,4-benzothiazin-3(4H)-one (1.15 g, 4.71 mmol) and 3-pyridineboronic acid (695 mg, 5.56 mmol) after flash chromatography on silica gel (petroleum ether/ethyl acetate, 1/1, $R_f = 0.20$) and crystallization from ethanol as colorless needles (486 mg, 2.01 mmol, 43 %), mp 238–240 °C. LC/MS m/z 242.99 (MH^+). Anal. ($C_{13}H_{10}N_2OS \cdot 0.2H_2O$) C, H, N.

Biological Methods. 1. Enzyme Preparations. CYP17 and CYP19 preparations were obtained by described methods: the 50,000 g sediment of *E. coli* expressing human CYP17³² and microsomes from human placenta for CYP19.³⁴ **2. Enzyme Assays.** The following enzyme assays were performed as previously described: CYP17³² and CYP19.³⁴ **3. Activity and Selectivity Assay Using V79 Cells.** V79 MZh 11B1 and V79 MZh 11B2 cells^{10,28} were incubated with [4-¹⁴C]-11-deoxycorticosterone as substrate and inhibitor in at least three different concentrations. The enzyme reactions were stopped by addition of ethyl acetate. After vigorous shaking and a centrifugation step (10,000 g, 2 min), the steroids were extracted into the organic phase, which was then separated. The conversion of the substrate was analyzed by HPTLC and a phosphoimaging system as described. **4. Inhibition of Human Hepatic CYP Enzymes.** The recombinantly expressed enzymes from baculovirus-infected insect microsomes (Supersomes) were used and the manufacturer's instructions (www.gentest.com) were followed. **5. In Vivo Pharmacokinetics.** Animal trials were conducted in accordance with institutional and international ethical guidelines for the use of laboratory animals. Cassette dosing: Male Wistar rats weighing 297–322 g (Janvier, France) were housed in a temperature-controlled room (20–24 °C) and maintained in a 12 h light/12 h dark cycle. Food and water were available ad libitum. The animals were anaesthetised with a ketamine (135 mg/kg)/xylazine (10 mg/kg) mixture, and cannulated with silicone tubing via the right jugular vein. Prior to the first blood sampling, animals were connected to a counterbalanced system and tubing, to perform blood sampling in the freely moving rat. Separate stock solutions (5 mg/mL) were prepared for the tested compounds in labrasol/water (1:1; v/v), leading to a clear solution. Immediately before application, the cassette dosing mixture was prepared by adding equal volumes of the stock solutions to end up with a final concentration of 1 mg/mL for each compound. The mixture was applied perorally to 3 rats with an injection volume of 5 mL/kg (Time 0). Blood samples (250 µl) were collected 1 hour before application and 1, 2, 4, 6, 8, and 24 hours thereafter. They were centrifuged at 650 g for 10 minutes at

4 °C and then the plasma was harvested and kept at -20 °C until LC/MS analysis. To 50 µL of rat plasma sample and calibration standard 100 µL acetonitrile containing the internal standard was added. Samples and standards were vigorously shaken and centrifuged for 10 minutes at 6000 g and 20 °C. For the test items, an additional dilution was performed by mixing 50 µL of the particle free supernatant with 50 µL water. An aliquot was transferred to 200 µL sampler vials and subsequently subjected to LC-MS/MS. HPLC-MS/MS analysis and quantification of the samples was carried out on a Surveyor-HPLC-system coupled with a TSQ Quantum (ThermoFinnigan) triple quadrupole mass spectrometer equipped with an electrospray interface (ESI). The mean of absolute plasma concentrations (\pm SEM) was calculated for the 3 rats and the regression was performed on group mean values. The pharmacokinetic analysis was performed using a noncompartment model (PK Solutions 2.0, Summit Research Services). Single dosing: The single dose experiments were performed as described for the cassette dosing procedure with male Wistar rats weighing 234–276 g (Janvier, France). Separate stock solutions (5 mg/mL) were prepared for compound **12** in PEG400/water/ethanol (50:40:10; v/v/v) and for compound **21** in labrasol/water (1:1; v/v), leading to clear solutions. Compound **12** was applied at 25 mg/kg perorally and 1 mg/kg intravenously and compound **21** at 25 mg/kg perorally to 4 rats each. Additional blood samples were taken 10 and 12 hours after application in case of peroral application and 0.08, 0.25, 0.50, and 0.75 hours in case of intravenous application of compound **12**, respectively.

6. Plasma Protein Binding. A 10 mM test compound solution and ketoprofen solution is prepared in acetonitrile. The test compound solution is diluted with solvent to the 50 fold concentration (150 µM, working solution) used in the assay (3 µM). In a 1.5 mL eppendorff vial, 3 µL working solution are given to 147 µL serum (rat or human) and mixed. For recovery the same dilutions are done in ultrafiltrated serum. The solutions are incubated for 1 hour at 37 °C. The whole samples (6 test solutions, 6 recovery samples) are centrifuged at 8000 g for 20 min using Centrifree micropartition devices (Millipore). 75 µL of ultra filtrate (UF) sample is removed for sample preparation. To 75 µL of sample or 150 µL calibration standard, 75 µL or 150 µL acetonitrile containing the internal standard (ketoprofen, 1 µM) is added to precipitate plasma proteins. Samples are then vigorously shaken (10 sec.) and centrifuged for 10 minutes at 6000 g and 20 °C. An aliquot (70 µL) of the particle-free supernatant is subsequently subjected to LC-MS/MS. The degree of binding to the plasma proteins (PPB) is calculated by the following equation: % Protein binding = $(1 - [\text{ligand}_{\text{ultrafiltrat}}]/[\text{ligand}_{\text{total}}]) \cdot 100$.

7. Cytotoxicity. Cell viability upon drug exposure was determined using a fluorimetric alamar blue conversion assay using a 96-well plate format. Briefly, U-937 cells (human monocytic leukemia) were seeded in growth medium into 96-well plates at a final density of 5×10^4 cells/ml and exposed to the respective compounds for the indicated time intervals (6 replicates per concentration). At the end of the exposure time, alamar blue (Biosource International, Camarillo, CA) was added at 10% (v/v) and incubated for 4 hours. Fluorescence intensity was quantitated using a Wallac Victor fluorescence plate reader (Perkin Elmer, Wellesley, MA) at 530 nm excitation and 590 nm emission. Relative viability of cells was determined in relation to the untreated control. Control

wells containing compound only were included to detect potential interference of the compound with the indicator system. Also, media only controls were included to account for background fluorescence. Viability of cells prior to cytotoxicity experiments was determined by Trypan Blue staining. Cells were diluted 1:3 in 0.4% (w/v) Trypan Blue (Sigma), and counted in a hemacytometer.

Acknowledgement. The assistance in performing the in vitro tests by Gertrud Schmitt and Jeannine Jung is highly appreciated. We would also like to acknowledge the undergraduate research participants Judith Horzel, Helena Rübél, and Thomas Jakoby whose work contributed to the presented results. S. L. is grateful to Saarland University for a scholarship (Landesgraduiererten-Förderung). Thanks are due to Prof. J. J. Rob Hermans, University of Maastricht, The Netherlands, for supplying the V79 CYP11B1 cells, and Prof. Rita Bernhardt, Saarland University, for supplying the V79 CYP11B2 cells. The determination of the cytotoxicity by Dr. Reiner Class, Pharmacelsus CRO, Saarbrücken, as well as the investigation of the hepatic CYP profile by Dr. Ursula Müller-Vieira, Pharmacelsus CRO, is gratefully acknowledged.

Supporting Information Available: Aldosterone concentrations in the individual animals at all sampling points, NMR spectroscopic data of the target compounds **1–4**, **6–11**, **13–26**, full experimental details and spectroscopic characterization of the reaction intermediates **1a**, **5a**, **5b**, **6a**, **14a–16a**, elemental analysis results of compounds **1–26**. This information is available free of charge via the Internet at <http://pubs.acs.org>.

References

- (1) Weber, K. T. Aldosterone in congestive heart failure. *N. Engl. J. Med.* **2001**, *345*, 1689–1697.
- (2) (a) Brilla, C. G. Renin-angiotensin-aldosterone system and myocardial fibrosis. *Cardiovasc. Res.* **2000**, *47*, 1–3. (b) Lijnen, P.; Petrov, V. Induction of cardiac fibrosis by aldosterone. *J. Mol. Cell. Cardiol.* **2000**, *32*, 865–879.
- (3) Satoh, M.; Nakamura, M.; Saitoh, H.; Satoh, H.; Akatsu, T.; Iwasaka, J.; Masuda, T.; Hiramori, K. Aldosterone synthase (CYP11B2) expression and myocardial fibrosis in the failing human heart. *Clin. Sci.* **2002**, *102*, 381–386.
- (4) (a) Pitt, B.; Zannad, F.; Remme, W. J.; Cody, R.; Castaigne, A.; Perez, A.; Palensky, J.; Wittes, J. The effect of spironolactone on morbidity and mortality in patients with severe heart failure. *N. Engl. J. Med.* **1999**, *341*, 709–717. (b) Pitt, B.; Remme, W.; Zannad, F.; Neaton, J.; Martinez, F.; Roniker, B.; Bittman, R.; Hurley, S.; Kleiman, J.; Gatlin, M. Eplerenone, a selective aldosterone blocker, in patients with left ventricular dysfunction after myocardial infarction. *N. Eng. J. Med.* **2003**, *348*, 1309–1321.
- (5) Izawa, H.; Murohara, T.; Nagata, K.; Isobe, S.; Asano, H.; Amano, T.; Ichihara, S.; Kato, T.; Ohshima, S.; Murase, Y.; Iino, S.; Obata, K.; Noda, A.; Okumura, K.; Yokota, M. Mineralocorticoid receptor antagonism ameliorates left ventricular diastolic dysfunction and myocardial fibrosis in mildly

- symptomatic patients with idiopathic dilated cardiomyopathy: a pilot study. *Circulation* **2005**, *112*, 2940–2945.
- (6) Juurlink, D. N.; Mamdani, M. M.; Lee, D. S.; Kopp, A.; Austin, P. C.; Laupacis, A.; Redelmeier, D. A. Rates of hyperkalemia after publication of the Randomized Aldactone Evaluation Study. *N. Engl. J. Med.* **2004**, *351*, 543–551.
- (7) Delcayre, C.; Swynghedauw, B. Molecular mechanisms of myocardial remodeling. The role of aldosterone. *J. Mol. Cell. Cardiol.* **2002**, *34*, 1577–1584.
- (8) (a) Wehling, M. Specific, nongenomic actions of steroid hormones. *Annu. Rev. Physiol.* **1997**, *59*, 365–393. (b) Lösel, R.; Wehling, M. Nongenomic actions of steroid hormones. *Nature Rev. Mol. Cell. Biol.* **2003**, *4*, 46–55.
- (9) Hartmann, R. W. Selective inhibition of steroidogenic P450 enzymes: Current status and future perspectives. *Eur. J. Pharm. Sci.* **1994**, *2*, 15–16.
- (10) Ehmer, P. B.; Bureik, M.; Bernhardt, R.; Müller, U.; Hartmann, R. W. Development of a test system for inhibitors of human aldosterone synthase (CYP11B2): Screening in fission yeast and evaluation of selectivity in V79 cells. *J. Steroid Biochem. Mol. Biol.* **2002**, *81*, 173–179.
- (11) Kawamoto, T.; Mitsuuchi, Y.; Toda, K.; Yokoyama, Y.; Miyahara, K.; Miura, S.; Ohnishi, T.; Ichikawa, Y.; Nakao, K.; Imura, H.; Ulick, S.; Shizuta, Y. Role of steroid 11 β -hydroxylase and steroid 18-hydroxylase in the biosynthesis of glucocorticoids and mineralocorticoids in humans. *Proc. Natl. Acad. Sci. U.S.A.* **1992**, *89*, 1458–1462.
- (12) Ulmschneider, S.; Müller-Vieira, U.; Mitrenga, M.; Hartmann, R. W.; Oberwinkler-Marchais, S.; Klein, C. D.; Bureik, M.; Bernhardt, R.; Antes, I.; Lengauer, T. Synthesis and evaluation of imidazolymethylenetetrahydronaphthalenes and imidazolymethyleneindanes: Potent inhibitors of aldosterone synthase. *J. Med. Chem.* **2005**, *48*, 1796–1805.
- (13) Ulmschneider, S.; Müller-Vieira, U.; Klein, C. D.; Antes, I.; Lengauer, T.; Hartmann, R. W. Synthesis and evaluation of (pyridylmethylene)tetrahydronaphthalenes/-indanes and structurally modified derivatives: Potent and selective inhibitors of aldosterone synthase. *J. Med. Chem.* **2005**, *48*, 1563–1575.
- (14) Voets, M.; Antes, I.; Scherer, C.; Müller-Vieira, U.; Biemel, K.; Barassin, C.; Oberwinkler-Marchais, S.; Hartmann, R. W. Heteroaryl substituted naphthalenes and structurally modified derivatives: Selective inhibitors of CYP11B2 for the treatment of congestive heart failure and myocardial fibrosis. *J. Med. Chem.* **2005**, *48*, 6632–6642.
- (15) Lucas, S.; Heim, R.; Negri, M.; Antes, I.; Ries, C.; Schewe, K. E.; Bisi, A.; Gobbi, S.; Hartmann, R. W. Novel aldosterone synthase inhibitors with extended carbocyclic skeleton by a combined ligand-based and structure-based drug design approach. *J. Med. Chem.* **2008**, in press.
- (16) Voets, M.; Antes, I.; Scherer, C.; Müller-Vieira, U.; Biemel, K.; Oberwinkler-Marchais, S.; Hartmann, R. W. Synthesis and evaluation of heteroaryl-substituted dihydronaphthalenes and indenes: Potent and selective inhibitors of aldosterone synthase (CYP11B2) for the treatment of congestive heart failure and myocardial fibrosis. *J. Med. Chem.* **2006**, *49*, 2222–2231.

- (17) Appukkuttan, P.; Orts, A. B.; Chandran, R., P.; Goeman, J. L.; van der Eycken, J.; Dehaen, W.; van der Eycken, E. Generation of a small library of highly electron-rich 2-(hetero)aryl-substituted phenethylamines by the Suzuki-Miyaura reaction: A short synthesis of an apogalanthamine analogue. *Eur. J. Org. Chem.* **2004**, 3277–3285.
- (18) Bengtson, A.; Hallberg, A.; Larhed, M. Fast synthesis of aryl triflates with controlled microwave heating. *Org. Lett.* **2002**, 4, 1231–1233.
- (19) Carreño, M. C.; García-Cerrada, S.; Urbano, A. From central to helical chirality: Synthesis of P and M enantiomers of [5]helicenequinones and bisquinones from (SS)-2-(p-tolylsulfinyl)-1,4-benzoquinone. *Chem. Eur. J.* **2003**, 9, 4118–4131.
- (20) Selnick, H. G.; Smith, G. R.; Tebben, A. J. An improved procedure for the cyanation of aryl triflates: A convenient synthesis of 6-cyano-1,2,3,4-tetrahydroisoquinoline. *Synth. Commun.* **1995**, 25, 3255–3261.
- (21) Tschaen, D. M.; Abramson, L.; Cai, D.; Desmond, R.; Dolling, U.-H.; Frey, L.; Karady, S.; Shi, Y.-J.; Verhoeven, T. R. Asymmetric Synthesis of MK-0499. *J. Org. Chem.* **1995**, 60, 4324–4330.
- (22) Mewshaw, R. E.; Edsall, R. J., Jr.; Yang, C.; Manas, E. S.; Xu, Z. B.; Henderson, R. A.; Keith, J. C., Jr.; Harris, H. A. ER β ligands. 3. Exploiting two binding orientations of the 2-phenylnaphthalene scaffold to achieve ER β selectivity. *J. Med. Chem.* **2005**, 48, 3953–3979.
- (23) DeBernardis, J. F.; Kerkman, D. J.; Winn, M.; Bush, E. N.; Arendsen, D. L.; McClellan, W. J.; Kyncl, J. J.; Basha, F. Z. Conformationally defined adrenergic agents. 1. Design and synthesis of novel α_2 selective adrenergic agents: Electrostatic repulsion based conformational prototypes. *J. Med. Chem.* **1985**, 28, 1319–1404.
- (24) Occhiato, E. G.; Ferrali, A.; Menchi, G.; Guarna, A.; Danza, G.; Comerci, A.; Mancina, R.; Serio, M.; Garotta, G.; Cavalli, A.; De Vivo, M.; Recanatini, M. Synthesis, biological activity, and three-dimensional quantitative structure-activity relationship model for a series of benzo[c]quinolizin-3-ones, nonsteroidal inhibitors of human steroid 5 α -reductase 1. *J. Med. Chem.* **2004**, 47, 3546–3560.
- (25) Fröhner, W.; Monse, B.; Braxmeier, T. M.; Casiraghi, L.; Sahagún, H.; Seneci, P. Regiospecific synthesis of mono-N-substituted indolopyrrolocarbazoles. *Org. Lett.* **2005**, 7, 4573–4576.
- (26) Bach, T.; Grosch, B.; Strassner, T.; Herdtweck, E. Enantioselective [6 π]-photocyclization reaction of an acrylanilide mediated by a chiral host. Interplay between enantioselective ring closure and enantioselective protonation. *J. Org. Chem.* **2003**, 68, 1107–1116.
- (27) Adams, N. D.; Darcy, M. G.; Dhanak, D.; Duffy, K. J.; Fitch, D. M.; Knight, S. D.; Newlander, K. A.; Shaw, A. N. Compounds, compositions and methods. PCT Int. Appl. WO2006113432, 2006.
- (28) (a) Denner, K.; Bernhardt, R. Inhibition studies of steroid conversions mediated by human CYP11B1 and CYP11B2 expressed in cell cultures. In *Oxygen Homeostasis and Its Dynamics*, 1st ed.; Ishimura, Y., Shimada, H., Suematsu, M., Eds.; Springer-Verlag: Tokyo, Berlin, Heidelberg, New York, 1998; pp 231–236. (b) Denner, K.; Doehmer, J.; Bernhardt, R. Cloning of CYP11B1 and CYP11B2 from normal human adrenal and their functional expression in COS-7 and V79 chinese hamster cells. *Endocr. Res.* **1995**, 21,

- 443–448. (c) Böttner, B.; Denner, K.; Bernhardt, R. Conferring aldosterone synthesis to human CYP11B1 by replacing key amino acid residues with CYP11B2-specific ones. *Eur. J. Biochem.* **1998**, *252*, 458–466.
- (29) Lamberts, S. W.; Bruining, H. A.; Marzouk, H.; Zuiderwijk, J.; Uitterlinden, P.; Blijd, J. J.; Hackeng, W. H.; de Jong, F. H. The new aromatase inhibitor CGS-16949A suppresses aldosterone and cortisol production by human adrenal cells in vitro. *J. Clin. Endocrinol. Metab.* **1989**, *69*, 896–901.
- (30) Demers, L. M.; Melby, J. C.; Wilson, T. E.; Lipton, A.; Harvey, H. A.; Santen, R. J. The effects of CGS 16949A, an aromatase inhibitor on adrenal mineralocorticoid biosynthesis. *J. Clin. Endocrinol. Metab.* **1990**, *70*, 1162–1166.
- (31) Heim, R.; Lucas, S.; Grombein, C. M.; Ries, C.; Schewe, K. E.; Negri, M.; Müller-Vieira, U.; Birk, B.; Hartmann, R. W. Overcoming undesirable CYP1A2 inhibition of pyridyl-naphthalene type aldosterone synthase inhibitors: Influence of heteroaryl derivatization on potency and selectivity. *J. Med. Chem.* **2008**, *51*, 5064–5074.
- (32) (a) Ehmer, P. B.; Jose, J.; Hartmann, R. W. Development of a simple and rapid assay for the evaluation of inhibitors of human 17 α -hydroxylase-C_{17,20}-lyase (P450c17) by coexpression of P450c17 with NADPH-cytochrome-P450-reductase in *Escherichia coli*. *J. Steroid Biochem. Mol. Biol.* **2000**, *75*, 57–63; (b) Hutschenreuter, T. U.; Ehmer, P. B.; Hartmann, R. W. Synthesis of hydroxy derivatives of highly potent nonsteroidal CYP17 inhibitors as potential metabolites and evaluation of their activity by a non cellular assay using recombinant enzyme. *J. Enzyme Inhib. Med. Chem.* **2004**, *19*, 17–32.
- (33) Thompson, E. A.; Siiteri, P. K. Utilization of oxygen and reduced nicotinamide adenine dinucleotide phosphate by human placental microsomes during aromatization of androstenedione. *J. Biol. Chem.* **1974**, *249*, 5364–5372.
- (34) Hartmann, R. W.; Batzl, C. Aromatase inhibitors. Synthesis and evaluation of mammary tumor inhibiting activity of 3-alkylated 3-(4-aminophenyl)piperidine-2,6-diones. *J. Med. Chem.* **1986**, *29*, 1362–1369.
- (35) Taymans, S. E.; Pack, S.; Pak, E.; Torpy, D. J.; Zhuang, Z.; Stratakis, C. A. Human CYP11B2 (aldosterone synthase) maps to chromosome 8q24.3. *J. Clin. Endocrinol. Metab.* **1998**, *83*, 1033–1036.
- (36) (a) Chohan, K. K.; Paine, S. W.; Mistry, J.; Barton, P.; Davis, A. M. A rapid computational filter for cytochrome P450 1A2 inhibition potential of compound libraries. *J. Med. Chem.* **2005**, *48*, 5154–5161. (b) Korhonen, L. E.; Rahnasto, M.; Mähönen, N. J.; Wittekindt, C.; Poso, A.; Juvonen, R. O.; Raunio, H. Predictive three-dimensional quantitative structure-activity relationship of cytochrome P450 1A2 inhibitors. *J. Med. Chem.* **2005**, *48*, 3808–3815.
- (37) Butler, M. A.; Iwasaki, M.; Guengerich, F. P.; Kadlubar, F. F. Human cytochrome P-450_{PA} (P-450IA2), the phenacetin O-deethylase, is primarily responsible for the hepatic 3-demethylation of caffeine and N-oxidation of carcinogenic arylamines. *Proc. Natl. Acad. Sci. U.S.A.* **1989**, *86*, 7696–7700.
- (38) Sesardic, D.; Boobis, A. R.; Murray, B. P.; Murray, S.; Segura, J.; de la Torre, R.; Davies, D. S. Furfurylline is a potent and selective inhibitor of cytochrome P450IA2 in man. *Br. J. Clin. Pharmacol.* **1990**, *29*, 651–663.

- (39) Ulmschneider, S.; Negri, M.; Voets, M.; Hartmann, R. W. Development and evaluation of a pharmacophore model for inhibitors of aldosterone synthase (CYP11B2). *Bioorg. Med. Chem. Lett.* **2006**, *16*, 25–30.

3.4 Fine-Tuning the Selectivity of Aldosterone Synthase Inhibitors: SAR Insights from Studies of Heteroaryl Substituted 1,2,5,6-Tetrahydropyrrolo[3,2,1-ij]quinolin-4-one Derivatives

Simon Lucas, Ralf Heim, Christina Ries, and Rolf W. Hartmann

This manuscript will be submitted for publication as an article to the

Journal of Medicinal Chemistry 2008

Paper IV

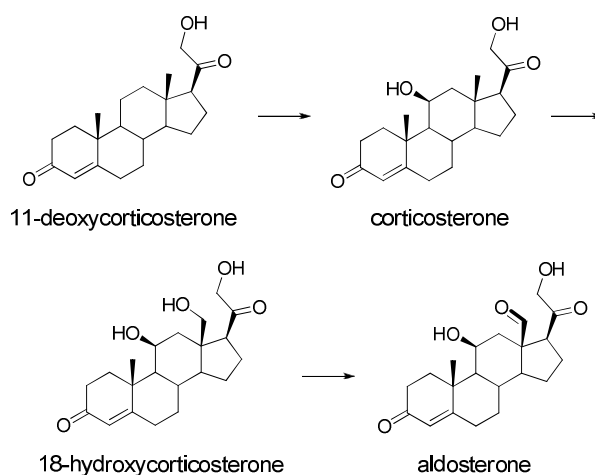
Abstract: Pyridine substituted 3,4-dihydro-1*H*-quinolin-2-ones (e.g., **I** and **II**) constitute a class of highly potent and selective inhibitors of aldosterone synthase (CYP11B2), a promising target for the treatment of hyperaldosteronism, congestive heart failure and myocardial fibrosis. Amongst the latter, ethyl-substituted **II** is particularly striking due to a pronounced CYP1A2 selectivity. Rigidification of **II** by incorporation of the ethyl group into a 5- or 6-membered ring affords compounds with a pyrroloquinolinone or pyridoquinolinone molecular scaffold (e.g., **1** and **2**). It was found that these molecules are even more potent and selective CYP11B2 inhibitors than their corresponding open-chain analogues. Moreover, pyrroloquinolinone **1** exhibits no inhibition of the six most important hepatic CYP enzymes ($IC_{50} > 10 \mu M$) as well as a bioavailability ($AUC_{0-\infty} = 3464 \text{ ng}\cdot\text{h/mL}$) in the range of the marketed drug fadrozole ($AUC_{0-\infty} = 3207 \text{ ng}\cdot\text{h/mL}$). The SAR studies disclose structural features for either strong or weak inhibition of the highly homologous 11 β -hydroxylase (CYP11B1). These results are not only important for fine-tuning the selectivity but also for the development of selective CYP11B1 inhibitors that are of interest for the treatment of Cushing's syndrome and metabolic syndrome.

Introduction

Congestive heart failure (CHF) is a condition of insufficient cardiac output and reduced systemic blood flow which provokes a chronic activation of the renin-angiotensin-aldosterone system (RAAS). As a consequence, the excessive release of angiotensin II (Ang II) and aldosterone leads to an increased blood pressure and finally to a further deterioration of heart function, mainly mediated via epithelial sodium retention by mineralocorticoid receptor (MR) activation as well as Ang II mediated vasoconstriction.¹ Moreover, aldosterone is known to exert direct effects on the heart. Activation of nonepithelial MRs stimulates the progressive synthesis and deposition of fibrillar collagens in fibroblasts and results in myocardial fibrosis.² Until today, various drug classes targeting the RAAS have been developed in order to interrupt the vicious circle of chronic neurohormonal activation, acting either by inhibition of the key regulator enzymes or by blocking the actions of the effector hormones by functional antagonism, affording a successful treatment of heart failure and hypertension. Inhibitors of the angiotensin converting enzyme (ACE) proved to trigger a down-regulation of circulating aldosterone, but increased levels of aldosterone may be seen after several months of therapy, presumably due to potassium stimulated secretion.³ The persistence of aldosterone secretion despite treatment with ACE inhibitors and the evidence of the deleterious effects of aldosterone on cardiovascular function led to the assumption that blocking the mineralocorticoid receptor might provide additional benefit. This hypothesis has been corroborated in two recent clinical trials by using the MR antagonists spironolactone and eplerenone in addition to standard therapy of patients with chronic congestive heart failure and in patients after myocardial infarction, respectively.⁴ Aldosterone antagonistic therapy, however, raises several issues. Spironolactone can induce severe side effects due to its low selectivity toward other steroid hormone receptors. Although eplerenone is more selective, clinically relevant hyperkalemia remains a principal therapeutic risk.⁵ Moreover, the elevated plasma aldosterone concentrations are left unaffected on a pathological level, promoting the up-regulation of MR expression⁶ and nongenomic aldosterone effects⁷ on the insufficient heart.

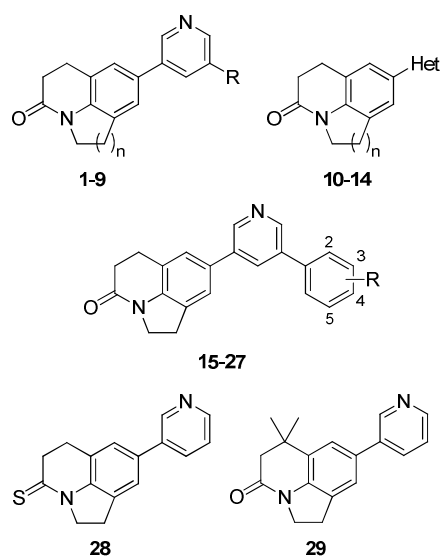
Hence, we hypothesized a novel approach for the treatment of hyperaldosteronism, congestive heart failure and myocardial fibrosis by combating the elevated plasma aldosterone levels via blockade of aldosterone synthase (CYP11B2), the key enzyme of mineralocorticoid biosynthesis.^{8,9} This mitochondrial cytochrome P450 enzyme is localized mainly in the zona glomerulosa of the adrenal gland and catalyzes the terminal three oxidation steps in the biogenesis of aldosterone in humans via initial hydroxylation of 11-deoxycorticosterone at 11 β -position to yield corticosterone, followed by two subsequent hydroxylations at C₁₈ and water release to yield aldosterone (Chart 1).¹⁰ In addition to the potential therapeutic utility in cardiovascular diseases, radiolabelled inhibitors of that enzyme might be a useful tool for molecular imaging of CYP11B expression in adrenocortical tissue and thus for the diagnosis of adrenal tumors.¹¹ Due to selectively binding to CYP11B2, these compounds are also interesting for the imaging of Conn adenomas which are characterized by high expression of CYP11B2.¹²

Chart 1. CYP11B2 Catalyzed Biosynthesis of Aldosterone



An obstacle in the development of a putative CYP11B2 inhibitor is to accomplish selectivity versus other cytochrome P450 (CYP) enzymes since complexation of the heme iron which is a widespread interaction motive is likely to occur in other CYP enzymes as well. The selectivity issue becomes especially critical with respect to 11 β -hydroxylase (CYP11B1), the key enzyme of glucocorticoid biosynthesis whose amino acid sequence exhibits a homology of 93 % compared to CYP11B2.¹³ A drug discovery program launched in our laboratory led to a series of nonsteroidal aldosterone synthase inhibitors with high selectivity versus other cytochrome P450 enzymes by consequent structural optimization of a hit discovered by compound library screening.^{14,15} Pyridine-substituted naphthalenes^{16,17} and dihydronaphthalenes,¹⁸ the most potent and selective compounds that emerged from the development process, however, revealed two major pharmacological drawbacks: A strong inhibition of the hepatic drug metabolizing enzyme CYP1A2 and no inhibitory effect on the aldosterone production in vivo by using a rat model.

Chart 2. Title Compounds



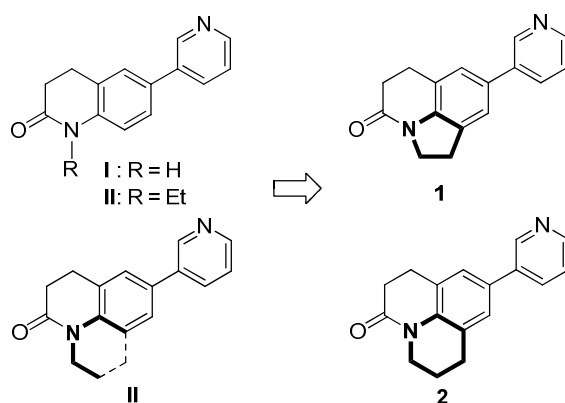
In the present study, we describe the development of 1,2,5,6-tetrahydropyrrolo[3,2,1-*ij*]quinolin-4-ones and structurally related compounds (Chart 2) as highly potent aldosterone synthase inhibitors with improved selectivity against other crucial CYP enzymes, such as CYP11B1, the steroidogenic enzymes CYP17 (17 α -hydroxylase-C17,20-lyase) and CYP19 (aromatase) as well as the six most important drug-metabolizing cytochrome P450 enzymes (CYP1A2, CYP2B6, CYP2C9, CYP2C19, CYP2D6 and CYP3A4). The *in vivo* pharmacokinetic profile of some promising compounds was determined in male Wistar rats.

Results

Inhibitor Design Concept

Preliminary studies aiming at the design of nonsteroidal aldosterone synthase inhibitors performed in our laboratory have demonstrated that 3-pyridine substituted naphthalenes provide an ideal molecular scaffold for a strong inhibition of the target enzyme CYP11B2 as well as high selectivity versus several other CYP enzymes (e.g., CYP11B1, CYP17, CYP19).^{16,18} These molecules, however, revealed two major pharmacological drawbacks: A strong inhibition of the hepatic drug metabolizing enzyme CYP1A2 and no inhibitory effect on the aldosterone production *in vivo* by using a rat model. In a recent study, we demonstrated that changing the naphthalene by a 3,4-dihydro-1*H*-quinolin-2-one skeleton affords highly potent CYP11B2 inhibitors such as **I** and **II** (Chart 3) with pronounced selectivity versus other CYP enzymes including CYP1A2, as well as aldosterone-lowering properties *in vivo*.¹⁹ Amongst the latter compounds, ethyl-substituted derivative **II** displayed a remarkably little inhibition of CYP1A2. Therefore, this molecule was chosen as starting point for further structural optimization. Incorporation of the ethyl group into a 5- or 6-membered ring affords the pyrroloquinolinone **1** and the pyridoquinolinone **2**, respectively. In the present study, the chemical modification is mainly directed to the heterocyclic moiety since both potency and selectivity have been identified in previous investigations to be highly dependent on heterocyclic derivatization.²⁰

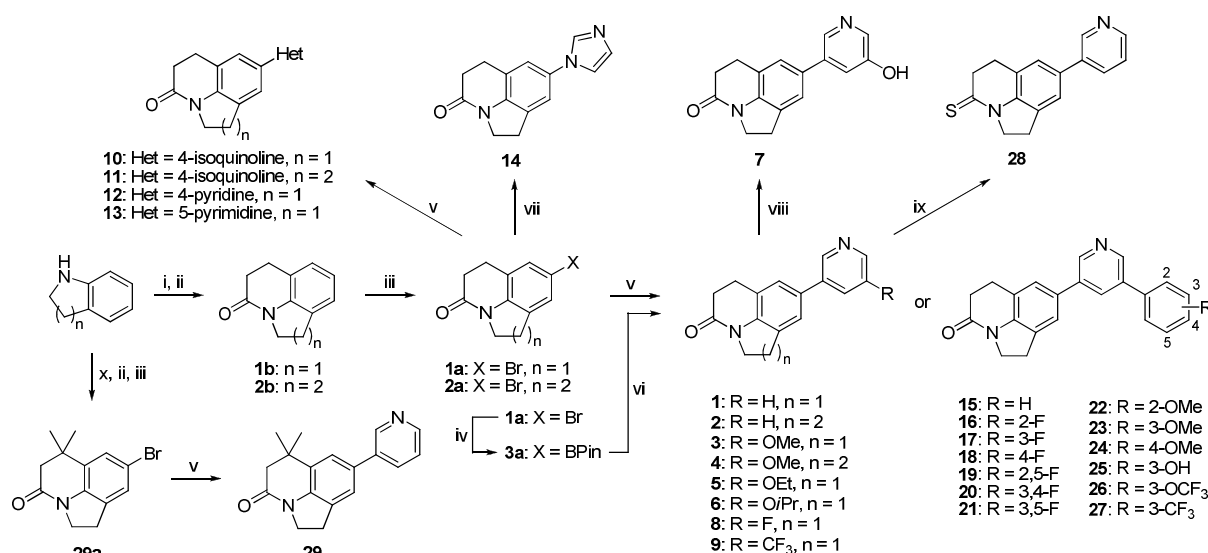
Chart 3. Development of Compounds **1** and **2**



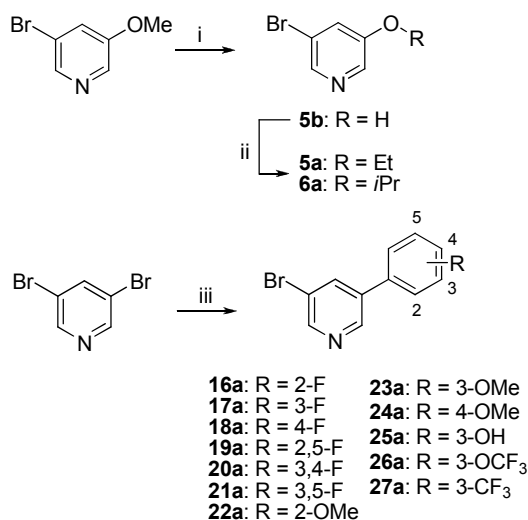
Chemistry

The key synthetic transformation toward the target compounds was a Suzuki coupling to connect the pyrrolo- or pyridoquinolinone scaffold to various *N*-heterocyclic systems, in most cases a derivative of 3-pyridine (Scheme 1). The advanced intermediates **1a**, **2a** as well as **29a** were prepared in three consecutive steps starting from commercially available indoline or 1,2,3,4-tetrahydroquinoline as initial building block. The sequence of amide formation and subsequent Friedel-Crafts cyclization to afford **1b** and **2b** has been described previously and was also used for the synthesis of the *gem*-dimethyl analog **29a**.²¹ Regioselective bromination was accomplished by treating the fused heterocycles with *N*-bromosuccinimide in DMF at 0 °C. The pyrrolo- or pyridoquinolinones **1–4**, **10–13**, and **29** were obtained by Suzuki coupling of the arylbromides **1a**, **2a** or **29a** with an *N*-heterocyclic boronic acid.²² Copper catalyzed *N*-arylation of **1a** with imidazole gave rise to the 1-imidazolyl derivative **14**.²³ Alternatively, the bromo-substituted pyrroloquinolinone **1a** was transformed into the corresponding pinacol boronate **3a** by treating with bis(pinacolato)diboron under palladium catalysis²⁴ and was subsequently used for cross-coupling with a derivatized 3-bromopyridine to afford compounds **5–9**, and **15–27**. If not commercially available, the 3-bromopyridines used in this step were prepared as outlined in Scheme 2 either from 3-bromo-5-methoxypyridine by demethylation and subsequent alkylation (**5a**, **6a**) or from 3,5-dibromopyridine by Suzuki coupling with a substituted arylboronic acid (**16a–27a**). The hydroxypyridine **7** was synthesized by treating the corresponding methoxy derivative **3** with concentrated hydrobromic acid under reflux. Thionation of pyrroloquinolinone **1** with Lawessons reagent in dry toluene afforded the thioanalog **28**.

Scheme 1^a



^a Reagents and conditions: i) 3-chloropropanoyl chloride, acetone reflux; ii) AlCl₃, NaCl, 150 °C; iii) NBS, DMF, 0 °C; iv) bis(pinacolato)diboron, Pd(dppf)Cl₂, KOAc, DMSO, 80 °C; v) heteroarylboronic acid, Pd(PPh₃)₄, aq. NaHCO₃, DMF, μw, 150 °C or: heteroarylboronic acid, Pd(PPh₃)₄, aq. Na₂CO₃, toluene/ethanol, reflux; vi) heteroarylboronic acid, Pd(PPh₃)₄, aq. Na₂CO₃, toluene/ethanol, reflux; vii) Cu₂SO₄, K₂CO₃, 180 °C; viii) conc HBr, reflux; ix) Lawessons reagent, toluene, reflux, x) 3,3-dimethylacryloylchloride, acetone reflux. (Het = heteroaryl, BPin = pinacol boronate)

Scheme 2^a

^a Reagents and conditions: i) conc HBr, reflux; ii) alkylhalogenide, K₂CO₃, DMF, rt; iii) arylboronic acid, Pd(PPh₃)₄, aq. Na₂CO₃, toluene/ethanol, reflux.

Biological Results

Inhibition of Human Adrenal Corticoid Producing CYP11B2 and CYP11B1 In Vitro (Table 1). The inhibitory activities of the compounds were determined in V79 MZh cells expressing either human CYP11B2 or CYP11B1.^{9,25} The V79 MZh cells were incubated with [¹⁴C]-deoxycorticosterone as substrate and the inhibitor in different concentrations. The product formation was monitored by HPTLC using a phosphoimager. Fadrozole, an aromatase (CYP19) inhibitor with proven ability to reduce corticoid formation in vitro²⁶ and in vivo²⁷ was used as a reference (CYP11B2, IC₅₀ = 1 nM; CYP11B1, IC₅₀ = 10 nM).

Most of the investigated molecules are highly potent aldosterone synthase inhibitors displaying IC₅₀ values in the low nanomolar range (< 5 nM). An extraordinary high activity is observed in case of the isoquinoline derivatives **10** and **11** with sub-nanomolar IC₅₀ values (0.2 nM). Replacing 3-pyridine by other nitrogen containing heterocycles induces a decrease in inhibitory potency. The 5-pyrimidine (**13**) and 1-imidazole (**14**) derivatives are less active (IC₅₀ = 56–89 nM) than the 3-pyridine analog **1** (IC₅₀ = 1.1 nM) and the corresponding 4-pyridine compound **12** lacks any inhibitory activity on CYP11B2 (< 10 % inhibition at a concentration of 500 nM). The same trend was observed previously for the binding properties of a series of substituted pyridynaphthalenes.¹⁶ A slight decrease in CYP11B2 potency (IC₅₀ = 16–33 nM) is also observed in case of some aryl-substituents in 5-position of the pyridine heterocycle (**21**, **26**, and **27**). A *gem*-dimethyl group in the quinolinone moiety as accomplished in compound **29** is not tolerated in terms of CYP11B2 potency. The inhibition of the highly homologous CYP11B1 is significantly lower than the CYP11B2 inhibition for all investigated molecules resulting in selectivity factors in the range of 15–957 (fadrozole, selectivity factor = 10).

Table 1. Inhibition of Human Adrenal CYP11B2 and CYP11B1 In Vitro

compd	n	R	Het	% inhibition ^a		IC ₅₀ value ^b (nM)		selectivity factor ^e
				V79 11B2 ^c hCYP11B2	V79 11B2 ^c hCYP11B2	V79 11B1 ^d hCYP11B1		
1	1	H		90	1.1	715	650	
2	2	H		95	2.4	2296	957	
3	1	OMe		98	0.6	247	412	
4	2	OMe		95	0.9	545	606	
5	1	OEt		92	1.0	158	158	
6	1	OiPr		96	2.2	103	47	
7	1	OH		94	4.3	2045	476	
8	1	F		97	4.4	1288	293	
9	1	CF ₃		96	5.9	141	24	
10	1		4-isoquinoline	98	0.2	13	65	
11	2		4-isoquinoline	95	0.2	34	170	
12	1		4-pyridine	7	n.d.	n.d.	n.d.	
13	1		5-pyrimidine	81	56	28546	510	
14	1		1-imidazole	87	89	2077	23	
15		H		97	1.3	58	45	
16		2-F		92	0.7	43	61	
17		3-F		97	1.4	490	350	
18		4-F		96	0.9	40	44	
19		2,5-F		80	3.6	183	51	
20		3,4-F		89	2.3	496	215	
21		3,5-F		81	18	1748	97	
22		2-OMe		86	2.4	128	53	
23		3-OMe		86	4.6	1374	299	
24		4-OMe		95	1.4	21	15	
25		3-OH		92	1.2	44	37	
26		3-OCF ₃		92	16	2058	129	
27		3-CF ₃		80	33	4646	141	
28				96	1.2	333	278	
29				48	n.d.	n.d.	n.d.	
fadrozole					1	10	10	

^a Mean value of at least four experiments, standard deviation less than 10 %; inhibitor concentration, 500 nM. ^b Mean value of at least four experiments, standard deviation usually less than 25 %, n.d. = not determined. ^c Hamster fibroblasts expressing human CYP11B2; substrate deoxycorticosterone, 100 nM. ^d Hamster fibroblasts expressing human CYP11B1; substrate deoxycorticosterone, 100 nM. ^e IC₅₀ CYP11B1/IC₅₀ CYP11B2, n.d. = not determined.

Inhibition of Steroidogenic and Hepatic CYP Enzymes (Tables 2 and 3). A subset of 12 compounds was investigated for inhibition of the steroidogenic enzymes CYP17 and CYP19 (Table 2). The inhibition of CYP17 was investigated using the 50,000 g sediment of the *E. coli* homogenate recombinantly expressing human CYP17 and progesterone (25 μ M) as substrate.²⁸ The inhibition values were measured at an inhibitor concentration of 2 μ M. The inhibition of CYP19 at an inhibitor concentration of 500 nM was determined in vitro with human placental microsomes and [1β - 3 H] androstenedione as substrate as described by Thompson and Siiteri²⁹ using our modification.³⁰ Pyridoquinolinone **2** is a moderately potent aromatase inhibitor (69 % inhibition). All other investigated molecules are highly selective toward both CYP17 and CYP19, usually displaying less than 10 % inhibition.

Table 2. Inhibition of Human CYP17 and CYP19 In Vitro

compd	% inhibition ^a		compd	% inhibition ^a	
	CYP17 ^b	CYP19 ^c		CYP17 ^b	CYP19 ^c
1	6	18	11	5	< 5
2	6	69	13	5	5
3	< 5	5	17	7	6
4	< 5	5	20	< 5	< 5
8	< 5	< 5	23	< 5	< 5
10	6	< 5	28	11	5

^a Mean value of three experiments, standard deviation less than 10 %. ^b *E. coli* expressing human CYP17; substrate progesterone, 25 μ M; inhibitor concentration, 2.0 μ M; ketoconazole, IC₅₀ = 2.78 μ M. ^c Human placental CYP19; substrate androstenedione, 500 nM; inhibitor concentration, 500 nM; fadrozole, IC₅₀ = 30 nM.

A selectivity profile relating to inhibition of crucial hepatic CYP enzymes (CYP1A2, CYP2B6, CYP2C9, CYP2C19, CYP2D6, and CYP3A4) was determined for compounds **1–4**, **11**, and **17** by use of recombinantly expressed enzymes from baculovirus-infected insect microsomes. The unsubstituted pyrroloquinolinone **1** exhibits a pronounced selectivity toward all investigated CYP enzymes. CYP2B6, CYP2C19, CYP2D6, and CYP3A4 are not inhibited at all (< 5 % inhibition at a concentration of 10 μ M). The inhibition of CYP1A2 and CYP2C9 is in the range of 41–43 % corresponding with IC₅₀ values of approximately 10 μ M or higher. Compounds **2–4**, and **11** display an increased CYP1A2 inhibition (24–47 % at a concentration of 1 μ M) compared to **1** whereas the CYP1A2 potency of **17** is in the range of the unsubstituted analog **1**. Furthermore, isoquinoline derivative **11** is a rather potent inhibitor of both CYP2C9 and CYP2C19 (IC₅₀ < 1 μ M). Compound **17** displays a distinct inhibition of CYP2C9 (79 % at a concentration of 10 μ M) but is otherwise rather selective toward the other CYP enzymes investigated (IC₅₀ > 10 μ M). However, it becomes apparent from the results presented in Table 3 that none of the substituted derivatives **2–4**, **11** and **17** matches the selectivity of the unsubstituted parent compound **1**.

Table 3. Inhibition of Selected Hepatic CYP Enzymes In Vitro

compd	% inhibition ^a											
	CYP1A2 ^{b,c}		CYP2B6 ^{b,d}		CYP2C9 ^{b,e}		CYP2C19 ^{b,f}		CYP2D6 ^{b,g}		CYP3A4 ^{b,h}	
	10 μ M	1 μ M	10 μ M	1 μ M	10 μ M	1 μ M	10 μ M	1 μ M	10 μ M	1 μ M	10 μ M	1 μ M
1	43	8	< 5	< 5	41	6	< 5	< 5	< 5	< 5	< 5	< 5
2	83	41	36	27	40	19	44	8	n.d.	n.d.	21	6
3	72	37	8	< 5	42	23	30	7	13	9	19	14
4	87	47	n.d.	n.d.	63	34	61	11	n.d.	n.d.	24	12
11	63	24	n.d.	n.d.	97	73	96	67	n.d.	n.d.	< 5	< 5
17	38	9	13	< 5	79	39	21	n.d.	9	< 5	43	37

^a Mean value of two experiments, standard deviation less than 5 %. ^b Recombinantly expressed enzymes from baculovirus-infected insect microsomes (Supersomes). ^c Furofylline, IC₅₀ = 2.42 μ M. ^d Tranylcypromine, IC₅₀ = 6.24 μ M. ^e Sulfaphenazole, IC₅₀ = 318 nM. ^f Tranylcypromine, IC₅₀ = 5.95 μ M. ^g Quinidine, IC₅₀ = 14 nM. ^h Ketoconazole, IC₅₀ = 57 nM.

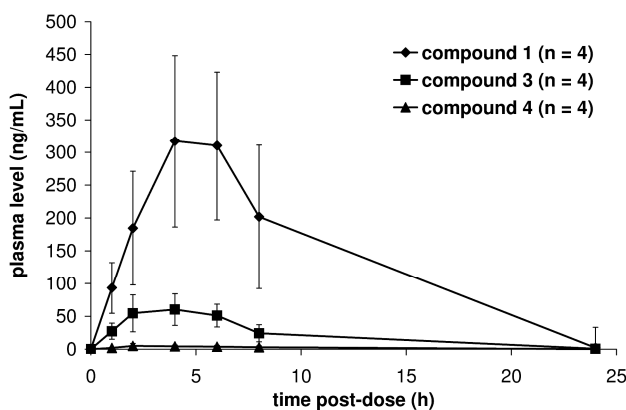
In Vivo Pharmacokinetics (Table 4). The pharmacokinetic profile of selected compounds was determined after peroral application to male Wistar rats. Plasma samples were collected over 24 h and the concentrations were determined by HPLC-MS/MS. Compounds **1**, **3**, and **4** were investigated in a cassette dosing approach (peroral dose = 5 mg/kg) and compared to fadrozole. All three compounds show comparable terminal half-lives ($t_{1/2z}$ = 2.0–2.9 h) which are in the range of the reference fadrozole ($t_{1/2z}$ = 3.2 h). Contrariwise, the absorbance of compounds **1** and **3** (t_{max} = 4 h) is slower as the absorbance of fadrozole (t_{max} = 1 h). Within this series, fadrozole shows the highest maximal concentration (C_{max}) in plasma (471 ng/mL) followed by compound **1** (317 ng/mL). The maximal amount of the other test items (**3** and **4**) found in the plasma after peroral application is significantly lower (< 50 ng/mL). Using the area under the curve (AUC_{0-∞}) as a ranking criterion, pyrroloquinolinone **1** exhibits the highest bioavailability (3464 ng·h/mL), thus slightly exceeding the bioavailability of the reference compound (3207 ng·h/mL). Methoxylation of the heterocycle as accomplished in **3** results in a significant decrease of the AUC_{0-∞} (557 ng·h/mL). A further decrease is observed for the corresponding pyridoquinolinone **4** (51 ng·h/mL). The influence of varying the molecular scaffold of compound **1** becomes particularly apparent from Figure 1 where the mean profile of plasma levels (ng/mL) in rat versus time after oral application (5 mg/kg) in a cassette of compounds **1**, **3** and **4** are shown. In the course of the in vivo experiment, no obvious sign of toxicity was noted in any animal over the duration of the experiment (24 h).

Table 4. Pharmacokinetic Profile of Compounds **1**, **3**, and **4**

compd	$t_{1/2z}$ (h) ^b	t_{max} (h) ^c	C_{max} (ng/mL) ^d	AUC _{0-∞} (ng·h/mL) ^e
1	2.4	4.0	317	3464
3	2.9	4.0	60	557
4	2.0	2.0	4.9	51
fadrozole ^f	3.2	1.0	471	3207

^a All compounds were applied perorally (5 mg/kg) to male Wistar rats in a cassette dosing approach. ^b Terminal half-life. ^c Time of maximal concentration. ^d Maximal concentration. ^e Area under the curve. ^f Mean value of two experiments.

Figure 1^a



^a Mean profile (\pm) SEM of plasma levels (ng/ml) in rat versus time after oral application (5 mg/kg) of compounds **1**, **3**, and **4** determined in a cassette dosing experiment.

Discussion and Conclusion

Within the present set of compounds, interesting structure-activity relationships (SAR) can be observed, especially with respect to the inhibition of 11 β -hydroxylase (CYP11B1) and thus selectivity. On the one hand, selectivity is influenced by the ring-size of the carbocycle condensed to the quinolinone moiety. Within the series of pyrido-condensed compounds (**2**, **4**, and **11**), the CYP11B1 inhibition is significantly decreased compared to the corresponding pyrroloquinolinone analogues (**1**, **3**, and **10**), whereas the CYP11B2 inhibition is in a comparable range. This leads to an enhanced selectivity for the pyridoquinolinone derivatives. Pyridoquinolinone **2** is the most selective compound of the present series (selectivity factor = 957). Hence, the selectivity increases nearly by a factor of 100 compared to fadrozole (selectivity factor = 10). This experimental result is particularly noteworthy with respect to the high homology of the two CYP11B isoforms. However, it was demonstrated by pharmacokinetic studies of **3** and **4** that ring expansion to the 6-membered carbocycle is accompanied by an approximately 10-fold decrease in bioavailability as indicated by an AUC_{0- ∞} of 557 ng·h/mL (**3**) and 51 ng·h/mL (**4**), respectively. On the other hand, the substitution pattern of the pyridine moiety was found to significantly influence the CYP11B1 selectivity. Obviously, the size of substituents in 5-position of the heterocycle plays a crucial role in CYP11B1 inhibition. This becomes particularly evident in the series of pyrroloquinolinone compounds with alkoxy derivatized heterocycle. The inhibitory potency at CYP11B1 increases with the substituent size in the order **1** (R = H, IC₅₀ = 715 nM) < **3** (R = OMe, IC₅₀ = 247 nM) < **5** (R = OEt, IC₅₀ = 158 nM) < **6** (R = OiPr, IC₅₀ = 103 nM). Contrariwise, the inhibition of CYP11B2 is in a comparable range for these compounds (IC₅₀ = 0.6–2.2 nM), that is the selectivity factor decreases in the same order from 650 (**1**) to 47 (**6**). A pronounced increase in CYP11B1 inhibition is observed in case of the introduction of additional aryl moieties. Replacing 3-pyridine by 4-isoquinoline results in a dramatic increase in CYP11B1 potency for both the pyrrolo-condensed (**10**, increase by a factor of 55) and pyrido-condensed (**11**, factor 68) derivative

whereas the CYP11B2 inhibition increases to a minor degree (factor 6–12). The same trend can be observed for several compounds with additional aryl substituent in 5-position of the pyridine moiety (e.g., **15**, **16**, **18**, **22**, **24**, and **25**). The latter compounds display a CYP11B2 inhibition in a range of 0.7–2.4 nM which is readily comparable to the unsubstituted parent compound **1** ($IC_{50} = 1.1$ nM). Contrariwise, the CYP11B1 inhibition increases up to 36-fold compared to **1** ($IC_{50} = 715$ nM) to IC_{50} values of 21–128 nM corresponding to a rather low selectivity (factor 15–61). Obviously, the introduction of additional aromatic rings and to a minor degree also sterically demanding aliphatic residues (e.g., isopropoxy) in the pyridine moiety leads to additional interactions of the inhibitors with CYP11B1, thus stabilizing the formed CYP11B1-inhibitor complexes considerably. This observation correlates with homology modeling results suggesting that the putative binding sites of both CYP11B isoforms contain many hydrophobic amino acids (e.g., Ala313, Phe321, Pro322, Val378, Phe381, Leu382, Tyr485, and Ile488).³¹ In principal, these residues can interact with the additional aryl moiety by hydrophobic or π - π stacking contacts. Docking studies of imidazolylmethyleneindanes into our CYP11B2 model revealed that the inhibitor is predominantly bound through hydrophobic interactions with residues of the I-helix and Phe106, except for the nitrogen-metal coordination with the heme iron.¹⁴ Since the position of the heme has been hypothesized to be shifted by approximately 20° in the two CYP11B enzymes,³² it is likely that the ‘network’ of hydrophobic groups in the binding pocket accommodates the inhibitors in a different way in CYP11B1, thus affording additional stabilization of the phenyl moiety.

Moreover, it is striking that *meta* substituents in the aryl moiety can trigger CYP11B1 selectivity again. With exception of the 3-hydroxy derivative **25**, all compounds bearing a substituent in 3-position of the benzene moiety (i.e., **17**, **20**, **21**, **23**, **26**, and **27**) exhibit a decreased CYP11B1 potency with IC_{50} values in a range of 490–4646 nM and thus selectivity factors up to 350 (**17**). This obvious off/on-switch of CYP11B1 potency is of particular interest. From unsubstituted parent compound **1** ($IC_{50} = 715$ nM), derivatization with phenyl in 5-position of the pyridine moiety leads to a significant increase of inhibitory potency in compound **15** ($IC_{50} = 58$ nM) whereas the *meta*-fluorophenyl analog **17** exhibits a low inhibitory potency again ($IC_{50} = 490$ nM). Coevally, these three compounds display virtually the same aldosterone synthase inhibition ($IC_{50} = 1.1$ – 1.4 nM), which means that a variety of sterically demanding substituents in the pyridine moiety is readily tolerated in the CYP11B2 binding pocket, however, lead to no further stabilization of the complexes formed by coordination of the heme iron by the heterocyclic nitrogen. Contrariwise, 3-pyridine substituted pyrroloquinolinone derivatives such as **1** are per se rather poor CYP11B1 inhibitors and require an additional benzene moiety, and thus a further stabilization of the formed complexes mainly through hydrophobic or π - π stacking interactions, for basal inhibitory potency. Amongst these compounds are highly potent CYP11B1 inhibitors, for example isoquinoline derivative **10** ($IC_{50} = 13$ nM) and *para*-methoxyphenyl derivative **24** ($IC_{50} = 21$ nM). Obviously the *meta*-substituted analogues do not adequately fit into the CYP11B1 binding pocket or loose contact to the heme iron while minimizing unfavorable contacts with the

enzyme. Only 3-hydroxy derivative **25** displays a pronounced CYP11B1 inhibition ($IC_{50} = 44$ nM). This is an indication for stabilizing interactions by the hydroxy group acting as hydrogen bond donor which might compensate an eventual weakening of the Fe–N interaction.

The above biological results that derivatization of the 3-pyridine moiety of pyrroloquinolinone type compounds is a tool for fine-tuning the CYP11B1 selectivity are in contrast to previous findings in the series of inhibitors with a naphthalene molecular scaffold. In the latter case, substituents in the heterocyclic moiety led to a change of inhibition of both the CYP11B isoforms in a comparable order of magnitude, resulting in a reasonable linear correlation of the corresponding pIC_{50} values ($r^2 = 0.86$) and thus a rather constant selectivity factor.²⁰ We interpreted this finding as a consequence of similar protein-inhibitor interactions of the heterocyclic moiety with both CYP11B isoforms due to structural similarities in the heterocyclic binding site. As a matter of fact, the selectivity is significantly influenced by the substitution pattern of the heterocycle within the present set of compounds which is an indication for a binding mode of the pyrroloquinolinone derivatives different from that of the naphthalene analogues.

In summary, the present study provides extensive SAR results relating to CYP11B2 and CYP11B1 inhibition. The influence of certain structural modifications on the 11β -hydroxylase (CYP11B1) activity is particularly noteworthy. On the one hand, CYP11B1 inhibition is an important selectivity criterion for aldosterone synthase inhibitors. On the other hand, selective CYP11B1 inhibitors could be used for the treatment of Cushing's syndrome and metabolic syndrome. Although several potent CYP11B1 inhibitors have been described previously, in-depth SAR studies were usually focused on the concurrent CYP11B2 activity. Herein, we clearly identified structural features important for high inhibitory CYP11B1 potency, namely sterically demanding lipophilic residues or aromatic residues in the heterocyclic moiety or condensed to the heterocycle, giving rise to a series of highly potent 11β -hydroxylase inhibitors (e.g., *para*-methoxyphenyl derivative **24**, $IC_{50} = 21$ nM). Slight variation of these compounds, for example introduction of *meta*-substituents into the phenyl moiety, led to a significant loss of CYP11B1 inhibition again, providing selective CYP11B2 inhibitors. In the majority of cases, the investigated molecules are potent aldosterone synthase inhibitors selective toward the steroidogenic enzymes CYP11B1, CYP17, and CYP19 displaying no significant inhibition (except for **2**). The unsubstituted parent compound **1** shows also no significant inhibition of the six most important hepatic CYP enzymes ($IC_{50} > 10$ μ M). In addition, this highly potent and selective aldosterone synthase inhibitor reaches high plasma concentrations ($AUC_{0-\infty} = 3464$ ng·h/mL) after peroral application to rats and even slightly exceeds the bioavailability of the marketed drug fadrozole ($AUC_{0-\infty} = 3207$ ng·h/mL). Currently, further studies with inhibitor **1** are underway to evaluate aldosterone-lowering effects in vivo.

Experimental section

Chemical and Analytical Methods. Melting points were measured on a Mettler FP1 melting point apparatus and are uncorrected. ^1H NMR and ^{13}C spectra were recorded on a Bruker DRX-500 instrument. Chemical shifts are given in parts per million (ppm), and tetramethylsilane (TMS) was used as internal standard for spectra obtained in $\text{DMSO-}d_6$ and CDCl_3 . All coupling constants (J) are given in hertz. Mass spectra (LC/MS) were measured on a TSQ Quantum (Thermo Electron Corporation) instrument with a RP18 100-3 column (Macherey Nagel) and with water/acetonitrile mixtures as eluents. GC/MS spectra were measured on a GCD Series G1800A (Hewlett Packard) instrument with an Optima-5-MS (0.25 μM , 30 m) column (Macherey Nagel). Elemental analyses were carried out at the Department of Chemistry, University of Saarbrücken. Reagents were used as obtained from commercial suppliers without further purification. Solvents were distilled before use. Dry solvents were obtained by distillation from appropriate drying reagents and stored over molecular sieves. Flash chromatography was performed on silica gel 40 (35/40–63/70 μM) with petroleum ether/ethyl acetate mixtures as eluents, and the reaction progress was determined by thin-layer chromatography analyses on Alugram SIL G/UV254 (Macherey Nagel). Visualization was accomplished with UV light and KMnO_4 solution. All microwave irradiation experiments were carried out in a CEM-Discover monomode microwave apparatus.

The following compounds were prepared according to previously described procedures: 1,2,5,6-tetrahydro-4*H*-pyrrolo[3,2,1-*ij*]quinolin-4-one (**1b**),²¹ 2,3,6,7-tetrahydro-1*H*,5*H*-pyrido[3,2,1-*ij*]quinolin-5-one (**2b**),²¹ 5-bromopyridin-3-ol (**5b**),²⁰ 3-bromo-5-ethoxypyridine (**5a**).²⁰

Synthesis of the Target Compounds

Procedure A.²² Boronic acid (0.75 mmol, 1 equivalent), aryl bromide or -triflate (0.9–1.3 equivalents), and tetrakis(triphenylphosphane)palladium(0) (43 mg, 37.5 μmol , 5 mol %) were suspended in 1.5 mL DMF in a 10 mL septum-capped tube containing a stirring magnet. To this was added a solution of NaHCO_3 (189 mg, 2.25 mmol, 3 equivalents) in 1.5 mL water and the vial was sealed with a Teflon cap. The mixture was irradiated with microwaves for 15 min at a temperature of 150 °C with an initial irradiation power of 100 W. After the reaction, the vial was cooled to 40 °C, the crude mixture was partitioned between ethyl acetate and water and the aqueous layer was extracted three times with ethyl acetate. The combined organic layers were dried over MgSO_4 and the solvents were removed in vacuo. The coupling products were obtained after flash chromatography on silica gel (petroleum ether/ethyl acetate mixtures) and/or crystallization. If an oil was obtained, it was transferred into the hydrochloride salt by 1N HCl solution in diethyl ether.

Procedure B. Boronic acid (1 equivalent), aryl bromide or (1.3–1.5 equivalents), and tetrakis(triphenylphosphane)palladium(0) (5 mol %) were suspended in toluene/ethanol 4/1 to give a 0.07–0.1 M solution of boronic acid under an atmosphere of nitrogen. To this was added a 1 N aqueous solution of Na_2CO_3 (6 equivalents). The mixture was then refluxed for 12–18 h, cooled to room temperature, diluted with water and extracted several times with ethyl acetate. The combined extracts

were dried over MgSO_4 , concentrated and purified by flash chromatography on silica gel (petroleum ether/ethyl acetate mixtures) and/or crystallization. If an oil was obtained, it was transferred into the hydrochloride salt by 1 N HCl solution in diethyl ether.

8-Pyridin-3-yl-1,2,5,6-tetrahydro-4H-pyrrolo[3,2,1-*ij*]quinolin-4-one (1) was obtained according to procedure B from **1a** (5.19 g, 20.6 mmol) and 3-pyridineboronic acid (2.30 g, 18.7 mmol) after flash chromatography on silica gel (ethyl acetate, $R_f = 0.08$) and crystallization from acetone/diethylether as colorless plates (83 mg, 0.33 mmol, 49 %), mp 153–154 °C. $^1\text{H-NMR}$ (500 MHz, CDCl_3): $\delta = 2.72$ (t, $^3J = 7.8$ Hz, 2H), 3.03 (t, $^3J = 7.8$ Hz, 2H), 3.25 (t, $^3J = 8.5$ Hz, 2H), 4.13 (t, $^3J = 8.5$ Hz, 2H), 7.20 (s, 1H), 7.28 (s, 1H), 7.32 (ddd, $^3J = 7.8$ Hz, $^3J = 4.8$ Hz, $^5J = 0.5$ Hz, 1H), 7.79 (ddd, $^3J = 7.8$ Hz, $^4J = 2.2$ Hz, $^4J = 1.6$ Hz, 1H), 8.54 (dd, $^3J = 4.7$ Hz, $^4J = 1.4$ Hz, 1H), 8.59 (d, $^4J = 2.0$ Hz, 1H). $^{13}\text{C-NMR}$ (125 MHz, CDCl_3): $\delta = 24.5, 27.7, 31.6, 45.5, 120.7, 122.4, 123.5, 124.7, 129.9, 133.5, 134.0, 136.7, 141.6, 148.1, 167.6$. MS m/z 251.22 (MH^+). Anal. ($\text{C}_{16}\text{H}_{14}\text{N}_2\text{O}$) C, H, N.

9-Pyridin-3-yl-1,2,6,7-tetrahydro-5H-pyrido[3,2,1-*ij*]quinolin-3-one (2) was obtained according to procedure A from **2a** (266 mg, 1.0 mmol) and 3-pyridineboronic acid (92 mg, 0.75 mmol) after flash chromatography on silica gel (petroleum ether/ethyl acetate, 2/3, $R_f = 0.12$) and crystallization from acetone/diethylether as colorless needles (116 mg, 0.44 mmol, 59 %), mp 122–123 °C. MS m/z 265.07 (MH^+). Anal. ($\text{C}_{17}\text{H}_{16}\text{N}_2\text{O}_2$) C, H, N.

8-(5-Methoxy-pyridin-3-yl)-1,2,5,6-tetrahydro-4H-pyrrolo[3,2,1-*ij*]quinolin-4-one (3) was obtained according to procedure A from **1a** (252 mg, 1.0 mmol) and 5-methoxy-3-pyridineboronic acid (115 mg, 0.75 mmol) after flash chromatography on silica gel (ethyl acetate, $R_f = 0.09$) as colorless needles (74 mg, 0.26 mmol, 35 %), mp 171–172 °C. MS m/z 281.02 (MH^+). Anal. ($\text{C}_{17}\text{H}_{16}\text{N}_2\text{O}_2$) C, H, N

9-(5-Methoxy-pyridin-3-yl)-1,2,6,7-tetrahydro-5H-pyrido[3,2,1-*ij*]quinolin-3-one (4) was obtained according to procedure A from **2a** (266 mg, 1.0 mmol) and 5-methoxy-3-pyridineboronic acid (115 mg, 0.75 mmol) after flash chromatography on silica gel (petroleum ether/ethyl acetate, 2/3, $R_f = 0.08$) and crystallization from acetone/diethylether as colorless needles (63 mg, 0.21 mmol, 28 %), mp 148–150 °C. MS m/z 295.02 (MH^+). Anal. ($\text{C}_{18}\text{H}_{18}\text{N}_2\text{O}_2 \cdot 0.2\text{H}_2\text{O}$) C, H, N.

8-(5-Ethoxy-pyridin-3-yl)-1,2,5,6-tetrahydro-4H-pyrrolo[3,2,1-*ij*]quinolin-4-one (5) was obtained according to procedure B from **3a** (300 mg, 1.0 mmol) and **5a** (242 mg, 1.2 mmol) after flash chromatography on silica gel (petroleum ether/ethyl acetate, 1/9, $R_f = 0.10$) and crystallization from acetone/diethylether as colorless needles (132 mg, 0.45 mmol, 45 %), mp 171–172 °C. MS m/z 295.16 (MH^+). Anal. ($\text{C}_{18}\text{H}_{18}\text{N}_2\text{O}_2$) C, H, N.

8-(5-Isopropoxy-pyridin-3-yl)-1,2,5,6-tetrahydro-4H-pyrrolo[3,2,1-*ij*]quinolin-4-one (6) was obtained according to procedure B from **3a** (359 mg, 1.20 mmol) and **6a** (281 mg, 1.30 mmol) after flash chromatography on silica gel (petroleum ether/ethyl acetate, 3/7, $R_f = 0.07$) as colorless plates (196 mg, 0.63 mmol, 53 %), mp 154–155 °C. MS m/z 309.15 (MH^+). Anal. ($\text{C}_{19}\text{H}_{20}\text{N}_2\text{O}_2 \cdot 0.2\text{H}_2\text{O}$) C, H, N.

8-(5-Hydroxypyridin-3-yl)-1,2,5,6-tetrahydro-4H-pyrrolo[3,2,1-*ij*]quinolin-4-one (7). A solution of **3** (95 mg, 0.34 mmol) in 35 ml concentrated hydrobromic acid was heated under reflux for 18 h. After cooling to room temperature, the reaction mixture was neutralized with saturated NaHCO₃ solution and extracted with ethyl acetate (3 x 200 ml). The crude product which was obtained after evaporation of the solvent was purified by flash chromatography on silica gel (ethyl acetate, *R_f* = 0.06) and washing with ethanol, yielding the hydroxy compound **7** as colorless solid (75 mg, 0.28 mmol, 83 %). The solid was dissolved in diethyl THF/methanol and transferred into the hydrochloride salt by 1N HCl solution in isopropanol/diethyl ether, followed by filtration and crystallization from acetone, mp (HCl salt) >300 °C. MS *m/z* 267.94 (MH⁺). Anal. (C₁₆H₁₄N₂O₂) C, H, N.

8-(5-Fluoropyridin-3-yl)-1,2,5,6-tetrahydro-4H-pyrrolo[3,2,1-*ij*]quinolin-4-one (8) was obtained according to procedure B from **3a** (359 mg, 1.2 mmol) and 3-bromo-5-fluoropyridine (211 mg, 1.2 mmol) after flash chromatography on silica gel (petroleum ether/ethyl acetate, 1/1, *R_f* = 0.09) and crystallization from acetone/diethylether as colorless needles (202 mg, 0.75 mmol, 63 %), mp 157–158 °C. MS *m/z* 269.83 (MH⁺). Anal. (C₁₆H₁₃FN₂O·0.3H₂O) C, H, N.

8-[5-(Trifluoromethyl)pyridin-3-yl]-1,2,5,6-tetrahydro-4H-pyrrolo[3,2,1-*ij*]quinolin-4-one (9) was obtained according to procedure B from **3a** (329 mg, 1.1 mmol) and 3-bromo-5-(trifluoromethyl)pyridine (249 mg, 1.1 mmol) after flash chromatography on silica gel (petroleum ether/ethyl acetate, 1/1, *R_f* = 0.14) and crystallization from acetone/diethylether as colorless needles (248 mg, 0.78 mmol, 71 %), mp 211–212 °C. MS *m/z* 318.95 (MH⁺). Anal. (C₁₇H₁₃F₃N₂O) C, H, N.

8-Isoquinolin-4-yl-1,2,5,6-tetrahydro-4H-pyrrolo[3,2,1-*ij*]quinolin-4-one (10) was obtained according to procedure A from **1a** (252 mg, 1.0 mmol) and 4-isoquinolineboronic acid (227 mg, 0.9 mmol) after flash chromatography on silica gel (petroleum ether/ethyl acetate, 2/3, *R_f* = 0.13) as colorless needles (93 mg, 0.31 mmol, 34 %), mp 184–185 °C. MS *m/z* 301.15 (MH⁺). Anal. (C₂₀H₁₆N₂O·0.2H₂O) C, H, N.

9-Isoquinolin-4-yl-1,2,6,7-tetrahydro-5H-pyrido[3,2,1-*ij*]quinolin-3-one (11) was obtained according to procedure A from **2a** (266 mg, 1.0 mmol) and 4-isoquinolineboronic acid (227 mg, 0.9 mmol) after flash chromatography on silica gel (petroleum ether/ethyl acetate, 2/3, *R_f* = 0.10) and crystallization from acetone/diethylether as colorless needles (173 mg, 0.55 mmol, 61 %), mp 158–159 °C. MS *m/z* 315.24 (MH⁺). Anal. (C₂₁H₁₈N₂O) C, H, N.

8-Pyridin-4-yl-1,2,5,6-tetrahydro-4H-pyrrolo[3,2,1-*ij*]quinolin-4-one (12) was obtained according to procedure B from **1a** (627 mg, 3.50 mmol) and 4-pyridineboronic acid (369 mg, 3.0 mmol) after crystallization from ethanol as yellow crystals (225 mg, 0.90 mmol, 30 %), mp 173–174 °C. MS *m/z* 251.01 (MH⁺). Anal. (C₁₆H₁₄N₂O) C, H, N.

8-Pyrimidin-5-yl-1,2,5,6-tetrahydro-4H-pyrrolo[3,2,1-*ij*]quinolin-4-one (13) was obtained according to procedure B from **1a** (627 mg, 3.50 mmol) and 5-pyrimidineboronic acid (372 mg, 3.0 mmol) after crystallization from acetone as a yellow crystals (324 mg, 1.29 mmol, 43 %), mp 185–186 °C. MS *m/z* 251.85 (MH⁺). Anal. (C₁₅H₁₃N₃O·0.3H₂O) C, H, N.

8-Imidazol-1-yl-1,2,5,6-tetrahydro-4H-pyrrolo[3,2,1-ij]quinolin-4-one (14). Imidazole (628 mg, 9.23 mmol), **1a** (2.12 g, 8.39 mmol), potassium carbonate (1.28 g, 9.23 mmol) and copper(II)sulfate (160 mg, 1.0 mmol) were mixed and heated at 180 °C for 10 h under an atmosphere of dry nitrogen. After being cooled to room temperature, the reaction mixture was poured into 150 ml water and extracted with ethyl acetate (3 x 100 ml). After drying with MgSO₄ and evaporating of the solvent, the crude product was purified by two subsequent crystallizations from acetone to yield a colorless solid (674 mg, 2.82 mg, 34 %), mp 123–124 °C. MS *m/z* 240.02 (MH⁺). Anal. (C₁₄H₁₃N₃O·0.2H₂O) C, H, N.

8-(5-Phenylpyridin-3-yl)-1,2,5,6-tetrahydro-4H-pyrrolo[3,2,1-ij]quinolin-4-one (15) was obtained according to procedure B from **3a** (325 mg, 1.07 mmol) and 3-bromo-5-phenylpyridine (301 mg, 1.28 mmol) after flash chromatography on silica gel (petroleum ether/ethyl acetate, 2/3, *R_f* = 0.09) as colorless plates (150 mg, 0.46 mmol, 43 %), mp 188–189 °C. MS *m/z* 326.79 (MH⁺). Anal. (C₂₂H₁₈N₂O·0.4H₂O) C, H, N.

8-[5-(2-Fluorophenyl)pyridin-3-yl]-1,2,5,6-tetrahydro-4H-pyrrolo[3,2,1-ij]quinolin-4-one (16) was obtained according to procedure B from **3a** (389 mg, 1.30 mmol) and **16a** (311 mg, 1.12 mmol) after flash chromatography on silica gel (petroleum ether/ethyl acetate, 2/3, *R_f* = 0.09) as colorless solid (239 mg, 0.69 mmol, 56 %), mp 245–247 °C. MS *m/z* 345.19 (MH⁺). Anal. (C₂₂H₁₇FN₂O·0.3H₂O) C, H, N.

8-[5-(3-Fluorophenyl)-pyridin-3-yl]-1,2,5,6-tetrahydro-4H-pyrrolo[3,2,1-ij]quinolin-4-one (17) was obtained according to procedure B from **3a** (360 mg, 1.20 mmol) and **17a** (378 mg, 1.50 mmol) after flash chromatography on silica gel (petroleum ether/ethyl acetate, 2/3, *R_f* = 0.08) as colorless needles (97 mg, 0.28 mmol, 23 %), mp 181–182 °C. MS *m/z* 345.26 (MH⁺). Anal. (C₂₂H₁₇FN₂O) C, H, N.

8-[5-(4-Fluorophenyl)-pyridin-3-yl]-1,2,5,6-tetrahydro-4H-pyrrolo[3,2,1-ij]quinolin-4-one (18) was obtained according to procedure B from **3a** (463 mg, 1.55 mmol) and **18a** (440 mg, 1.75 mmol) after flash chromatography on silica gel (petroleum ether/ethyl acetate, 2/3, *R_f* = 0.05) as colorless needles (189 mg, 0.55 mmol, 35 %), mp 233–234 °C. MS *m/z* 345.05 (MH⁺). Anal. (C₂₂H₁₇FN₂O·0.6H₂O) C, H, N.

8-[5-(2,5-Difluorophenyl)pyridin-3-yl]-1,2,5,6-tetrahydro-4H-pyrrolo[3,2,1-ij]quinolin-4-one (19) was obtained according to procedure B from **3a** (430 mg, 1.44 mmol) and **19a** (338 mg, 1.25 mmol) after flash chromatography on silica gel (petroleum ether/ethyl acetate, 3/7, *R_f* = 0.08) as colorless solid (371 mg, 1.02 mmol, 82 %), mp 189–190 °C. MS *m/z* 362.97 (MH⁺). Anal. (C₂₂H₁₆F₂N₂O·0.2H₂O) C, H, N.

8-[5-(3,4-Difluorophenyl)pyridin-3-yl]-1,2,5,6-tetrahydro-4H-pyrrolo[3,2,1-ij]quinolin-4-one (20) was obtained according to procedure B from **3a** (449 mg, 1.50 mmol) and **20a** (367 mg, 1.36 mmol) after flash chromatography on silica gel (petroleum ether/ethyl acetate, 1/4, *R_f* = 0.07) as

colorless needles (110 mg, 0.30 mmol, 22 %), mp 204–205 °C. MS m/z 363.11 (MH^+). Anal. ($C_{22}H_{16}F_2N_2O \cdot 0.3H_2O$) C, H, N.

8-[5-(3,5-Difluorophenyl)pyridin-3-yl]-1,2,5,6-tetrahydro-4H-pyrrolo[3,2,1-*ij*]quinolin-4-one (21) was obtained according to procedure B from **3a** (404 mg, 1.35 mmol) and **21a** (315 mg, 1.17 mmol) after flash chromatography on silica gel (petroleum ether/ethyl acetate, 3/7, $R_f = 0.10$) as colorless solid (104 mg, 0.29 mmol, 25 %), mp 228–229 °C. MS m/z 363.81 (MH^+). Anal. ($C_{22}H_{16}F_2N_2O \cdot 0.6H_2O$) C, H, N.

8-[5-(2-Methoxyphenyl)pyridin-3-yl]-1,2,5,6-tetrahydro-4H-pyrrolo[3,2,1-*ij*]quinolin-4-one (22) was obtained according to procedure B from **3a** (512 mg, 1.71 mmol) and **22a** (430 mg, 1.63 mmol) after flash chromatography on silica gel (petroleum ether/ethyl acetate, 1/4, $R_f = 0.10$) as colorless needles (106 mg, 0.29 mmol, 18 %), mp 186–187 °C. MS m/z 356.95 (MH^+). Anal. ($C_{23}H_{20}N_2O_2$) C, H, N.

8-[5-(3-Methoxyphenyl)pyridin-3-yl]-1,2,5,6-tetrahydro-4H-pyrrolo[3,2,1-*ij*]quinolin-4-one (23) was obtained according to procedure B from **3a** (329 mg, 1.10 mmol) and **23a** (270 mg, 1.02 mmol) after flash chromatography on silica gel (ethyl acetate, $R_f = 0.09$) as colorless solid (62 mg, 0.17 mmol, 17 %), mp 207–208 °C. MS m/z 357.09 (MH^+). Anal. ($C_{23}H_{20}N_2O_2 \cdot 0.2H_2O$) C, H, N.

8-[5-(4-Methoxyphenyl)pyridin-3-yl]-1,2,5,6-tetrahydro-4H-pyrrolo[3,2,1-*ij*]quinolin-4-one (24) was obtained according to procedure B from **3a** (389 mg, 1.30 mmol) and **24a** (315 mg, 1.19 mmol) after flash chromatography on silica gel (ethyl acetate, $R_f = 0.08$) as colorless needles (182 mg, 0.51 mmol, 43 %), mp 220–221 °C. MS m/z 357.09 (MH^+). Anal. ($C_{23}H_{20}N_2O_2 \cdot 0.5H_2O$) C, H, N.

8-[5-(3-hydroxyphenyl)pyridin-3-yl]-1,2,5,6-tetrahydro-4H-pyrrolo[3,2,1-*ij*]quinolin-4-one (25) was obtained according to procedure B from **3a** (430 mg, 1.44 mmol) and **25a** (313 mg, 1.25 mmol) after crystallization from ethanol as colorless needles (93 mg, 0.27 mmol, 22 %), mp 286–288 °C. MS m/z 343.03 (MH^+). Anal. ($C_{22}H_{18}N_2O_2 \cdot 0.7H_2O$) C, H, N.

8-[5-[3-(Trifluoromethoxy)phenyl]pyridin-3-yl]-1,2,5,6-tetrahydro-4H-pyrrolo[3,2,1-*ij*]quinolin-4-one (26) was obtained according to procedure B from **3a** (382 mg, 1.28 mmol) and **26a** (370 mg, 1.16 mmol) after flash chromatography on silica gel (petroleum ether/ethyl acetate, 1/4, $R_f = 0.11$) as colorless solid (332 mg, 0.81 mmol, 70 %), mp 160–161 °C. MS m/z 410.90 (MH^+). Anal. ($C_{23}H_{17}F_3N_2O_2$) C, H, N.

8-[5-[3-(Trifluoromethyl)phenyl]pyridin-3-yl]-1,2,5,6-tetrahydro-4H-pyrrolo[3,2,1-*ij*]quinolin-4-one (27) was obtained according to procedure B from **3a** (344 mg, 1.15 mmol) and **27a** (330 mg, 1.09 mmol) after flash chromatography on silica gel (petroleum ether/ethyl acetate, 2/3, $R_f = 0.05$) as colorless solid (276 mg, 0.70 mmol, 64 %), mp 154–153 °C. MS m/z 395.01 (MH^+). Anal. ($C_{23}H_{14}F_3N_2O$) C, H, N.

8-Pyridin-3-yl-1,2,5,6-tetrahydro-4H-pyrrolo[3,2,1-*ij*]quinoline-4-thione (28). A suspension of **1** (900 mg, 3.60 mmol) and Lawesson's reagent (1.45 g, 3.60 mmol) in 50 ml dry toluene and 5 ml dry THF was refluxed for 30 min under an atmosphere of nitrogen. After cooling to room temperature, the

solvent was removed in vacuo and the residue was purified by flash chromatography on silica gel (petroleum ether/ethyl acetate, 1/1, $R_f = 0.25$) to afford **28** as yellow solid (155 mg, 0.58 mmol, 16 %). The solid was dissolved in diethyl ether/methanol and transferred into the hydrochloride salt by 1N HCl solution in isopropanol/diethyl ether, followed by filtration and crystallization from acetone, mp (HCl salt) 281–283 °C. MS m/z 267.10 (MH^+). Anal. ($C_{16}H_{14}N_2S \cdot HCl \cdot 0.2H_2O$) C, H, N.

6,6-Dimethyl-8-pyridin-3-yl-1,2,5,6-tetrahydro-4H-pyrrolo[3,2,1-ij]quinolin-4-one (29) was obtained according to procedure B from **29a** (280 mg, 1.0 mmol) and 3-pyridineboronic acid (92 mg, 0.75 mmol) after flash chromatography on silica gel (petroleum ether/ethyl acetate, 1/9, $R_f = 0.09$) and crystallization from acetone as colorless needles (48 mg, 0.17 mmol, 23 %), mp 178–180 °C. MS m/z 279.14 (MH^+). Anal. ($C_{18}H_{18}N_2O \cdot 0.2H_2O$) C, H, N.

Biological Methods. 1. Enzyme Preparations. CYP17 and CYP19 preparations were obtained by described methods: the 50,000 g sediment of *E. coli* expressing human CYP17²⁸ and microsomes from human placenta for CYP19.³⁰ **2. Enzyme Assays.** The following enzyme assays were performed as previously described: CYP17²⁸ and CYP19.³⁰ **3. Activity and Selectivity Assay Using V79 Cells.** V79 MZh 11B1 and V79 MZh 11B2 cells^{9,25} were incubated with [4-¹⁴C]-11-deoxycorticosterone as substrate and inhibitor in at least three different concentrations. The enzyme reactions were stopped by addition of ethyl acetate. After vigorous shaking and a centrifugation step (10,000 g, 2 min), the steroids were extracted into the organic phase, which was then separated. The conversion of the substrate was analyzed by HPTLC and a phosphoimaging system as described.^{9,25} **4. Inhibition of Human Hepatic CYP Enzymes.** The recombinantly expressed enzymes from baculovirus-infected insect microsomes (Supersomes) were used and the manufacturer's instructions (www.gentest.com) were followed. **5. In Vivo Pharmacokinetics.** Animal trials were conducted in accordance with institutional and international ethical guidelines for the use of laboratory animals. Male Wistar rats weighing 260–280 g (Janvier, France) were housed in a temperature-controlled room (20–24 °C) and maintained in a 12 h light/12 h dark cycle. Food and water were available ad libitum. The animals were anaesthetised with a ketamine (90 mg/kg)/xylazine (10 mg/kg) mixture, and cannulated with silicone tubing via the right jugular vein. Prior to the first blood sampling, animals were connected to a counterbalanced system and tubing, to perform blood sampling in the freely moving rat. Separate stock solutions (5 mg/mL) were prepared for the tested compounds in labrasol/water (1:1; v/v), leading to a clear solution. Immediately before application, the cassette dosing mixture was prepared by adding equal volumes of the stock solutions to end up with a final concentration of 1 mg/mL for each compound. The mixture was applied perorally to 4 rats with an injection volume of 5 mL/kg (Time 0). Blood samples (250 μ l) were collected 1 hour before application and 1, 2, 4, 6, 8, and 24 hours thereafter. They were centrifuged at 650 g for 10 minutes at 4 °C and then the plasma was harvested and kept at –20 °C until LC/MS analysis. To 50 μ L of rat plasma sample and calibration standard 100 μ L acetonitrile containing the internal standard was added. Samples and standards were vigorously shaken and centrifuged for 10 minutes at 6000 g and 20 °C. For the test items, an additional

dilution was performed by mixing 50 μL of the particle free supernatant with 50 μL water. An aliquot was transferred to 200 μL sampler vials and subsequently subjected to LC-MS/MS. HPLC-MS/MS analysis and quantification of the samples was carried out on a Surveyor-HPLC-system coupled with a TSQ Quantum (ThermoFinnigan) triple quadrupole mass spectrometer equipped with an electrospray interface (ESI). The mean of absolute plasma concentrations ($\pm\text{SEM}$) was calculated for the 4 rats and the regression was performed on group mean values. The pharmacokinetic analysis was performed using a noncompartment model (PK Solutions 2.0, Summit Research Services).

Acknowledgement. We thank Gertrud Schmitt and Jeannine Jung for their help in performing the in vitro tests. We would also like to acknowledge the undergraduate research participants Judith Horzel and Helena Rubel whose work contributed to the presented results. The investigation of the hepatic CYP profile by Dr. Ursula Muller-Vieira and the pharmacokinetic studies by Dr. Barbara Birk, Pharmacelsus CRO, Saarbrucken, are highly appreciated. S. L. is grateful to Saarland University for a scholarship (Landesgraduierten-Forderung). Thanks are due to Prof. J. J. Rob Hermans, University of Maastricht, The Netherlands, for supplying the V79 CYP11B1 cells, and Prof. Rita Bernhardt, Saarland University, for supplying the V79 CYP11B2 cells.

Supporting Information Available: NMR spectroscopic data of the target compounds **2–29**, full experimental details and spectroscopic characterization of the reaction intermediates **1a–3a**, **6a**, **16a–27a**, **29a**, **29b**, elemental analysis results and purity data (LC-MS) of compounds **1–29**. This information is available free of charge via the Internet at <http://pubs.acs.org>.

References

- (1) Weber, K. T. Aldosterone in congestive heart failure. *N. Engl. J. Med.* **2001**, *345*, 1689–1697.
- (2) (a) Brilla, C. G. Renin-angiotensin-aldosterone system and myocardial fibrosis. *Cardiovasc. Res.* **2000**, *47*, 1–3. (b) Lijnen, P.; Petrov, V. Induction of cardiac fibrosis by aldosterone. *J. Mol. Cell. Cardiol.* **2000**, *32*, 865–879.
- (3) (a) Struthers, A. D. Aldosterone escape during angiotensin-converting enzyme inhibitor therapy in chronic heart failure. *J. Card. Fail.* **1996**, *2*, 47–54. (b) Sato, A.; Saruta, T. Aldosterone escape during angiotensin-converting enzyme inhibitor therapy in essential hypertensive patients with left ventricular hypertrophy. *J. Int. Med. Res.* **2001**, *29*, 13–21.
- (4) (a) Pitt, B.; Zannad, F.; Remme, W. J.; Cody, R.; Castaigne, A.; Perez, A.; Palensky, J.; Wittes, J. The effect of spironolactone on morbidity and mortality in patients with severe heart failure. *N. Engl. J. Med.* **1999**, *341*, 709–717. (b) Pitt, B.; Remme, W.; Zannad, F.; Neaton, J.; Martinez, F.; Roniker, B.; Bittman, R.; Hurley, S.; Kleiman, J.; Gatlin, M. Eplerenone, a selective aldosterone blocker, in patients with left ventricular dysfunction after myocardial infarction. *N. Eng. J. Med.* **2003**, *348*, 1309–1321.

- (5) Juurlink, D. N.; Mamdani, M. M.; Lee, D. S.; Kopp, A.; Austin, P. C.; Laupacis, A.; Redelmeier, D. A. Rates of hyperkalemia after publication of the Randomized Aldactone Evaluation Study. *N. Engl. J. Med.* **2004**, *351*, 543–551.
- (6) Delcayre, C.; Swynghedauw, B. Molecular mechanisms of myocardial remodeling. The role of aldosterone. *J. Mol. Cell. Cardiol.* **2002**, *34*, 1577–1584.
- (7) (a) Wehling, M. Specific, nongenomic actions of steroid hormones. *Annu. Rev. Physiol.* **1997**, *59*, 365–393. (b) Lösel, R.; Wehling, M. Nongenomic actions of steroid hormones. *Nature Rev. Mol. Cell. Biol.* **2003**, *4*, 46–55.
- (8) Hartmann, R. W. Selective inhibition of steroidogenic P450 enzymes: Current status and future perspectives. *Eur. J. Pharm. Sci.* **1994**, *2*, 15–16.
- (9) Ehmer, P. B.; Bureik, M.; Bernhardt, R.; Müller, U.; Hartmann, R. W. Development of a test system for inhibitors of human aldosterone synthase (CYP11B2): Screening in fission yeast and evaluation of selectivity in V79 cells. *J. Steroid Biochem. Mol. Biol.* **2002**, *81*, 173–179.
- (10) Kawamoto, T.; Mitsuuchi, Y.; Toda, K.; Yokoyama, Y.; Miyahara, K.; Miura, S.; Ohnishi, T.; Ichikawa, Y.; Nakao, K.; Imura, H.; Ulick, S.; Shizuta, Y. Role of steroid 11 β -hydroxylase and steroid 18-hydroxylase in the biosynthesis of glucocorticoids and mineralocorticoids in humans. *Proc. Natl. Acad. Sci. U.S.A.* **1992**, *89*, 1458–1462.
- (11) (a) Hahner, S.; Stuermer, A.; Kreissl, M.; Reiners, C.; Fassnacht, M.; Haenscheid, H.; Beuschlein, F.; Zink, M.; Lang, K.; Allolio, B.; Schirbel, A. [¹²³I]Iodometomidate for Molecular Imaging of Adrenocortical Cytochrome P450 Family 11B Enzymes. *J. Clin. Endocrinol. Metab.* **2008**, *93*, 2358–65. (b) Zolle, I. M.; Berger, M. L.; Hammerschmidt, F.; Hahner, S.; Schirbel, A.; Peric-Simov, B. New selective inhibitors of steroid 11 β -hydroxylation in the adrenal cortex. Synthesis and structure–activity relationship of potent etomidate analogues. *J. Med. Chem.* **2008**, *51*, 2244–2253.
- (12) Bassett, M. H.; Mayhew, B.; Rehman, K.; White, P. C.; Mantero, F.; Arnaldi, G.; Stewart, P. M.; Bujalska, I.; Rainey, W. E. Expression profiles for steroidogenic enzymes in adrenocortical disease. *J. Clin. Endocrinol. Metab.* **2005**, *90*, 5446–5455.
- (13) Taymans, S. E.; Pack, S.; Pak, E.; Torpy, D. J.; Zhuang, Z.; Stratakis, C. A. Human CYP11B2 (aldosterone synthase) maps to chromosome 8q24.3. *J. Clin. Endocrinol. Metab.* **1998**, *83*, 1033–1036.
- (14) Ulmschneider, S.; Müller-Vieira, U.; Mitrenga, M.; Hartmann, R. W.; Oberwinkler-Marchais, S.; Klein, C. D.; Bureik, M.; Bernhardt, R.; Antes, I.; Lengauer, T. Synthesis and evaluation of imidazolymethylenetetrahydronaphthalenes and imidazolymethyleneindanes: Potent inhibitors of aldosterone synthase. *J. Med. Chem.* **2005**, *48*, 1796–1805.
- (15) Ulmschneider, S.; Müller-Vieira, U.; Klein, C. D.; Antes, I.; Lengauer, T.; Hartmann, R. W. Synthesis and evaluation of (pyridylmethylene)tetrahydronaphthalenes/-indanes and structurally modified derivatives: Potent and selective inhibitors of aldosterone synthase. *J. Med. Chem.* **2005**, *48*, 1563–1575.
- (16) Voets, M.; Antes, I.; Scherer, C.; Müller-Vieira, U.; Biemel, K.; Barassin, C.; Oberwinkler-Marchais, S.; Hartmann, R. W. Heteroaryl substituted naphthalenes and structurally modified derivatives: Selective

- inhibitors of CYP11B2 for the treatment of congestive heart failure and myocardial fibrosis. *J. Med. Chem.* **2005**, *48*, 6632–6642.
- (17) Lucas, S.; Heim, R.; Negri, M.; Antes, I.; Ries, C.; Schewe, K. E.; Bisi, A.; Gobbi, S.; Hartmann, R. W. Novel aldosterone synthase inhibitors with extended carbocyclic skeleton by a combined ligand-based and structure-based drug design approach. *J. Med. Chem.* **2008**, in press.
- (18) Voets, M.; Antes, I.; Scherer, C.; Müller-Vieira, U.; Biemel, K.; Oberwinkler-Marchais, S.; Hartmann, R. W. Synthesis and evaluation of heteroaryl-substituted dihydronaphthalenes and indenes: Potent and selective inhibitors of aldosterone synthase (CYP11B2) for the treatment of congestive heart failure and myocardial fibrosis. *J. Med. Chem.* **2006**, *49*, 2222–2231.
- (19) Lucas, S.; Heim, R.; Ries, C.; Schewe, K. E.; Birk, B.; Hartmann, R. W. Nonsteroidal aldosterone synthase inhibitors with improved selectivity: Lead optimization providing a series of pyridine substituted 3,4-dihydro-1*H*-quinolin-2-one derivatives. *J. Med. Chem.* **2008**, submitted.
- (20) Heim, R.; Lucas, S.; Grombein, C. M.; Ries, C.; Schewe, K. E.; Negri, M.; Müller-Vieira, U.; Birk, B.; Hartmann, R. W. Overcoming undesirable CYP1A2 inhibition of pyridynaphthalene type aldosterone synthase inhibitors: Influence of heteroaryl derivatization on potency and selectivity. *J. Med. Chem.* **2008**, *51*, 5064–5074.
- (21) Crabb, T. A.; Soilleux, S. L.; Microbiological transformations. Part 9.: Microbiological transformations of 1,2,5,6-tetrahydropyrrolo[3,2,1-*i,j*]-quinolin-4-one and of derivatives of 1,2,3,5,6,7-hexahydropyrrolo[3,2,1-*i,j*]quinoline with the fungus *Cunninghamella elegans*. *Tetrahedron* **1986**, *42*, 5407–5413.
- (22) Appukkuttan, P.; Orts, A. B.; Chandran, R., P.; Goeman, J. L.; van der Eycken, J.; Dehaen, W.; van der Eycken, E. Generation of a small library of highly electron-rich 2-(hetero)aryl-substituted phenethylamines by the Suzuki-Miyaura reaction: A short synthesis of an apogalanthamine analogue. *Eur. J. Org. Chem.* **2004**, 3277–3285.
- (23) Zhu, H.-F.; Zhao, W.; Okamura, T.; Fan, J.; Sun, W.-Y.; Ueyama, N. Syntheses and crystal structures of 1D tubular chains and 2D polycatenanes built from the asymmetric 1-(1-imidazolyl)-4-(imidazol-1-ylmethyl)benzene ligand with metal salts. *New J. Chem.* **2004**, *28*, 1010–1018.
- (24) Ishiyama, T.; Murata, M.; Miyaura, N. Palladium(0)-catalyzed cross-coupling reaction of alkoxydiboron with haloarenes: A direct procedure for arylboronic esters. *J. Org. Chem.* **1995**, *60*, 7508–7510.
- (25) (a) Denner, K.; Bernhardt, R. Inhibition studies of steroid conversions mediated by human CYP11B1 and CYP11B2 expressed in cell cultures. In *Oxygen Homeostasis and Its Dynamics*, 1st ed.; Ishimura, Y., Shimada, H., Suematsu, M., Eds.; Springer-Verlag: Tokyo, Berlin, Heidelberg, New York, 1998; pp 231–236. (b) Denner, K.; Doehmer, J.; Bernhardt, R. Cloning of CYP11B1 and CYP11B2 from normal human adrenal and their functional expression in COS-7 and V79 chinese hamster cells. *Endocr. Res.* **1995**, *21*, 443–448. (c) Böttner, B.; Denner, K.; Bernhardt, R. Conferring aldosterone synthesis to human CYP11B1 by replacing key amino acid residues with CYP11B2-specific ones. *Eur. J. Biochem.* **1998**, *252*, 458–466.

- (26) Lamberts, S. W.; Bruining, H. A.; Marzouk, H.; Zuiderwijk, J.; Uitterlinden, P.; Blijd, J. J.; Hackeng, W. H.; de Jong, F. H. The new aromatase inhibitor CGS-16949A suppresses aldosterone and cortisol production by human adrenal cells in vitro. *J. Clin. Endocrinol. Metab.* **1989**, *69*, 896–901.
- (27) Demers, L. M.; Melby, J. C.; Wilson, T. E.; Lipton, A.; Harvey, H. A.; Santen, R. J. The effects of CGS 16949A, an aromatase inhibitor on adrenal mineralocorticoid biosynthesis. *J. Clin. Endocrinol. Metab.* **1990**, *70*, 1162–1166.
- (28) (a) Ehmer, P. B.; Jose, J.; Hartmann, R. W. Development of a simple and rapid assay for the evaluation of inhibitors of human 17 α -hydroxylase-C_{17,20}-lyase (P450c17) by coexpression of P450c17 with NADPH-cytochrome-P450-reductase in *Escherichia coli*. *J. Steroid Biochem. Mol. Biol.* **2000**, *75*, 57–63; (b) Hutschenreuter, T. U.; Ehmer, P. B.; Hartmann, R. W. Synthesis of hydroxy derivatives of highly potent nonsteroidal CYP17 inhibitors as potential metabolites and evaluation of their activity by a non cellular assay using recombinant enzyme. *J. Enzyme Inhib. Med. Chem.* **2004**, *19*, 17–32.
- (29) Thompson, E. A.; Siiteri, P. K. Utilization of oxygen and reduced nicotinamide adenine dinucleotide phosphate by human placental microsomes during aromatization of androstenedione. *J. Biol. Chem.* **1974**, *249*, 5364–5372.
- (30) Hartmann, R. W.; Batzl, C. Aromatase inhibitors. Synthesis and evaluation of mammary tumor inhibiting activity of 3-alkylated 3-(4-aminophenyl)piperidine-2,6-diones. *J. Med. Chem.* **1986**, *29*, 1362–1369.
- (31) Belkina, N. V.; Lisurek, M.; Ivanov, A. S.; Bernhardt, R. Modelling of three-dimensional structures of cytochromes P450 11B1 and 11B2. *J. Inorg. Biochem.* **2001**, *87*, 197–207.
- (32) Hakki, T.; Bernhardt, R.; CYP17- and CYP11B-dependent steroid hydroxylases as drug development targets. *Pharmacol. Ther.* **2006**, *111*, 27–52.

4 Summary and conclusion

The aim of the present work was the development of novel compounds as potent and highly selective inhibitors of aldosterone synthase (CYP11B2) as prospective agents for the treatment of cardiovascular diseases. On the basis of a previously established pharmacophore model,⁹⁰ new molecules were designed with the primary goal to reach selectivity versus a range of other cytochrome P450 enzymes and CYP1A2 in particular as well as supplying experimental evidence for the *in vivo* efficacy of nonsteroidal CYP11B2 inhibitors and thus providing a proof of concept.

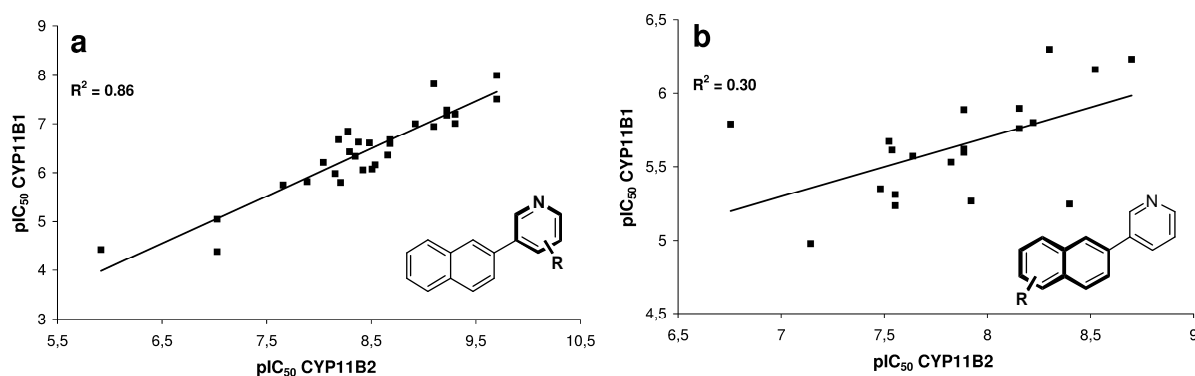
In Chapter 3.1, the synthesis and biological evaluation of a series of 30 pyridylnaphthalenes and -dihydronaphthalenes **I/1–I/30**[†] bearing various substituents in the pyridine moiety is described to examine their influence on potency and selectivity. In preceding studies, the attention was focused on the optimization of the naphthalene skeleton. The substitution pattern of the heme complexing 3-pyridine moiety, however, was not investigated in detail. In the present study, it was found that derivatization of the heterocycle has dramatic effects on the inhibitory action of the pyridylnaphthalenes on the target CYP11B2. Acidic residues (e.g., carboxylic acids, amides, hydroxy groups) generally resulted in a decrease in inhibitory potency whereas the nonprotic bioisosteric analogues turned out to inhibit CYP11B2 strongly. Most of the tested compounds turned out to be even more active than the unsubstituted parent compound **MV23** with IC₅₀ values in the low nanomolar range and even subnanomolar potencies in some cases. On the other hand, the selectivity toward 11 β -hydroxylase (CYP11B1) was not significantly influenced by most of the residues in the pyridine moiety.

This interesting experimental result was found to be due to a precise relationship between the inhibition of CYP11B2 and CYP11B1: an increased or decreased inhibitory activity at the one enzyme was accompanied by an increased or decreased inhibitory activity at the other enzyme. This trend becomes particularly evident when plotting the CYP11B2 versus the CYP11B1 pIC₅₀ values (Figure 17) revealing a reasonable linear correlation ($r^2 = 0.86$, $n = 29$). The finding, that it is to some extent possible to change the inhibitory potency by the heteroaryl derivatization without significantly changing the selectivity versus either CYP11B2 or CYP11B1 is an indication that the inhibitor binding proceeds via similar protein-inhibitor interactions of the heterocyclic moiety with both CYP11B isoforms. Contrariwise, it has been shown earlier by us that variation of the carbocyclic skeleton instead of the heterocycle can significantly influence the selectivity. Therefore, no correlation is observed for

[†] For the sake of clarity, all compounds that are referred to in chapter 4 are characterized by a Roman numeral I–IV to identify the paper in which they are published, and an Arabic numeral that is identical with the corresponding compound number of the particular publication (e.g., **II/6** is compound **6** from paper II)

a plot of the CYP11B2 and CYP11B1 pIC₅₀ values of the naphthalenes and dihydronaphthalenes described previously by Voets *et al.* that are functionalized with an unsubstituted 3-pyridine as heme complexing heterocycle ($r^2 = 0.30$, $n = 20$). Consistent with these findings, it can be assumed that both enzymes, CYP11B2 and CYP11B1, are structurally more diverse in the naphthalene binding site than in the heterocyclic binding site.

Figure 17. Correlation of pIC₅₀ values of pyridylnaphthalenes with modifications in the heterocyclic moiety (a) or in the naphthalene skeleton (b).

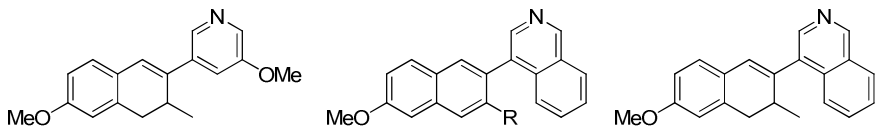


Contrary to the selectivity toward CYP11B1, some pyridine substituents had a significant impact on the CYP1A2 potency. It was found that the decrease of unwanted CYP1A2 inhibition correlates inversely with the planarity and aromaticity of the molecules. The reduced inhibition of CYP1A2 with reduced planarity reflects the affinity of the enzyme to both its typical substrates (e.g., caffeine⁹⁷) and inhibitors (e.g., furafylline⁹⁸) which are usually small-volume molecules with a planar shape. For example, in compounds **I/28–I/30**, the isoquinoline constrains the rotation around the carbon–carbon bond between the heterocycle and the naphthalene core, especially in presence of the additional *ortho*-methyl groups in **I/29** and **I/30** (Table 2). Thus, a coplanar conformation becomes energetically disfavored compared to the pyridine analogues and the sterically demanding heterocycle rotates out of the naphthalene plane. The latter molecules display a remarkably low CYP1A2 inhibition (< 60 % at a concentration of 2 μ M). The dihydronaphthalenes are again more selective, for example compounds **I/13** and **I/30** inhibit CYP1A2 less than 20 % at a concentration of 2 μ M. This result correlates with recent QSAR studies that have identified the CYP1A2 inhibition to be highly dependent on the number of sp²-hybridized carbons.⁹⁶

In summary, it has been demonstrated that modifying the lead compound **MV23** by introduction of substituents in the heterocyclic moiety has a clear effect on the activity and selectivity profile. The undesirable high CYP1A2 inhibition that is present in the previously investigated derivatives could be overcome by certain residues, giving rise to compounds with an advantageous overall selectivity profile. The results obtained are of great relevance for the design of aldosterone synthase inhibitors. A variety of substituents in the heterocyclic moiety is tolerated with respect to the inhibitory action on the target enzyme and even induces an increase in potency in most cases. What is even more important is the fact, that the selectivity toward CYP11B1 is rather constant, independent of the heterocyclic

substituent. This allows the introduction of residues into the pyridine moiety to improve for example pharmacokinetic (PK) parameters or the selectivity toward other competitive targets such as hepatic CYP enzymes. Therefore, the concept of varying the heterocyclic substitution pattern was used in the following sub-projects (Chapter 3.2 – Chapter 3.4) to investigate PK or selectivity effects.

Table 1. Inhibition of human CYP11B2, CYP11B1 and CYP1A2 *in vitro* by heteroaryl substituted naphthalenes

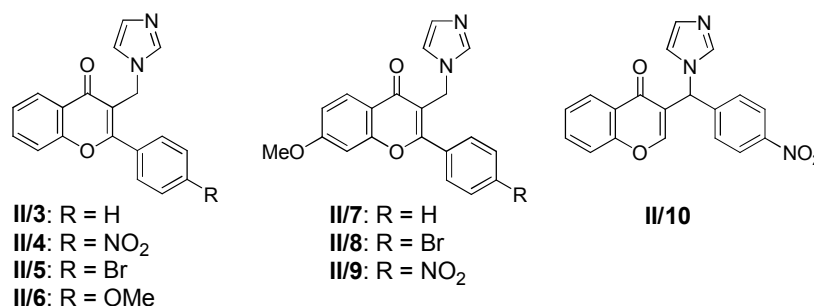


compd	R	IC ₅₀ value ^a (nM)		selectivity factor ^d	% inhibition ^e CYP1A2 ^f
		CYP11B2 ^b	CYP11B1 ^c		
I/13		1.2	100	83	18
I/28	H	0.6	67	112	57
I/29	Me	3.1	843	272	45
I/30		0.5	64	128	6

^a Mean value of at least four experiments, standard deviation usually less than 25 %. ^b Hamster fibroblasts expressing human CYP11B2; substrate deoxycorticosterone, 100 nM. ^c Hamster fibroblasts expressing human CYP11B1; substrate deoxycorticosterone, 100 nM. ^d IC₅₀ CYP11B1/IC₅₀ CYP11B2. ^e Mean value of two experiments, standard deviation less than 5 %. ^f Recombinantly expressed enzyme from baculovirus-infected insect microsomes (Supersomes); inhibitor concentration, 2.0 μM; furafylline, 55 % inhibition.

Chapter 3.2 deals with an *in silico* approach toward CYP11B2 inhibitors with extended carbocyclic skeleton. The inhibitor design concept is based on the discovery of imidazolylmethylene-substituted flavones as aldosterone synthase inhibitors with moderate to high inhibitory potency by compound library screening (Figure 18). These compounds that originally have been described as aromatase inhibitors⁹⁵ display CYP11B2 inhibition in a range of 73–94 % at a concentration of 500 nM with methoxy-functionalized **II/6** being most active (IC₅₀ = 11 nM), albeit without showing selectivity versus the highly homologous CYP11B1.

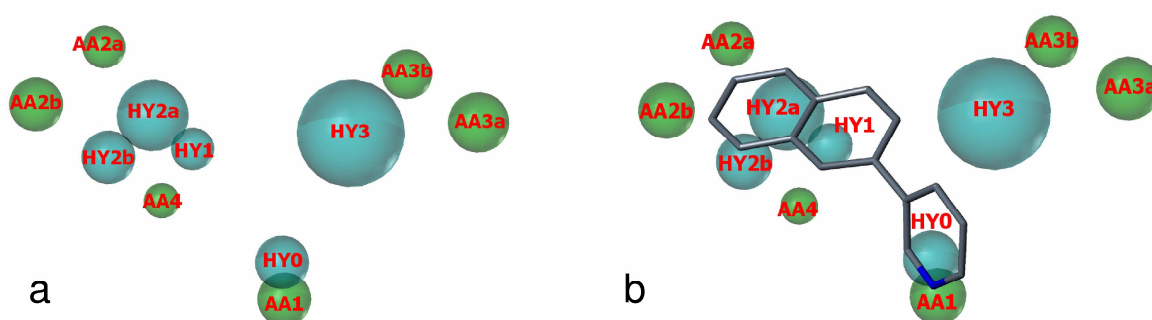
Figure 18. Imidazolylmethylene-substituted flavones with inhibitory action on CYP11B2



Using the chemical structures of the most potent flavone type inhibitors together with potent inhibitors of the naphthalene as well as methyleneindane type as a training set, an extended pharmacophore model was generated by applying the GALAHAD pharmacophore generation module of the SYBYL molecular modeling software.¹⁰¹ In the top ranked pharmacophore model, best in three of the

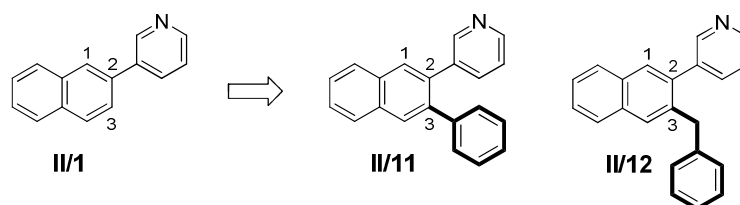
most indicative ranking criteria of this software, the earlier pharmacophoric points⁹⁰ were confirmed, namely the hydrophobic features HY0, HY1, HY2a, HY2b as well as the acceptor atom features AA1, AA2a, and AA2b (Figure 19a). A novel and voluminous hydrophobic area HY3 was identified next to HY1, along with the acceptor atom features AA3a and AA3b as well as an additional acceptor atom feature AA4. Figure 19b shows the unsubstituted naphthalene type inhibitor **II/1** mapped into the pharmacophore model. It becomes apparent that the hydrophobic feature HY3 and the corresponding acceptor atom features AA3a and AA3b are not exploited by inhibitors of the naphthalene type.

Figure 19. Pharmacophore model (a) and compound **II/1** mapped to the pharmacophore model (b). The newly identified hydrophobic feature HY3 as well as the acceptor atom features AA3a and AA3b are not exploited by inhibitors with a naphthalene molecular scaffold. Pharmacophoric features are color-coded: Cyan for hydrophobic regions (HY0–HY3) and green for acceptor atom features (AA1–4).



In order to exploit the newly discovered pharmacophoric feature HY3, the two model compounds **II/11** and **II/12** were designed (Figure 20). As suggested by the model and visualized in Figure 19, introduction of a hydrophobic substituent in 3-position of the naphthalene skeleton should be favorable to exploit the voluminous hydrophobic feature HY3 of the pharmacophore. The phenyl residue directly bound to the naphthalene core in compound **II/11** creates a conformationally constrained structure in which both rotational degrees of freedom of the two aryl–aryl bonds are limited since they are located *ortho* to each other. The benzyl motive in compound **II/12** leads to an increased flexibility of the spatial property distribution by rotation around the two benzylic carbon–carbon bonds. Furthermore, the aromatic ring moves apart from the naphthalene core by one methylene unit.

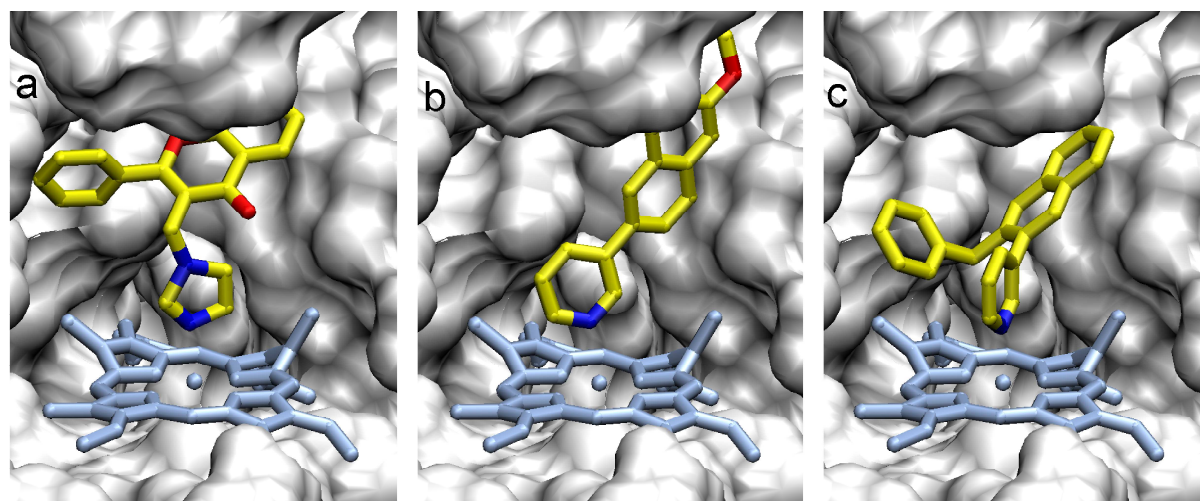
Figure 20. Proposed new lead structures **II/11** and **II/12**



In order to elucidate the role of conformational flexibility and the exact position of the aryl moiety for optimal inhibitor binding, docking studies were performed prior to synthesis. The analysis of the docking mode of compound **II/3** led to the identification of a new sub-pocket which interacts with the

aryl moiety (Figure 21a). This sub-pocket was not considered as potential binding site during our previous design efforts due to the fact that the formerly investigated compounds such as **II/2** (**MV23**) did not occupy this binding site (Figure 21b). However, the proposed new lead structure **II/11** proved to be too rigid to fit into the binding site and could thus not be docked successfully into the binding pocket under the given pharmacophore constraint, that is a directed heme-Fe–N interaction perpendicular to the heme-plane. This pharmacophore constraint was applied to ensure the right binding mode of the inhibitors with the heme-cofactor. The constraint requires the existence of an inhibitor-nitrogen-atom on the surface of an interaction cone with a 20 degree radius, which has its origin at the Fe-atom and points perpendicular to the heme-plane with a length of 2.2 Å. Obviously, the conformationally restricted phenyl moiety of compound **II/11** undergoes repulsive interaction with amino acids of the binding pocket or with the heme-cofactor under the above mentioned constraint, thus preventing that the molecule successfully docks into the CYP11B2 protein model. Contrariwise, the 3-benzyl substituted analog **II/12** is more flexible due to an additional methylene spacer between the two ring systems and thus fitted adequately into the binding site (Figure 21c). From these docking results it can be concluded that the methylene group of the potential inhibitor should provide the flexibility necessary to adapt to the binding site geometry.

Figure 21. Structure of the CYP11B2–inhibitor complexes of **II/3** (a), **II/2** (b) and **II/12** (c). Surface of the binding pocket (grey) surrounding the inhibitor and the heme co-factor (light blue). The inhibitors are presented in yellow; nitrogen atoms are colored in blue and oxygen atoms are in red. Unlike **II/2**, the inhibitors **II/3** and **II/12** exploit an additional sub-pocket of the inhibitor binding site.



The latter *in silico* experiments were confirmed by experimental results showing that 3-phenyl-substituted pyridynaphthalene **II/11** exhibits no significant CYP11B2 inhibition *in vitro*. In accordance with the docking results, benzyl analog **II/12**, however, is a moderately potent aldosterone synthase inhibitor ($IC_{50} = 154$ nM), albeit showing poor selectivity toward CYP11B1 (Table 2). Upon identification of **II/12** as promising hit, 25 new compounds were synthesized, most of which are highly potent CYP11B2 inhibitors with pronounced selectivity toward important steroidogenic and hepatic CYP enzymes. The inhibitory effects showed sharp structure-activity relationships for the investigated molecules, particularly for the substitution pattern of the benzyl moiety. A selection of

pharmacological data is presented in Table 2 for some representative compounds. It was found, that both high inhibitory potency and selectivity are due to substituents in *para*-position of the benzyl moiety (e.g., **II/16–II/18**) whereas derivatization of other positions is tolerated only to minor degree (e.g., **II/14**, **II/15**). Within this set of compounds, the outstanding selectivity toward CYP11B1 of **II/17** (factor 724) and **II/18** (factor 913) is particularly noteworthy with respect to the high homology of the two CYP11B isoforms. In the naphthalene molecular scaffold, introduction of a methoxy substituent in 7-position results in a decrease in inhibitory potency (e.g., **II/20**). On the other hand, the same substituent is readily tolerated in 6-position and even slightly increases the CYP11B1 selectivity in most cases (e.g., **II/19**).

Table 2. Inhibition of human CYP11B2 and CYP11B1 *in vitro* by 3-benzyl-naphthalene derivatives

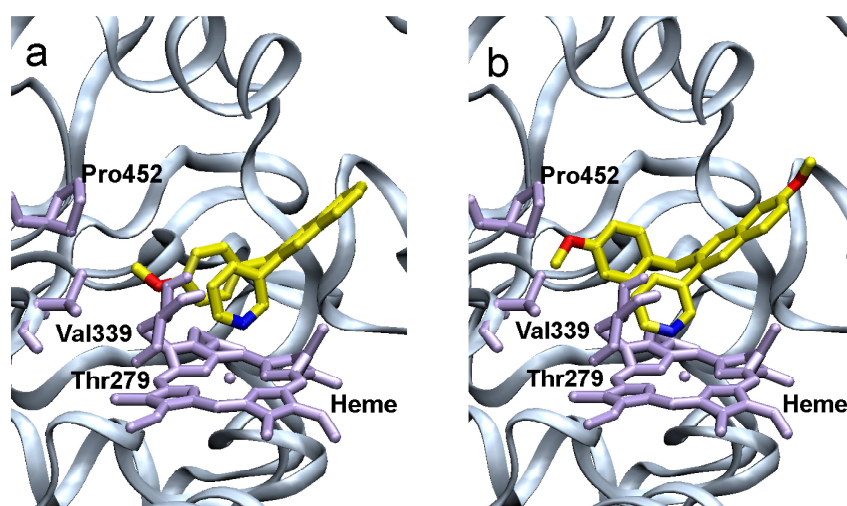
compd	R	% inhibition ^a		IC ₅₀ value ^b (nM)		selectivity factor ^e
		CYP11B2 ^c	CYP11B2 ^c	CYP11B2 ^c	CYP11B1 ^d	
II/12	H	76	154	953	6	
II/14	<i>o</i> -OMe	24	n.d.	n.d.	n.d.	n.d.
II/15	<i>m</i> -OMe	62	n.d.	n.d.	n.d.	n.d.
II/16	<i>p</i> -OMe	89	7.8	2804	359	
II/17	<i>p</i> -CN	93	2.7	1956	724	
II/18	<i>p</i> -OCF ₃	95	3.9	3559	913	
II/19	6-OMe	95	11	4329	394	
II/20	7-OMe	35	n.d.	n.d.	n.d.	n.d.

^a Mean value of at least two experiments, standard deviation usually less than 10 %; inhibitor concentration, 500 nM. ^b Mean value of at least four experiments, standard deviation usually less than 25 %, n.d. = not determined. ^c Hamster fibroblasts expressing human CYP11B2; substrate deoxycorticosterone, 100 nM. ^d Hamster fibroblasts expressing human CYP11B1; substrate deoxycorticosterone, 100 nM. ^e IC₅₀ CYP11B1/IC₅₀ CYP11B2, n.d. = not determined.

The pharmacological data can be explained by the docking results of compounds **II/16** and **II/19**, both bearing a *para*-methoxy group (Figure 22). The introduction of this substituent into the benzyl moiety as accomplished in **II/16** leads to interactions of the compound with the residues of Pro452, Val339, and Thr279, thus stabilizing the complex formed by coordination of the heme iron by the heterocyclic nitrogen considerably (Figure 22a). In compound **II/19**, a second methoxy group was introduced at the 6-position of the naphthalene scaffold (Figure 22b). This leads to no additional stabilization of the complex, but to a slightly increased selectivity versus CYP11B1. The same trend was observed previously for the binding properties of a series of substituted pyridyl-naphthalenes.^{88,89}

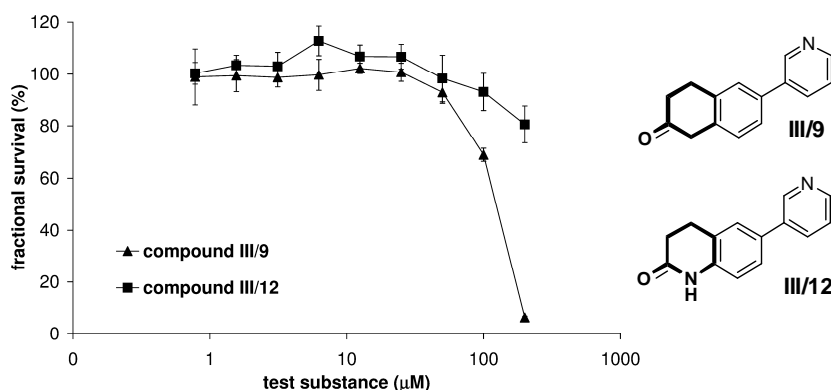
In summary, it has been shown in this sub-project that our novel CYP11B2 pharmacophore model has predictive power to identify prospective lead structures. Based on the results of the pharmacophore modeling, a new class of pyridynaphthalene derivatives with extended carbocyclic skeleton was designed. In addition, docking studies using our CYP11B2 protein model proved to be a useful tool to estimate the inhibitory properties of proposed new molecules and to explain structure-activity relationships. The results obtained are of significant relevance for the future design of CYP11B2 inhibitors because specific pharmacophoric features as well as interactions with certain amino acids have been identified to correlate with high potency at the target enzyme and, at the other hand, high selectivity toward CYP11B1.

Figure 22. Structure of the CYP11B2 binding pocket with the docked inhibitors **II/16** (a) and **II/19** (b). Details of the active site, showing inhibitor, heme co-factor and the interacting residues of Pro452, Val339, and Thr279.



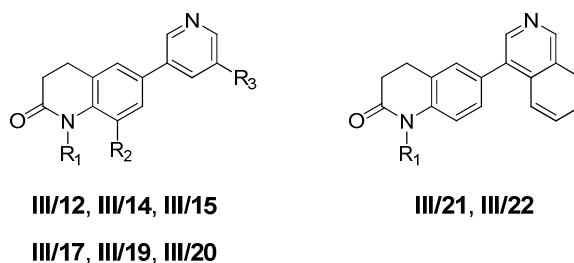
Chapter 3.3 describes the effort of reducing unwanted CYP1A2 activity of aldosterone synthase inhibitors by systematically reducing the aromaticity and planarity of the **MV23** scaffold. As already mentioned, these molecular descriptors have been hypothesized to be the most important variables influencing CYP1A2 inhibition. Among the molecules with partly saturated carbocyclic core structure, tetralone **III/9** (Figure 23), a potent aldosterone synthase inhibitor ($IC_{50} = 7.8$ nM), was found to be highly selective toward both CYP11B1 ($IC_{50} = 3.95$ μ M) and CYP1A2 ($IC_{50} = 1.55$ μ M) as well as a range of other hepatic CYP enzymes and even showed a good PK profile. However, tetralone **III/9** turned out to be cytotoxic to the human cell line U-937 at a concentration of 100 μ M (Figure 23). Subsequent bioisosteric exchange of the cyclic ketone in **III/9** by a lactam culminated in the discovery of dihydro-1*H*-quinolin-2-one **III/12** which exhibits no distinct cytotoxic effect on U-937 cells up to the highest concentration tested (Figure 23). In addition, compound **III/12** is an even slightly less potent inhibitor of CYP1A2 ($IC_{50} = 1.95$ μ M) than the analogous tetralone. Furthermore, it is more selective toward other CYP enzymes and significantly exceeds the bioavailability of **III/9**.

Figure 23. Mean profile (\pm SEM) of fractional survival (%) of human U-937 cells in presence of compound **III/9** or **III/12**.



Based on the molecular scaffold of **III/12**, several structurally modified derivatives were synthesized and tested for biological activity. The inhibitory data of some representative compounds out of this series are shown in Table 3. It becomes apparent that the dihydro-1*H*-quinolin-2-ones are highly potent CYP11B2 inhibitors with IC_{50} values in the low nanomolar range. Indeed, isoquinoline derivative **III/22** is the most active CYP11B2 inhibitor known so far with an IC_{50} value in the picomolar range ($IC_{50} = 90$ pM). Furthermore, the investigated compounds are selective toward CYP11B1, CYP1A2 as well as other competing enzymes, for example isoquinoline derivative **III/21** shows no CYP1A2 inhibition at all ($IC_{50} > 150$ μ M).

Table 3. Inhibition of human CYP11B2, CYP11B1 and CYP1A2 *in vitro* by dihydro-1*H*-quinolin-2-one derivatives

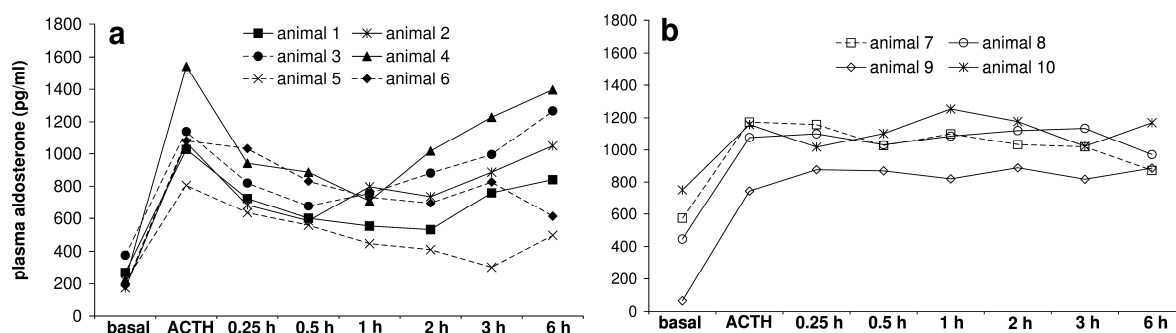


compd	R ₁	R ₂	R ₃	IC_{50} value ^a (nM)		selectivity factor ^d	IC_{50} value ^e (nM)
				CYP11B2 ^b	CYP11B1 ^c		
III/12	H	H	H	28	6746	241	1.95
III/14	Me	H	H	2.6	742	289	1.79
III/15	Et	H	H	22	5177	235	3.48
III/17	H	Cl	H	3.8	1671	440	30.6
III/19	H	H	OMe	2.7	339	126	5.24
III/20	Me	H	OMe	0.18	87	483	16.5
III/21	H			0.18	33	183	> 150
III/22	Me			0.09	6.9	77	n.d.

^a Mean value of at least four experiments, standard deviation usually less than 25 %. ^b Hamster fibroblasts expressing human CYP11B2; substrate deoxycorticosterone, 100 nM. ^c Hamster fibroblasts expressing human CYP11B1; substrate deoxycorticosterone, 100 nM. ^d IC_{50} CYP11B1/ IC_{50} CYP11B2. ^e Mean value of two experiments, standard deviation less than 5 %. ^f Recombinantly expressed enzymes from baculovirus-infected insect microsomes (Supersomes); furafylline, $IC_{50} = 2.42$ μ M.

In order to determine a suitable candidate to investigate aldosterone-lowering effects in rats, the synthesized inhibitors of the dihydro-1*H*-quinolin-2-one series were investigated for their ability to block aldosterone biosynthesis in V79 MZh cells expressing *rat* CYP11B2 prior to *in vivo* experiments. The results revealed that only compound **III/21** (and to a minor degree also the *N*-methyl analog **III/22**) shows a moderate inhibitory action on *rat* CYP11B2 *in vitro* (unpublished results). This compound is a highly potent inhibitor of human CYP11B2 *in vitro* (IC₅₀ = 0.18 nM) and also exhibits a pronounced selectivity toward other CYP enzymes. Examination of availability in plasma following peroral administration of this compound to rats revealed a good half-life (2.9 h) and reasonable plasma levels (AUC_{0-∞} = 1658 ng·h/mL following a 25 mg/kg dose). To investigate aldosterone-lowering effects *in vivo* (unpublished results), adult male rats received a subcutaneous injection of ACTH (1 mg/kg) 16 hours before test item application to stimulate the gluco- and mineralocorticoid biosynthesis (Figure 24). It becomes apparent, that ACTH treatment induces a significant increase of the aldosterone levels. Within the vehicle-treated group (Figure 24b), the concentrations found in the plasma are rather constant over the duration of the experiment (6 h). After intravenous application of a 20 mg/kg dose of **III/21** to ACTH stimulated rats, however, a significant lowering of the plasma aldosterone levels is already observed after 15 min (Figure 24a). The inhibitory effect persists up to three hours upon injection before returning to the ACTH levels again. The aldosterone levels are maximally reduced to 36–63 % in a timeframe of 0.5–3 hours (n = 6).

Figure 24. Lowering of aldosterone plasma levels *in vivo*. (a) **III/21**-treated group (animals 1–6), (b) vehicle-treated group (animals 7–10)

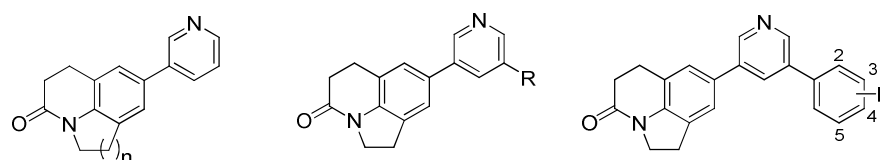


In conclusion, nonsteroidal aldosterone synthase inhibitors with dihydro-1*H*-quinolin-2-one molecular scaffold proved to be significantly superior to the previously investigated pyridyl-naphthalenes such as **MV23**. These molecules are highly selective toward a range of cytochrome P450 enzymes and CYP1A2 in particular. Furthermore, most of the investigated compounds show a good PK profile. Moreover, isoquinoline derivative **III/21** proved to be capable of reducing the aldosterone plasma levels in ACTH stimulated rats after intravenous application. The structural motives obtained in this sub-project were pursued and refined in Chapter 3.4.

Rigidification of the latter substances by incorporation of the lactam *N*-alkyl group into a 5- or 6-membered ring afforded compounds with a pyrroloquinolinone or pyridoquinolinone molecular

scaffold (Chapter 3.4). Analysis of the biological data of these molecules, whereof some are presented in Table 4, reveals interesting structure-activity relationships with regard to 11 β -hydroxylase (CYP11B1) potency and thus selectivity while, on the contrary, the CYP11B2 activity is influenced only to a minor degree and is in a very narrow activity range with IC₅₀ values of typically less than 5 nM. As a general rule, a majority of the fused heterocycles is more selective toward CYP11B1 than their corresponding open-chain analogues due to a decreased CYP11B1 inhibition with pyrido- being more selective than the pyrrolo-fused derivatives (e.g., **IV/2**). The influence of certain structural modifications on the 11 β -hydroxylase activity is particularly noteworthy. On the one hand, CYP11B1 inhibition is an important selectivity criterion for aldosterone synthase inhibitors. On the other hand, selective CYP11B1 inhibitors could be used for the treatment of Cushing's syndrome and metabolic syndrome. Although several potent CYP11B1 inhibitors have been described previously, in-depth SAR studies were usually focused on the concurrent CYP11B2 activity. Herein, we clearly identified structural features important for high inhibitory CYP11B1 potency.

Table 4. Inhibition of human CYP11B2 and CYP11B1 *in vitro* by pyrrolo- and pyridoquinolinone derivatives



compd	n	R	IC ₅₀ value ^b (nM)		selectivity factor ^e
			CYP11B2 ^c	CYP11B1 ^d	
IV/1	1	H	1.1	715	650
IV/2	2	H	2.4	2296	957
IV/3		OMe	0.6	247	412
IV/5		OEt	1.0	158	158
IV/6		O <i>i</i> Pr	2.2	103	47
IV/15		H	1.3	58	45
IV/16		2-F	0.7	43	61
IV/17		3-F	1.4	490	350
IV/18		4-F	0.9	40	44
IV/22		2-OMe	2.4	128	53
IV/23		3-OMe	4.6	1374	299
IV/24		4-OMe	1.4	21	15

^a Mean value of at least four experiments, standard deviation usually less than 25 %. ^b Hamster fibroblasts expressing human CYP11B2; substrate deoxycorticosterone, 100 nM. ^c Hamster fibroblasts expressing human CYP11B1; substrate deoxycorticosterone, 100 nM. ^d IC₅₀ CYP11B1/IC₅₀ CYP11B2.

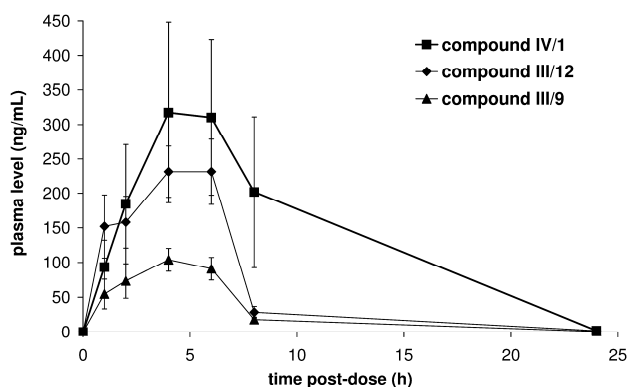
The main impact on CYP11B1 inhibition is exerted by substituents in the 3-pyridine moiety. Obviously, the size of substituents plays a crucial role for the CYP11B1 potency. For instance, this trend becomes evident in the series of pyrroloquinolinone compounds with alkoxy derivatized heterocycle (**IV/3**, **IV/5**, **IV/6**) where the CYP11B1 inhibition increases with the substituent size in the order

IV/1 (R = H, IC₅₀ = 715 nM) < **IV/3** (R = OMe, IC₅₀ = 247 nM) < **IV/5** (R = OEt, IC₅₀ = 158 nM) < **IV/6** (R = OiPr, IC₅₀ = 103 nM). The same shift of CYP11B1 activity can be observed for several compounds with additional aryl substituent in 5-position of the pyridine moiety (e.g., **IV/15**, **IV/16**, **IV/18**, **IV/22**, **IV/24**). The CYP11B1 inhibition exerted by these molecules increases up to 36-fold compared to the unsubstituted parent compound **IV/1** to IC₅₀ values in the range of 21–128 nM corresponding with a rather low selectivity (factor 15–61). Moreover, it is striking that *meta* substituents in the aryl moiety as accomplished in compounds **IV/17** and **IV/23** can trigger CYP11B1 selectivity again, thus constituting an intriguing on/off-switch of CYP11B1 potency. This tendency implicates that a variety of sterically demanding substituents at the pyridine moiety is readily tolerated in the CYP11B2 binding pocket, however, lead to no further stabilization of the complexes formed by coordination of the heme iron by the heterocyclic nitrogen. Contrariwise, 3-pyridine substituted pyrroloquinolinone derivatives such as **IV/1** are per se rather poor CYP11B1 inhibitors and require an additional benzene moiety, and thus a further stabilization of the formed complexes mainly through hydrophobic or π - π stacking interactions, for basal inhibitory potency. Amongst these compounds are highly potent CYP11B1 inhibitors (e.g., **IV/24**). On the other hand, *meta*-substituted analogues obviously do not adequately fit into the CYP11B1 binding pocket or loose contact to the heme iron while minimizing unfavorable contacts with the enzyme leading to a decrease in potency.

The latter observations contravene the results obtained in case of the substituted pyridyl-naphthalenes (Chapter 3.1), in which substituents at the heterocyclic moiety led to a change of inhibition of both the CYP11B isoforms in a comparable order of magnitude resulting in a reasonable linear correlation of the corresponding pIC₅₀ values ($r^2 = 0.86$) and thus a rather constant selectivity factor. This is an indication for a binding mode of the pyrroloquinolinone derivatives different from that of the naphthalene analogues. Recently performed docking studies of 3-pyridyl-naphthalenes with extended carbocyclic skeleton suggest a previously unexplored sub-pocket of the inhibitor binding site that can interact with additional aryl moieties next to the heterocycle.⁹⁴ It can be assumed that this sub-pocket is similarly exploited by the aryl-substituted pyrroloquinolinones of the present study.

In addition to the high CYP11B1 selectivity of most of the investigated compounds, the pyrroloquinolinone type inhibitors also exhibit a good selectivity toward hepatic CYP enzymes. For instance, the unsubstituted parent compound **IV/1** shows no significant inhibition of the six most important hepatic CYP enzymes (IC₅₀ > 10 μ M). In addition, this highly potent and selective aldosterone synthase inhibitor reaches higher plasma concentrations (AUC_{0- ∞} = 3464 ng·h/mL) after peroral application to rats (following a 5 mg/kg dose) than for example **III/9** or **III/12**, both compounds with good pharmacological profile (Figure 25), and even slightly exceeds the bioavailability of the marketed drug fadrozole (AUC_{0- ∞} = 3207 ng·h/mL). Currently, further studies with inhibitor **IV/1** and structurally related compounds are underway to evaluate aldosterone-lowering effects *in vivo*.

Figure 25. Mean profile (\pm) SEM of plasma levels (ng/ml) in rat versus time after oral application (5 mg/kg) of compounds **IV/1**, **III/12**, and **III/9** determined in a cassette dosing experiment.



In summary, the present work describes the pharmacophore-based design of nonsteroidal aldosterone synthase inhibitors, that combine the advantages of the previously described pyridyl-naphthalenes (i.e., high inhibitory CYP11B2 potency and selectivity toward CYP11B1) with a simultaneously improved pharmacological overall profile. Beside a strong CYP11B2 inhibition with IC_{50} values in the low to sub-nanomolar range and outstanding CYP11B1 selectivity with up to 1000-fold lower activity in comparison to the CYP11B2 isoform, the most promising compounds of the actual study show virtually no inhibition of the six most important hepatic CYP enzymes as well as CYP17 and CYP19, both crucial enzymes for the metabolism of steroid hormones. Amongst the last-mentioned, the selectivity toward CYP1A2 is particularly noteworthy because this drug-metabolizing enzyme was strongly inhibited by all compounds with pyridyl-naphthalene scaffold. In view of the pharmacokinetic properties, a subset of the investigated inhibitors reaches excellent plasma-levels in the range of the marketed drug fadrozole after peroral application to rats. Furthermore, it has been shown that a nonsteroidal CYP11B2 inhibitor of the dihydro-1*H*-quinolin-2-one series exerts aldosterone-lowering effects *in vivo* using a modified rat model as described by Häusler *et al.*⁹² Current *in vivo* investigations in disease oriented models toward evidence to prevent or reverse myocardial fibrosis and reduce CHF induced mortality are under scrutiny to determine a potential development candidate out of the most promising CYP11B2 inhibitors. In addition, the investigations of the present work provide precise structure-activity studies for both CYP11B2 and CYP11B1 inhibition which can be used in the future development of new molecules interacting either with CYP11B2 or CYP11B1. The latter might be of particular interest for the treatment of cortisol-dependent disorders such as Cushing's syndrome or metabolic syndrome since in-depth SAR studies dealing with 11 β -hydroxylase potency are essentially absent so far. The utility of the pharmacophore model generated in the course of the present study has already been shown by the success in the development of pyridyl-naphthalenes with extended carbocyclic skeleton. However, its scope has not yet been exploited in full and might thereto serve as a sign post for continual pharmacophore-based drug design. Currently, several drug design projects based on the concepts elucidated herein are in progress.

5 References

- 1 Kawamoto, T.; Mitsuuchi, Y.; Toda, K.; Yokoyama, Y.; Miyahara, K.; Miura, S.; Ohnishi, T.; Ichikawa, Y.; Nakao, K.; Imura, H.; Ulick, S.; Shizuta, Y. Role of steroid 11 β -hydroxylase and steroid 18-hydroxylase in the biosynthesis of glucocorticoids and mineralocorticoids in humans. *Proc. Natl. Acad. Sci. U.S.A.* **1992**, *89*, 1458–1462.
- 2 Tait, S. A.; Tait, J. F.; Coghlan, J. P. The discovery, isolation and identification of aldosterone: reflections on emerging regulation and function. *Mol. Cell. Endocrinol.* **2004**, *217*, 1–21.
- 3 Connell, J. M. C.; Davies, E. The new biology of aldosterone. *J. Endocrinol.* **2005**, *186*, 1–20.
- 4 Eaton, D. C.; Malik, B.; Saxena, N. C. Al-Khalili, O. K.; Yue, G. Mechanisms of aldosterone's action on epithelial Na⁺ transport. *J. Membrane Biol.* **2001**, *184*, 313–319.
- 5 Therien, A. G.; Blostein, R. Mechanisms of sodium pump regulation. *Am. J. Physiol. Cell. Physiol.* **2000**, *279*, C541–C566.
- 6 (a) Bonvalet, J. P. Regulation of sodium transport by steroid hormones. *Kidney Int.* **1998**, *53*, 49–56. (b) Palmer, L. G.; Frindt, G. Aldosterone and potassium secretion by the cortical collecting duct. *Kidney Int.* **2000**, *57*, 1324–1328.
- 7 (a) Reul, J. M. H. M.; de Kloet, E. R. Anatomical resolution of two types of corticosterone receptor sites in rat brain with in vitro autoradiography and computerized image analysis. *J. Steroid Biochem. Mol. Biol.* **1986**, *24*, 269–272. (b) Agarwal, M. K.; Mirshahi, F.; Mirshahi, M.; Rostene, W. Immunochemical detection of the mineralocorticoid receptor in rat brain. *Neuroendocrinology* **1993**, *58*, 575–580.
- 8 (a) Lombes, M.; Oblin, M. E.; Gasc, J. M.; Baulieu, E. E.; Farman, N.; Bonvalet, J. P. Immunohistochemical and biochemical evidence for a cardiovascular mineralocorticoid receptor. *Circ. Res.* **1992**, *71*, 503–510. (b) Lombes, M.; Alfaidy, N.; Eugene, E.; Lessana, A.; Farman, N.; Bonvalet, J. P. Prerequisite for cardiac aldosterone action. Mineralocorticoid receptor and 11 β -hydroxysteroid dehydrogenase in the human heart. *Circulation* **1995**, *92*, 175–182.
- 9 Quinn, S. J.; Williams, G. H. Regulation of aldosterone secretion. *Annu. Rev. Physiol.* **1988**, *50*, 409–426.
- 10 (a) Wehling, M. Specific, nongenomic actions of steroid hormones. *Annu. Rev. Physiol.* **1997**, *59*, 365–393. (b) Lösel, R.; Wehling, M. Nongenomic actions of steroid hormones. *Nature Rev. Mol. Cell. Biol.* **2003**, *4*, 46–55.
- 11 Spach, C.; Streeten, D. H. Retardation of sodium exchange in dog erythrocytes by physiological concentrations of aldosterone, in vitro. *J. Clin. Invest.* **1964**, *43*, 217–227.

- 12 Haseroth, K.; Gerdes, D.; Berger, S.; Feuring, M.; Günther, A.; Herbst, C.; Christ, M.; Wehling, M. Rapid nongenomic effects of aldosterone in mineralocorticoid-receptor-knockout mice. *Biochem. Biophys. Res. Commun.* **1999**, *266*, 257–261.
- 13 (a) Christ, M.; Douwes, K.; Eisen, C.; Bechtner, G.; Theisen, K.; Wehling, M. Rapid Effects of aldosterone on sodium transport in vascular smooth muscle cells. *Hypertension* **1995**, *25*, 117–123. (b) Wehling, M.; Kasmayr, J.; Theisen, K. Rapid effects of mineralocorticoids on sodium-proton exchanger: genomic or nongenomic pathway? *Am. J. Physiol. Endocrinol. Metab.* **1995**, *260*, E719–E726.
- 14 Eisen, C.; Meyer, C.; Christ, M.; Theisen, K.; Wehling, M. Novel membrane receptors for aldosterone in human lymphocytes: a 50 kDa protein on SDS-PAGE. *Cell. Mol. Biol.* **1994**, *40*, 351–358.
- 15 Davies, E.; MacKenzie, S. M. Extra-adrenal production of corticosteroids. *Clin. Exp. Pharmacol. Physiol.* **2003**, *30*, 437–445.
- 16 (a) Strömstedt, M.; Waterman, M. R. Messenger RNAs encoding steroidogenic enzymes are expressed in rodent brain. *Mol. Brain Res.* **1995**, *34*, 75–88. (b) Gomez-Sanchez, C. E.; Zhou, M. Y.; Cozza, E. N.; Morita, H.; Foecking, M. F.; Gomez-Sanchez, E. P. Aldosterone biosynthesis in the rat brain. *Endocrinology* **1997**, *138*, 3369–3373.
- 17 (a) Ahmad, N.; Romero, D. G.; Gomez-Sanchez, E. P.; Gomez-Sanchez, C. E. Do human vascular endothelial cells produce aldosterone? *Endocrinology* **2004**, *145*, 3626–3629. (b) Funder, J. W. Cardiac synthesis of aldosterone: Going, going, gone...? *Endocrinology* **2004**, *145*, 4793–4795.
- 18 Silvestre, J. S.; Robert, V.; Heymes, C.; Aupetit-Faisant, B.; Mouas, C.; Moalic, J. M.; Swynghedauw, B.; Delcayre, C. Myocardial production of aldosterone and corticosterone in the rat: Physiological regulation. *J. Biol. Chem.* **1998**, *273*, 4883–4891.
- 19 Fiebeler, A.; Nussberger, J.; Shagdarsuren, E.; Rong, S.; Hilfenhaus, G.; Al-Saadi, N.; Dechend, R.; Wellner, M.; Meiners, S.; Maser-Gluth, C.; Jeng, A. Y.; Webb, R. L.; Luft, F. C.; Muller, D. N. Aldosterone synthase inhibitor ameliorates angiotensin II-induced organ damage. *Circulation* **2005**, *111*, 3087–3094.
- 20 Hu, X.; Bolten, C. W. Adrenal corticosteroids, their receptors and hypertension. *Drug Dev. Res.* **2006**, *67*, 871–883.
- 21 Schacke, H.; Docke, W.D.; Asadullah, K. Mechanisms involved in the side effects of glucocorticoids. *Pharmacol. Ther.* **2002**, *96*, 23–43.
- 22 (a) Krozowski, Z. S.; Funder, J. W. Renal mineralocorticoid receptors and hippocampal corticosterone-binding species have identical intrinsic steroid specificity. *Proc. Natl. Acad. Sci. U.S.A.* **1983**, *80*, 6056–6060. (b) Myles, K.; Funder, J. W. Type I (mineralocorticoid) receptors in the guinea pig. *Am. J. Physiol. Endocrinol. Metab.* **1994**, *267*, E268–E272.
- 23 Funder, J. W.; Feldman, D.; Edelman, I. S. The roles of plasma binding and receptor specificity in the mineralocorticoid action of aldosterone. *Endocrinology* **1973**, *92*, 994–1004.
- 24 Lombes, M.; Kenouch, S.; Souque, A.; Farman, N.; Rafestin-Oblin, M. E. The mineralocorticoid receptor discriminates aldosterone from glucocorticoids independently of the 11 β -hydroxysteroid dehydrogenase. *Endocrinology* **1994**, *135*, 834–840.

- 25 Funder, J. W.; Pearce, P. T.; Smith, R.; Smith, A. I. Mineralocorticoid action: target tissue specificity is enzyme, not receptor, mediated. *Science* **1988**, *242*, 583–585.
- 26 Funder, J. W. Mineralocorticoid receptor activation and oxidative stress. *Hypertension* **2007**, *50*, 840–841.
- 27 Hasler, J. A.; Estabrook, R.; Murray, M.; Pikuleva, I.; Waterman, M.; Capdevila, J.; Holla, V.; Helvig, C.; Falck, J. R.; Farrell, G.; Kaminsky, L. S.; Spivack, S. D.; Boitier, E.; Beaune, P. Human cytochromes P450. *Mol. Aspects Med.* **1999**, *20*, 1–137.
- 28 Garfinkel, D. Studies on pig liver microsomes. I. Enzymic and pigment composition of different microsomal fractions. *Arch. Biochem. Biophys.* **1958**, *77*, 493.
- 29 Klingenberg, M. Pigments of rat liver microsomes. *Arch. Biochem. Biophys.* **1958**, *75*, 376–386.
- 30 (a) Omura, T.; Sato, R. A new cytochrome in liver microsomes. *J. Biol. Chem.* **1962**, *237*, 1375–1376. (b) Omura, T.; Sato, R. The carbon monoxide-binding pigment of liver microsomes. I. Evidence for its hemoprotein nature. *J. Biol. Chem.* **1964**, *239*, 2370–2378. (c) Omura, T.; Sato, R. The carbon monoxide-binding pigment of liver microsomes. II. Solubilization, purification, and properties. *J. Biol. Chem.* **1964**, *239*, 2379–2385.
- 31 Meunier, B.; de Visser, S. P.; Shaik, S. Mechanism of oxidation reactions catalyzed by cytochrome P450 enzymes. *Chem. Rev.* **2004**, *104*, 3947–3980.
- 32 Miller, W. L. Regulation of steroidogenesis by electron transfer. *Endocrinology* **2005**, *146*, 2544–2550.
- 33 BIASON-LAUBER, A. Molecular medicine of steroid hormone biosynthesis. *Mol. Aspects Med.* **1998**, *19*, 155–220.
- 34 Lieberman, S.; Lin, Y. Y. Reflections on sterol sidechain cleavage process catalyzed by cytochrome P450(scc). *J. Steroid Biochem. Mol. Biol.* **2001**, *78*, 1–14.
- 35 Mornet, E.; Dupont, J.; Vitek, A.; White, P. C. Characterization of two genes encoding human steroid 11 β -hydroxylase (P-450_{11 β}). *J. Biol. Chem.* **1989**, *264*, 20961–20967.
- 36 Bureik, M.; Lisurek, M.; Bernhardt, R. The human steroid hydroxylases CYP11B1 and CYP11B2. *Chem. Biol.* **2002**, *383*, 1537–1551.
- 37 Belkina, N. V.; Lisurek, M.; Ivanov, A. S.; Bernhardt, R. Modelling of three-dimensional structures of cytochromes P450 11B1 and 11B2. *J. Inorg. Biochem.* **2001**, *87*, 197–207.
- 38 Fisher, A.; Friel, E. C.; Bernhardt, R.; Gomez-Sanchez, C.; Connell, J. M.; Fraser, R.; Davies, E. Effects of 18-hydroxylated steroids on corticosteroid production by human aldosterone synthase and 11 β -hydroxylase. *J. Clin. Endocrinol. Metab.* **2001**, *86*, 4326–4329.
- 39 (a) Böttner, B.; Schrauber, H.; Bernhardt, R. Engineering a mineralocorticoid- to a glucocorticoid-synthesizing cytochrome P450. *J. Biol. Chem.* **1996**, *271*, 8028–8033. (b) Böttner, B.; Denner, K.; Bernhardt, R. Conferring aldosterone synthesis to human CYP11B1 by replacing key amino acid residues with CYP11B2-specific ones. *Eur. J. Biochem.* **1998**, *252*, 458–466.
- 40 Roumen, L.; Sanders, M. P. A.; Pieterse, K.; Hilbers, P. A. J.; Plate, R.; Custers, E.; de Gooyer, M.; Smits, J. F. M.; Beugels, I.; Emmen, J.; Ottenheijm, H. C. J.; Leysen, D.; Hermans, J. J. R. Construction

- of 3D models of the CYP11B family as a tool to predict ligand binding characteristics. *J. Comput.-Aided Mol. Des.* **2007**, *21*, 455–471.
- 41 Ulmschneider, S.; Müller-Vieira, U.; Mitrenga, M.; Hartmann, R. W.; Oberwinkler-Marchais, S.; Klein, C. D.; Bureik, M.; Bernhardt, R.; Antes, I.; Lengauer, T. Synthesis and evaluation of imidazolymethylenetetrahydronaphthalenes and imidazolymethyleneindanes: Potent inhibitors of aldosterone synthase. *J. Med. Chem.* **2005**, *48*, 1796–1805.
- 42 Ulmschneider, S.; Müller-Vieira, U.; Klein, C. D.; Antes, I.; Lengauer, T.; Hartmann, R. W. Synthesis and evaluation of (pyridylmethylene)tetrahydronaphthalenes/-indanes and structurally modified derivatives: Potent and selective inhibitors of aldosterone synthase. *J. Med. Chem.* **2005**, *48*, 1563–1575.
- 43 Cowie, M. R.; Mosterel, A.; Wood, D. A.; Deckers, J. W.; Poole-Wilson, P. A.; Grobbee, D. E. The epidemiology of heart failure. *Eur. Heart J.* **1997**, *18*, 208–225.
- 44 Laragh, J. H. Hormones and the pathogenesis of congestive heart failure: vasopressin, aldosterone, and angiotensin II: further evidence for renal-adrenal interaction from studies in hypertension and in cirrhosis. *Circulation* **1962**, *25*, 1015–1023
- 45 Weber, K. T. Aldosterone in congestive heart failure. *N. Engl. J. Med.* **2001**, *345*, 1689–1697.
- 46 (a) Brilla, C. G. Renin-angiotensin-aldosterone system and myocardial fibrosis. *Cardiovasc. Res.* **2000**, *47*, 1–3. (b) Brilla, C. G. Aldosterone and myocardial fibrosis in heart failure. *Herz* **2000**, *25*, 299–306. (c) Lijnen, P.; Petrov, V. Induction of cardiac fibrosis by aldosterone. *J. Mol. Cell. Cardiol.* **2000**, *32*, 865–879.
- 47 Robert, V.; van Thiem, N.; Cheav, S. L.; Mouas, C.; Swynghedauw, B.; Delcayre, C. Increased cardiac types I and III collagen mRNAs in aldosterone-salt hypertension. *Hypertension* **1994**, *24*, 30–36.
- 48 (a) Fullerton, M. J.; Funder, J. W. Aldosterone and cardiac fibrosis: in vitro studies. *Cardiovasc. Res.* **1994**, *28*, 1863–1867. (b) Fullerton, M. J.; Funder, J. W. Aldosterone regulates collagen output of rat cardiac fibroblasts by up-regulation of endothelin receptors. *Endocrin. Soc. Proc.* **1998**, *93*, 511.
- 49 Brilla, C. G.; Zhou, G.; Matsubara, L.; Weber, K. T. Collagen metabolism in cultured adult rat cardiac fibroblasts: response to angiotensin II and aldosterone. *J. Mol. Cell. Cardiol.* **1994**, *26*, 809–820.
- 50 Satoh, M.; Nakamura, M.; Saitoh, H.; Satoh, H.; Akatsu, T.; Iwasaka, J.; Masuda, T.; Hiramori, K. Aldosterone synthase (CYP11B2) expression and myocardial fibrosis in the failing human heart. *Clin. Sci. (Lond.)* **2002**, *102*, 381–386.
- 51 (a) The CONSENSUS trial study group. Effects of enalapril on mortality in severe congestive heart failure. Results of the cooperative north scandinavian enalapril survival study (CONSENSUS). *N. Engl. J. Med.* **1987**, *316*, 1429–1435. (b) Kjekshus J, Swedberg K, Snapinn S. Effects of enalapril on long-term mortality in severe congestive heart failure. *Am. J. Cardiol.* **1992**, *69*, 103–107.
- 52 (a) Struthers, A. D. Aldosterone escape during angiotensin-converting enzyme inhibitor therapy in chronic heart failure. *J. Card. Fail.* **1996**, *2*, 47–54. (b) Sato, A.; Saruta, T. Aldosterone escape during angiotensin-converting enzyme inhibitor therapy in essential hypertensive patients with left ventricular hypertrophy. *J. Int. Med. Res.* **2001**, *29*, 13–21.
- 53 Ruilope, L. M.; Rosei, E. A.; Bakris, G. L.; Mancía, G.; Poulter, N. R.; Taddei, S.; Unger, T.; Volpe, M.; Waeber, B.; Zannad, F. Angiotensin receptor blockers: Therapeutic targets and cardiovascular protection. *Blood Press.* **2005**, *14*, 196–209.

- 54 Maibaum, J.; Stutz, S.; Göschke, R.; Rigollier, P.; Yamaguchi, Y.; Cumin, F.; Rahuel, J.; Baum, H.-P.; Cohen, N.-C.; Schnell, C. R.; Fuhrer, W.; Gruetter, M. G.; Schilling, W.; Wood, J. M. Structural modification of the P2' position of 2,7-dialkyl-substituted 5(S)-amino-4(S)-hydroxy-8-phenyl-octane-carboxamides: The discovery of aliskiren, a potent nonpeptide human renin inhibitor active after once daily dosing in marmosets. *J. Med. Chem.* **2007**, *50*, 4832–4844.
- 55 Siragy, H. M.; Kar, S.; Kirkpatrick, P. Aliskiren. *Nature Rev. Drug Discov.* **2007**, *6*, 779–780.
- 56 Pitt, B.; Zannad, F.; Remme, W. J.; Cody, R.; Castaigne, A.; Perez, A.; Palensky, J.; Wittes, J. The effect of spironolactone on morbidity and mortality in patients with severe heart failure. *N. Engl. J. Med.* **1999**, *341*, 709–717.
- 57 (a) Zannad, F.; Alla, F.; Dousset, B.; Perez, A.; Pitt, B. Limitation of excessive extracellular matrix turnover may contribute to survival benefit of spironolactone therapy in patients with congestive heart failure: insights from the randomized aldactone evaluation study (RALES). Rales Investigators. *Circulation* **2000**, *102*, 2700–2706. (b) Izawa, H.; Murohara, T.; Nagata, K.; Isobe, S.; Asano, H.; Amano, T.; Ichihara, S.; Kato, T.; Ohshima, S.; Murase, Y.; Iino, S.; Obata, K.; Noda, A.; Okumura, K.; Yokota, M. Mineralocorticoid receptor antagonism ameliorates left ventricular diastolic dysfunction and myocardial fibrosis in mildly symptomatic patients with idiopathic dilated cardiomyopathy: a pilot study. *Circulation* **2005**, *112*, 2940–2945.
- 58 MacFadyen, R. J.; Barr, C. S.; Struthers, A. D. Aldosterone blockade reduces vascular collagen turnover, improves heart rate variability and reduces early morning rise in heart rate in heart failure patients. *Cardiovasc. Res.* **1997**, *35*, 30–34.
- 59 Juurlink, D. N.; Mamdani, M. M.; Lee, D. S.; Kopp, A.; Austin, P. C.; Laupacis, A.; Redelmeier, D. A. Rates of hyperkalemia after publication of the Randomized Aldactone Evaluation Study. *N. Engl. J. Med.* **2004**, *351*, 543–551.
- 60 Pitt, B.; Remme, W.; Zannad, F.; Neaton, J.; Martinez, F.; Roniker, B.; Bittman, R.; Hurley, S.; Kleiman, J.; Gatlin, M. Eplerenone, a selective aldosterone blocker, in patients with left ventricular dysfunction after myocardial infarction. *N. Engl. J. Med.* **2003**, *348*, 1309–1321.
- 61 Young, M.; Funder, J. W. Eplerenone, but not steroid withdrawal, reverses cardiac fibrosis in deoxycorticosterone/salt-treated rats. *Endocrinology* **2004**, *145*, 3153–3157.
- 62 Bell, M. G.; Gernert, D. L.; Grese, T. A.; Belvo, M. D.; Borromeo, P. S.; Kelley, S. A.; Kennedy, J. H.; Kolis, S. P.; Lander, P. A.; Richey, R.; Sharp, V. S.; Stephenson, G. A.; Williams, J. D.; Yu, H.; Zimmerman, K. M.; Steinberg, M. I.; Jadhav, P. K. (S)-N-{3-[1-Cyclopropyl-1-(2,4-difluoro-phenyl)-ethyl]-1H-indol-7-yl}-methanesulfonamide: A potent, nonsteroidal, functional antagonist of the mineralocorticoid receptor. *J. Med. Chem.* **2007**, *50*, 6443–6445.
- 63 (a) Delcayre, C.; Swynghedauw, B. Molecular mechanisms of myocardial remodeling. The role of aldosterone. *J. Mol. Cell. Cardiol.* **2002**, *34*, 1577–1584. (b) de Resende, M. M.; Kauser, K.; Mill, J. G. Regulation of cardiac and renal mineralocorticoid receptor expression by captopril following myocardial infarction in rats. *Life Sci.* **2006**, *78*, 3066–3073.
- 64 Chai, W.; Garrelds, I. M.; de Vries, R.; Batenburg, W. W.; van Kats, J. P.; Danser, A. H. J. Nongenomic effects of aldosterone in the human heart: Interaction with angiotensin II. *Hypertension* **2005**, *46*, 701–706.

- 65 Hartmann, R. W. Selective inhibition of steroidogenic P450 enzymes: Current status and future perspectives. *Eur. J. Pharm. Sci.* **1994**, *2*, 15–16.
- 66 Ehmer, P. B.; Bureik, M.; Bernhardt, R.; Müller, U.; Hartmann, R. W. Development of a test system for inhibitors of human aldosterone synthase (CYP11B2): Screening in fission yeast and evaluation of selectivity in V79 cells. *J. Steroid Biochem. Mol. Biol.* **2002**, *81*, 173–179.
- 67 Hartmann, R. W.; Müller, U.; Ehmer, P. B. Discovery of selective CYP11B2 (aldosterone synthase) inhibitors for the therapy of congestive heart failure and myocardial fibrosis. *Eur. J. Med. Chem.* **2003**, *38*, 363–366.
- 68 Schenkman, J. B.; Sligar, S. G.; Cinti, D. L. Substrate interaction with cytochrome P-450. *Pharmacol. Ther.* **1981**, *12*, 43–71.
- 69 Taymans, S. E.; Pack, S.; Pak, E.; Torpy, D. J.; Zhuang, Z.; Stratakis, C. A. Human CYP11B2 (aldosterone synthase) maps to chromosome 8q24.3. *J. Clin. Endocrinol. Metab.* **1998**, *83*, 1033–1036.
- 70 Lamberts, S. W.; Bruining, H. A.; Marzouk, H.; Zuiderwijk, J.; Uitterlinden, P.; Blijd, J. J.; Hackeng, W. H.; de Jong, F. H. The new aromatase inhibitor CGS-16949A suppresses aldosterone and cortisol production by human adrenal cells in vitro. *J. Clin. Endocrinol. Metab.* **1989**, *69*, 896–901.
- 71 Demers, L. M.; Melby, J. C.; Wilson, T. E.; Lipton, A.; Harvey, H. A.; Santen, R. J. The effects of CGS 16949A, an aromatase inhibitor on adrenal mineralocorticoid biosynthesis. *J. Clin. Endocrinol. Metab.* **1990**, *70*, 1162–1166.
- 72 Minnaard-Huiban, M.; Emmen, J. M. A.; Roumen, L.; Beugels, I. P. E.; Cohuet, G. M. S.; van Essen, H.; Ruijters, E.; Pieterse, K.; Hilbers, P. A. J.; Ottenheijm, H. C. J.; Plate, R.; de Gooyer, M. E.; Smits, J. F. M.; Hermans, J. J. R. Fadrozole reverses cardiac fibrosis in spontaneously hypertensive heart failure rats: Discordant enantioselectivity versus reduction of plasma aldosterone. *Endocrinology* **2008**, *149*, 28–31.
- 73 Funder, J. W. Aldosterone synthase and mineralocorticoid receptors as targets in cardiovascular disease. *Drug Discov. Today Ther. Strat.* **2005**, *2*, 231–235.
- 74 Hahner, S.; Stuermer, A.; Kreissl, M.; Reiners, C.; Fassnacht, M.; Haenscheid, H.; Beuschlein, F.; Zink, M.; Lang, K.; Allolio, B.; Schirbel, A. [¹²³I]Iodometomidate for Molecular Imaging of Adrenocortical Cytochrome P450 Family 11B Enzymes. *J. Clin. Endocrinol. Metab.* **2008**, *93*, 2358–65.
- 75 Bassett, M. H.; Mayhew, B.; Rehman, K.; White, P. C.; Mantero, F.; Arnaldi, G.; Stewart, P. M.; Bujalska, I.; Rainey, W. E. Expression profiles for steroidogenic enzymes in adrenocortical disease. *J. Clin. Endocrinol. Metab.* **2005**, *90*, 5446–5455.
- 76 (a) Weindel, K.; Lewicka, S.; Vecsei, P. Inhibitory effects of the novel anti-aldosterone compound mespirenone on adrenocortical steroidogenesis in vitro. *Arzneimittelforschung* **1991**, *41*, 946–949. (b) Weindel, K.; Lewicka, S.; Vecsei, P. Interference of C17-spirosteroids with late steps of aldosterone biosynthesis. Structure-activity studies. *Arzneimittelforschung* **1991**, *41*, 1082–1091.
- 77 (a) Delorme, C.; Piffeteau, A.; Viger, A.; Marquet, A. Inhibition of bovine cytochrome P-450_{11β} by 18-unsaturated progesterone derivatives. *Eur. J. Biochem.* **1995**, *232*, 247–256. (b) Delorme, C.; Piffeteau, A.; Sobrio, F.; Marquet, A. Mechanism-based inactivation of bovine cytochrome P-450_{11β} by 18-unsaturated progesterone derivatives. *Eur. J. Biochem.* **1997**, *248*, 252–260.
- 78 Davioud, E.; Piffeteau, A.; Delorme, C.; Coustal, S.; Marquet, A. 18-Vinyldeoxycorticosterone: a potent inhibitor of the bovine cytochrome P-450_{11β}. *Bioorg. Med. Chem.* **1998**, *6*, 1781–1788.

- 79 Bureik, M.; Hubel, K.; Dragan, C. A.; Scher, J.; Becker, H.; Lenz, N.; Bernhardt, R. Development of test systems for the discovery of selective human aldosterone synthase (CYP11B2) and 11 β -hydroxylase (CYP11B1) inhibitors. Discovery of a new lead compound for the therapy of congestive heart failure, myocardial fibrosis and hypertension. *Mol. Cell. Endocrinol.* **2004**, *217*, 249–254.
- 80 Bureik, M.; Mion, A.; Kenyon, C. J.; Bernhardt, R. Inhibition of aldosterone biosynthesis by staurosporine. *Biol. Chem.* **2005**, *386*, 663–669.
- 81 Avgerinos, P. C.; Nieman, L. K.; Oldfield, E. H.; Cutler Jr., G. B. A comparison of the overnight and the standard metyrapone test for the differential diagnosis of adrenocorticotrophin-dependent Cushing's syndrome. *Clin. Endocrinol.* **1996**, *45*, 483–491.
- 82 Fellows, I. W.; Bastow, M. D.; Byrne, A. J.; Allison, S. P. Adrenocortical suppression in multiply injured patients: a complication of etomidate treatment. *Br. Med. J.* **1983**, *287*, 1835–1837.
- 83 Schieweck, K.; Bhatnagar, A. S.; Matter, A. CGS 16949A, a new nonsteroidal aromatase inhibitor: effects on hormone-dependent and -independent tumors in vivo. *Cancer Res.* **1988**, *48*, 834–838.
- 84 Ménard, J.; Gonzalez, M.-F.; Guyene, T.-T.; Bissery, A. Investigation of aldosterone-synthase inhibition in rats. *J. Hypertension* **2006**, *24*, 1147–1155.
- 85 (a) Herold, P.; Mah, R.; Tschinke, V.; Stojanovic, A.; Marti, C.; Jelakovic, S.; Stutz, S. Preparation of imidazo compounds as aldosterone synthase inhibitors. PCT Int. Appl. WO2007116099, 2007. (b) Herold, P.; Mah, R.; Tschinke, V.; Stojanovic, A.; Marti, C.; Jelakovic, S.; Bennacer, B.; Stutz, S. Preparation of spiro-imidazo derivatives as aldosterone synthase inhibitors. PCT Int. Appl. WO2007116098, 2007. (c) Herold, P.; Mah, R.; Tschinke, V.; Stojanovic, A.; Marti, C.; Stutz, S. Preparation of imidazo compounds as aldosterone synthase inhibitors. PCT Int. Appl. WO2007116097, 2007. (d) Herold, P.; Mah, R.; Tschinke, V.; Quirnbach, M.; Marti, C.; Stojanovic, A.; Stutz, S. Preparation of fused imidazoles as aldosterone synthase inhibitors. PCT Int. Appl. WO2007065942, 2007. (e) Herold, P.; Mah, R.; Tschinke, V.; Stojanovic, A.; Marti, C.; Jotterand, N.; Schumacher, C.; Quirnbach, M. Preparation of heterocyclic spiro-compounds as aldosterone synthase inhibitors. PCT Int. Appl. WO2006128853, 2006. (f) Herold, P.; Mah, R.; Tschinke, V.; Stojanovic, A.; Marti, C.; Jotterand, N.; Schumacher, C.; Quirnbach, M. Preparation of heterocyclic spiro-compounds as aldosterone synthase inhibitors. PCT Int. Appl. WO2006128852, 2006. (g) Herold, P.; Mah, R.; Tschinke, V.; Stojanovic, A.; Marti, C.; Jotterand, N.; Schumacher, C.; Quirnbach, M. Preparation of fused imidazoles as aldosterone synthase inhibitors. PCT Int. Appl. WO2006128851, 2006. (h) Herold, P.; Mah, R.; Tschinke, V.; Schumacher, C.; Marti, C.; Quirnbach, M. Preparation of fused heterocycles as aldosterone synthase inhibitors. PCT Int. Appl. WO2006005726, 2006. (i) Herold, P.; Mah, R.; Tschinke, V.; Schumacher, C.; Quirnbach, M. Preparation of imidazopyridines and related analogs as aldosterone synthase inhibitors. PCT Int. Appl. WO2005118557, 2005. (j) Herold, P.; Mah, R.; Tschinke, V.; Schumacher, C.; Quirnbach, M. Preparation of tetrahydro-imidazo[1,5-a]pyridin derivatives as aldosterone synthase inhibitors. PCT Int. Appl. WO2005118581, 2005. (k) Herold, P.; Mah, R.; Tschinke, V.; Schumacher, C.; Behnke, D.; Quirnbach, M. Preparation of nitrogen-containing heterobicyclic compounds as aldosterone synthase inhibitors. PCT Int. Appl. WO2005118541, 2005.
- 86 (a) Hu, Q.-Y.; Ksander, G. M. Preparation of imidazoles as inhibitors of aldosterone synthase. PCT Int. Appl. WO2008076862, 2008. (b) Hu, Q.-Y.; Ksander, G. M. Preparation of 4-imidazolyl-1,2,3,4-tetrahydroquinoline derivatives as aldosterone/11 β -hydroxylase inhibitors. PCT Int. Appl.

- WO2008076860, 2008. (c) Adams, C.; Hu, Q.-Y.; Ksander, G. M.; Papillon, J. Preparation of imidazole derivatives as inhibitors of CYP11B2, CYP11B1 and/or aromatase. PCT Int. Appl. WO2008076336, 2008. (d) Ksander, G. M.; Hu, Q.-Y. Fused imidazole derivatives for the treatment of disorders mediated by aldosterone synthase and/or 11-beta-hydroxylase and/or aromatase. PCT Int. Appl. WO2008027284, 2008. (e) Papillon J.; Ksander, G. M.; Hu, Q.-Y. Preparation of tetrahydroimidazo[1,5-a]pyrazine derivatives as aldosterone synthase and/or 11 β -hydroxylase inhibitors. PCT Int. Appl. WO2007139992, 2007. (f) Adams, C.; Papillon, J.; Ksander, G. M. Preparation of imidazole derivatives as aldosterone synthase inhibitors. PCT Int. Appl. WO2007117982, 2007. (g) Ksander, G. M.; Meredith, E.; Monovich, L. G.; Papillon, J.; Firooznia, F.; Hu, Q.-Y. Preparation of condensed imidazole derivatives for the inhibition of aldosterone synthase and aromatase. PCT Int. Appl. WO2007024945, 2007. (h) Firooznia, F. Preparation of imidazo[1,5a]pyridine derivatives for treatment of aldosterone mediated diseases. PCT Int. Appl. WO2004046145, 2004. (i) McKenna, J. Preparation of imidazopyrazines and imidazodiazepines as agents for the treatment of aldosterone mediated conditions. PCT Int. Appl. WO2004014914, 2004.
- 87 Anzenbacher, P.; Anzenbacherová, E. Cytochromes P450 and metabolism of xenobiotics. *Cell. Mol. Life Sci.* **2001**, *58*, 737–747.
- 88 Voets, M.; Antes, I.; Scherer, C.; Müller-Vieira, U.; Biemel, K.; Barassin, C.; Oberwinkler-Marchais, S.; Hartmann, R. W. Heteroaryl substituted naphthalenes and structurally modified derivatives: Selective inhibitors of CYP11B2 for the treatment of congestive heart failure and myocardial fibrosis. *J. Med. Chem.* **2005**, *48*, 6632–6642.
- 89 Voets, M.; Antes, I.; Scherer, C.; Müller-Vieira, U.; Biemel, K.; Oberwinkler-Marchais, S.; Hartmann, R. W. Synthesis and evaluation of heteroaryl-substituted dihydronaphthalenes and indenenes: Potent and selective inhibitors of aldosterone synthase (CYP11B2) for the treatment of congestive heart failure and myocardial fibrosis. *J. Med. Chem.* **2006**, *49*, 2222–2231.
- 90 Ulmschneider, S.; Negri, M.; Voets, M.; Hartmann, R. W. Development and evaluation of a pharmacophore model for inhibitors of aldosterone synthase (CYP11B2). *Bioorg. Med. Chem. Lett.* **2006**, *16*, 25–30.
- 91 (a) Eaton, D. L.; Gallagher, E. P.; Bammler, T. K.; Kunze, K. L. Role of cytochrome P4501A2 in chemical carcinogenesis: Implications for human variability in expression and enzyme activity. *Pharmacogenetics* **1995**, *5*, 259–274. (b) Guengerich, F.; Parikh, A.; Turesky, R. J.; Josephy, P. D. Interindividual differences in the metabolism of environmental toxicants: Cytochrome P450 1A2 as a prototype. *Mutat. Res.* **1999**, *428*, 115–124.
- 92 Häusler, A.; Monnet, G.; Borer, C.; Bhatnagar, A. S. Evidence that corticosterone is not an obligatory intermediate in aldosterone biosynthesis in the rat adrenal. *J. Steroid Biochem.* **1989**, *34*, 567–570.
- 93 Heim, R.; Lucas, S.; Grombein, C. M.; Ries, C.; Schewe, K. E.; Negri, M.; Müller-Viera, U.; Birk, B.; Hartmann, R. W. Overcoming undesirable CYP1A2 inhibition of pyridynaphthalene type aldosterone synthase inhibitors: Influence of heteroaryl derivatization on potency and selectivity. *J. Med. Chem.* **2008**, *51*, 5064–5074.
- 94 Lucas, S.; Heim, R.; Negri, M.; Antes, I.; Ries, C.; Schewe, K. E.; Bisi, A.; Gobbi, S.; Hartmann, R. W. Novel aldosterone synthase inhibitors with extended carbocyclic skeleton by a combined ligand-based and structure-based drug design approach. *J. Med. Chem.* **2008**, in press.

- 95 (a) Cavalli, A.; Bisi, A.; Bertucci, C.; Rosini, C.; Paluszczak, A.; Gobbi, S.; Giorgio, E.; Rampa, A.; Belluti, F.; Piazzzi, L.; Valenti, P.; Hartmann, R. W.; Recanatini M. Enantioselective nonsteroidal aromatase inhibitors identified through a multidisciplinary medicinal chemistry approach. *J. Med. Chem.* **2005**, *48*, 7282–7289. (b) Gobbi, S.; Cavalli, A.; Rampa, A.; Belluti, F.; Piazzzi, L.; Paluszczak, A.; Hartmann, R. W.; Recanatini, M.; Bisi, A. Lead optimization providing a series of flavone derivatives as potent nonsteroidal inhibitors of the cytochrome P450 aromatase enzyme. *J. Med. Chem.* **2006**, *49*, 4777–4780.
- 96 (a) Chohan, K. K.; Paine, S. W.; Mistry, J.; Barton, P.; Davis, A. M. A rapid computational filter for cytochrome P450 1A2 inhibition potential of compound libraries. *J. Med. Chem.* **2005**, *48*, 5154–5161. (b) Korhonen, L. E.; Rahnasto, M.; Mähönen, N. J.; Wittekindt, C.; Poso, A.; Juvonen, R. O.; Raunio, H. Predictive three-dimensional quantitative structure-activity relationship of cytochrome P450 1A2 inhibitors. *J. Med. Chem.* **2005**, *48*, 3808–3815.
- 97 Butler, M. A.; Iwasaki, M.; Guengerich, F. P.; Kadlubar, F. F. Human cytochrome P-450PA (P-450IA2), the phenacetin O-deethylase, is primarily responsible for the hepatic 3-demethylation of caffeine and N-oxidation of carcinogenic arylamines. *Proc. Natl. Acad. Sci. U.S.A.* **1989**, *86*, 7696–7700.
- 98 Sesardic, D.; Boobis, A. R.; Murray, B. P.; Murray, S.; Segura, J.; de la Torre, R.; Davies, D. S. Furfurylline is a potent and selective inhibitor of cytochrome P450IA2 in man. *Br. J. Clin. Pharmacol.* **1990**, *29*, 651–663.
- 99 Lucas, S.; Heim, R.; Ries, C.; Schewe, K. E.; Birk, B.; Hartmann, R. W. Nonsteroidal aldosterone synthase inhibitors with improved selectivity: Lead optimization providing a series of pyridine substituted 3,4-dihydro-1*H*-quinolin-2-one derivatives. *J. Med. Chem.* **2008**, submitted.
- 100 Lucas, S.; Heim, R.; Ries, C.; Hartmann, R. W. Fine-tuning the selectivity of aldosterone synthase inhibitors: SAR insights from studies of heteroaryl substituted 1,2,5,6-tetrahydropyrrolo[3,2,1-*ij*]quinolin-4-one derivatives. *J. Med. Chem.* **2008**, submitted.
- 101 (a) Richmond, N. J.; Abrams, C. A.; Wolohan, P. R.; Abrahamian, E.; Willett, P.; Clark, R. D. GALAHAD: 1. Pharmacophore identification by hypermolecular alignment of ligands in 3D. *J. Comput.-Aided Mol. Des.* **2006**, *20*, 567–587. (b) Shepphird, J. K.; Clark, R. D. A marriage made in torsional space: Using GALAHAD models to drive pharmacophore multiplet searches. *J. Comput.-Aided Mol. Des.* **2006**, *20*, 763–771.

6 Acknowledgements

I would like to express my sincere gratitude to the following people, without whom the work described in this thesis would have been much less enjoyable or, in some cases, not even possible.

My supervisor Prof. Rolf W. Hartmann for believing in me in the first place, for the competent guidance during my PhD work and for providing lot of scope for creative ideas. Your vast knowledge in medicinal chemistry and your ability to inspire and enthuse others have made these past years very pleasant and instructive.

My official referee Prof. Uli Kazmaier for the reviewing of this dissertation, for your kind support and, not least, for teaching me all I know about organic chemistry. Your great didactical skills made all the lectures and seminars so enjoyable.

My co-supervisor Dr. Ralf Heim for the excellent collaboration during the past years, all the stimulating discussions, the readiness to supply help whenever needed and your valuable suggestions and scientific criticism on this work.

Matthias Negri for the generation of the extended pharmacophore model, some other very interesting contributions to this work and the discussion of all the computational results.

Gertrud Schmitt and Jeannine Jung for performing the *in vitro* tests and for measuring the elemental analyses.

All past and present members of the CYP11B2 team, especially the members of the first hour Dr. Katarzyna Schewe and Christina Ries for the very successful and inspiring teamwork.

The undergraduate research participants Judith Horzel, Helena Rübel, and Thomas Jakoby whose enthusiastic work contributed to the presented results.

Dr. Stefan Boettcher for measuring the LC/MS samples.

All other co-workers of the RWH group for practical support and collegiality, as well as the excellent working atmosphere.

Dr. Josef Zapp for the help with the performance and interpretation of some NMR experiments.

The colleagues from Pharmacelsus CRO, and Dr. Ursula Müller-Vieira, Dr. Barbara Birk, and Dr. Reiner Class in particular, for the hepatic CYP testing as well as for performing the in vivo and cytotoxicity experiments.

Prof. Iris Antes, Max Planck Institute for Informatics, now Technical University Munich, for performing the homology and docking studies and the good collaboration for our joint paper.

Prof. Alessandra Bisi and Dr. Silvia Gobbi, University of Bologna, for providing the flavone inhibitors for testing and the collaboration for our publication.

Thanks are also due to Prof. J. J. Rob Hermans, University of Maastricht, The Netherlands, for supplying the V79 CYP11B1 cells, and Prof. Rita Bernhardt, Saarland University, for supplying the V79 CYP11B2 cells.

This work was supported by a scholarship of the Saarland University (Landesgraduierten-Förderung).